

**ANALYSIS OF RADIOISOTOPE DEPLETION AND
GENERATION USING KLOPFENSTEIN-SHAMPINE
FAMILY OF
NUMERICAL DIFFERENTIATION FORMULA**

By
GYAN CHANDRA CHAUTHWANI
PHYS01201304036

Bhabha Atomic Research Centre, Mumbai

*A thesis submitted to the
Board of Studies in Physical Sciences*

*In partial fulfillment of requirements
for the degree of*

DOCTOR OF PHILOSOPHY

of

HOMI BHABHA NATIONAL INSTITUTE

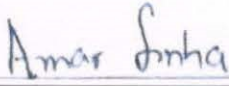
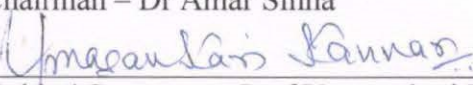
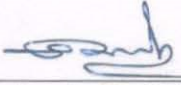
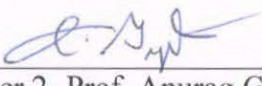
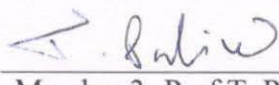


AUGUST, 2013

HomiBhabha National Institute

RECOMMENDATIONS OF THE VIVA VOCE COMMITTEE

As members of the Viva Voce Committee, we certify that we have read the dissertation prepared by Gyan Chandra Chauthwani entitled "**Analysis of radio-isotope depletion and generation using Klopfenstein-Shampine family of Numerical Differentiation Formula**" and recommend that it may be accepted as fulfilling the thesis requirement for the award of Degree of Doctor of Philosophy.

	(Attended through video conferencing)
Chairman – Dr Amar Sinha	Date :17/12/2020
	(Attended through video conferencing)
Guide / Convener – Prof.Umasankari Kannan	Date :17/12/2020
Co-guide - NIL	(Attended through video conferencing)
	(Attended through video conferencing)
Examiner - Prof. K.V. Subbaiah	Date:17/12/2020
	(Attended through video conferencing)
Member 1- Prof. K. Devan	Date :17/12/2020
	(Attended through video conferencing)
Member 2- Prof. Anurag Gupta	Date :17/12/2020
	(Attended through video conferencing)
Member 3- Prof.T. Palaniselvam	Date :17/12/2020

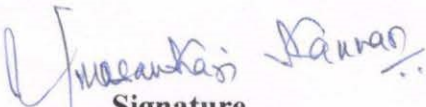
Final approval and acceptance of this thesis is contingent upon the candidate's submission of the final copies of the thesis to HBNI.

I/We hereby certify that I/we have read this thesis prepared under my direction and recommend that it may be accepted as fulfilling the thesis requirement.

Date: 17/12/2020

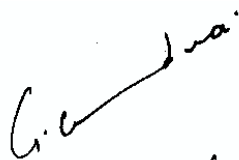
Place: Mumbai

Signature
Co-guide (if any)


Signature
Guide

Statement by Author

This dissertation has been submitted in partial fulfillment of requirements for an advanced degree at the Homi Bhabha National Institute (HBNI). It is deposited in the library to be made available to borrowers under the rules of the HBNI.


(Gyan Chandra
Chauthwani)

Name & Signature of the student

Declaration

I hereby declare that except where specific reference is made to others' work, this dissertation's contents are original and have not been submitted in whole or in part for consideration for any other degree or qualification in this or any other University. This dissertation results from my work and includes nothing which is the outcome of work done in collaboration, except where specifically indicated in the text or reference. This dissertation contains less than 45,000 words, including appendices, bibliography, footnotes, tables, equations, and has less than 50 figures.

G.C. Chauthwani
(Gyan Chandra
Chauthwani)

Name & Signature of the student

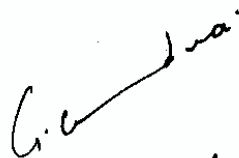
List of Publications arising from the thesis

Journal

1. G. C. Chauthwani, Umasankari Kannan, "Development of computer code IGDC for generation and depletion of fission products and actinides in pressure tube type heavy water reactors (PT-HWRs) using Klopfenstien-Shampine Numerical Differentiation Formula (NDF)." *Journal of Nuclear Engineering and Design*, **341** (2019), 220-238.
2. G C Chauthwani, Umasankari Kannan, "Analysis for Decay heat in natural uranium fuelled Pressure Tube Type Heavy Water Reactor estimated using the indigenous computer code IGDC", *Journal of Nuclear Engineering and Design*, **352** (2019), 110159.

Conferences

1. G. C. Chauthwani, L. K. Gupta, Anil Chauhan, Umasankari Kannan, "Estimation of isotopic inventory and activity for 220 MW(e) pressurized heavy water reactor." Symposium on Advances in Reactor Physics (ARP2017), Mumbai Dec 6-9, 2017.


(Gyan Chandra
Chauthwani)

Name & Signature of the student

Dedication

I would like to dedicate this thesis to my loving parents and my wife.

Acknowledgments

Foremost, I would like to express my sincere gratitude to my Ph.D. guide, Prof Umasankari Kannan, for the continuous support of my Ph.D. study and research, for her patience, motivation, enthusiasm, and immense knowledge. Her guidance helped me in all the time of research and writing of this thesis. I could not have imagined having a better advisor and mentor for my Ph.D. study. At the same time, I would also like to express my gratitude towards my technical advisor Shri L K Gupta, for his technical guidance during the research work. Besides my guide and advisor, I would like to thank the rest of my doctoral committee: Dr. S.B. Degweker, Dr. Amar Sinha, Dr. K. Devan, Dr. Anurag Gupta, and Dr. T. Palani Selvam for their encouragement, insightful comments, and of course, challenging questions. My sincere thanks also go to Professor Emeritus L.F. Shampine of Southern Methodist University and Professor Raju K. George of the Indian Institute of Space Science and Technology (IIST) for stimulating discussions and suggestions on numerical methods for first-order stiff ODEs. I thank Dr. G. Pandikumar for his valuable insights on nuclear data and enlightening me on the first glance of research. Finally, I would like to thank my family: for supporting me spiritually throughout my life.

Table of Contents

<i>Declaration</i>	iii
<i>Dedication</i>	v
<i>Acknowledgments</i>	vi
<i>Summary</i>	2
<i>Chapter 1 Introduction to fuel cycle analysis</i>	3
1.0 Statement of the problem and solution methodology	3
1.1 Objective of the research	4
1.2 Development of Actinide and fission product nuclide chains	6
1.3 Generation of Nuclear reaction database for PHWR applications.....	7
1.4 Study and use of Fission yield data	7
1.5 Study of the Decay process of nuclides and their decay-data.....	8
1.6 Estimation of average Neutron flux.....	10
1.7 Isotopic decay energy and dose conversion factors.....	11
1.8 Summary.....	11
<i>Chapter 2 Literature Survey</i>	12
2.0 Introduction	12
2.1 Study of the transmutation chains.....	12
2.2 Survey of nuclear data required for fuel cycle analysis.....	13
2.3 Literature survey of solution recipes	14
2.3.1 Matrix exponential method	15
2.3.2 Eigen value method	17
2.3.3 Analytical Methods.....	17
2.3.4 Numerical Methods	18
2.4 A summary of burn-up codes currently used.....	19
2.4.1 Nuclear Inventory Codes	19
2.4.1.1 ORIGEN-S	19
2.4.1.2 ORIGEN-ARP.....	20
2.4.1.3 FISPIN.....	22
2.4.1.4 FISPACT	23
2.4.1.5 ACAB.....	25

2.4.1.6	RICE.....	25
2.4.1.7	FISP.....	26
2.4.1.8	ISOGEN.....	26
2.4.2	Burn-up modules in lattice codes.....	27
2.4.2.1	SERPENT.....	27
2.4.2.2	CASMO.....	28
2.4.2.3	CLUB.....	29
2.4.2.4	WIMS.....	29
2.4.2.5	MONTE CARLO METHODS.....	30
2.4.3	Fuel cycle simulation codes.....	30
2.4.3.1	ORION.....	30
2.4.3.2	COSI.....	32
2.4.3.3	Nuclear fuel simulation system (VISTA).....	32
2.4.4	Other important codes.....	33
2.4.4.1	DARWIN.....	33
2.4.4.2	APOLLO.....	34
2.4.4.3	SNF.....	34
2.5	Description of the code under development.....	34
2.6	Benchmarks for fuel cycle analysis codes.....	35
2.7	Conclusion.....	36
	<i>Chapter 3 Generation of Cross-section Library.....</i>	38
3.0	Introduction.....	38
3.1	Weighting Spectrum.....	38
3.2	Generation of spectrum dependent one group cross-section.....	40
3.3	Evaluated Nuclear Data format (ENDF) Files.....	41
3.3.1	Reading an ENDF tape.....	42
3.3.2	Symbol Nomenclature.....	43
3.3.3	Types of Records.....	43
3.3.4	Retrieving data from an ENDF file.....	43
3.4	Estimation of spectrum dependent of cross-sections.....	44
3.5	Preparation of Generalised Cross-section sets.....	49
3.5.1	Linearization.....	49
3.5.2	Resonance Reconstruction.....	50
3.5.3	Doppler broadening.....	51

3.5.4 Multi-grouping.....	52
3.6 Reactor specific cross-section set	54
3.7 Results	55
3.8 Conclusion	58
<i>Chapter 4 Development of computer code IGDC.....</i>	60
4.0 Introduction	60
4.1 Development of transmutation model	61
4.1.1 Fission term	62
4.1.2 Radioactive decay terms	62
4.2 Numerical method for solution of Bateman equations	69
4.3 Suitability of Klopfenstein - Shampine family of NDF.....	70
4.3.1 Backward Differentiation Formula.....	70
4.3.2 Klopfenstein- Shampine Family of NDFS	75
4.3.3 Novelty of NDFs over Matrix exponential methods	77
4.3.4 Novelty of NDFs over BDFs	77
4.3.3 Implementation of NDF.....	80
4.3.4 Algorithm of K-S family of NDFs.....	81
4.4 Flow diagram of the code	82
4.5 Summary.....	83
<i>Chapter 5 Benchmarking and Analysis of PT-HWR fuel cycle with IGDC.....</i>	86
5.0 Introduction	86
5.1 Validation of the computer code IGDC	87
5.1.1 Validation for isotopic inventory.....	87
5.1.2 Validation for decay heat.....	89
5.1.3 Validation for Activities and concentration.....	94
5.2 Concentration of important radio-nuclides	95
5.3 Non-linear coupling of neutron flux	100
5.4 Radio-activity and Radio-toxicities	102
5.5 Decay heat analysis	108
5.5.1 Decay heat factor for actinides & fission products.....	112
5.5.2 Decay factor for alpha, beta, and gamma emitters	114
5.6 Neutron absorption	121
5.6.1 Poisoning factor of different fission products	122
5.5.2 Relative absorption of neutron.....	123

5.7	Summary.....	125
	<i>Chapter 6 Summary and future work</i>.....	128
6.0	Summary of the research work done	128
6.1	Numerical method of IGDC	128
6.2	Benchmarking of IGDC.....	129
6.3	Decay heat analysis with IGDC.....	129
6.4	Analysis for neutron absorbing isotopes.....	130
6.5	Important conclusions of analysis using IGDC	130
6.6	Future work with IGDC.....	133
	<i>Annexure-1</i>.....	136
	<i>The decay chain of fission products</i>	136
	<i>Annexure-2</i>.....	155
	<i>Generation and depletion of actinides</i>.....	155
	<i>Annexure-3</i>.....	160
	<i>Numerical Methods for ODEs</i>.....	160
A3-1.	Introduction	160
A3-2.	Methods of solution of initial value problem.....	161
A3-2.1.	Analytical method	161
A3-2.2.	Numerical method	162
A3-2.2.1.	Single-step methods	163
A3-2.2.1.1.	Picard's method	163
A3-2.2.1.2.	Euler's method.....	163
A3-2.2.1.3.	Modified Euler's method.....	165
A3-2.2.1.4.	RungeKutta second order method.....	165
A3-2.2.1.5.	RungeKutta fourth-order method.....	165
A3-2.2.1.6.	Numerical Solution of stiff differential equations	166
A3-2.2.2.	Baily's criteria for step size.....	169
A3-2.2.3.	Multi-step methods.....	171
A3-2.2.4.	Numerical solution with Multi-step methods[83]	171
A3-2.2.5.	Gears BDF method[83]	172
A3-2.2.6.	Adams-Bashford Method[83].....	174
A3-2.2.7.	Adams-Moulton Method[83]	175
A3-2.2.8.	Predictor-corrector methods[83]	176

A3-2.2.9.	Adaptive step-size control[83]	178
A3-2.2.10.	Some basic concepts	179
A3-2.2.10.1.	Differential equation	179
A3-2.2.10.2.	Order and degree of Differential equation	180
A3-2.2.10.3.	Linear and non-linear Differential equation.....	180
A3-2.2.10.4.	Initial and boundary value problem	181
A3-2.2.10.5.	Existence and uniqueness of the solution	181
A3-2.2.10.6.	Solving differential equation numerically.....	182
A3-2.2.10.7.	Error in numerical solution and concept of order	182
A3-2.2.10.8.	Concept of stability	184
A3-3.	Summary.....	186
<i>Annexure-4</i>	187
<i>Nuclear data for fuel cycle analysis</i>	187
A4-1.	Introduction	187
A4-2.	Brookhaven National Laboratory's (BNL)	187
A4-3.	Decay-data library	188
A4-4.	data library for Dose conversion factors.....	191
A4-5.	Decay Energy data library	198
A4-6.	Branching ratio	206
A4-7.	Fission yield.....	209
A4-8.	Summary.....	210
References	211

List of Figures

Figure 1.1: JANIS browser window	9
Figure 1.2: JANIS rendering window	9
Figure 3.1: Unit cell of PT-HWR fuelled with natural uranium	38
Figure 3.2: Neutron spectrum in small size PT-HWR fuelled with NU	40
Figure 3.3: Total and fission cross-section of Pu ²³⁹ using JENDL-4.0	44
Figure 3.4: Interval halving technique for resonance reconstruction	50
Figure 3.5: Effect of Doppler broadening on resonances in cross-section	52
Figure 3.6: Multi-group cross-sections of U ²³³ , U ²³⁵ , and Pu ²³⁹ in WIMS library	53
Figure 4.1: Generation and depletion chain of few fission products	65
Figure 4.2: Generation and depletion chain of few actinides	67
Figure 4.3: Stability regionsof BDF (Solid) and NDF (Dotted)[68]	80
Figure 4.4: Detailed flow chart of the computer code “IGDC.”	84
Figure 5.1: Benchmarking workflow for the bundle ID T0906.....	92
Figure 5.2: Variation of uranium and plutonium isotopes with burn-up	96
Figure 5.3: Variation of plutonium, americium & curium with burn-up.....	97
Figure 5.4: Variation of U ²³⁶ and U ²³⁸ concentration with burn-up.....	97
Figure 5.5: Variation of non-saturating fission products with burn-up	98
Figure 5.6: Generation of actinium isotopes with burn-up	98
Figure 5.7: Generation of americium isotopes with burn-up.....	99
Figure 5.8: Generation of californium isotopes with burn-up	99
Figure 5.9: Generation of curium isotopes with burn-up.....	100
Figure 5.10: ²³⁵ U Concentrationwith/out nonlinear coupling of neutron flux	101
Figure 5.11: Variation of activity in PT-HWR fuel (Long Time Scale - LTS)	103
Figure 5.12: Variation of activity in PT-HWR fuel (Short Time Scale - STS)	104
Figure 5.13: Radio-toxicity due to ingestion by different recipients	107
Figure 5.14: Inhalation radio-toxicity of different size particles	107
Figure 5.15: Variation of total decay factor and gamma decay factor.....	110
Figure 5.16: Variation of thermal and gamma decay power after shut down.....	110
Figure 5.17: Decay heat (W/te) contribution of fission products and actinides	114

Figure 5.18: Variation of decay heat of essential fission products	120
Figure 5.19: Variation of decay heat of important actinides	121
Figure A1. 1: Radioactive decay chains of fission products.....	136
Figure A2. 1: Radioactive decay chains of actinides.....	155
Figure A4. 1: National Nuclear Data Centre of BNL	188
Figure A4. 2: Radioactive decay chain of U^{235}	206
Figure A4. 3: Radioactive decay chain of Am^{242}	207
Figure A4. 4: Radioactive decay chain of Am^{242m}	208
Figure A4. 5: Independent fission yield of U^{235}	209

List of Tables

Table 3.1: Unit cell parameters of PT-HWR fuelled with NU [58].....	39
Table 3.2: Spectrum averaged Reaction cross-section of important Actinides	56
Table 3.3: Spectrum averaged cross-section of important Fission Products	57
Table 4.1: Co-efficient of NDFs and A(α) comparisons relative to BDFs	78
Table 5.1: Comparison of ^{235}U and ^{239}Pu inventory with different codes	88
Table 5.2: Difference of concentration of U^{235} and Pu^{239} with different codes	88
Table 5.3: Irradiation history Fuel Assemblies of Douglas Point reactor.....	89
Table 5.4: Decay heat of Douglas Point Reactor with different codes	93
Table 5.5: Comparison of Gama decay heat of Douglas Point Reactor	93
Table 5.6: Measured and estimated activities in PT-HWR [69].....	95
Table 5.7: Measured and estimated concentrations in PT-HWR [69]	95
Table 5.8: Comparison of concentration of U^{235} and Pu^{239}	101
Table 5.9: Comparison of specific activity in the discharged fuel of PT-HWR.....	105
Table 5.10: Radio-toxicity in the discharged fuel in PT-HWR	106
Table 5.11: Gamma decay power after shut down at 7500 MWd/t in PT-HWR.....	111
Table 5.12: Thermal decay power after shut down at 7500 MWd/t in PT-HWR.....	111
Table 5.13: Decay heat fraction at cooling period = 0 Years	112
Table 5.14: Variation of decay heat fraction at cooling period = 30 Years.....	113
Table 5.15: Variation of actinide and fission product decay heat with a time.....	113
Table 5.16: Variation of decay heat fraction at cooling period = 0 Years.....	115
Table 5.17: Variation of decay heat fraction at cooling period = 30 Years.....	115
Table 5.18: Decay heat contribution of different actinides after discharge.....	116
Table 5.19: Isotopic contribution to decay heat from individual actinides.....	117
Table 5.20: Decay heat of fission products after discharge (in Watt/te)	117
Table 5.21: FP isotopes contributing to the decay heat over time	119
Table 5.22: Poisoning factor and the nature of essential Fission Products.....	122
Table 5.23: RELIFIX parameters of essential fission products	124
Table A4. 1: Decay data of radio-isotopes for PT-HWR.....	189
Table A4. 2: Dose conversion factors.....	192
Table A4. 3: Energy released in radio-isotopic decay	199

In this research work on nuclear fuel cycle analysis, modeling of fission generated radio-nuclides and actinides generated through neutron activation or radio-active decay of other radionuclides was carried out. A model of radio-isotopes is developed in a most general form consisting of coupled nonlinear stiff first-order differential equations of 619 fission products and 112 actinides. Klopfenstein-Shampine Family of Numerical Differentiation Formulas (K-S family of NDFs) were used for solving the developed model. Nuclear data consists of decay data, fission yields, branching ratios, dose conversion factors, and nuclear reaction data. Decay data were extracted using available software tools viz. JANIS, dose conversion factors were extracted from ICRP (International Commission on Radiological Protection) publications, and nuclear reaction cross-section libraries were generated by processing ENDF (Evaluated Nuclear Data Format) files using the computer code PREPRO.

The model and nuclear data libraries developed during the research were utilized for developing an indigenous nuclear fuel burn-up code **Isotopic Generation and Depletion Code: IGDC**. This code can be used for both in-core and ex-core applications. The use of efficient and new numerical techniques is the major novelty of this research. The significant outcome of the study is to have an own tool developed for the Indian community to reduce the dependence on foreign codes and resolve accessibility problems.

Results of the code can be used for identifying the important isotopes in the spent fuel, preparation of consignment for spent fuel transportation, identifying the reactivity anomaly during reactor operation and estimation of source term for Radiological Impact Analysis (RIA).

Presently this code is used for the analysis of Pressure Tube Type Heavy Water Reactor. However, this can be used for any type of nuclear facility (e.g. BWR, PWR, MSR ...) where nuclear fission is the primary process for the generation and depletion of radioisotopes for the estimation of concentration, decay heat, radioactivity, ingestion, and inhalation radiotoxicity and reactivity changes due to fission products and actinides both during irradiation and cooling periods.

Chapter 1

Introduction to fuel cycle analysis

In a nuclear fission reactor, the isotopic composition of nuclear fuel changes continuously due to the transformation of nuclides to the other nuclides by neutron-induced transmutation reactions and spontaneous radioactive decay. The radioactive decay process continues even when nuclear fuel is removed from the reactor. The fuel cycle analysis entails detailed tracking of each nuclide formed and destroyed, their consequences w.r.t. radioactivity and radiotoxicity, the heat generated, and many other related consequences. This complex phenomenon involves several reaction mechanisms and decay, ranging from several orders of magnitude in the time scale. Thus the tracking of nuclide concentrations is very involved and requires efficient computations. The nature of the governing equations and their complexity will be discussed below. The present research study's objective is to simulate these changes over the time domain and capture the related physics phenomena.

1.0 STATEMENT OF THE PROBLEM AND SOLUTION METHODOLOGY

The radio-isotope depletion and generation equations govern the changes in nuclide concentrations over time. These equations form a system of first-order coupled ordinary differential equations (ODEs) called burn-up equations or Bateman Equations [1]. These systems of equations are stiff owing to the enormous changes in the half-lives. For example, the aforesaid system of equation will have to incorporate very short-lived fission products, e.g., Nd^{157} with a half-life of about 300 ns and very long-lived fission

product Zr^{96} with a half-life of about 2×10^{19} years, i.e., stiffness approximately is of the order of 10^{33} . Furthermore, these systems of equations are nonlinear due to the explicit variation of neutron flux.

Method of Backward Differentiation formulae (BDFs) proposed by C.W. Gear [2] is commonly used for the aforesaid system of coupled nonlinear stiff first-order differential equations. However, their most significant drawback is the low stability properties of the higher-order formula. Several efforts to derive methods with better accuracy and stability properties than those in BDFs have been made. One of the modifications made to the BDFs in this line is the NDFs (Numerical Differentiation Formulae) done by Klopfenstein and Shampine [3]. In this research, an algorithm based on the Klopfenstein-Shampine family of Numerical Differentiation Formulae (K-S family of NDFs) in particular is proposed, which is a novel method for solving these burn-up equations.

In other types of solution methods, such as the exponential matrix method, which is widely used, partitioning short and long-lived isotopes is essential [4]. K-S family of NDFs can handle the stiffness of any order; therefore, partitioning of short and long-lived isotopes is not required. K-S family of NDFs can also address the nonlinear set of first-order differential equations. Thus explicit flux variation can be coupled with Bateman equations, and hence neutron flux need not be treated as constant during the time step of integration.

1.1 OBJECTIVE OF THE RESEARCH

To cater to the need, as mentioned earlier in nuclear fuel cycle analysis, it is required to model the generation and depletion of various radio-isotopes considering several

neutron-induced transmutation reactions and spontaneous radioactive decay. The research included studying the isotopic changes over the fuel's life in and out of the reactor. It led to developing a computer code Isotopic Generation and Depletion Code (IGDC) to estimate number density, concentration, activity, decay heat, radiotoxicity, and relative absorption of various actinides fission products accumulated during the reactor operation. The code has been benchmarked in detail with the natural uranium fuel of Pressure Tube Type Heavy Water Reactors (PT-HWRs).

PT-HWR of small and large sizes are being operated successfully worldwide. Countries like China, France, India, Japan, Netherland, and Russian Federation have their nuclear program based on the closed fuel cycle. In addition to these countries, Germany, Switzerland, and the United Kingdom have their nuclear program based on both open and closed nuclear fuel cycle [5]. There are 22 PHWRs in operation in India, and the program is based on a closed fuel cycle. The discharged fuel from PT-HWRs is being reprocessed for deployment in the next fuel cycle. Therefore, it is required to perform a complete fuel cycle analysis of the spent fuel. It is necessary to simulate the behavior of isotopes, both actinides and fission products, in-situ, and when the fuel is out of the core. It is also essential to know the exact concentration, decay heat, activity, radiotoxicity, and clearance potential index of all isotopes produced over the fuel cycle to estimate future waste streams/ amounts and their characteristics.

However, the research is not limited to the fuel cycle analysis of pressure tube type heavy water reactor. The solution methodology developed is general and can be used for the analysis of other nuclear reactors also. Development of nuclear transmutation

model and the computer code Isotopic Generation and Depletion Code (IGDC) as an outcome of this research can be used for nuclear fuel cycle analysis of various nuclear reactor types viz. Fast breeder reactor, Boiling water reactor, Pressurized water reactor, Advanced CANDU reactors, Gen-IV reactors, etc. It should be noted that the nuclear constants required for such analysis would have to be derived from the corresponding neutron spectrum. It can be seen that research requires a multi-dimensional approach. The problem of the research has been studied in different stages. These are discussed in detail in the next sections:

1.2 DEVELOPMENT OF ACTINIDE AND FISSION PRODUCT NUCLIDE CHAINS

Generation and depletion equations or Burn-up equations or Bateman equations of several isotopes under consideration are the primary input for the research problem. This will require a detailed study to identify the nuclear transmutation chains of an individual isotope of actinides and fission products for any type of fuel. These decay chains are given in annexure-1 and 2 for fission products and actinides, respectively [6, 7]. These equations are coupled first-order stiff nonlinear ordinary differential equations. For example, a simplified model for U^{235} and Ru^{102} is given as follows:

$$\begin{aligned} \frac{dN^{U235}}{dt} = & -N^{U235}\lambda_5^{U235} - N^{U235}\lambda_6^{U235} - N^{U235}\sigma_c^{U235}\phi - N^{U235}\sigma_{cc}^{U235}\phi \\ & - N^{U235}\sigma_f^{U235}\phi + N^{Pu239}\lambda_6^{Pu239} + N^{U234}\sigma_c^{U234}\phi + N^{U236}\sigma_{cc}^{U236}\phi \end{aligned} \quad (1.1)$$

$$\begin{aligned} \frac{dn^{Ru^{102}}}{dt} = & \gamma^{Ru^{102}}\Sigma_f\phi + \lambda_1^{Tc^{102M}}N^{Tc^{102M}} + \lambda_1^{Tc^{102}}N^{Tc^{102}} + \lambda_2^{Rh^{102m}}N^{Rh^{102m}} + \lambda_2^{Rh^{102}}N^{Rh^{102}} \\ & - N^{Ru^{102}}\sigma_a^{Ru^{102}}\phi + N^{Ru^{101}}\sigma_a^{Ru^{101}}\phi \end{aligned} \quad (1.2)$$

Where N indicates the number density (in cc^{-3}), λ_1 , λ_2 , λ_5 , and λ_6 indicates the decay constant for β^- decay, β^+ decay, spontaneous fission, and alpha decay respectively (s^{-1}), σ_c represents the capture cross-section (cm^2), σ_{cc} represents the cross-section for (n,2n) reaction (cm^2), σ_a represents the absorption cross-section (cm^2), and ϕ is the neutron flux (neutrons/ cm^2/s). The analysis requires a complete formulation of all the different actinide and fission product chains. As part of this work, 112 actinides and 619 fission products for the fuel of a PT-HWR have been individually formulated and solved numerically.

1.3 GENERATION OF NUCLEAR REACTION DATABASE FOR PHWR APPLICATIONS

The solution of burn-up equations modeled as mentioned above will require PT-HWR fuel spectrum weighted averaged one-group self-shielded nuclear reaction cross-sections. This database can be created using ENDF.B-VII.0 [8] / TENDL [9] files as raw data files, PREPRO code system [10] as the nuclear data processing code, and Bondarenko self-shielding factors for generating self-shielded cross-sections for essential nuclei.

1.4 STUDY AND USE OF FISSION YIELD DATA

Nuclear fission splits a heavy nucleus such as uranium into two or more lighter nuclei depending upon the fission process called fission products, 2 to 3 neutrons and delivers about 200 MeV energy. Yield refers to the fraction of a fission product produced per fission [11]. JANIS (**J**ava-based **N**uclear **I**nformation **S**oftware) [12] is utilized for parent independent fission yield of the fission product considered for the calculation

from ENDF files. A fission yield database has been prepared for different actinides and different neutron energies. Linear interpolation of the fission yield is utilized for the estimation of isotopic generation and depletion after normalization.

1.5 STUDY OF THE DECAY PROCESS OF NUCLIDES AND THEIR DECAY-DATA

Decay data, which consists of β -decay, electron capture decay, isomeric transition, spontaneous fission, α -decay, and branching ratios, will also be required. Decay data library for various nuclei will be prepared through NUBASE [13], nuclear wallet cards [14], and ENSDF (evaluated nuclear structure data format) [15] files with the help of the computer code JANIS (Java-based nuclear information system). JANIS is developed by the OECD Nuclear Energy Agency to facilitate the visualization and manipulation of nuclear data. Mainly a graphical interface giving access to:

- Bibliographical nuclear reaction data (CINDA)
- Experimental nuclear reaction data (EXFOR)
- Evaluated nuclear reaction and decay data (e.g., JEFF, ENDF/B)
- Basic properties of nuclei (NUBASE)

Supports several nuclear data formats as input:

- ENDF and derived formats (PENDF, GENDF)
- Processed covariance formats (BOXER, COVERX)
- EXFOR, CINDA exchange formats

It has the capabilities for exploring and displaying content of nuclear data libraries and databases, visualization and comparison of data, simple arithmetic operations

(normalization, ratio, product, linear combination), and more complex processing (weighted average of evaluated data). Plots and numerical values can be exported in several formats viz. PNG for images, WMF/EMF, PS, PDF for vectorial images, CSV, copy & paste to Excel for numerical values. JANIS browser and renderer windows are shown in Figures 1.1 and 1.2, respectively.

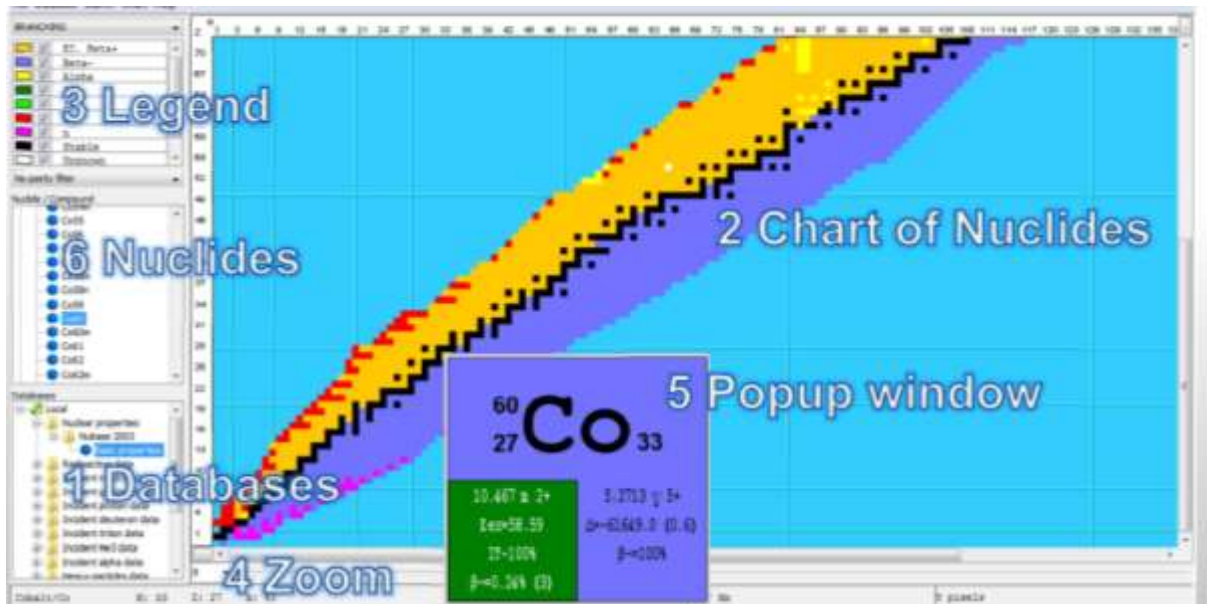


Figure 1.1: JANIS browser window

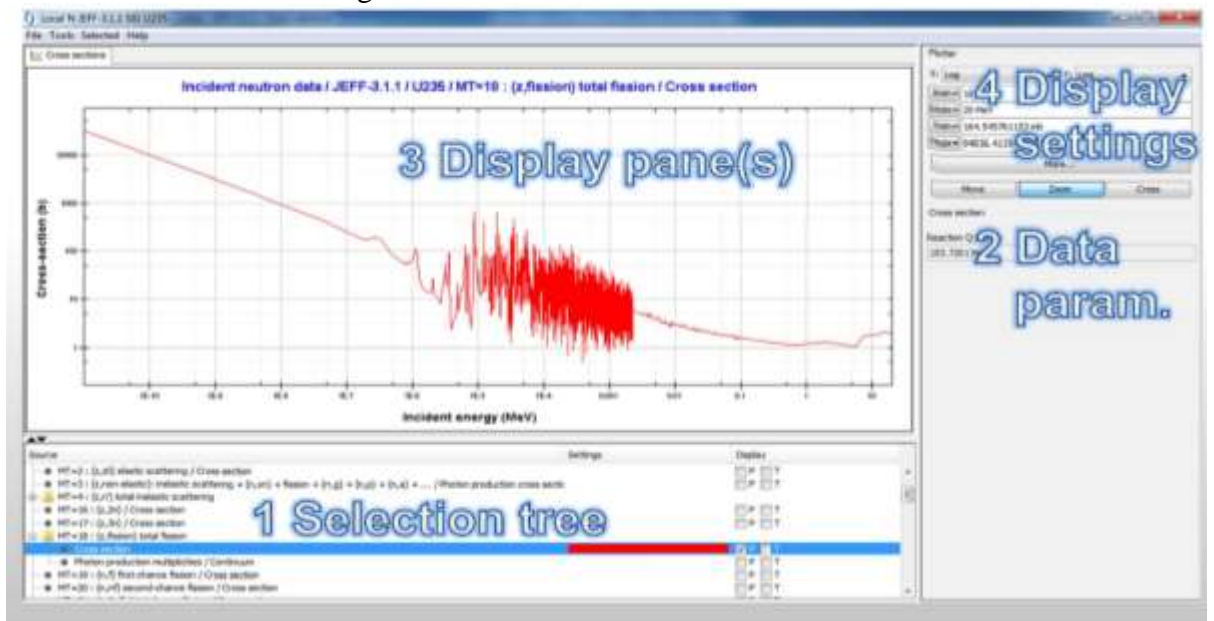


Figure 1.2: JANIS rendering window

1.6 ESTIMATION OF AVERAGE NEUTRON FLUX

The neutron flux, which depends on the core composition, reactor power level, and recoverable energy per fission, is essential for the burn-up calculations. It varies with time and is defined in equation (1.3).

$$Flux (\phi) = \frac{Power (P)}{\sum N_i \sigma_i E_i V} \quad (1.3)$$

Where,

N_i is the number of i^{th} nuclei per unit volume

σ_i is the fission cross section of i^{th} nuclei

E_i is the recoverable energy per fission of i^{th} nuclei and is defined as

$$E_i \left(\frac{MeV}{fission} \right) = 1.29927e - 3 (Z^2 A^5) + 33.12$$

V is the core volume

Differentiating equation (1.3) w.r.t. time,

$$\frac{dP}{dt} = \phi V \frac{d}{dt} \sum (N_i \sigma_i E_i) + \sum V N_i \sigma_i E_i \frac{d}{dt} (\phi) \quad (1.4)$$

Reactor power is assumed to be constant; therefore, equation (1.4) is written as

$$\frac{d}{dt} (\phi) = - \frac{\phi}{\sum N_i \sigma_i E_i} \frac{d}{dt} \left(\sum N_i \sigma_i E_i \right) \quad (1.5)$$

As defined in equation (1.5), the explicit variation of neutron flux will be considered while solving the Bateman equations to account for core composition changes with time.

1.7 ISOTOPIC DECAY ENERGY AND DOSE CONVERSION FACTORS

Estimation of decay heat and radio-toxicity are also part of fuel cycle analysis. In this connection, the energy of isotopic decay and dose conversion factors is required. Library of the former can be prepared using JENDL (Japanese Evaluated Nuclear Data File) [16], whereas the library for dose conversion factors (DCF) of different radio-nuclides for both inhalation and ingestion for the public as well as radiation worker has been prepared using ICRP-102 publication [17].

1.8 SUMMARY

In summary, the generation and depletion of actinides and fission products over the reactor's irradiation and out of the reactor core is selected as a research problem. The governing equation's complexity is evident from the different branching reaction mechanisms and their behavior over time. The stiffness of the problem has been well elaborated. The resulting stiff equation has been solved numerically for the first time using the algorithm based on the Klopfenstein-Shampine family of Numerical Differentiation Formulae (K-S family of NDF). The research work focused on developing code IGDC based on this numerical technique and tested extensively for different fuel cycle aspects. The next chapter focuses on the literature survey before describing the exhaustive work done on the research topic.

2.0 INTRODUCTION

Before starting the work on any problem, it is essential to understand the background, available resources, and problem-solving methodologies available to date with their pros and cons. This objective is achieved by a thorough and broad literature survey on the problem at hand. The present nuclear fuel cycle analysis problem requires a comprehensive literature survey on radio-isotopic transmutation chains, nuclear data, solving methodologies for transmutation equations, and available benchmarks for isotopic inventories, decay heat, radio-activity, and radiotoxicity.

2.1 STUDY OF THE TRANSMUTATION CHAINS

Ab initio start at the problem requires the decay chains, which can be used to develop the generation and depletion model. The papers by R.C. Bolles and N.E. Ballou entitled, “calculated activities and abundances of ^{235}U fission products” [18] was the first paper that gives these details. The computed disintegration rates and numbers of atoms (abundances) of each fission product radio-nuclide at various times after simultaneous slow neutron fission of 10,000 atoms of U^{235} are presented. The decay chains of fission products were introduced in the paper by R. Crocker entitled “Fission product decay chains: Schematics with branching fractions, half-lives and literature references”. The article entitled, “Nuclear Data Requirements for Decay Heat Calculations” originated by the lectures given at the workshop on Nuclear Reaction Data and Nuclear Reactors

by A. Nicholas, contains the fission product decay chains with branching details and is detailed in the Annexure-1 and transmutation chains of actinides are detailed in the Annexure-2. Generation and depletion equations can be generated based on the chains provided in the last paper.

2.2 SURVEY OF NUCLEAR DATA REQUIRED FOR FUEL CYCLE

ANALYSIS

Nuclear data viz. nuclear decay data (Decay constants and decay energies), branching ratios, nuclear reaction data, and fission product yields are required after the generation of nuclear transmutation equations. Fission product yield and reaction cross-section data are spectrum dependent, whereas others are spectrum independent. The fission product yields can be measured in the lab; the measurement of decay constants and decay energies are complicated because of different ways of disintegration and varying half-lives of the decay process.

It is seen that primary nuclear data are produced by experimental results and calculated values by different theoretical models [19]. These data are then compiled and evaluated through a critical process by evaluators for each nucleus. Finally, these primary nuclear data are made available in evaluated nuclear data files (viz. ENDF, JENDL, CENDL, TENDL, etc.).

The evaluated data requires further processing, verification, and validation before being utilized for the application. The nuclear data processing codes available are mainly ENDF utility codes [20], ENDF pre-processing codes (PREPRO), and nuclear data processing code NJOY [21].

Depending upon availability, ENDF files are used for primary nuclear data. For nuclides not available in the ENDF, TENDL files may be used. It is also seen that the PREPRO system of codes can be utilized for processing the ENDF nuclear data files for the current research.

2.3 LITERATURE SURVEY OF SOLUTION RECIPES

Bateman proposed an analytic solution for the chain of nuclides resulting from a single radioactive isotope. The modern version of the Bateman equation used in nuclear fuel cycle analysis has been solved in a number of ways by various authors, and these methods are successfully implemented in their codes. Bateman equations are depletion and generation equations of different nuclei via transmutation and natural decay.

These equations are set of first-order coupled differential equations describing the radioactive decay and transmutation of nuclides (by fission or nuclear reactions) in a nuclear reactor during and after irradiation and can be written as:

$$\frac{dN_i}{dt} = \sum_j \gamma_{j,i} \sigma_{f,j} N_j \phi + \sigma_{c,i-1} N_{i-1} \phi + \sum_k \lambda_{k,i} N_k - \lambda_i N_i - \sigma_{f,i} N_i \phi - \sigma_{c,i} N_i \phi \quad (2.1)$$

Where,

- ϕ = Neutron flux
- $\gamma_{j,i}$ = Fission yield of i^{th} nuclei by fission of j^{th} nuclei
- $\sigma_{f,i}, \sigma_{f,j}$ = Fission cross-section of i^{th} and j^{th} nuclei respectively
- $\lambda_{k,i}$ = Decay constant of k^{th} nuclei which transmutes to i^{th} nuclei
- λ_i = Decay constant of i^{th} nuclei
- i, N_j, k, N_{i-1} = Number density of $i^{\text{th}}, j^{\text{th}}, k^{\text{th}}$, and $(i-1)^{\text{th}}$ nuclei, respectively
- $\sigma_{c,i}, \sigma_{c,i-1}$ = Capture cross-section of $(i)^{\text{th}}$ and $(i-1)^{\text{th}}$ nuclei

Equation (2.1) shows the rate of change of i^{th} nuclei is given by the algebraic sum of:

- i) Formation of i^{th} nuclei by the fission of all other nuclei.
- ii) Formation of i^{th} nuclei by the capture of $(i-1)^{\text{th}}$ nuclei.
- iii) Formation of i^{th} nuclei by the decay of other nuclei.
- iv) Depletion of i^{th} nuclei by its decay.
- v) Depletion of i^{th} nuclei by its fission.
- vi) Depletion of i^{th} nuclei by capture

Each of the coefficients in this equation will have to be carefully derived for the particular reactor spectrum and a specific application type. The different solution methods available in the literature are presented in the following section.

2.3.1 MATRIX EXPONENTIAL METHOD

Considering the set of equations (2.1) to be linear, one can rewrite equation (2.1) as follows:

$$y'(t) = Ay(t) \tag{2.2}$$

Initial conditions are given as:

$$y(0) = y_0 \tag{2.3}$$

Where,

A is the $M \times M$ square matrix formed by the coefficients of Bateman Equations.

(M is the number of isotopes considered for the estimation).

$y(0)$ is the initial values of number densities of each of the nuclei (N_0)

$y(t)$ are the number densities of each of the nuclei at time t $N(t)$

$y(t)'$ Denotes the rate of change of number densities with time $\left(\frac{dN}{dt}\right)$

The solution of the system of equations is of the form:

$$y = y_0 \exp([A]t) = y_0(1 + [A]t + [A] \frac{t^2}{2!} + \dots) \quad (2.4)$$

This series will converge if the matrix's norm, say, the largest eigenvalue is less than unity. Then the number of terms in the series is determined by the specified degree of accuracy. In ORIGEN-2, “the calculation of the terms in the series is facilitated by using a recursion relationship”. The matrix exponential method has some inherent difficulties because half-lives vary from milliseconds to billions of years. This results in very widely spaced eigenvalues. So one cannot apply the series’ method blindly. A three-step procedure is followed in the most commonly used nuclear fuel cycle analysis code ORIGEN:

- Short-lived fission products with short-lived parents having a half-life less than 14 % of the time step. These will saturate within a time step. So their asymptotic value is considered sufficient.
- Reduced transition matrix for long-lived nuclides, which is solved by the above matrix series method.
- A Gauss-Seidel method to solve for asymptotic solutions of short-lived nuclides whose parents are long-lived.

This method works with the linear form of the Bateman equation considering the neutron flux to be constant for the time step of integration and requires partitioning short and long-lived radioisotopes.

2.3.2 EIGEN VALUE METHOD

The differential equation defined by Eq. (2.2) is solved exactly by calculating the distinct eigenvalues and eigenvectors of the matrix A and the solution will be of the form:

$$y = c_1 \exp(\lambda_1 t) y_1 + c_2 \exp(\lambda_2 t) y_2 + \dots \quad (2.5)$$

Where, c_1, c_2 , etc. are constants to be determined using initial conditions and λ_1, λ_2 , etc. are the eigenvalues of the matrix.

This method has been used in DECROI (Inventory formation and decay code) [22]. Suitable sub-routines for this procedure come from the LAPACK library of linear algebra, which is sufficiently stable numerically to treat the broad span of half-lives and irradiating flux. This method is more applicable when no fission production terms are present [23] and works with the simple transition matrix considering the linear form's Bateman equation.

2.3.3 ANALYTICAL METHODS

The first analytical solution was given by Bateman for a chain of n members with the particular assumption that at $t = 0$, the parent nucleus alone is present (as in natural decay series of Uranium). The general solution was obtained by performing a Laplace transform and its subsequent inverse transform. Bateman's approach cannot also be extended to branching systems. However, the procedure by Pressyanov [24] claims to be extended to branching systems. This analytical method may not be suitable for generation and depletion inside the nuclear reactor because it is a radioactivity problem and the nuclear interaction in a particle (neutron in this case) flux.

A paper by Cetnar [25] on the general solution of Bateman equations for nuclear transmutation is quite instructive. This reference provides the procedure for branching decay, nuclear interaction in particle flux, and nuclides (FPs) production from fission. This method is incorporated in MCB code, which is a Monte Carlo burn-up code.

2.3.4 NUMERICAL METHODS

We have already explained the method followed in ORIGEN. The algebraic techniques also use numerical computational packages to evaluate the eigenvalues and eigenvectors of the transition matrix. The analytical method generally encounters round-off errors in the evaluations of the “pi” functions and requires certain fix-ups to avoid infinities, like slightly altering the decay constants, etc.

A number of codes have been written using different numerical schemes, notably the modified Euler scheme used in FISPIN and FISPACT and implicit methods for stiff differential equations in RICE [26]. Sometimes they use the numerical method during the burn-up / irradiation phase and the analytical method during the decay phase. For burn-up periods the nonlinear physical system is approximated by a linear physical system with cross-sections. Flux levels are held constant in any given time step and changed discontinuously between time steps, the length of the time step being chosen to make the approximations as useful as required.

Some of these codes are the local adaptation of ORIGEN code (like KORIGEN [27], ORIGEN-JR [28], and ACAB [29], etc.). ORIGEN is now part of a modular code system in the ORNL safety analysis code system SCALE (Standardized Computer Analyses for Licensing Evaluation).

A method used for a highly stiff general nonlinear form of transmutation equations is based on Backward Differentiation Formulae (BDF) by Gear or Numerical Differentiation Formulae (NDF) by Klopfenstein and Shampine.

2.4 A SUMMARY OF BURN-UP CODES CURRENTLY USED

Several burn-up codes are available worldwide, used for nuclear fuel cycle analysis of different reactors [30]. These codes can be categorized into different categories:

2.4.1 NUCLEAR INVENTORY CODES

These are widely used computer codes for calculating the radio-nuclide inventories, radioactivity, and radiotoxicity. A few essential codes in this category are:

2.4.1.1 ORIGEN-S

The **ORIGEN-S** code (ORIGEN stands for **O**ak **R**idge National Lab **G**ENERated) [31] uses several different kinds of data libraries containing nuclear decay data, neutron reaction cross-sections, and delayed photon yield and neutron emission data. The nuclear data libraries contain nuclear decay data and cross-sections for about 698 activation products and structural materials, 129 actinides, and 1119 fission products. ORIGEN-S is used to perform fuel cycle analysis using the matrix method explained earlier.

The nuclear cross-section library contains multi-group cross-sections in three energy groups that are collapsed from continuous energy cross-sections using a weighting spectrum for light water reactor (LWR) fuel. The cross-section evaluations are obtained from ENDF/B-VI, FENDL-2.0, and EAF-99. Explicit ENDF/B-VI fission-product yields are available for 30 fissionable actinides. Photon yield data libraries are public

for 1132 isotopes that include activation products, actinides, and fission product nuclides. The photon libraries contain discrete photon line energy and intensity data and continuum photon data, for decay gamma and X-rays, prompt and equilibrium fission-product gamma rays from spontaneous fission, gamma rays associated with (α ,n) reactions in oxide fuel, and bremsstrahlung from decay beta (negatron and positron) particles slowing down in either UO₂ fuel or water matrix. Neutron production data libraries are also provided to calculate the neutron yields and energy spectra for spontaneous fission, (α , n) reactions in any matrix, and delayed neutron emission.

2.4.1.2 ORIGEN-ARP

The **ORIGEN-ARP** (Automatic Rapid Processing) version of the **ORIGEN-S** code is available as a SCALE module [32]. ORIGEN-ARP is the currently supported version of ORIGEN and is included in the SCALE software package. It contains the latest version of the ORIGEN-ARP Windows user interface, and PlotOPUS is the interactive plotting program of ORIGEN results. ORIGEN-ARP is a sequence in SCALE that serves as a fast and easy-to-use system to perform nuclear irradiation and decay calculations with the ORIGEN code using problem-dependent cross-sections. ORIGEN-ARP uses an algorithm that allows the generation of cross-section libraries for the ORIGEN code by interpolation over pre-generated cross-section libraries. The interpolations are carried out on the different variables viz. burn-up, enrichment, and moderator density. The ORIGEN-ARP GUI provides easy-to-use windows interface with menus, toolbars, and forms that allow the user to set up, run, and view the results

of ORIGEN-ARP calculations in a user-friendly integrated environment. PlotOPUS [33] is a Windows GUI designed to plot ORIGEN results post-processed with the OPUS utility. Input for OPUS and viewing plots with PlotOPUS are handled automatically by the integrated ORIGEN-ARP GUI. The ORIGEN-ARP libraries in SCALE include a large number of fuel assembly designs. All light water reactor (LWR) libraries and VVER libraries are based on TRITON / NEWT 2-D depletion models. All BWR libraries contain moderator density-dependent cross-sections. The available libraries include:

- Boiling Water Reactor (BWR):
 1. GE 7x7, 8x8, 9x9, 10x10
 2. ABB 8x8
 3. ATRIUM-9 and ATRIUM-10
 4. SVEA-64 and SVEA-100
- Pressurized Water Reactor (PWR):
 1. Siemens 14x14
 2. Westinghouse CE 14x14 and 16x16
 3. Westinghouse 14x14, 15x15, 17x17, 17x17 OFA
- CANDU reactor fuel (28- and 37-element bundle designs)
- MAGNOX graphite reactor fuel
- Advanced Gas Cooled (AGR) fuel
- VVER-440 enrichment (1.6% - 3.6%) and profiled enrichment (3.82%, 4.25%, 4.38%)
- VVER-1000
- MOX BWR 8x8-2, 9x9-1, 9x9-9, 10x10-9
- MOX PWR 14x14, 15x15, 16x16, 17x17, 18x18

Significant features of the ORIGEN-ARP nuclear data in SCALE is described below.

1. The essential neutron reaction cross-sections are based on ENDF/B-VI evaluations, the European Activation File (EAF-99), and FENDL-2 data. There are 854 nuclides with evaluated cross-section data in SCALE.
2. Fission product yields are from ENDF/B-VI, Release 2 (ENDF/B-VI.2), with data for 1119 fission products.
3. Explicit fission product yields for 30 actinides.
4. Photon emission line-energy data from ENDF/B-VI, ENSDF, and JEF-2.2 evaluated data for 2101 nuclides.

2.4.1.3 FISPIN

FISPIN[34] is an acronym for the **F**ission **P**roduct **I**nventory code. This code was developed in UKAEA. The code models the time-dependent behavior of three groups of nuclides: the fission product group, the actinide group, and the structural material group. For each nuclide, an equation describing the time rate of change of the nuclide number density is solved. The equation includes production and removal due to radioactive decay, production, and removal due to neutron reactions, and in the case of fission products, production due to neutron-induced fission. The neutron reactions may be calculated in any number of energy groups, but the model assumes that the neutron flux spectrum and flux (or power) level is known. A modified Euler method (for stiff ODEs) [35] is used. The procedure employed is to split the total time interval into two steps, perform the calculation, test for convergence of all nuclides and, if the accuracy is not sufficient, repeat the operations with double the number of time steps. The process is repeated until enough accuracy is achieved.

2.4.1.4 FISPACT

FISPACT (**F**ission **P**roduct **A**ctivation) [36] is an inventory code that has been developed for neutron, deuteron, and proton-induced activation calculations for materials in fusion devices. It is a robust code that can answer the fundamental questions about the numbers of atoms and the activity in the material following neutron or charged particle irradiation. Other options include calculating sensitivity coefficients (i.e., how the amount of a particular nuclide depends on cross-sections or half-life data) and the identification of pathways (i.e., series of reactions and decays) from the parent to a specific daughter. It can treat trace amounts of actinides that can fission and include sequential charged particle reactions (only neutron irradiation).

FISPACT was developed from the FISPIN inventory code designed for fission reactor calculations and dealt in greater detail with inventories arising from the irradiated fuel in a reactor. FISPACT is complementary to FISPIN and has been designed for activation calculations; however, it can be used with any type of particle (neutron) spectrum and is not restricted to only fusion applications.

FISPACT uses external libraries of reaction cross-sections and decay data for all relevant nuclides to calculate an inventory of nuclides produced as a result of the irradiation of a starting material with a flux of neutrons. The actual output quantities include the amount (number of atoms/cm³ or gm/kg), the activity (Bq), α , β , γ -energies (kW), γ dose-rate (Sv h⁻¹), the potential ingestion and inhalation doses (Sv), the legal transport limit, and the clearance index. Clearance potential index is defined as the ratio between specific radioactivity and clearance level, the state in which the radioactivity material became un-dangerous. So, the clearance potential index is a non-dimensional

quantity, which, if greater than unity, shows the measure of radiotoxicity for the radioactive material. When it is equal to unity or less, the radioactive material is clean, i.e., it can be handled without restrictions. The code's output consists of the concentration of different isotopes, heat outputs for the elements, and the γ -ray spectrum for the material. It also contains various summed quantities, such as total activity and total dose-rate.

The neutron spectrum must be available either in one of the standard energy structures used by FISPACT or in an arbitrary energy structure. The user must supply details of the energy boundaries. The standard energy structures are the WIMS-69 group (**Winfrith Improved Multi-group Scheme**), GAM-II 100 groups (General Atomic Multi-group-II), XMAS (172 groups), VITAMIN-J (175 groups), VITAMIN-J+ (211 groups), TRIPOLI (315 groups) and TRIPOLI+ (351 groups). Cross-section data in these seven energy structures are available for the EAF (European Activation File) [37] neutron-induced cross-section library and in the VITAMIN-J+ structure for the deuteron and proton-induced reaction library. One of the seven group format libraries is used to form the 1-group 'effective' cross-sections that FISPACT requires by 'collapsing' the library with the neutron spectrum. The FISPACT code is user friendly and runs by the input of a series of keywords. FISPACT is now used by many research groups throughout Europe and adopted by the ITER project as the reference activation code. It is a part of the European Activation System (EASY).

2.4.1.5 ACAB

The ACAB (Activation ABacus) [38] code is a computer program for performing the activation and transmutation calculations for different nuclear systems such as fusion, ADS (Accelerator Driven Systems), and fission reactors. Various calculations performed by the code ACAB are:

- i) Space dependent isotopic inventory calculations for “multidimensional” neutron flux distributions.
- ii) All the neutron reactions that may occur are treated in the code
- iii) Dealing with charged particle reactions
- iv) Treat actinides and fission products
- v) Generation of radionuclide activities, decay heat, neutron emission, radio-toxicity, decay gamma spectra, contact dose rates, doses to the exposed individual, as well as collective doses and its consequences, etc.

The mathematical structure is based on that of the ORIGEN code.

2.4.1.6 RICE

RICE (**R**eactor **I**nventory **C**od**E**) [39] is another inventory code developed in UKAEA. It is used to calculate the actinide and fission product inventories of irradiated nuclear fuel. The range of actinide and fission product isotopes considered is large enough to permit studies to be made of the effect of decades-long irradiations and geological cooling times. The output consists of inventories, activities, biological hazards, decay heating, gamma spectra, and macroscopic cross-sections. The code can be used to

perform a coupled actinide-fission product calculation, a sole actinide calculation, or an exclusive fission product calculation. The stiff set of differential equations for the actinide case is solved using the implicit trapezoidal rule and Aitken's formula for accelerated convergence of a series. For the fission product case, the implicit Euler rule is used; the algorithm is specially designed to solve sets of linear first-order differential equations. For cooling periods, analytical solutions are used.

2.4.1.7 FISP

FISP (**F**ission **P**roduct **I**nventory code) code series was developed by Clarke and Tobias [40, 41] specifically for FPs. FISP6 calculates fission product inventory and energy release rates in irradiated fuel using a point model for irradiation and cooling conditions specified by the user. FISP6 is a nuclide inventory summation code similar to the RICE computer code. The main difference between the two codes is that RICE treats both actinides and fission products, whereas FISP6 treats only fission products but considers approximately twice the number that RICE does. These additional fission products mostly have half-lives less than 2 minutes. Besides, FISP6 can calculate the beta and gamma spectra emitted by fission products in some detail. The code was designed mainly for decay heat studies. The code uses an analytical solution with linearized build-up and decay chains of the fission products. The FISP5 version has been validated against many experimental decay heat results, as given in [42].

2.4.1.8 ISOGEN

ISOGEN (Interactive isotope generation and depletion code) [43] is an interactive inventory code for solving first order coupled linear differential equations with constant

coefficients for a large number of isotopes, which are produced or depleted by the processes of radioactive decay or through neutron transmutation or fission. The mathematical structure of ISOGEN is similar to that of ORIGEN. ISOGEN code is written in a modern computer language, VB.NET version 2013 for Windows operating system version 7, which enables one to provide many interactive features between the user and the program.

2.4.2 BURN-UP MODULES IN LATTICE CODES

There are several lattice codes, which in addition to the lattice property modules, also consist of burn-up modules to estimate radionuclides' inventory. The flux and spectrum averaged nuclide cross sections is generated at every step from a detailed spatial simulation of the lattice. It is to be noted that the burnup simulation in lattice codes are extensively used for in-core assessment of the nuclide inventories for operating flux levels and is limited to the nuclides available in the multi-group library. A few essential codes of this category are described briefly below:

2.4.2.1 SERPENT

SERPENT [44] is a continuous energy Monte Carlo reactor physics code primarily developed for lattice physics calculations. However, afterward, its capabilities were extended to fuel cycle studies also. Two techniques are used for solving the Bateman equations in SERPENT. The first method is the Transmutation Trajectory Analysis method (TTA), based on the analytical solution of linearized depletion chains and the

second method is Chebyshev Rational Approximation Method (CRAM), an advanced matrix exponential solution developed at VTT.

2.4.2.2 CASMO

CASMO [45] is a two-dimensional depletion transport theory code designed for fuel rods inside a fuel assembly. This program aims to place the fuel assembly in an infinite lattice to simulate the neutron transport inside and around the assembly. CASMO computes multi-dimensional neutron flux distributions by solving the neutron transport eigenvalue problem. The solutions are used to calculate different types of reactor physics' parameters such as neutron flux, cross-sections, neutron age, buckling, isotope concentrations, etc. CASMO contains a library of the microscopic cross-section for a large number of nuclides.

CASMO is coupled with another code SIMULATE. SIMULATE is a three-dimensional calculation program used for both the PWR and BWR cores. In the calculation, the neutron flux is divided into high energy flux (fast) and thermal flux, and the core is divided into a specific set of nodes. For example, a fuel assembly is divided into 24 axial and four radial nodes, i.e., 96 nodes per fuel assembly. Simply, this means that SIMULATE solves a three-dimensional diffusion equation for the neutron flux at each node and connect the solutions between the different nodes with boundary conditions to describe the entire fuel core. Necessary input to SIMULATE is cross-sectional data describing the fuel design calculated by CASMO and is accessed through a linking program, CMSLINK. As further input to SIMULATE,

core operating information and the included fuel assemblies' specification with their burnout histories can be mentioned.

The output of SIMULATE is given as input of CASMO. The input data is provided to CASMO via a file, which specifies lattice data (the fuel geometry, construction material, fuel enrichment, and density), and boron level, power, fuel temperature, moderator density, and temperature. The output consists of a large amount of data; the most important for this study is the isotope concentrations of the predefined nuclides. CASMO also uses the CRAM algorithm to solve Bateman equations for the given cross-sections and flux.

2.4.2.3 CLUB

CLUB code [46] is the workhorse of lattice analysis of PHWRs. It uses a combination of methods namely interference current formalism and collision probability methods to solve for the fluxes in each annular region of the lattice or fuel cluster. One group condensed cross section in each element of fuel regions is calculated and used in the burnup equations for nuclide inventories which are solved by either trapezoidal rule or Runge Kutta method.

2.4.2.4 WIMS

In the WIMS formalism, a heterogeneous infinite lattice cell calculation followed by a homogeneous leakage calculation is performed [47]. The flux distribution across the cluster is obtained using either discrete ordinates method or collision probability methods for solving the differential or integral form of the transport equation. The burnup calculations are performed with critical flux spectrum, energy averaged cross

sections and operating temperatures. The number densities of actinides and fission products are calculated for the operating conditions at each burnup step by solving the Bateman equations.

2.4.2.5 MONTE CARLO METHODS

In the literature survey done, it is also seen that Monte Carlo methods are used in tandem with the burnup simulations. The methods involves estimating the region wise reaction rate tallies from a detailed Monte Carlo simulation of the lattice or core and using them directly in the Bateman equations for estimating the nuclide densities.

2.4.3 FUEL CYCLE SIMULATION CODES

To model nuclear energy and its correlated needs viz. an exploration of uranium, fuel manufacturing, spent fuel storage, and reprocessing, fuel cycle simulators are developed. A few simulators are described below:

2.4.3.1 ORION

ORION developed by Gregg, R. and C. Grove [48], is a fuel cycle modeling code (written in C++) that has been developed for more than 15 years by the UK National Nuclear Laboratory (NNL) and can be used on a Windows, Linux, or Apple computer. This code is independent of the other tools and provides some unique features such as long-range radioactive decay for over 2000 nuclides. Furthermore, the graphical user interface is relatively easy and intuitive to use. It allows the user to construct a visual representation of the fuel cycle with run times of seconds to a few minutes. ORION can model various nuclear facilities as individual objects. Several of these objects can be

grouped to represent many small-scale facilities that support one reactor. One object can represent a large-scale facility that represents a fleet's behavior. Therefore, the objects in ORION can be used to represent individual facilities or a fleet of facilities. The Reactor Dynamic Control tool in ORION can be used to automate the commissioning and decommissioning of selected reactors based on the electricity demand and decommissioning or commissioning profiles of other reactors. The “change order” feature allows for prioritizing facilities, allowing mass flows through various streams to be prioritized over others. ORION also enables the user to specify individual reactor lifetimes for multiple years in addition to the “year vs. mass demand” and “year vs. energy demand” features that were available in previous versions. The program can track over 2500 nuclides (most of which are short-lived) and can model both decay and in-reactor irradiation. Prior to an ORION analysis, detailed lattice physics calculations are completed using external codes to generate either burnup-dependent cross-section libraries or fuel recipes for each reactor and fuel type. Using burn-up-dependent cross-sections, ORION can model in-reactor radionuclide inventory changes and estimate any feedback effects on new fuel compositions.

ORION can explicitly model driver and blanket fuel streams and the isotopic evolution with burn-up in those streams, separately for multi-region systems. This feature of ORION enables changes in fuel, core, and reactor designs, including breeding ratios and mass demands for each fuel supply component, to be explicitly tracked. ORION has the functionality to scale the blanket region (or others) with a parent reactor to ensure fuel demands scale appropriately.

ORION can simulate the full range of nuclear-related facilities and all reactor types (*e.g.*, LWRs, FRs, MSRs, *etc.*) and fuel types (*e.g.*, U, Pu, Th, MA, *etc.*). It is also capable of modeling detailed individual reactors or entire fleets. The user also has the flexibility to choose material flows, separations, and stream priorities.

2.4.3.2 COSI

Commelini-Sicart (COSI) [49] is a java based nuclear fuel cycle simulator, developed by the CEA, the French Atomic, and Alternative Energies Commission. The user inputs the period to be simulated as well as the deployment and decommissioning dates of each reactor in the simulation. The user also provides stock usage preference, *i.e.*, the order spent fuel for use (recently discharged or piled-up stock). In COSI, the reactor depletion calculations are done using the CESAR code. CESAR is similar to ORIGEN and solves the coupled ordinary differential equations governing nuclide populations due to irradiation and decay over time.

2.4.3.3 NUCLEAR FUEL SIMULATION SYSTEM (VISTA)

The Nuclear Fuel Cycle Simulation System (VISTA) was developed by the IAEA [50]. The code's objective is to calculate the nuclear fuel cycle material and service requirements and material arisings for the different fuel cycle options for a year. VISTA is a simulator used to design nuclear parks with varying types of nuclear reactors and nuclear fuel. VISTA consists of two modules. The first one is the overall nuclear material flow module, which is the main part of the VISTA calculation. The second one is the fuel depletion module CAIN, which calculates the spent fuel composition in

discharge time and after a cooling period. In CAIN, analytical expressions are available for the solution of the equations, which makes the code computationally very efficient.

2.4.4 OTHER IMPORTANT CODES

In addition to the codes described above, few other codes are developed which have burn-up routines to estimate the radionuclide inventories and are described below:

2.4.4.1 DARWIN

Computer code system DARWIN is developed at CEA, France [51]. DARWIN is devoted not only to the nuclear fuel cycle studies, but it can be used in several other dimensions also viz. dismantling, thermonuclear fusion, accelerator-driven system, and in medicine. In the nuclear fuel cycle analysis, the depletion unit of DARWIN is PEPIN2. It solves the generalized Bateman equations which govern the time dependence of isotope concentrations for actinides, fission products, and activation products. Physical quantities estimated by the code are isotope concentration, isotope mass, activity, radiotoxicity, decay heat for any cooling times until final disposal of the nuclear waste. Both analytical and numerical schemes are developed in the PEPIN2 depletion module of DARWIN to solve the generalized coupled differential depletion equations. A fourth-order Runge-Kutta scheme is used for irradiation, and analytical solutions are performed during cooling stages. The depletion module PEPIN2 is automatically linked to various international evaluations (JEF2, ENDF /B6, EAF97..) both for decay data and cross-sections and to some transport codes such as TRIPOLI, APOLL02, and ERANOS. These transport codes provide neutronics data as self-shielded cross-sections and neutron fluxes. DARWIN includes a generator of

radioisotope chain built automatically from decay modes and nuclear reaction types specified in the evaluation libraries. A "searchengine" allows us to determine all formation ways of a considered isotope.

2.4.4.2 APOLLO

APOLLO [52] solves the Boltzman transport equation using multi-group modeling. The APOLLO code generates the two-group macroscopic cross-sections. The code also supports a sophisticated self-shielding model and a predictor/corrector method for isotopic depletion of the fuel.

2.4.4.3 SNF

SNF [53] has capabilities for back-end calculations consistent with and utilizing in-core fuel management (ICFM), multi-dimensional analyses performed with, e.g., the CASMO/SIMULATE system.

SNF generates isotopic concentrations, decay heat, and radiation source terms of fuel assemblies and individual fuel rods for cooling times upto 100,000 years.

2.5 DESCRIPTION OF THE CODE UNDER DEVELOPMENT

Based on the primary literature survey, it was decided to develop a code with the following features:

- a) The code under development is an inventory code.
- b) This code will be independent and will have versatile use, i.e., it can be used for any reactor type, a facility with nuclear fission as a primary process of generation and depletion of radionuclides.

- c) This code can be used for isotopic inventories, radioactivity, decay heat, radiotoxicity, relative neutron absorption by different fission products, and reactivity of the core in various conditions.
- d) The solution algorithm for Bateman equations in this code will be based upon the Klopfenstein-Shampine family of Numerical differentiation formula (K-S family of NDFs). This method treats the Batemen equations in their most general form and can handle stiffness of any order.
- e) The development of this code will solve the accessibility problem and reduce the dependency on foreign codes.

2.6 BENCHMARKS FOR FUEL CYCLE ANALYSIS CODES

Benchmarking and validation is an essential aspect of any newly developed code. Several types of results are available from theoretical benchmarked codes and experiments for concentration and activity [54, 55] & decay heat [56]. For in-core inventories for PT type heavy water reactors, benchmarking of the code can be carried out with results available in IAEA TECDOC-887 [57] for the estimation of the concentration of U235 and Pu239 at 4000 MWd/te and 8000 MWd/te burn-up.

The radioactive decay for the discharged fuel is available as theoretical estimates from other codes. Experimental measurements for actinide and fission product concentrations are also found in open literature but limited. The decay heat measurements on spent fuel performed by Ontario Hydro using Douglas point CANDU reactor irradiated fuel bundles of varying irradiation histories is a useful benchmark for this research work [56]. Experimental verification for the decay heat estimation can be carried out by comparing the decay heat measurements, estimation by ORIGEN-S, and those of the ANSI / ANS-5.1-1979, the American National Standard for decay heat

power. In this reference, in addition to the total decay heat and gamma decay heat for irradiated fuel assemblies was also estimated and compared with those of the ORIGEN-S estimations.

2.7 CONCLUSION

Having studied various papers, it is obvious that the research study is very vast. Internationally many codes exist, and users have developed based on their requirements. It may be noted that these specialized codes are not available openly. Thus in the study, it was decided to comprehend all the concepts, references, and necessary tools needed to develop a model and implement it in computer code on nuclear fuel cycle analysis using a modern computer language. As mentioned earlier, the immediate focus was on fuel cycle analysis of PT-HWRs. The literature survey led to the following:

- The depletion –generation equation can be modeled using efficient ODE solver tools
- MATLAB is one such solver that can be used as a modern language in the Windows environment.
- Nuclear transmutation chains available in the reference “Nuclear Data Requirements for Decay Heat Calculations” by A.L. Nichols can be used for developing the model on isotopic generation and depletion.
- The method of solving the generation and depletion model can be an efficient numerical method that can handle a highly stiff system of non-linear form of Bateman equations. Therefore, one of the best methods available to date to cater

to the need mentioned earlier is the Klopfenstein-Shampine Family of numerical differentiation formulae (K-S family of NDFs) and can be used for nuclear fuel cycle analysis code.

- Nuclear decay data which consists of β -decay, electron capture decay, isomeric transition, spontaneous fission, α -decay, and branching ratios can be obtained for various nuclei through NUBASE, nuclear wallet cards, and ENSDF (evaluated nuclear structure data format) files with the help of the computer code JANIS (Java-based nuclear information system). The decay data for each isotope has been carefully collected, and a database has been made.
- The reaction cross-sections, which are coefficients of the Bateman equation, form a library and are reactor specific. The library for the nuclear reaction data can be developed by processing the point nuclear data through pre-processing code PREPRO using the appropriate weighting spectrum.
- Benchmarking and validation of the newly developed code can be carried out with the results available in the references.

Generation of problem dependent cross sections is one of the major aspects of fuel cycle analysis codes. It has already been emphasised that the spectrum averaging has to be done carefully. The next chapter focuses on generating one group reaction cross-section library for different reactions for PT-HWR. These reaction libraries will be utilized while solving the Bateman equations.

Chapter 3

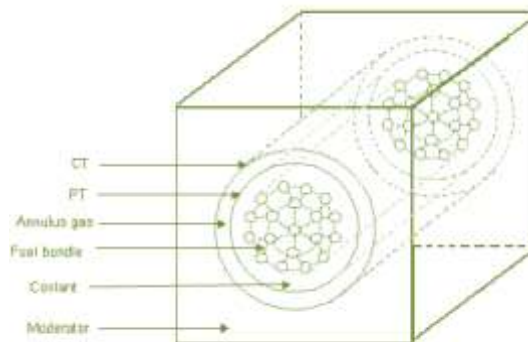
Generation of Cross-section Library

3.0 INTRODUCTION

The necessary coefficients of the burn-up equations viz. decay data, branching ratios, and spectrum dependent interaction cross-sections & fission yield are problems dependent and required to be as accurate as possible. Estimating nuclear data viz. decay data, fission yield data, branching ratios, Dose conversion factors, and energy released during radio-isotope decay are described in chapter-1. This chapter is devoted to the generation of spectrum dependent nuclear interaction data.

3.1 WEIGHTING SPECTRUM

Reaction cross-sections are averaged over a fuel spectrum to obtain reactor specific cross-section. The PT-HWR lattice cell is shown in Figure 3.1, consisting of fuel, Zr-4 cladding, heavy water coolant, Calandria tube, and heavy water moderator. The properties of the lattice cell are given in Table 3.1.



CT: Calandria Tube; PT: Pressure Tube

Figure 3.1: Unit cell of PT-HWR fuelled with natural uranium

Table 3.1: Unit cell parameters of PT-HWR fuelled with NU [58]

Parameter	Description
Fuel material	Nat. UO ₂
U ²³⁴	0.0054 %
U ²³⁵	0.711 %
U ²³⁸	99.2836 %
N ^{U234} number density	1.36669E+17 atoms/gm
N ^{U235} number density	1.79947E+19 atoms/gm
N ^{U238} number density	2.51277E+21 atoms/gm
Moderator material	D2O
Coolant material	D2O
Average Coolant temperature	271.0 °C
Average Moderator temperature	53.6 °C
Pitch of the unit cell	22.86 Cm
Cell array	Square
Fuel mass in the bundle	13.4 kg (U)
Total number of elements in the fuel bundle	19
Mass of UO ₂ in a fuel bundle	15.2 kg
Density of UO ₂	10.6 g/cm ³

The lattice cell has been simulated in the WIMS-D code system to obtain the spectrum in the fuel regions and the average neutron spectrum. This neutron spectrum has been used as the weighting spectrum for further calculations. The weighting neutron spectrum in the fuel is shown in Figure 3.2. This spectrum is obtained for average in-core burn-up, which is about 3500MWd/te. This spectrum consists of three regions; in the thermal region, the spectrum is similar to the Maxwell-Boltzmann distribution, slowing down the spectrum in the resonance region, and Watt's fission spectrum in the fast energy region.

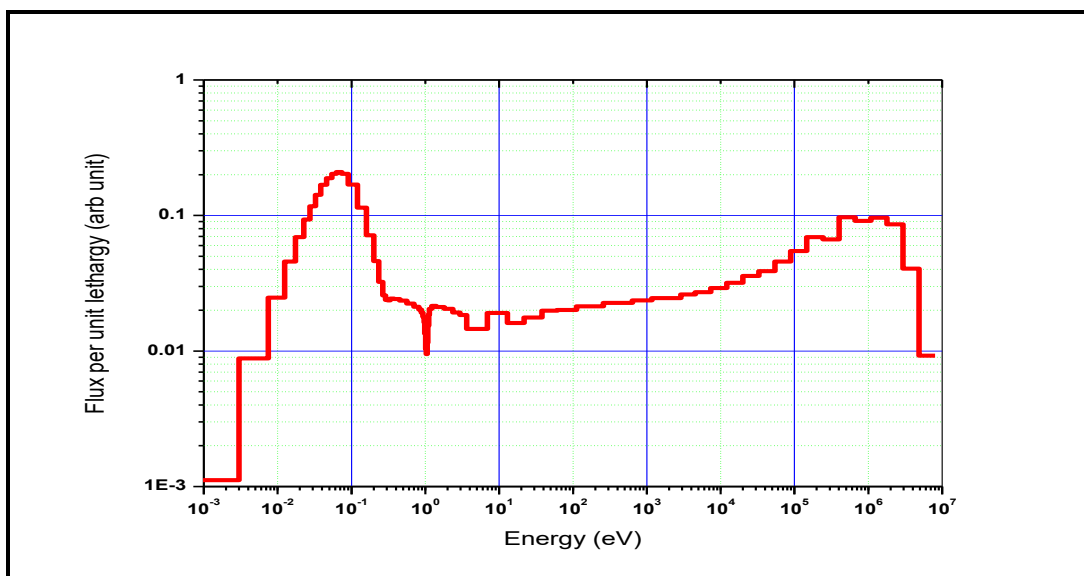


Figure 3.2: Neutron spectrum in small size PT-HWR fuelled with NU

3.2 GENERATION OF SPECTRUM DEPENDENT ONE GROUP CROSS-SECTION

One group spectrum dependent neutron cross-sections are essential elements for burn-up calculations. The primary data for the generation of cross-section libraries are evaluated nuclear data format (ENDF) files and available for each isotope in separate files. The cross-section data available in ENDF files are point energy cross-section data. For the point reactor codes, direct use of these data into the nuclear reactor applications viz. calculation for generation and depletion of radio-isotopes in a nuclear reactor is not possible because these cross-section data are available at different energies and one requires one group cross-sections properly weighted with the reactor neutron spectrum for these simulations or calculations.

3.3 EVALUATED NUCLEAR DATA FORMAT (ENDF) FILES

Nuclear reaction cross-section data and isotope masses are stored in a format called ENDF, or Evaluated Nuclear Data Files. Nuclear data from ENDF-format libraries can be extracted easily for particular nuclear reaction cross-sections, the distributions in energy and angle of reaction products, the various nuclei produced during nuclear reactions, the decay modes resulting from the decay of radioactive nuclei, and the estimated errors in these quantities [59, 60 and 61].

An ENDF-format nuclear data library has a hierarchical structure by tape, material, file, and section. (When the first libraries were compiled, the data was stored on punch cards and magnetic tape, hence the term tape and the 80-column data width of ENDF records). Each of these levels has a characteristic numerical identifier [62]. An ENDF 'tape' is a file that contains one or more ENDF materials.

MAT labels an ENDF material. It is computed from the target Z and A. It equals 100 Z plus an isotope indicator, starting at 25 for the lightest of the common isotopes. The MAT number steps by threes to allow for isomers. Thus, 125 is H1, 128 is H2, 2625 is Fe54, 6153 is Pm148m, and 9228 is U235. MF labels an ENDF file. Files are usually used to store different types of data:

MF=1 contains descriptive and miscellaneous data
MF=2 contains resonance parameter data
MF=3 contains reaction cross-sections vs. energy
MF=4 contains angular distributions
MF=5 contains energy distributions
MF=6 contains energy-angle distributions
MF=7 contains thermal scattering data
MF=8 contains radioactivity data
MF=9-10 contains nuclide production data
MF=12-15 contains photon production data, and
MF=30-36 contains covariance data

MT labels an ENDF section, which is used to hold different reactions. E.g.

MT=1 is the total cross-section

MT=2 is the elastic scattering

MT=16 is the (n, 2n) reaction

MT=18 is fission and

MT=102 is radiative capture.

3.3.1 READING AN ENDF TAPE

An ENDF tape contains one or more materials in increasing order by MAT. Each material contains several files in increasing order by MF. Each file contains several sections in increasing order by MT. An ENDF ‘tape’ is built up from a small number of basic structures called ‘records’, such as TPID, TEND, CONT, TAB1, and so on. These ‘records’ usually consist of one or more 80-character FORTRAN records. It is also possible to use binary mode, where each of the basic structures is implemented as a FORTRAN logical record. The design of an ENDF Tape (file) is as follows:

The tape contains a single record at the beginning that identifies the tape. The major subdivision between these records is by material (identified by the MAT number). The data for the material is divided into files, and each file (determined by the MF number) contains the data for a particular class of information. A file is subdivided into sections, containing data for a specific reaction type (identified by the MT number). Finally, a section is divided into records. Every record on a tape contains three identification numbers: MAT, MF, and MT. These numbers are always in increasing numerical order, and the hierarchy is MAT, MF, and MT. The end of a section, file, or material is divided into special records called SEND, FEND, and MEND, respectively.

3.3.2 SYMBOL NOMENCLATURE

ENDF data use an internally consistent notation based on the following rules derived from FORTRAN.

1. Symbols starting with the letter I, J, K, L, M, or N are integers. All other symbols refer to floating-point (real numbers).
2. The letter I or a symbol, starting with I, refers to an interpolation code.
3. Letters J, K, L, M, or N, when used alone, are indices.
4. A symbol starting with M is a control number. Examples are MAT, MF, and MT.
5. A symbol starting with L is a test number.
6. A symbol starting with N is a count of items.

3.3.3 TYPES OF RECORDS

All records on an ENDF tape are one of six possible types, denoted by TEXT, CONT, LIST, TAB1, TAB2, and INTG. The CONT record has six exceptional cases called DIR, HEAD, SEND, FEND, MEND, and TEND. The TEXT record has a unique case TPID. Every record contains the essential control numbers MAT, MF, MT, and the sequence number NS. The definitions of the other fields in each record will depend on its usage.

3.3.4 RETRIEVING DATA FROM AN ENDF FILE

The complete ENDF tape is over 100MB in size and almost two million lines in length. Searching for data in it while doing depletion calculations would place a heavy toll on memory and processor resources. Therefore, only the required data after cross-sections

(After processing, which will be discussed in the next section) and fission yields were extracted and stored in separate files used by the depletion code. For example, fission and total cross-section of ^{239}Pu using point cross-section data of JENDL-4.0 is shown in Figure 3.3.

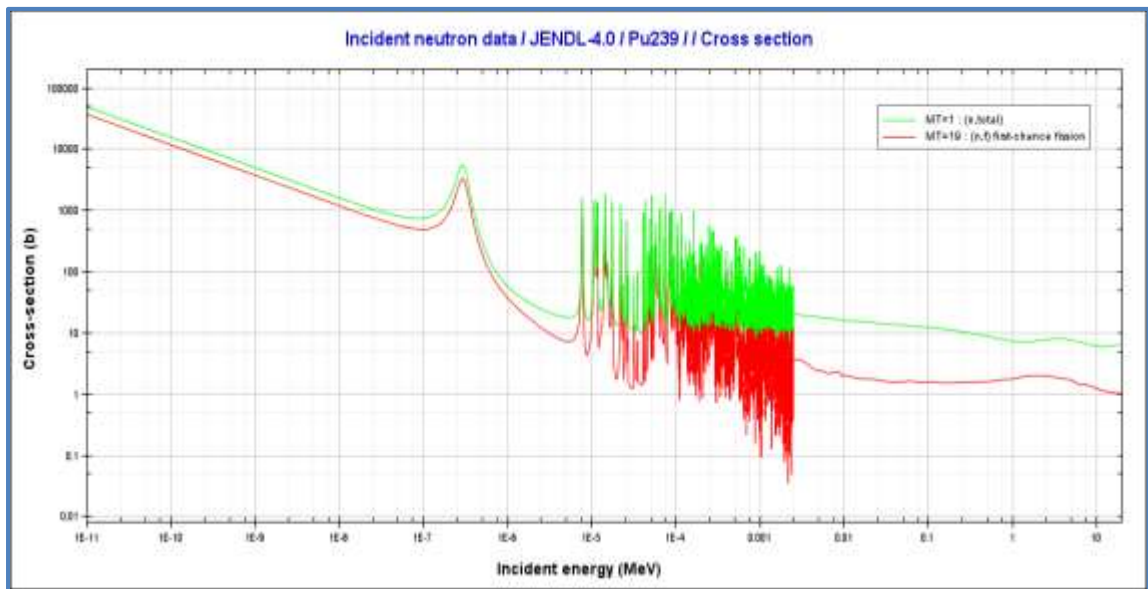


Figure 3.3: Total and fission cross-section of Pu^{239} using JENDL-4.0

3.4 ESTIMATION OF SPECTRUM DEPENDENT OF CROSS-SECTIONS

Point reactor calculations such as burn-up calculations require spectrum averaged one group cross-section for each nuclide. It is essential to estimate the average behavior of a particular nuclide in a typical slowing down medium. These effective cross-sections can be parameterized as a function of a background cross-section derived from the absorber's relative concentration in the medium. This is mostly done through Bondarenko self-shielding factor approach [63]. The self-shielding factor for a given material is a factor that accounts for energy self-shielding, which means that the factors that account for the presence of other absorbers. Bondarenko self-shielding factor

approach has been adopted to calculate the one group cross-section of each nuclide.

This is carried out in two steps:

Step-1: In the first step, generalized multi-group cross-section is obtained for a given nuclide as a function of background cross-section. The primary aim of reactor physics calculations is to study the variation of neutron flux and multiplication factor in the reactor under various operating conditions. The transport equation is solved for this purpose in a multi-group format. Multi-grouping is done by conserving the reaction rates. The diffusion equation is obtained by integrating the transport equation over all the angles. The multi-group diffusion equation can be written as [63]:

$$-\nabla \cdot D_g \nabla \Phi_g + \Sigma_g \Phi_g = S_g \quad (3.1)$$

Where,

$$\Sigma_g = \frac{\int_{E_{g+1}}^{E_g} \Sigma(E) \Phi(E) dE}{\int_{E_{g+1}}^{E_g} \Phi(E) dE} \quad (3.2)$$

Equation (3.2) represents the macroscopic cross-section in energy group **g**.

$$\text{Or, } \sigma_{gx}^i = \frac{\int_{E \in g} \sigma_x^i(E) \Phi(E) dE}{\int_{E \in g} \Phi(E) dE} \quad (3.3)$$

Equation (3.3) represents the microscopic group cross-section in energy group **g** for the reaction “x” and nuclei “i” and S_g neutron source for the group “g”.

Total reaction rate at energy **E** is defined as [63]:

$$\Sigma_t(E) \Phi(E) = S(E) \quad (3.4)$$

Where,

$\Sigma_t(E)$ = Macroscopic mixture Cross – section

$\Phi(E)$ = Neutron Flux

S (E) = Source at energy E

Substituting Φ (E) from eq. (3-5) to (3-4), one can get

$$\sigma_{gx}^i = \frac{\int_{E \in g} \sigma_x^i(E)(S(E)/\Sigma_t)dE}{\int_{E \in g} (S(E)/\Sigma_t)dE} \quad (3.5)$$

Group averaged values of energy-dependent parameters such as cross-section is defined as:

$$\langle \sigma_x^i \rangle_g = \frac{\int_{E_{g+1}}^{E_g} \sigma_{gx}^i(E)w(E)dE}{\int_{E_{g+1}}^{E_g} w(E)dE} \quad (3.6)$$

Where,

σ_x^i is the parameter to be averaged

w is the weighting function.

E_g is the energy group boundary

g is the group index

The weighting function can be chosen arbitrarily, but to conserve the reaction rate weighting function must be the incident particle spectrum.

The generalized cross-section set is obtained using the standard procedures of the PREPRO code system. The primary cross-section data is obtained from the ENDF (Evaluated Nuclear Data Format) files. In PREPRO, unshielded cross-sections are calculated, and self-shielding factors are generated as a function of background dilution for each nuclide.

Step-2: In the second part, actual background dilution (\mathbf{B}_0) is calculated for each isotope for the given material composition. This section aims to explain the theory behind the estimation of one group self-shielded cross-section. The group averaged cross-sections for any nuclide would depend upon the effectiveness of that nuclide in a mixture of all nuclides in a slowing down medium. The macroscopic mixture cross-section can be assumed to be consisting of two parts, the macroscopic total cross-section of the nuclide of interest and the macroscopic total cross-section of the remainder of the mixture [63]. Thus,

$$\Sigma_t = \sum_k N_k \sigma_t^k(E) = N_i \sigma_t^i(E) + \sum_{j \neq i} N_j \sigma_t^j(E) \quad (3.7)$$

If we assume all the resonances are narrow and the flux depression due to i^{th} a nuclide is only due to its resonance at energy E, then

$$\Sigma_t = N_i \left(\sigma_t^i(E) + \frac{1}{N_i} \sum_{j \neq i} N_j \sigma_t^j(E) \right) = N_i (\sigma_t^i(E) + \sigma_0^i) \quad (3.8)$$

Where,

σ_t^i is the total microscopic cross-section due to i^{th} nuclei

$$\sigma_0^i = \frac{1}{N_i} \sum_{j \neq i} N_j \sigma_t^j \quad (3.9)$$

σ_0^i is the microscopic cross-section of all nuclei except i^{th} nuclei per i^{th} nuclide, which is known as ‘**dilution cross-section**’ or ‘**background dilution**’ for i^{th} nuclei. Using Bondarenko approximation, we assume that σ_t^i is independent of energy. Thus multi-group cross-section (3-6) can be written as [63]:

$$\sigma_{gx}^i = \frac{\int_{E_{g+1}}^{E_g} \frac{\sigma_x^i(E)S(E)}{\sigma_{tx}^i(E)+\sigma_{0x}^i} dE}{\int_{E_{g+1}}^{E_g} \frac{S(E)}{\sigma_{tx}^i(E)+\sigma_{0x}^i} dE} \quad (3.10)$$

Here S(E) takes the form as defined in equation (3.4). Background dilution σ_0^i varies inversely as the atom density of nuclide i, and it goes from zero to several thousand barns. When σ_{0x}^i is large in comparison to σ_{tx}^i , then multi-group cross-section becomes:

$$\sigma_{gx}^{i\infty} = \frac{\int_{E_{g+1}}^{E_g} \sigma_x^i(E)S(E)dE}{\int_{E_{g+1}}^{E_g} S(E)dE} \quad (3.11)$$

$\sigma_{gx}^{i\infty}$ is called the infinite dilution cross-section or unshielded cross-section. The unshielded cross-section is mixture independent and can be calculated for any nuclide from a basic evaluated nuclear data file using processing code PREPRO.

Self-Shielding Factor (SSF) is defined as the ratio of the group cross-section (self-shielded cross-section) for any dilution to that corresponding infinite dilution cross-section (unshielded cross-section).

$$f_{xg}^i(\sigma_0) = \frac{\sigma_{xg}^i(\sigma_0)}{\sigma_{xg}^{i\infty}} \quad (3.12)$$

Self-Shielding Factor $f_{xg}^i(\sigma_0)$ is a smooth function of σ_0 and it ranges from zero to one but depending on the shape of the cross-section and group structure, it can exceed unity.

These factors as a function of σ_0 can also be obtained through the processing code PREPRO. Self-shielding factors are interpolated for the actual background cross-section to get the self-shielding factor (**SSF0**). This factor is then used to get one group self-shielded cross-section for different nuclei as follows:

$$1G \text{ self - shielded cross - section} = \frac{\sum_i \Delta E_i b_i \text{SSF}_0}{\sum_i \Delta E_i} \quad (3.13)$$

3.5 PREPARATION OF GENERALISED CROSS-SECTION SETS

As stated in the previous section that unshielded cross-sections can be generated through the PREPRO system of codes. PREPRO code is used to create a multi-group dataset from point data in the ENDF files. The procedure entails linearizing, resonance reconstruction, Doppler broadening and grouping of the primary point cross-section. This dataset is then condensed to a multi-group format using the standard of a specific reactor spectrum. The modules of PREPRO 2012 (The latest version of PREPRO available at the time of research work started) that have been used to generate multi-group data are described below.

3.5.1 LINEARIZATION

This linearization module is required because for the neutron transport calculations, cross-sections must be defined at all energies. Interpolation laws are used to reduce the number of points needed to specify cross-section vs. energy for the specified accuracy. These laws lend themselves to accurately and simply representing some cross-section shapes, e.g., $1/V$ cross-section can be exactly represented using log-log interpolation. But it can introduce inconsistencies during the evaluation process and result in a non-unique representation of the cross-section for later application. A module “linear” of PREPRO is used for the treatment of *linearization* of cross-section data. Following are the significant advantages of linearization:

- The cross-section can be easily plotted / integrated
- Can be Doppler Broadened efficiently
- Retrieved efficiently for continuous energy MONTE CARLO codes

3.5.2 RESONANCE RECONSTRUCTION

We need to generate many energy points such that the resonance is adequately reconstructed. There are three methods to follow.

- From the resonance peak, using the total width to measure the length and defining energy points on either side of the peak.
- Starting from the two adjacent resonances' peaks, the intervening energy between the interval is subdivided using the interval halving technique.
- Combines the above two methods; Uses the total width of two adjacent resonances to subdivide the intervening energy into subintervals. Each subinterval is then divided using the interval halving technique until the cross-section is linearly interpolable. The above points are pictorially shown in the following Figure 3.4.

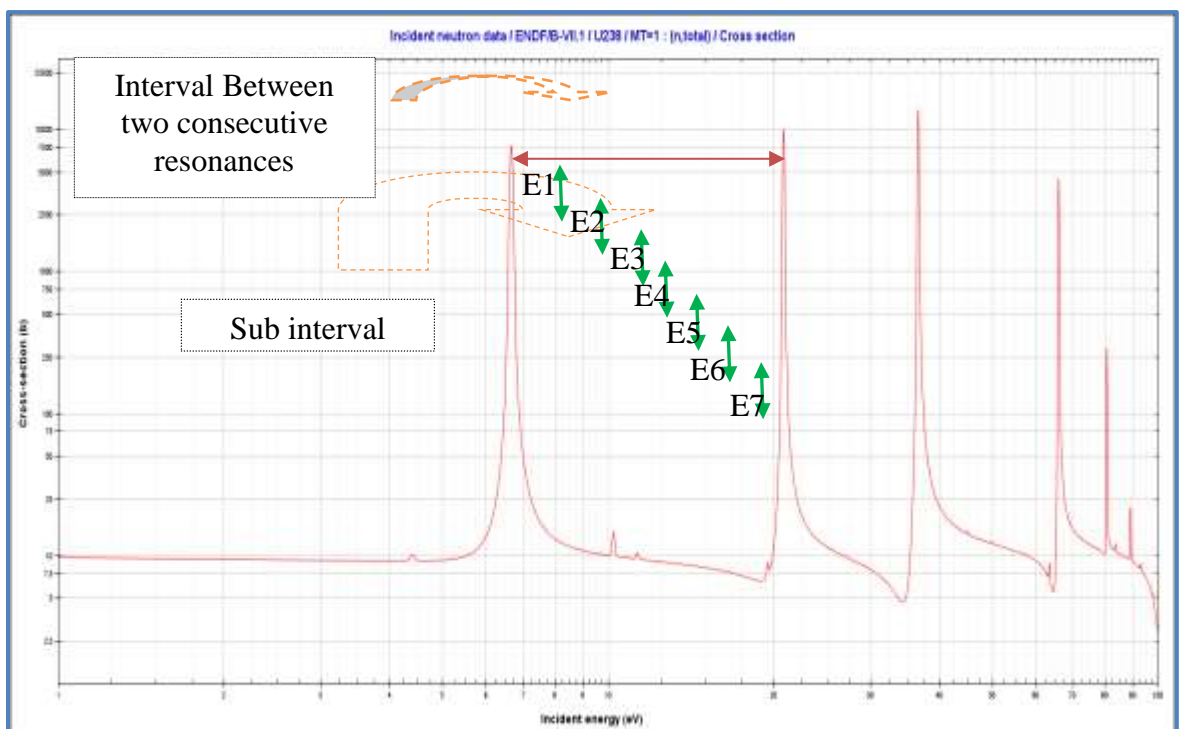


Figure 3.4: Interval halving technique for resonance reconstruction

If E lies between E_1 and E_2 , let the cross section at E is $\sigma_i(E)$, estimate the cross-section at E as follows:

$$\sigma_i^*(E) = \frac{1}{2} (\sigma_i(E_1) + \sigma_i(E_2))$$

While carrying out the interval halving procedure following acceptance criteria is followed:

$$\frac{|\sigma_i(E) - \sigma_i^*(E)|}{\sigma_i(E)} \leq \varepsilon_{max} \quad (3.14)$$

A module “Recent” of PREPRO is used for the treatment of *resonance reconstruction*.

3.5.3 DOPPLER BROADENING

Cross-section or the probability of neutron interacting with the nucleus depends on the relative speed between them. ENDF gives cross-section as a function of neutron energy, assuming the target nucleus at rest. This is true at 0K target temperature, but in practice, even at room temperature, the target nucleus is having a distribution of kinetic energies and moving about randomly due to thermal agitation. There will be a spectrum of relative energy for any given neutron energy in the lab frame reference. By convention, the cross-section is given for neutron kinetic energies. A practical way to account for the thermal motion of the target nuclei is to re-compute the cross-section at neutron energy by averaging out the cross-sections corresponding to all the relative energies about given neutron energy.

Neutron interaction cross-section depends upon the relative energy of neutron and nuclei. Let us consider a neutron with energy corresponding to the peak of a resonance incident upon a medium. In the medium, the nuclei are moving about due to thermal

motion. The collision of a neutron with the nucleus moves (toward or away from neutron), then the relative energy will be either more or less than the actual energy (Peak value). The cross-section will be lower than the peak value. Due to this resonance peak will be broadened, as shown in Figure 3.5 below.

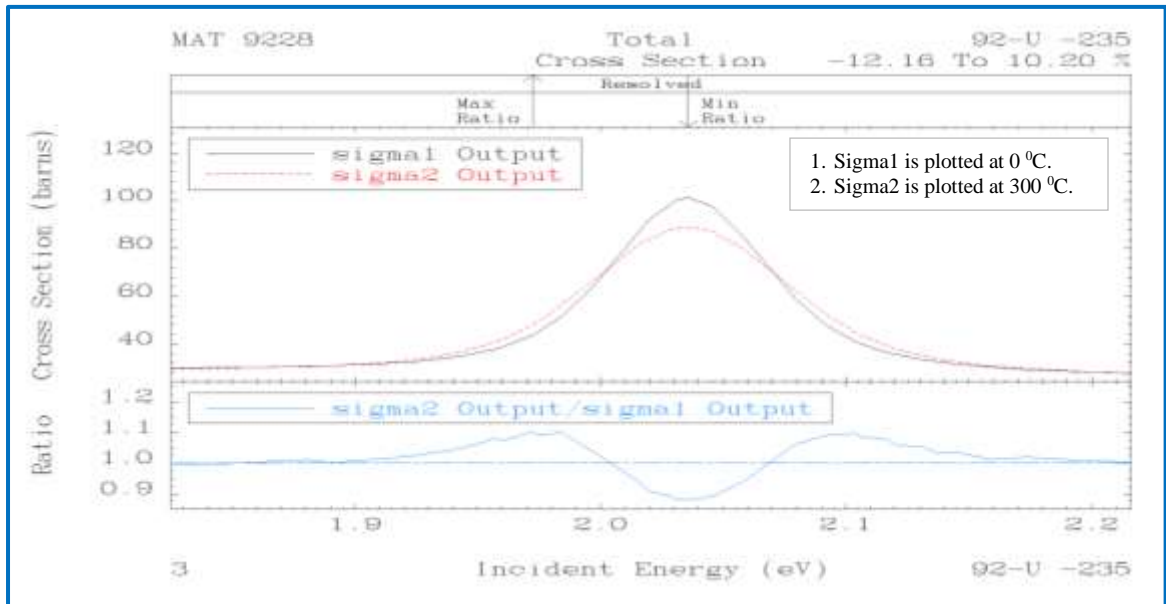


Figure 3.5: Effect of Doppler broadening on resonances in cross-section

A module “Sigma1” of PREPRO is used for the treatment of *Doppler broadening*.

3.5.4 MULTI-GROUPING

In reactor physics calculations for solving diffusion, transport, or burn-up equations, cross-section data are required up-to 20MeV. The point cross-section is forbiddingly too much to use in the balance equation. Therefore, a multi-grouping of the cross-section data is carried out. Multi-group cross-section is obtained by dividing the energy range into energy bins and defining the average cross-section in each bin, with reaction

rate conservation. The number of groups and group limits are selected based on the following parameters.

- Depends on manageability w.r.t. computer time & memory availability
- Energy region of importance w.r.t. flux spectrum
- For thermal reactors, a higher number of groups are defined in the lower energy (eV) range
- For fast reactors, many groups are defined in the higher energy (K eV) range

Multi-group cross-sections of U^{233} , U^{235} , and Pu^{239} in the WIMS library are shown in Figure 3.6 below:

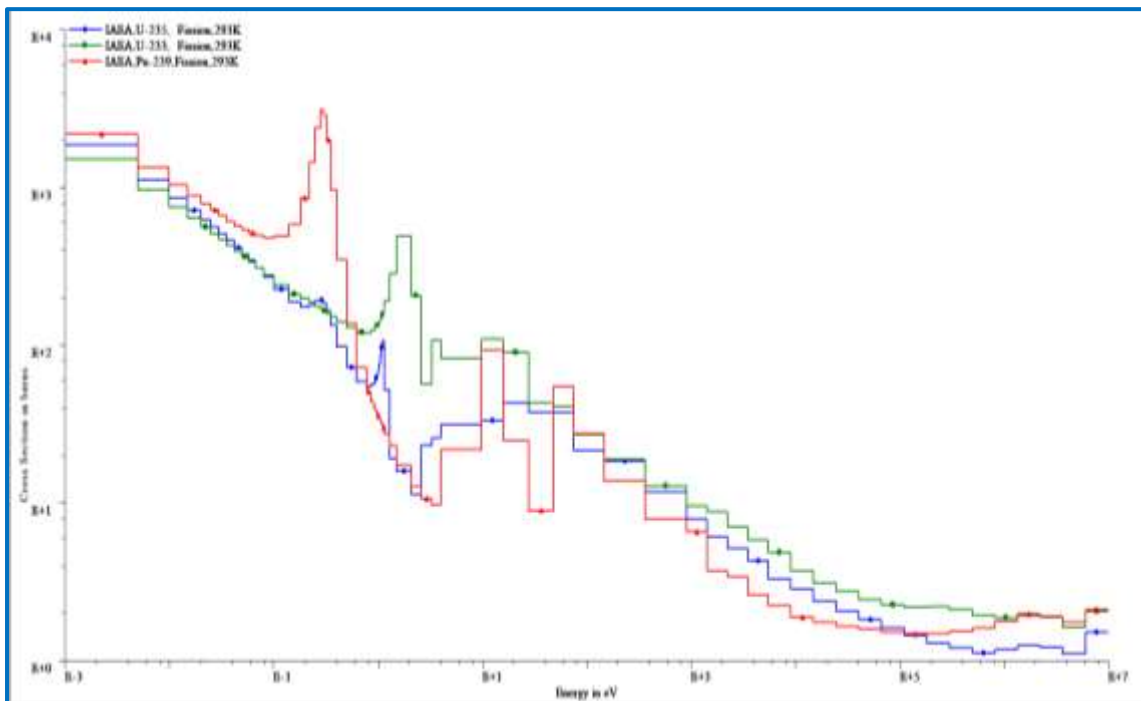


Figure 3.6: Multi-group cross-sections of U^{233} , U^{235} , and Pu^{239} in WIMS library

In the absence of any specific condition, group limits are generally arrived at by dividing the logarithmic range of the energy into an equal number of divisions. Seven important group structures are given below [64]:

1. 175 group (TART structure)
2. 50 group (ORNL structure)
3. 126 group (ORNL structure)
4. 171 group (ORNL structure)
5. 620 group (SAND-II structure, up to 18 MeV)
6. 640 group (SAND-II structure, up to 20 MeV)
7. 69 group (WIMS structure)
8. 68 group (GAM-I structure)
9. 99 group (GAM-II structure)
10. 54 group (MUFT structure)
11. 28 group (ABBN structure)
12. 616 group (TART structure to 20 MeV)
13. 700 group (TART structure to 1 GeV)
14. 665 group (SAND-II structure, 1.0e-5 eV, up to 18 MeV)
15. 685 group (SAND-II structure, 1.0e-5 eV, up to 20 MeV)
16. 666 group (TART structure to 200 MeV)
17. 725 group (SAND-II structure, 1.0e-5 eV, up to 60 MeV)
18. 755 group (SAND-II structure, 1.0e-5 eV, up to 150 MeV)
19. 765 group (SAND-II structure, 1.0e-5 eV, up to 200 MeV)

3.6 REACTOR SPECIFIC CROSS-SECTION SET

In this step effective cross-section is calculated for each material from the generalized cross-section set. The background dilution is calculated for each material, and then the self-shielding factor is interpolated from the $f_{xg}^i(\sigma_0)$ obtained from the generalized cross-section calculation for total, fission, and capture reaction.

The evaluation of the effective cross-section for each nuclide is an iterative process as the background dilution for a given nuclide depends on the effective total cross-section of other nuclides present in the mixture, and the effective total cross-section depends

on the background dilution. In the first iteration, the unshielded total cross-section is assumed to be the total cross-section, and the background dilution is estimated using Eq. (3.9). Then self-shielding factor is interpolated for this dilution, and effective total cross-section is obtained using the eq. (3.12). The background dilution is recalculated using these effective cross-sections. Thus this continues until the fractional change in every value of effective total cross-section is less than the selected convergence criteria. After the convergence is achieved, the final values for background dilution and effective total cross-section for each nuclide are obtained.

Using this background dilution, the self-shielding factors are interpolated, and hence the effective cross-sections are calculated for total, fission, and capture reactions. The self-shielded cross-sections are estimated only for important nuclei, e.g., For PT-HWR, self-shielded cross-sections are estimated only for ^{235}U and ^{238}U , and for other nuclei, unshielded cross-sections as estimated in the previous section are utilized for nuclear fuel cycle analysis.

3.7 RESULTS

One group spectrum averaged cross-section library generated for different nuclei using the method described in this chapter can be used in the nuclear database of the nuclear fuel cycle code prepared in this research work for the calculation of generation and depletion of different actinides and fission products inside the nuclear reactor during irradiation as well as outside the reactor after discharge. The reaction cross-sections of important actinides and fission products are given in Table 3.2 and Table-3.3, respectively. It is seen that the spectrum averaged fission cross section of ^{235}U and ^{239}Pu for a typical PHWR spectrum is 156 barns and 267 barns. The corresponding 0.0253

eV values are ~586 barns and ~746.9 barns [8]. The fission cross section in a slightly harder LWR spectrum is quoted in literature as 40.65 barns and 105.75 barns for ^{235}U and ^{239}Pu [65]

Table 3.2: Spectrum averaged Reaction cross-section of important Actinides

Isotope	Fission Cross-section (barn)	Absorption Cross-section (barn)	Isotope	Fission Cross-section (barn)	Absorption Cross-section (barn)	Isotope	Fission Cross-section (barn)	Absorption Cross-section (barn)
Am242m	1.83E+03	2.24E+03	Cf250	3.77E+01	8.57E+02	Pa231	2.11E-01	8.88E+01
Cf251	1.77E+03	2.85E+03	Cm247	3.54E+01	6.12E+01	Ra223	1.78E-01	3.84E+01
Pu237	8.85E+02	8.87E+02	Th229	2.05E+01	6.56E+01	Np239	1.75E-01	1.63E+01
Np236	8.67E+02	9.13E+02	Np240	1.99E+01	2.34E+01	Pu244	1.69E-01	1.51E+00
Am244m	7.11E+02	7.13E+02	Th231	1.63E+01	4.51E+01	Th228	1.69E-01	5.36E+01
Cm241	6.60E+02	6.63E+02	Ac228	1.53E+01	2.01E+01	Ra224	1.29E-01	5.42E+00
Am242	6.59E+02	7.57E+02	Ac226	1.17E+01	1.53E+01	Am245	1.16E-01	9.27E+00
Am244	6.53E+02	6.64E+02	Cf252	1.04E+01	1.70E+01	Pa233	1.15E-01	2.84E+01
Am240	6.21E+02	6.24E+02	Th233	1.00E+01	8.96E+02	Ra227	1.13E-01	1.01E+01
Pa232	5.14E+02	6.03E+02	Th235	6.51E+00	9.98E+00	Ac225	9.64E-02	3.38E+00
Cm245	5.10E+02	5.95E+02	Es253	6.33E+00	1.00E+02	Fr222	9.14E-02	7.44E+00
Np238	4.65E+02	5.58E+02	Pu238	4.88E+00	9.52E+01	U238	6.82E-02	1.22E+00
Cf249	4.60E+02	5.94E+02	Bk249	4.02E+00	6.84E+02	Pa235	6.64E-02	2.32E+01
Pu241	3.26E+02	4.39E+02	Cm249	2.34E+00	6.20E+00	Ra225	6.41E-02	7.39E+00
Cf253	2.85E+02	2.91E+02	Cm242	2.31E+00	8.67E+00	Th234	6.00E-02	2.31E+00
Pu239	2.67E+02	3.94E+02	Ra228	2.20E+00	4.69E+01	Th230	3.97E-02	2.60E+01
Bk250	2.33E+02	3.25E+02	Am241	1.51E+00	2.19E+02	Th232	1.72E-02	3.61E+00
Cm243	1.96E+02	2.32E+02	U237	1.50E+00	1.33E+02	Ra226	9.13E-03	1.14E+01
Pa234	1.94E+02	1.97E+02	Np241	9.44E-01	7.50E+01	Cm250	5.68E-03	1.37E+01
U235	1.56E+02	1.85E+02	Th226	8.40E-01	2.82E+02	Pu246	3.87E-03	2.15E+00
U233	1.54E+02	1.70E+02	Cm244	8.09E-01	1.57E+01	Rn219	2.29E-03	6.89E+00
Pu245	1.38E+02	1.85E+02	U240	7.43E-01	5.47E+00	At218	1.83E-03	1.71E+00
Pa234m	7.41E+01	7.46E+01	Cm246	5.16E-01	2.92E+00	Fr223	1.48E-03	1.06E+01
Pu243	6.33E+01	8.85E+01	Pu240	4.06E-01	1.83E+02	Rn221	1.28E-03	4.20E+00
Th227	6.19E+01	6.99E+01	Cm248	3.87E-01	5.61E+00	Fr221	1.23E-03	8.68E+00
Pu236	6.08E+01	6.69E+01	Am243	3.55E-01	5.71E+01	Ac227	7.53E-04	1.59E+02
Am246	4.54E+01	4.89E+01	Np237	3.41E-01	6.53E+01	At219	4.44E-05	3.63E+00

Isotope	Fission Cross-section (barn)	Absorption Cross-section (barn)	Isotope	Fission Cross-section (barn)	Absorption Cross-section (barn)	Isotope	Fission Cross-section (barn)	Absorption Cross-section (barn)
U239	4.37E+01	1.29E+02	U234	3.27E-01	3.80E+01	Rn222	3.40E-06	9.97E-01
Am246m	4.04E+01	4.25E+01	Pu242	2.81E-01	2.70E+01	Rn220	3.00E-07	1.08E-01
U232	3.84E+01	6.00E+01	U236	2.25E-01	8.17E+00	Po218	2.00E-07	3.23E-01

Table 3.3: Spectrum averaged cross-section of important Fission Products

Isotope	Absorption Cross-section (barn)						
Xe135m	2.22E+06	Rh103m	1.86E+02	Pr145	3.95E+01	Eu159	2.21E+01
Xe135	8.48E+05	Dy161	1.74E+02	Cs134	3.90E+01	Tc102	2.18E+01
Gd157	4.95E+04	Tb163	1.74E+02	Dy160	3.57E+01	I133m	2.15E+01
Sm149	2.34E+04	Pm153	1.56E+02	Eu164	3.52E+01	In114	2.09E+01
Eu152m	1.56E+04	Xe133m	1.44E+02	Cd115m	3.49E+01	Sb122	2.05E+01
Gd155	1.12E+04	Pm157	1.42E+02	Tb161	3.39E+01	Pr144	2.04E+01
Cd113	1.08E+04	Nd147	1.24E+02	Cd111m	3.28E+01	Pm156	1.96E+01
Pm148m	6.99E+03	In115	1.23E+02	Ag113m	3.26E+01	Tb165	1.95E+01
Rh105	6.01E+03	Tb164	1.23E+02	Pm152	3.25E+01	Tb162	1.88E+01
Gd161	4.53E+03	Te127	1.21E+02	Sm150	3.21E+01	Rh110	1.83E+01
Gd153	3.47E+03	Ag118	1.13E+02	Ag108m	3.19E+01	Xe131m	1.83E+01
Sm151	3.07E+03	Ho167	1.13E+02	Ho165	3.04E+01	Ag117	1.78E+01
Eu152	3.06E+03	Pr144m	1.06E+02	Pm160	3.03E+01	In120	1.77E+01
Se81m	2.23E+03	Sm152	1.04E+02	Eu157	3.00E+01	Nd145	1.77E+01
Eu151	2.18E+03	Dy162	1.03E+02	Sm147	2.99E+01	Pr147	1.75E+01
I126	2.02E+03	Eu153	9.92E+01	Sm163	2.97E+01	Cd113m	1.69E+01
Eu155	1.83E+03	Xe133	9.02E+01	Pr142m	2.94E+01	Ag116	1.69E+01
Te127m	1.71E+03	Nd143	8.74E+01	In122m	2.83E+01	Ag117m	1.69E+01
Ho166m	1.60E+03	Pm147	8.33E+01	Eu163	2.76E+01	Eu162	1.68E+01
Dy165	1.14E+03	Pr149	7.85E+01	Sm162	2.75E+01	Cd117m	1.67E+01
Ho166	8.44E+02	Cs134m	7.82E+01	Ag108	2.71E+01	Br80m	1.65E+01
Kr81m	7.38E+02	As77	6.78E+01	Pr143	2.67E+01	Pr151	1.61E+01
Dy164	6.78E+02	Dy163	6.71E+01	Rh106	2.66E+01	Ag112	1.59E+01
Eu154	6.36E+02	In114m	6.42E+01	Kr83m	2.62E+01	Ag114	1.58E+01
Dy165m	5.54E+02	Rh103	5.89E+01	Gd154	2.60E+01	Nb98m	1.56E+01
Pm148	5.37E+02	In116m	5.81E+01	Pd111m	2.55E+01	Tc100	1.56E+01
Pm149	5.20E+02	Ag116m	5.79E+01	Eu158	2.55E+01	Cs132	1.56E+01
Er167	3.22E+02	Rh108m	5.64E+01	Y97m	2.49E+01	Sn115	1.55E+01
Cd109	3.20E+02	Kr83	5.47E+01	Pm152m	2.48E+01	Cs133	1.54E+01
Er167m	3.13E+02	Ag109	5.16E+01	In115m	2.47E+01	Rh108	1.53E+01

Isotope	Absorption Cross-section (barn)						
Sm153	2.86E+02	Se77m	4.97E+01	Ag115m	2.46E+01	Nd149	1.52E+01
Ag109m	2.82E+02	In118m	4.81E+01	Pr148	2.45E+01	Nd151	1.51E+01
Rh104m	2.81E+02	Eu156	4.79E+01	Sb122m	2.43E+01	In124m	1.50E+01
Te123m	2.74E+02	Y89m	4.66E+01	Pr150	2.41E+01	Cd121m	1.48E+01
Te123	2.26E+02	In120m	4.60E+01	Eu160	2.38E+01	Pr146	1.47E+01
Gd152	2.13E+02	Nb100m	4.58E+01	Se76	2.30E+01	La147	1.46E+01
Tb160	2.07E+02	Pm150	4.40E+01	I131	2.30E+01	I128	1.41E+01
Pm151	2.01E+02	Ag110	4.22E+01	Ag110m	2.28E+01	Tb159	1.41E+01

3.8 CONCLUSION

Nuclear reaction cross-sections are the essential elements for reactor physics calculations. These cross-sections for various reactions viz. fission, capture, absorption, etc. are available in ENDF files in the form of point data. These data need to be pre-processed because they cannot be used directly to estimate radionuclides in the point reactor burn-up codes. The methodology for processing nuclear data and generating the cross-sectional nuclear library for a particular reactor type is explained in this chapter. The spectrum averaged cross-sections are very sensitive to the input weighting spectrum. Although the neutron spectrum changes over the irradiation, the deviations are not very significant. In this research, the PT-HWR neutron spectrum has been used to generate the reactor specific one-group cross-section database for the problem chosen. In advanced simulations, burn-up dependent spectrum averaged cross-sections are being used to track the isotopes during irradiation.

In fuel cycle analysis, the best possible solution of the Bateman equations form the core of the fuel cycle design. This is still an emerging field and even today better and better methods are being evolved to treat the coupled ODEs and their stiffness. The next

chapter focuses on the methodology adopted to solve Bateman equations and development the computer code IGDC.

Chapter 4

Development of computer code IGDC

4.0 INTRODUCTION

Theoretical modeling of physical phenomena allows computer simulation of experiments for an understanding of the underlying physics. In the early days, simple analytical techniques were used. With the advancement of computer technology, a new area of computational science was evolved, and numerical methods were used extensively. Computational methods are very useful tools for modeling complex physical situations. Numerical methods are used for mathematical problems when analytic solutions are not possible and to avoid lengthy & cumbersome mathematical processes, particularly when closed-form solutions are not needed [66].

As an initiation towards the nuclear fuel cycle analysis, we have to develop a model of generation and depletion of fission products and actinides in the nuclear reactor and also outside the reactor. As mentioned in the earlier chapter, the problem is defined by a set of equations describing the production and depletion of nuclides through various mechanisms. The equations are then formulated for each nuclide of concern. This model consists of first-order coupled nonlinear stiff differential equations technically called Bateman equations. These equations will be solved using mathematical methods with the help of nuclear data libraries generated as inputs. These solutions will then be used to estimate the concentration of different radio-nuclides under consideration,

decay heat of the nuclear reactor, radio-activity, radiotoxicity associated with the spent fuel and neutron poisoning factors of different fission products.

The research focused on implementing a new method for solving the coupled depletion equations for fuel cycle analysis. A computer code “**I**sotopic **G**eneration and **D**epletion **C**ode: **IGDC**” is developed as an outcome of this research to cater the need described above for the nuclear fuel cycle analysis. In this chapter, the development of this computer code and its solution is discussed.

4.1 DEVELOPMENT OF TRANSMUTATION MODEL

This is the first step towards the development of the computer code IGDC. The transmutation model consists of generation and depletion equations of various fission products and actinides in a nuclear reactor. The depletion equation describes the rate of change of the number density N_i of isotope i [67]:

$$\frac{dN_i}{dt} = \text{Generation Rate} - \text{Depletion Rate} \quad (4.1)$$

In a reactor core, the generation of a number of atoms of an isotope in a specific volume is due to:

1. Fission products produced by fission
2. Neutron capture of a parent isotope
3. Radio-active decay of a parent isotope
4. Movement of material from a neighboring volume into the volume

Depletion terms are corresponding to:

1. Neutron capture that leads to fission

2. Neutron capture forming a daughter isotope
3. Radio-active decay into a daughter isotope
4. Outward movement of material into neighboring volume.

These processes are described in detail in the next sub-sections: Equation 4.1 is generally written as

$$\frac{dN_i}{dt} = \sum_j \gamma_{j,i} \sigma_{f,j} N_j \phi + \sigma_{c,i-1} N_{i-1} \phi + \sum_k \lambda_{k,i} N_k - \lambda_i N_i - \sigma_{f,i} N_i \phi - \sigma_{c,i} N_i \phi \quad (4.2)$$

4.1.1 FISSION TERM

A fission reaction is a reaction in which one fissile isotope fissions into two lighter fission products. Rate of depletion of i^{th} fissile isotope due to fission reaction is given by the fission reaction rate:

$$\frac{dN_i}{dt} = - \sum_i \sigma_{f,i} N_i \phi \quad (4.3)$$

$\sigma_{f,i}$ is the microscopic fission cross-section of i^{th} nuclei, ϕ is the neutron flux. Similarly, k^{th} isotope may also be produced by the fission of j^{th} isotope. This term may be given as:

$$\frac{dN_k}{dt} = \sum_j \gamma_{j,k} \sigma_{f,j} N_j \phi \quad (4.4)$$

$\gamma_{j,k}$ is the fission yield of k^{th} nuclei due to the fission of j^{th} nuclei.

4.1.2 RADIOACTIVE DECAY TERMS

Many of the fission products are unstable, so all the radioactive decay modes viz. (α), (γ), (β^-), (β^+), (β^- , n), (β^- , α), (β^- , p) and (p) are possible in a nuclear reactor. Few common decay modes are:

Alpha decay:



Beta-decay:



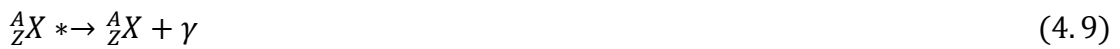
Or



Neutron decay:



Gamma decay:



Where X^* is an excited state of the isotope. The changes in mass number A and the atomic number Z are shown in the above reactions. The decay terms in the depletion equations are then

$$\frac{dN_i}{dt} = -\lambda_i N_i + \sum_{j \neq i} \lambda_{ji} N_j$$

The summation on the right-hand side is the gain of the daughter isotope i due to the decay of the parent isotope j . The first term is the loss rate of isotope i due to all the decay reactions. Because there is no radioactive decay between an actinide and fission product, the fission products' decay chains and actinides are independent. Coupling between the fission product and actinide equations will be through neutron flux.

1.1.3. Neutron capture terms

In neutron capture reactions, a parent isotope i captures a neutron forming a daughter isotope j . The only exception is fission, where two daughter isotopes are created for

each neutron capture. The rate of loss of the parent isotope and rate of gain of the daughter isotope is given by the neutron capture reaction rate

$$\frac{dN_j}{dt} = - \sum_i \sigma_{c,i \rightarrow j} N_i \phi \quad (4.10)$$

Where $\sigma_{c,i \rightarrow j}$ is the microscopic cross-section for the neutron capture reaction. Some examples of neutron capture reactions, showing the changes in mass number A and atomic number Z , are:



Although many different reactions are possible, most isotopes are only involved in one or two types of neutron capture reactions. All the generation and depletion equations of the various nuclei will be coupled, forming one extensive system of first-order differential equations. An example of a fission product chain is shown in Figure 4.1. Consider the following chain for ${}^{72}\text{Co}$ and ${}^{73}\text{Co}$.

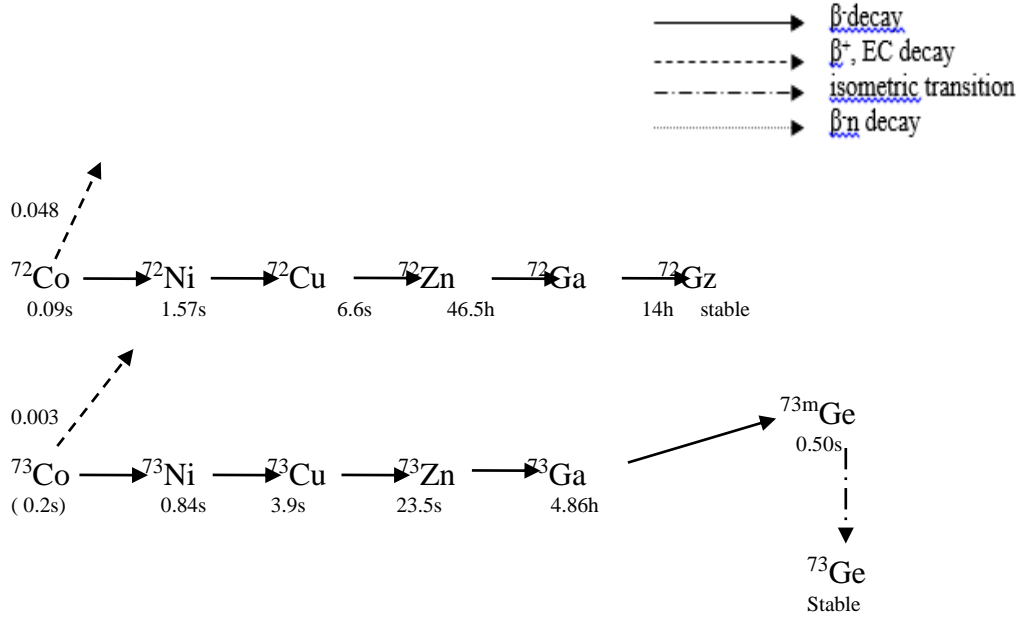


Figure 4.1: Generation and depletion chain of few fission products

N.B. Complete decay chain of fission products is given in *Annexure-1*

The explicit governing equations for production and depletion of all the isotopes shown in Fig. 4.1 are given below in equations 4.15 through 4.23.

$$\frac{dN^{Ni^{72}}}{dt} = -\lambda_1^{Ni^{72}} N^{Ni^{72}} - N^{Ni^{72}} \sigma_a^{Ni^{72}} \phi + r^{Ni^{72}} \Sigma_f \phi \quad (4.15)$$

$$\frac{dN^{Cu^{72}}}{dt} = \lambda_1^{Ni^{72}} N^{Ni^{72}} - \lambda_1^{Cu^{72}} N^{Cu^{72}} - N^{Cu^{72}} \sigma_a^{Cu^{72}} \phi + r^{Cu^{72}} \Sigma_f \phi + \lambda_3^{Ni^{73}} N^{Ni^{73}} \quad (4.16)$$

$$\frac{dN^{Zn^{72}}}{dt} = \lambda_1^{Cu^{72}} N^{Cu^{72}} - \lambda_1^{Zn^{72}} N^{Zn^{72}} - N^{Zn^{72}} \sigma_a^{Zn^{72}} \phi + r^{Zn^{72}} \Sigma_f \phi \quad (4.17)$$

$$\frac{dN^{Ga^{72}}}{dt} = \lambda_1^{Zn^{72}} N^{Zn^{72}} - \lambda_1^{Ga^{72}} N^{Ga^{72}} - N^{Ga^{72}} \sigma_a^{Ga^{72}} \phi + r^{Ga^{72}} \Sigma_f \phi \quad (4.18)$$

$$\frac{dN^{Ge72}}{dt} = \lambda_1^{Ga72} N^{Ga72} - N^{Ge72} \sigma_a^{Ge72} \phi + r^{Ge72} \Sigma_f \phi \quad (4.19)$$

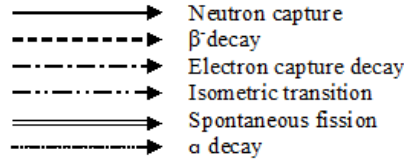
$$\frac{dN^{Cu73}}{dt} = -\lambda_1^{Cu73} N^{Cu73} + N^{Cu72} \sigma_a^{Cu72} \phi + \gamma^{Cu73} \Sigma_f \phi + \lambda_1^{Ni73} N^{Ni74} - N^{Cu73} \sigma_a^{Cu73} \phi \quad (4.20)$$

$$\frac{dN^{Zn73}}{dt} = N^{Zn72} \sigma_a^{Zn72} \phi - \lambda_1^{Zn73} N^{Zn73} + \gamma^{Zn73} \Sigma_f \phi + \lambda_1^{Cu73} N^{Cu73} - N^{Zn73} \sigma_a^{Zn73} \phi \quad (4.21)$$

$$\frac{dN^{Ga73}}{dt} = \lambda_1^{Zn73} N^{Zn73} - \lambda_1^{Ga73} N^{Ga73} + \gamma^{Ga73} \Sigma_f \phi + N^{Ga72} \sigma_a^{Ga72} \phi - N^{Ga73} \sigma_a^{Ga73} \phi \quad (4.22)$$

$$\frac{dN^{Ge73}}{dt} = \lambda_1^{Ga73} N^{Ga73} + N^{Ge72} \sigma_a^{Ge72} \phi - N^{Ge73} \sigma_a^{Ge73} \phi + \gamma^{Ge73} \Sigma_f \phi \quad (4.23)$$

Similarly, let us consider the build-up and decay chain of actinides explicitly shown in Figure 4.2 below (Meaning of pictorial representation in the decay chain is as follows):



Build-up and decay of actinides through various modes like neutron capture, β^- decay, β^+ decay, isomeric transition, spontaneous fission, and alpha decay as an example of the transmutation model actinides is shown in Figure 4.2. Burn-up equations for IGDC considered isotopes in the above chain can be given in equations 4.24 through 4.34.:

$$\frac{dN^{U235}}{dt} = -N^{U235}\lambda_5^{U235} - N^{U235}\lambda_6^{U235} - N^{U235}\sigma_c^{U235}\phi - N^{U235}\sigma_{cc}^{U235} * \phi - N^{U235}\sigma_f^{U235}\phi + N^{Pu239}\lambda_6^{Pu239} + N^{U234}\sigma_c^{U234} * \phi + N^{U236}\sigma_{cc}^{U236}\phi \quad (4.24)$$

$$\frac{dN^{Pu239}}{dt} = -N^{Pu239}\lambda_5^{Pu239} - N^{Pu239}\lambda_6^{Pu239} - N^{Pu239}\sigma_c^{Pu239}\phi - N^{Pu239}\sigma_{cc}^{Pu239}\phi - N^{Pu239}\sigma_f^{Pu239}\phi + N^{Np239}\lambda_2^{Np239} + N^{Cm243}\lambda_6^{Cm243} + N^{Pu238}\sigma_c^{Pu238}\phi + N^{Pu240}\sigma_{cc}^{Pu240}\phi \quad (4.25)$$

$$\frac{dN^{Pu241}}{dt} = -N^{Pu241}\lambda_2^{Pu241} - N^{Pu241}\lambda_6^{Pu241} - N^{Pu241}\sigma_c^{Pu241}\phi - N^{Pu241}\sigma_{cc}^{Pu241}\phi - N^{Pu241}\sigma_f^{Pu241}\phi + N^{Np241}\lambda_2^{Np241} + N^{Cm245}\lambda_6^{Cm245} + N^{Pu240}\sigma_c^{Pu240}\phi + N^{Pu242}\sigma_{cc}^{Pu242}\phi \quad (4.26)$$

$$\frac{dN^{Pu243}}{dt} = -N^{Pu243}\lambda_2^{Pu243} - N^{Pu243}\sigma_c^{Pu243}\phi - N^{Pu243}\sigma_{cc}^{Pu243}\phi - N^{Pu243}\sigma_f^{Pu243}\phi + N^{Cm247}\lambda_6^{Cm247} + N^{Pu242}\sigma_c^{Pu242}\phi + N^{Pu244}\sigma_{cc}^{Pu244}\phi \quad (4.27)$$

$$\frac{dN^{Am241}}{dt} = -N^{Am241}\lambda_5^{Am241} - N^{Am241}\lambda_6^{Am241} - N^{Am241}\sigma_{cc}^{Am241}\phi - N^{Am241}\sigma_f^{Am241}\phi - N^{Am241}\sigma_c^{11Am241}\phi - N^{Am241}\sigma_{c12}^{Am241}\phi + N^{Pu241}\lambda_2^{Pu241} + N^{Am240}\sigma_c^{Am240}\phi + N^{Am242}\sigma_{cc}^{Am242}\phi + N^{Am242}\sigma_{cc}^{Am242m}\phi \quad (4.28)$$

$$\frac{dN^{Am243}}{dt} = -N^{Am243}\lambda_6^{Am243} - N^{Am243}\sigma_{cc11}^{Am243}\phi - N^{Am243}\sigma_{cc12}^{Am243}\phi - N^{Am243}\sigma_f^{Am243}\phi - N^{Am243}\sigma_{c11}^{Am243}\phi - N^{Am243}\sigma_{c12}^{Am243}\phi + N^{Pu243}\lambda_2^{Pu243} + N^{Cm243}\lambda_3^{Cm243} + N^{Am242}\sigma_c^{Am242}\phi + N^{Am242}\sigma_c^{Am242m}\phi + N^{Am244}\sigma_{cc}^{Am244m}\phi + N^{Am244}\sigma_{cc}^{Am244}\phi \quad (4.29)$$

$$\frac{dN^{Np237}}{dt} = -N^{Np237}\lambda_6^{Np237} - N^{Np237}\sigma_c^{Np237}\phi - N^{Np237}\sigma_{cc}^{Np237}\phi - N^{Np237}\sigma_f^{Np237}\phi + N^{U237}\lambda_2^{U237} + N^{Pu237}\lambda_3^{Pu237} + N^{Np236}\sigma_c^{Np236}\phi + N^{Np238}\sigma_{cc}^{Np238}\phi \quad (4.30)$$

$$\frac{dN^{Cm241}}{dt} = -N^{Cm241}\lambda_5^{Cm241} - N^{Cm241}\lambda_6^{Cm241} - N^{Cm241}\sigma_c^{Cm241}\phi - N^{Cm241}\sigma_f^{Cm241}\phi + N^{Am241}\lambda_5^{Am241} + N^{Cm242}\sigma_{cc}^{Cm241}\phi \quad (4.31)$$

$$\frac{dN^{Cm243}}{dt} = -N^{Cm243}\lambda_3^{Cm243} - N^{Cm243}\lambda_6^{Cm243} - N^{Cm243}\sigma_c^{Cm243}\phi - N^{Cm243}\sigma_{cc}^{Cm243}\phi - N^{Cm243}\sigma_f^{Cm243}\phi + N^{Cm242}\sigma_c^{Cm242}\phi + N^{Cm244}\sigma_{cc}^{Cm244}\phi \quad (4.32)$$

$$\frac{dN^{Cf252}}{dt} = -N^{Cf252}\lambda_5^{Cf252} - N^{Cf252}\lambda_6^{Cf252} - N^{Cf252}\sigma_c^{Cf252}\phi - N^{Cf252}\sigma_{cc}^{Cf252}\phi - N^{Cf252}\sigma_f^{Cf252}\phi + N^{Cf251}\sigma_c^{Cf251}\phi + N^{Cf253}\sigma_{cc}^{Cf253}\phi \quad (4.33)$$

$$\frac{dN^{Cf253}}{dt} = N^{Cf253}\lambda_2^{Cf253}(-1) + N^{Cf253}\lambda_6^{Cf253}(-1) + N^{Cf253}\sigma_{cc}^{Cf253}\phi(-1) + N^{Cf252}\sigma_c^{Cf252}\phi \quad (4.34)$$

Note: In above equations symbols have following meaning.

λ_1 = Beta- decay

λ_2 = Beta+ decay

λ_3 = Beta-n decay

λ_4 = Isomeric transition

λ_5 = Spontaneous decay

λ_6 = Alpha decay

λ_{11} = Beta- decay towards Meta stable state nuclei

λ_{12} = Beta- decay towards stable state nuclei

λ_{21} = Beta+ decay towards Meta stable state nuclei

λ_{22} = Beta+ decay towards stable state nuclei

λ_{31} = Beta-n decay towards Meta stable state nuclei

λ_{32} = Beta-n decay towards stable state nuclei

σ_c = Capture cross-section

σ_{cc} = (n, 2n) cross-section

σ_f = Fission cross-section

It can be seen that these are a complicated set of non-linear equations and can be effectively solved by numerical methods.

4.2 NUMERICAL METHOD FOR SOLUTION OF BATEMAN EQUATIONS

Professor Rutherford gave the first mathematical model of isotopic generation and depletion in 1905, and H. Bateman gave the analytical solution of the model in 1910.

In that paper, Bateman used Laplace transformations and complex integrals to achieve the solution. This approach becomes very cumbersome as the number of nuclei under consideration becomes large. In such cases, this problem is solved numerically. The methods to tackle this problem can be broadly categorized into two categories:

1. In the first category, the decay chains are linearized, i.e. progeny does not produce the parent [40,41]. In this method, the generation and depletion path of all the nuclei under consideration are separated, and the differential equation corresponding to each path is solved separately. Once the solution for each linear chain is generated, they can be summed together as a result of the superposition principle. The advantage of the linear

chain method is the ability to find solutions explicitly and directly. This approach works effectively for a problem involving a low number of nuclides, but the need to explicitly model each pathway for each nuclide being tracked hinders the extension of these methods to problems involving several hundreds of nuclides.

2. In the second category, an alternative approach for dealing with burn-up problems is to solve the Bateman equations using matrix exponential methods. This method has been applied with varied success in multiple fuel decay and transmutation codes [4, 31, 43]. But in this method, the system of coupled ordinary differential equations is linearized by ignoring the non-linear coupling of neutron flux in Bateman equations. At the same time, this method also requires partitioning of short and long half-life radionuclides.

To avoid these limitations associated with the above two categories, for the first time, Klopfenstein–Shampine family of numerical differentiation formula (NDF) is used for solving nonlinear coupled ordinary differential equations without the need to partition the short and long-lived radio-isotopes is attempted. Basically, NDFs are corrections to the Gear’s Backward Differentiation Formula (BDF).

4.3 SUITABILITY OF KLOPFENSTEIN - SHAMPINE FAMILY OF NDF

Since the model of nuclear fuel cycle equations is highly stiff, a numerical method based on Backward Differentiation Formulae (BDFs) can be the first choice. Therefore, we will first derive these formulae, and then we will examine their suitability for the problem.

4.3.1 BACKWARD DIFFERENTIATION FORMULA

The Bateman equations (4.1) may also be written in the form:

$$y'(t) = f(t, y), \quad y(t_0) = y_0 \quad (4.35)$$

Where,

$y(0)$ are the initial values of the number densities of each of the nuclei (N_0).

$y(t)$ are the number densities of each nucleus at time t (N_t).

$y(t)'$ Denotes the rate of change of number densities with time ($\frac{dN_t}{dt}$)

In BDFs, the solution function $y(t)$ is approximated with a polynomial, and then the approximating function is differentiated. Newton's backward difference formula generates the polynomial functions that are used in these approximations.

Newton Backward Difference interpolation of k known values between y_n and y_{n+k} , i.e., $y_{n-k+1}, y_{n-k+2} \dots y_{n-1}, y_n$ is as follows:

$$\begin{aligned} y(t) &= y(t_n + sh) \\ &= y_n + s\nabla y_n + \frac{s(s+1)}{2!} \nabla^2 y_n + \dots + \frac{s(s+1) \dots (s+k-1)}{(k-1)!} \nabla^{k-1} y_n \end{aligned} \quad (4.36)$$

Where, $s = \frac{t-t_n}{h}$, $t_n \leq t \leq t_{n+1}$

From discrete mathematics,

$$\begin{aligned} -s c_j &= \binom{-s}{j} \\ &= \frac{(-s)(-s-1) \dots (-s-j+1)}{j!} \end{aligned} \quad (4.37)$$

Equation (4.36 and 4.37) will yield,

$$\begin{aligned} y(t) &= y(t_n + sh) \\ &= \sum_{j=0}^{k-1} (-1)^j \binom{-s}{j} \nabla^j y_n \end{aligned} \quad (4.38)$$

If the interpolation is done by considering 'k' known values $y_{n-k+1}, y_{n-k+2} \dots \dots y_{n-1}, y_n$ and one unknown value y_{n+1} . The polynomial approximation $q(t)$ of $y(t)$ can be written as:

$$q(t) = q(t_n + sh) = \sum_{j=0}^k (-1)^j \binom{-s+1}{j} \Delta^j y_{n+1} \quad (4.39)$$

We know that,

$$\frac{dq}{dt} = \frac{dq}{ds} \frac{ds}{dt}, \quad \text{or} \quad \frac{dq}{dt} = \frac{1}{h} \left(\frac{dq}{ds} \right) \quad (4.40)$$

Since $q(t)$ is this polynomial function of $y(t)$, then dq/dt can be equated to y' in equation (4.35), which leads to:

$$\frac{1}{h} \frac{dq}{ds} = f(t, y), \quad \text{or} \quad \frac{1}{h} \left[\sum_{j=0}^k (-1)^j \frac{d}{ds} \binom{-s+1}{j} \nabla^j y_{n+1} \right] = f_{n+1}$$

or

$$\frac{1}{h} \sum_{j=0}^k (-1)^j \nabla^j y_{n+1} \frac{d}{ds} \binom{-s+1}{j} = f_{n+1} \quad (4.41)$$

Since,

$$\binom{-s+1}{j} = (-1)^j \frac{(s-1)s(s+1)\dots\dots(s-1+j-1)}{j!} \&t_{n+1} = t_n + sh$$

For $s = 1$,

$$\frac{d}{ds} \left[\binom{-s+1}{j} \right]_{s=1} = (-1)^j \frac{d}{ds} \frac{(s-1)s(s+1)\dots\dots(s+j-1)}{j!} \Big|_{s=1}$$

$$\begin{aligned}
&= \frac{(-1)^j}{j!} \{(s)(s+1) \dots (s+j-2) \\
&\quad + (s-1)(s+1) \dots (s+j-2) + \dots \\
&\quad + (s-1)s(s+1) \dots (s+j-3)\}_{s=1}
\end{aligned}$$

For $s = 1, j = 0,$

$$\frac{d}{ds} \left[\begin{matrix} -(s-1) \\ 0 \end{matrix} \right]_{s=1} = \frac{d}{ds} \frac{(-s+1)!}{0!(-s+1)!} \Big|_{s=1} = \frac{d}{ds} 1 \Big|_{s=1} = 0.$$

For $s = 1, j = 1,$

$$\frac{d}{ds} \left[\begin{matrix} -(s-1) \\ 1 \end{matrix} \right]_{s=1} = \frac{d}{ds} \frac{(-s+1)!}{0!(-s+1-1)!} \Big|_{s=1} = \frac{d}{ds} (-s+1) \Big|_{s=1} = -1 = (-1)^1 0!$$

For $s = 1, j = 2,$

$$(s)(s+1) \dots (s+j-2) = (s) = 1!,$$

For $s = 1, j = 3,$

$$(s)(s+1) \dots (s+j-2) = (s)(s+1) = 2!$$

For $s = 1, j = k,$

$$(s)(s+1) \dots (s+j-2) = (1)(2) \dots (k-1) = (k-1)!, k \geq 2, \text{ then}$$

$$\frac{d}{ds} \left[\begin{matrix} -(s-1) \\ j \end{matrix} \right]_{s=1} = \frac{(-1)^j}{j!} \begin{cases} 0 \text{ for } j = 0 \\ (j-1)! \text{ for } j \geq 1 \end{cases} = (-1)^j \begin{cases} 0 \text{ for } j = 0 \\ \frac{1}{j} \text{ for } j \geq 1 \end{cases} \quad (4.42)$$

By substituting (4.42) into (4.41), we have

$$\sum_{j=1}^k (-1)^{2j} \left(\frac{1}{j} \right) \nabla^j y_{n+1} = h f_{n+1}$$

Since $(-1)^{2j} = 1$, for all $j \geq 1$, then

$$\sum_{j=1}^k \left(\frac{1}{j} \right) \nabla^j y_{n+1} = h f_{n+1} \quad (4.43)$$

These multistep methods are called backward differentiation formulae (BDF) methods [66]. \mathbf{K} is the order of the BDFs. For the case $k= 1, 2, 3, 4,$ and $5,$ the equation (4.43) gives

k= 1,

$$y_{n+1} = y_n + hf_{n+1} \quad (4.44)$$

k= 2,

$$y_{n+1} = \left(\frac{4}{3}\right)y_n - \left(\frac{1}{3}\right)y_{n-1} + \left(\frac{2}{3}\right)hf_{n+1} \quad (4.45)$$

k= 3,

$$y_{n+1} = \left(\frac{18}{11}\right)y_n - \left(\frac{9}{11}\right)y_{n-1} + \left(\frac{2}{11}\right)y_{n-2} + \left(\frac{6}{11}\right)hf_{n+1} \quad (4.46)$$

k= 4,

$$y_{n+1} = \left(\frac{48}{25}\right)y_n - \left(\frac{36}{25}\right)y_{n-1} + \left(\frac{16}{25}\right)y_{n-2} - \left(\frac{3}{25}\right)y_{n-3} \\ + \left(\frac{12}{25}\right)hf_{n+1} \quad (4.47)$$

k= 5,

$$y_{n+1} \\ = \left(\frac{300}{137}\right)y_n - \left(\frac{300}{137}\right)y_{n-1} + \left(\frac{200}{137}\right)y_{n-2} - \left(\frac{75}{137}\right)y_{n-3} + \left(\frac{12}{137}\right)y_{n-4} \\ + \left(\frac{60}{137}\right)hf_{n+1} \quad (4.48)$$

The stability of numerical methods is an important parameter and is indicated by their region of absolute stability. If the region contains the left half of the complex plane, the method is said to be A-stable. However, linear multistep methods with an order greater than two cannot be A-stable. The stability region of the higher-order BDF methods

contains a large part of the left half-plane and, in particular, the whole of the negative real axis. The BDF methods are the most efficient linear multistep methods of this kind [68].

4.3.2 KLOPFENSTEIN- SHAMPINE FAMILY OF NDFS

BDFs allow us to use high-order formulae, but their most significant drawback is the poor stability properties for higher-order. Several efforts to derive methods with better accuracy and stability properties than those in BDFs have been made.

One of the modifications made to the BDFs in this line is the NDFs (Numerical Differentiation Formulae) done by Klopfenstein and Shampine. It is a computationally cheap modification that consists of anticipating a difference of the order $(n+1)$ term multiplied by a constant $\kappa\gamma_k$ in the BDF formulae of order k . This term is equivalent to the error in the (k^{th}) term occurring in the BDFs and thus reduces the error constant of BDF and owing to which larger time step can be taken with the same accuracy as of BDFs and not much less stable. Then the k -step NDF of order k is

$$\sum_{m=1}^k \frac{1}{m} \nabla^m y_{n+1} = hf_{n+1} + \kappa\gamma_k (y_{n+1} - y_{n+1}^{[0]}) \quad (4.49)$$

Where “ κ ” is a scalar parameter and $\gamma_k = \sum_{j=1}^k \frac{1}{j}$

Klopfenstein found numerically the value of “ κ ” that maximizes the angle of A-stability. The addition of this new term has this advantage of giving rise to the same accuracy and higher stability for stiff ODEs as that of BDFs but with a bigger time step. These multistep methods are called numerical differentiation formulae (NDF) methods. It is also to be noted that for $\kappa = 0$ or $\gamma_{\kappa=0}$, NDFs reduces to BDFs. \mathbf{K} is the order of

the NDFs. Because NDFs, like BDFs, are implicit integrators, they have to be solved iteratively, usually using a Newton method. For both methods, the recommended initial starting point for the iteration is

$$y_{n+1}^{[0]} = \sum_{j=0}^k \nabla^j y_n \quad (4.50)$$

This represents an extrapolation from k past values and provides an estimate from which to start the iteration process. The last term in the bracket of equation (4.49) can be given as:

$$y_{n+1} - y_{n+1}^{[0]} = \nabla^{k+1} y_{n+1} \quad (4.51)$$

For the case k= 1, 2, 3, 4 and 5 the equation (4.49) for NDFs gives [68]

k= 1,

$$hf_{n+1} = y_{n+1} - y_n - \kappa_1 \gamma_1 (y_{n+1} - 2y_n + y_{n-1}) \quad (4.52)$$

k= 2,

$$hf_{n+1} = \frac{3}{2}y_{n+1} - 2y_n + \frac{1}{2}y_{n-1} + \kappa_2 \gamma_2 (y_{n+1} - 3y_n + 3y_{n-1} - y_{n-2}) \quad (4.53)$$

k= 3,

$$hf_{n+1} = \frac{11}{6}y_{n+1} - 3y_n + \frac{3}{2}y_{n-1} - \frac{1}{3}y_{n-2} + \kappa_3 \gamma_3 (y_{n+1} - 4y_n + 6y_{n-1} - 4y_{n-2} + y_{n-3}) \quad (4.54)$$

k= 4,

$$\begin{aligned}
hf_{n+1} = & \frac{25}{12}y_{n+1} - 4y_n + 3y_{n-1} - \frac{4}{3}y_{n-2} + \frac{1}{4}y_{n-3} \\
& + \kappa_4\gamma_4(y_{n+1} - 5y_n + 10y_{n-1} - 10y_{n-2} + 5y_{n-3} \\
& - y_{n-4})
\end{aligned} \tag{4.55}$$

k= 5,

$$\begin{aligned}
hf_{n+1} = & \frac{137}{60}y_{n+1} - 5y_n + 5y_{n-1} - \frac{10}{3}y_{n-2} + \frac{5}{4}y_{n-3} - \frac{1}{5}y_{n-4} \\
& + \kappa_5\gamma_5(y_{n+1} - 6y_n + 15y_{n-1} - 20y_{n-2} + 15y_{n-3} - 6y_{n-4} \\
& + y_{n-1})
\end{aligned} \tag{4.56}$$

4.3.3 NOVELTY OF NDFS OVER MATRIX EXPONENTIAL METHODS

Use of K-S family of NDFs in the fuel cycle analysis is new and has not been used before. The advantage of this method is that the stiffness of any order can be handled, therefore partitioning of short and long lived isotopes is not required as in the case of other codes [31]. K-S family of NDFs used in IGDC can also handle the non-linear set of first order differential equations and therefore explicit flux variation can be coupled with Bateman equations and hence neutron flux need not be treated as constant for the time step of integration as in the other codes [31].

4.3.4 NOVELTY OF NDFs OVER BDFs

To understand the difference between BDF and NDF, consider the BDF1 and NDF1.

BDF1:

$$y_{n+1} = y_n + hf_{n+1} \tag{4.57}$$

NDF1:

$$y_{n+1} = y_n + hf_{n+1} + \kappa_1 \gamma_1 (y_{n+1} - 2y_n + y_{n-1}) \quad (4.58)$$

BDF1 is Euler's implicit method, and error in this method can be obtained by comparing it with the Taylor series.

$$\text{TE in BDF1} = \frac{h^2}{2} y''_{n+1} = \frac{h^2}{2} \frac{(y_{n+1} - y_n)'}{h} = \frac{1}{2} (y_{n+1} - 2y_n + y_{n-1}) \quad (4.59)$$

Equation (4.57), (4.58), and (4.59) shows that in NDF1, a term analogous to the Truncation error (TE) of BDF1 is added to improve the accuracy of NDF1 over BDF1.

A similar comparison of NDF and BDF of higher order can also be carried out. A comparison of various order BDF and NDF is given in the Table-4.1 [3].

Table 4.1: Co-efficient of NDFs and $A(\alpha)$ comparisons relative to BDFs

Order	NDF co-efficient		Step ratio (%)	Stability angle $A(\alpha)$ (Degree)		Percentage change
	κ	γ_κ		BDF	NDF	
1	-0.185	1	26	90	90	0
2	-1/9	3/2	26	90	90	0
3	-0.0823	11/6	26	86	80	7
4	-0.0415	25/12	12	73	66	10
5	0	137/60	0	51	51	0

From this table, a clear difference between BDFs and NDFs can be observed and is summarized below:

1. NDFs for orders 1 and 2 can provide the same accuracy and stability as BDFs with increased step size for about 26%.

2. NDFs for order three can provide the same accuracy and stability as that of BDFs with increased step size for about 26% but at the cost of reduced stability by about 7%.
3. NDFs for order four can provide the same accuracy and stability as that of BDFs with increased step size for about 12% but at the cost of reduced stability by about 10%.
4. NDFs of order 5 are the same as the BDF of order 5 concerning accuracy and stability with the same step size.

Therefore, the choice of the method becomes problem-dependent. However, to increase the accuracy with a higher time step, the Klopfenstein-Shampine family of NDFs is used for nuclear fuel cycle analysis. Stability regions (external to the contours) of BDF and NDF are shown in Figure 4.3 below (In this figure, h is the time step of integration, and λ is the Eigenvalues of the matrix for linear system and Eigenvalues of the Jacobian matrix for a non-linear system of ODEs).

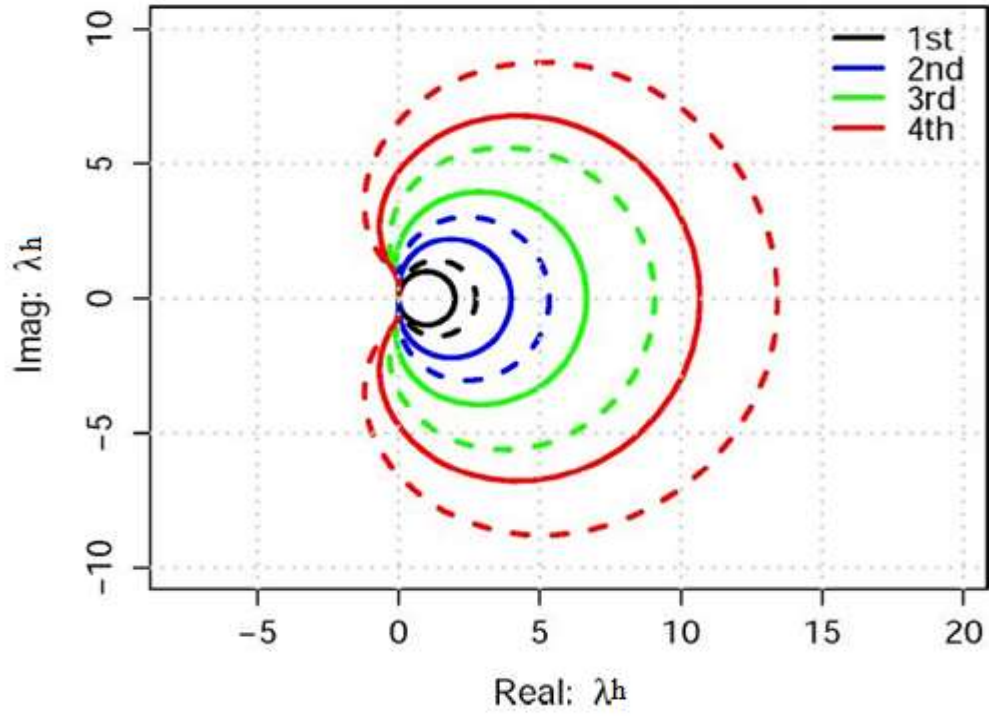


Figure 4.3: Stability regions of BDF (Solid) and NDF (Dotted)[68]

4.3.3 IMPLEMENTATION OF NDF

To implement the algorithm based on NDFs, one has to find the solution of (4.49) by iteration [68].

$$\text{Let } g = \sum_{m=1}^k \frac{1}{m} \nabla^m y_{n+1} - hf(t_{n+1}, y_{n+1}) - \kappa \gamma_\kappa \nabla^{k+1} y_{n+1} = 0 \quad (4.57)$$

Jacobian of the function g is defined as:

$$J = \frac{dg}{dy_{n+1}} = - \left[-(\alpha_0 - \kappa \gamma_\kappa) + h \frac{df(t_{n+1}, y_{n+1})}{dy_{n+1}} \right] \quad (4.58)$$

Applying Newton's method iteration scheme to get y_{n+1} , one can get

$$\Delta y^s = -J^{s-1} g^s \quad (4.59)$$

$$y^{s+1} = y^s + \Delta y^s \quad (4.60)$$

$$\text{i.e. } y_{n+1} = y_n + \left(\frac{\Delta t}{\rho(J_0)}\right) f(t, y) + \kappa\gamma(y_{n+1} - 2y_n + y_{n-1}) \dots (4.63)$$

Since $\mathbf{f}(t, \mathbf{y})$ is a non-linear function of \mathbf{y} , therefore equation (4.63) will also be a non-linear and its solution can be obtained by Newton's method till the error tolerance condition is reached i.e.

$$y^s - y^{s-1} < \varepsilon \dots \dots \dots (4.64)$$

Step 6: If the condition (4.64) is not satisfied, change the order and repeat the steps from (4) and (5).

Step 7: If the condition (4.64) is satisfied, the system of equations are solved for the first time step.

Step 8: Repeat the steps from (1) to (7) for all remaining time steps.

4.4 FLOW DIAGRAM OF THE CODE

To have a clear understanding of the development of this code, all the steps should be understood sequentially. These steps are described below:

1. In the **first step** towards developing the computer code IGDC, a model for the generation and depletion of fission products and actinides was developed. Technically these are called Bateman equations, which are formulated and solved in computer code IGDC.
2. Spectrum averaged self-shielded nuclear cross-sections are an essential part of the burn-up code; therefore, the neutron spectrum in a PHWR fuel was generated through the computer code WIMS-D in the **second step**. As mentioned in Chapter 1, this code and its method were tested for the fuel cycle analysis of PT-HWR.

3. ENDF files were processed using PREPRO-2012, and different nuclear reaction cross-sections were weighted for PT-HWR fuel spectra, and complete library for 1-Group unshielded cross-section for various nuclei is prepared in the **third step**.
4. It is essential to generate the self-shielded cross-section for the important nuclei initially present in the fuel of PT-HWR (U^{235} and U^{238}). Self-shielded 1-Group cross-sections of these isotopes were generated using Bondarenko self-shielding factor approach in the **fourth step**.
5. Nuclear data (Decay data, Fission yield data, Energy released in isotopic decay and Dose Conversion Factors) library is prepared using various sources like JANIS, ENSDF files, NUBASE, JENDL FP Decay Data File 2011 and Fission Yields Data File 2011 and Compendium of Dose Coefficients based on ICRP Publication 60 & ICRP publication 119 in the **fifth step**.
6. The computer code IGDC (Isotopic Generation and Depletion Code) is written on MATLAB14 based on the algorithm of Klopfenstein–Shampine family of NDFs and can be used for any reactor type in the **sixth step**.

The flow diagram of the computer code IGDC is shown in Figure 4.4.

4.5 SUMMARY

The complex problem of the simultaneous solution of isotope generation and depletion has been solved for the first time using a numerical technique that can be used for decay half-lives of varying order (Pico seconds to millions of years). The stiff ODEs are required to be solved for several isotopes for any instant of time, taking into account the neutron flux distribution and the nuclide concentrations. The code IGDC has been

developed for a fuel cycle analysis using the numerical differentiation formula and successfully implemented for the solution of the fuel of PT-HWR.

The flow of development of the computer code IGDC

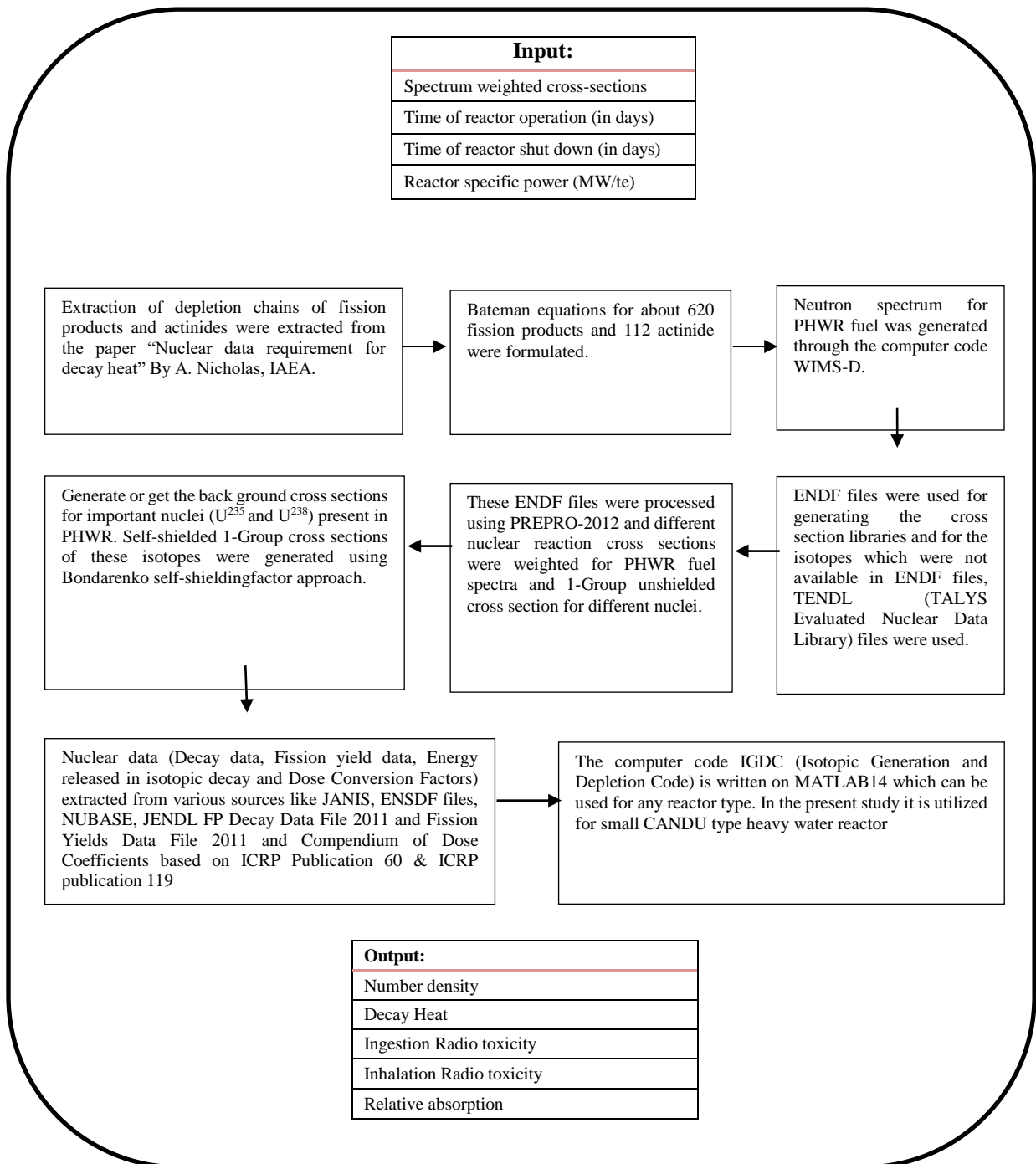


Figure 4.4: Detailed flow chart of the computer code “IGDC.”

In order to benchmark the code and its method, the analysis of PT-HWR fuel was taken up. After the development of the computer code IGDC, this code was utilized for the PT-HWR. The next chapter focuses on the benchmarking of the newly developed code IGDC.

Chapter 5

Benchmarking and Analysis of PT-HWR fuel cycle with IGDC

5.0 INTRODUCTION

The objective of the nuclear fuel cycle analysis in this research work is to simulate the nuclear fuel during irradiation in a nuclear reactor and out of the reactor after discharge to estimate the inventory of radionuclides generated during irradiation in the core. This necessary information on isotopic inventory is further utilized to estimate radio-activity, radiotoxicity, decay heat, relative neutron absorption by different fission products, and clearance potential of various radionuclides.

IGDC code is developed based on the new numerical technique. The next step is to validate the method and benchmark the new code. Although several simulations were done earlier for the natural uranium fuelled PT-HWR fuel, a comprehensive front end and back end analysis with spectrum average nuclear data has not been done before. Therefore, as mentioned earlier (in chapter-4), the fuel cycle studies for PT-HWR was taken up for this validation exercise. From the detailed literature survey, specific benchmarks for this type of fuel were selected. The concentrations of radionuclides, their activity, decay heat, and potential radio-toxicities have been calculated for the PT-HWR wherever possible; the results were compared with other code systems and experiments.

Results of the fuel cycle analysis of PT-HWR with the developed computer code IGDC and their benchmarking with other similar codes and through different experimental results are presented in this chapter. The fuel used in a PT-HWR is the standard 19 element UO_2 as mentioned in Chapter 3.

5.1 VALIDATION OF THE COMPUTER CODE IGDC

Computer codes should be well validated for their intended use. The purpose of validation of computer code is to ensure an acceptable degree of documented evidence that establishes confidence in the accuracy, reliability, and consistency in the performance of the code. To this end, computer code IGDC has been validated against different benchmarked codes and experiments.

5.1.1 VALIDATION FOR ISOTOPIC INVENTORY

Validation of the code is carried out with inter-code comparison results presented in IAEA TECDOC-887. In this validation the aim was to benchmark the in-core inventories of the fuel irradiated in PT-HWR. Estimating the concentration of U^{235} and Pu^{239} at 4000 MWd/te and 8000 MWd/te (approximately average in-core and discharge burn-up of 220 MWe class PT-HWRs respectively) by the code “IGDC” is comparable with the concentration of these isotopes by other codes. The comparison of concentrations is given in Table 5.1. The percentage difference in the concentration of U^{235} and Pu^{239} with different computer codes used worldwide is shown in Table 5.2. This table shows that the estimation of concentrations by the computer code IGDC matches reasonably well with the computations carried out by other codes.

Table 5.1: Comparison of ^{235}U and ^{239}Pu inventory with different codes

CODE	Nation	U^{235} (g/kg)		Pu^{239} (g/kg)		REF.
		4000 MWd/t	8000 MWd/t	4000 MWd/t	8000 MWd/t	
PPV	Argentina	3.822	2.044	1.928	2.407	[57]
PPV	Canada	3.786	1.996	1.941	2.414	[57]
PPV	Romania	3.789	1.997	1.939	2.413	[57]
WIMSD-4	Argentina	3.837	2.073	1.979	2.539	[57]
WIMSD-4	Korea	3.800	2.029	1.928	2.483	[57]
WIMSD-4	Pakistan	3.791	2.006	2.021	2.557	[57]
WIMSD-4	Romania	3.747	1.961	2.095	2.728	[57]
CLUB	India	3.796	2.020	1.931	2.490	[57]
CLIMAX	India	3.807	2.049	1.947	2.512	[57]
RHEA	India	3.984	2.204	1.861	2.470	[57]
IGDC	-	3.832	1.982	2.102	2.688	Present study
Mean Value		3.817	2.033	1.970	2.518	-
Std. Dev.		0.061	0.065	0.074	0.107	-

N.B.: The version of the lattice code WIMS used in Argentina, Korea, Pakistan, and Romania is the WIMSD-4, which uses 69 group WIMS library.

Table 5.2: Difference of concentration of U^{235} and Pu^{239} with different codes

CODE	Nation	Percentage difference in U^{235} (%)		Percentage difference in Pu^{239} (%)	
		4000 MWd/t	8000 MWd/t	4000 MWd/t	8000 MWd/t
PPV	Argentina	-0.3	3.1	-8.3	-10.5
PPV	Canada	-1.2	0.7	-7.6	-10.2
PPV	Romania	-1.1	0.8	-7.7	-10.3
WIMS	Argentina	0.1	4.6	-5.8	-5.6
WIMS	Korea	-0.8	2.4	-8.2	-7.6
WIMS	Pakistan	-1.1	1.2	-3.8	-4.9
WIMS	Romania	-2.2	-1.1	-0.3	1.5
CLUB	India	-0.9	1.9	-8.1	-7.4
CLIMAX	India	-0.7	3.4	-7.3	-6.6
RHEA	India	4.0	11.2	-11.4	-8.1
Average		-0.4	2.8	-6.9	-7.0

Minor differences may be due to the difference in the method used for solving the Bateman equations and the cross-section library.

5.1.2 VALIDATION FOR DECAY HEAT

IGDC was also validated with experiments. Experimental verification of the computer code IGDC for the decay heat estimation was carried out by comparing the decay heat measurements performed by Ontario Hydro using Douglas point CANDU reactor irradiated fuel bundles of varying irradiation histories, estimation by ORIGEN-S and those of the ANSI / ANS-5.1-1979, the American National Standard for decay heat power. In addition to the total decay heat, gamma decay heat for irradiated fuel assemblies was also estimated and compared with those of the ORIGEN-S estimations. The spent CANDU fuel was simulated in IGDC as per the power history given in Table 5.3 of the fuel bundles independently, i.e., a multi-step simulation of IGDC was carried out for each fuel bundle.

Table 5.3: Irradiation history Fuel Assemblies of Douglas Point reactor

Bundle ID	IRRADIATION DAYS (D)	Bundle Power (kW)	Average Burn-up (MWh/kgU)	Average Corrected Power (kW)	Total Cooling Time (Days)
T0906	106	157.7	29.6	161.2	224
	103	125	52.2	127.8	
	33	0	52.2	0	
	196	186.4	116.9	190.6	
	13	0	116.9	0	
	273	165	196.7	168.7	
	37	0	196.7	0	
	78	132.5	215	135.5	
B1106	162	252.3	72.4	257	596
	11	0	72.4	0	
	9	175.6	75.2	178.9	
	88	0	75.2	0	

Bundle ID	IRRADIATION DAYS (D)	Bundle Power (kW)	Average Burn-up (MWh/kgU)	Average Corrected Power (kW)	Total Cooling Time (Days)
	229	130.4	128.1	132.8	
	33	0	128.1	0	
	184	195.4	191.8	199.1	
	13	0	191.8	0	
	15	207	197.3	210.9	
R1206	40	220.2	15.6	223.9	776
	270	0	15.6	0	
	214	256.7	112.9	261	
	88	0	112.9	0	
	65	231.9	139.6	235.8	
	31	105.6	145.4	107.4	
	135	143.4	179.7	145.8	
	33	0	179.7	0	
	299	186.9	189.13	190	
G1706	165	272.1	80	276.4	1048
	273	0	80	0	
	76	292.3	119.4	296.9	
	7	0	119.4	0	
	106	287.6	173.4	292.1	
	16	0	173.4	0	
	9	250.9	177.4	254.9	
	88	0	177.4	0	
	15	293.6	185.2	298.2	
H0906	105	395.2	73.5	407.9	1050
	76	0	73.5	0	
	166	314.6	166	324.7	
	270	0	166	0	
	192	294.1	266	303.5	
	13	0	266	0	
	9	282.3	270.5	291.4	
	88	0	270.5	0	
	17	338.7	280.7	349.6	
5622	102	259.9	46.6	269.6	1749
	31	0	46.6	0	
	161	229	111.9	237.5	
	165	244	183.2	253.1	
	41	0	183.2	0	
	258	270	306.4	280	
	76	0	306.4	0	

Bundle ID	IRRADIATION DAYS (D)	Bundle Power (kW)	Average Burn-up (MWh/kgU)	Average Corrected Power (kW)	Total Cooling Time (Days)
	53	282.3	333.9	292.8	
4821	230	26	10.6	27	2014
	181	169.1	64.8	175.4	
	243	187.3	145.4	194.3	
	127	0	145.4	0	
	113	152.4	175.9	158.1	
	181	159.1	226.9	165	
	165	206.3	287.2	214	
	41	0	287.2	0	
	120	223.1	334.6	231.4	
4640	230	7.6	3.1	7.8	2200
	151	59.4	19	60.9	
	50	0	19	0	
	227	127.8	70.4	131	
	127	0	70.4	0	
	105	200.6	107.5	205.5	
	31	0	107.5	0	
	161	208.7	167	213.8	
	144	236.3	227.3	242.1	

Benchmarking workflow for the fuel bundle ID T0906 is shown in Figure 5.1. A similar benchmarking procedure based on their operating history was followed for other fuel bundles also.

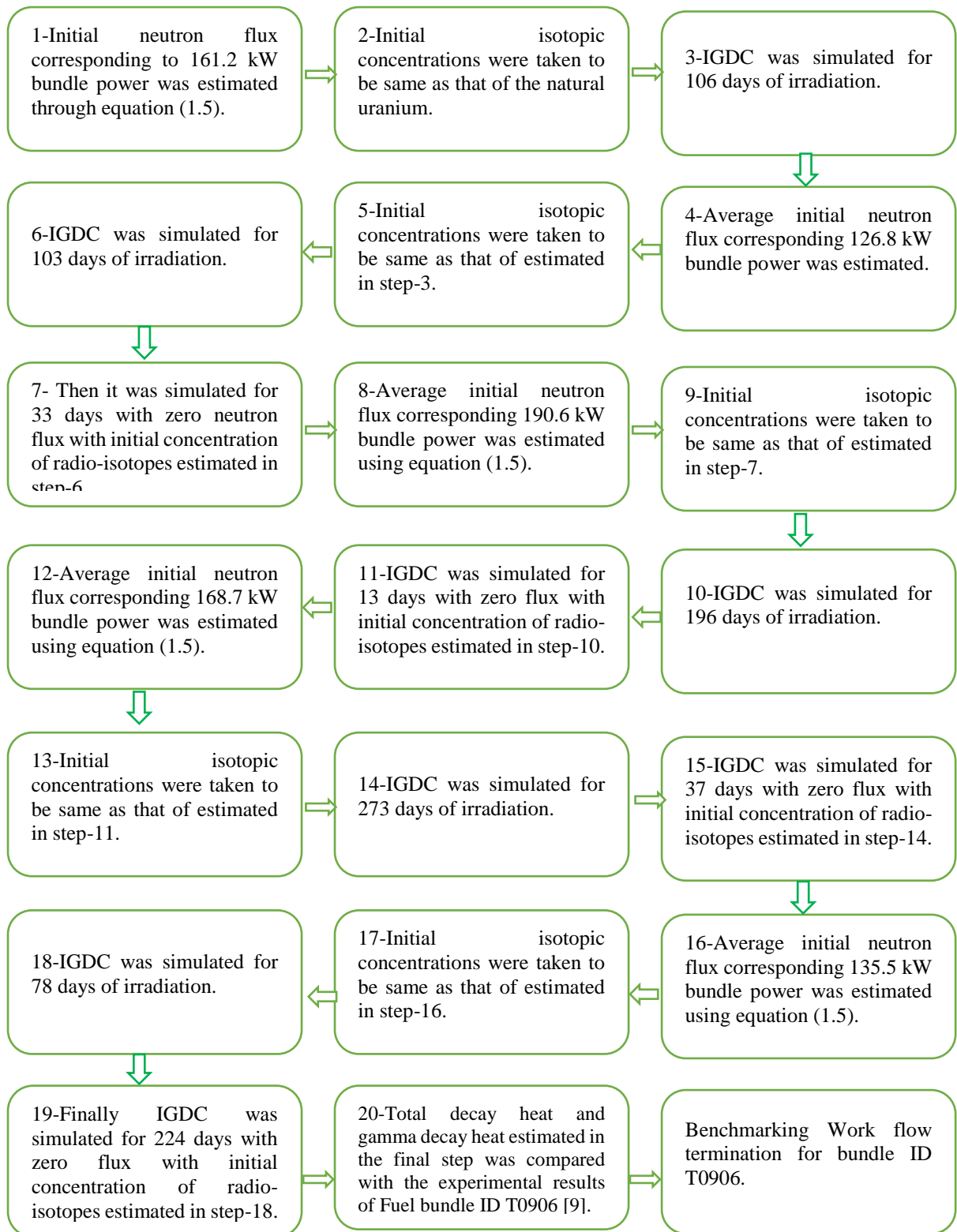


Figure 5.1: Benchmarking workflow for the bundle ID T0906

The comparison of total decay heat and gamma decay heat is provided in Table 5.4 & Table 5.5.

Table 5.4: Decay heat of Douglas Point Reactor with different codes

Bundle ID	Total Cooling Time (Days)	Decay Heat (Watt)				Percentage difference (%)		
		Measured* (M) Ref: [56]	ANS-5.1 (A) Ref: [5656]	ORIGEN-S (O) Ref: [5656]	IGDC (I) Present Study	((M-A) 100/M)	((M-O) 100/M)	((M-I) 100/M)
T0906	224	53.6	51.8	53.5	50.5	3.4	0.2	5.8
B1106	596	20.8	20.4	21.8	20.1	1.9	-4.8	3.4
R1206	776	15.4	13.7	15	13.1	11.0	2.6	14.9
G1706	1048	9.9	8.79	9.8	9.13	11.2	1.0	7.8
H0906	1050	14.7	12.5	14.4	13.9	15.0	2.0	5.4
5622	1749	10.1	7.92	9.6	10.9	21.6	5.0	-7.9
4821	2014	8.8	6.66	7.4	9.59	24.3	15.9	-9.0

* The overall combined uncertainty of the experiment and irradiation history parameters of $\pm 7\%$.

Table 5.5: Comparison of Gama decay heat of Douglas Point Reactor

Bundle ID	Total Cooling Time (Days)	Gamma Decay Heat (Watt)		Percentage difference (%)
		ORIGEN-S (O) Ref: [56]	IGDC (I) Present Study	((O-I)100/O)
T0906	224	13.1	14.6	-11.5
B1106	596	3.8	3.8	-0.8
R1206	776	2.9	2.6	10.3
G1706	1048	2.2	2.3	-4.5
H0906	1050	3.8	4.1	-7.9
5622	1749	3.4	3.7	-9.4
4821	2014	3.0	3.2	-8.3

Experimental verification of the decay heat was carried out with the measured decay heat of Douglas Point Reactor. The difference between measured and estimated (through IGDC) total decay heat $\leq \pm 15.0\%$ compared to the measurement and irradiation history uncertainty of $\pm 7.0\%$. The unaccounted difference may be attributed to the different factors viz. exact weight of uranium in the fuel assembly, uncertainties in the cross-sections, fission yield data, decay data, and the number of isotopes considered for analysis. This validation exercise proved the correctness of programming and the stability of the code. However, we need more validation in the future to make the code available for broader use for other reactor types.

5.1.3 VALIDATION FOR ACTIVITIES AND CONCENTRATION

Experimental results are available for specific activities and concentrations of different isotopes [69] for pressure tube type reactors. IGDC was simulated in similar conditions of neutron flux and power to verify the theoretical predictions with experimental results. Table 5.6 shows a significant difference of about 30 and 45% in the estimated activity with respect to the experimental results for Tc^{99} and I^{129} . These differences are outside the analytical uncertainty and must be attributed to the losses during a chemical separation or, in the case of Tc^{99} , to incomplete recovery due to its association with metallic residues that could not be dissolved entirely [69]. However, Am^{241} and Cs^{137} activities were evaluated within the experimental accuracy of 5%.

Table 5.6: Measured and estimated activities in PT-HWR [69]

Isotope	*Measured (Bq/kg U) M	Measurement uncertainty [%]	IGDC (Bq/kg U) I	*ORIGEN-S (Bq/kg U) O	<u>(I-M)</u> <u>100/M (%)</u>	<u>(O-M)</u> <u>100/M (%)</u>
Am ²⁴¹	1.86E+10	± 20	1.78E+10	1.92E+10	-4.3	3.23
Tc ⁹⁹	1.08E+08	± 10	1.56E+08	1.50E+08	44.44	38.89
I ¹²⁹	2.44E+05	± 0	1.73E+05	3.62E+05	-29.1	48.36
Cs ¹³⁷	8.05E+11	± 5	8.32E+11	7.88E+11	3.35	-2.11

Table 5.7 shows a noticeable difference of about 21% in the estimation of ²³⁴U concentration with respect to the experimental results. These differences may be due to the experimental uncertainty. The reported results from ORIGEN-S also show such deviations.

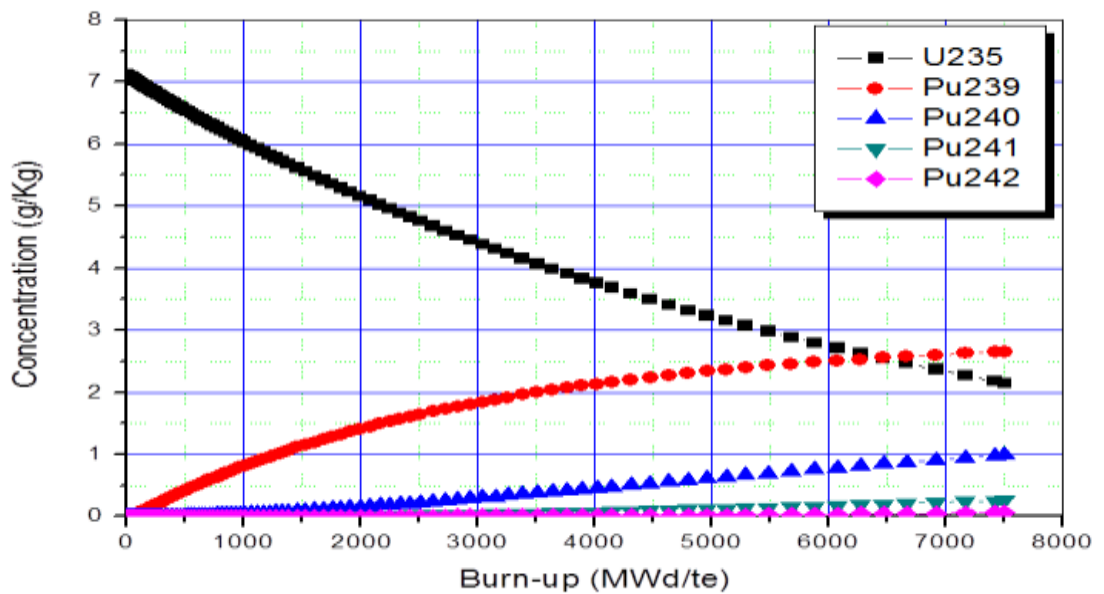
Table 5.7: Measured and estimated concentrations in PT-HWR [69]

Isotope	*Measured (g/kg U) M	Measurement uncertainty [%]	IGDC (g/kg U) I	*ORIGEN-S (g/kg U) O	<u>(I-M)</u> <u>100/M (%)</u>	<u>(O-M)</u> <u>100/M (%)</u>
U ²³⁴	3.39E-02	± 55	4.10E-02	4.23E-02	20.94	24.78
U ²³⁵	1.64E+00	± 2.4	1.62E+00	1.64E+00	-1.22	0.00
U ²³⁶	8.02E-01	± 3.7	8.19E-01	8.13E-01	2.12	1.37
U ²³⁸	9.83E+02	± 0.01	9.83E+02	9.83E+02	0.00	0.00
Pu ²³⁹	2.69E+00	± 2.5	2.82E+00	2.72E+00	4.83	1.12

5.2 CONCENTRATION OF IMPORTANT RADIO-NUCLIDES

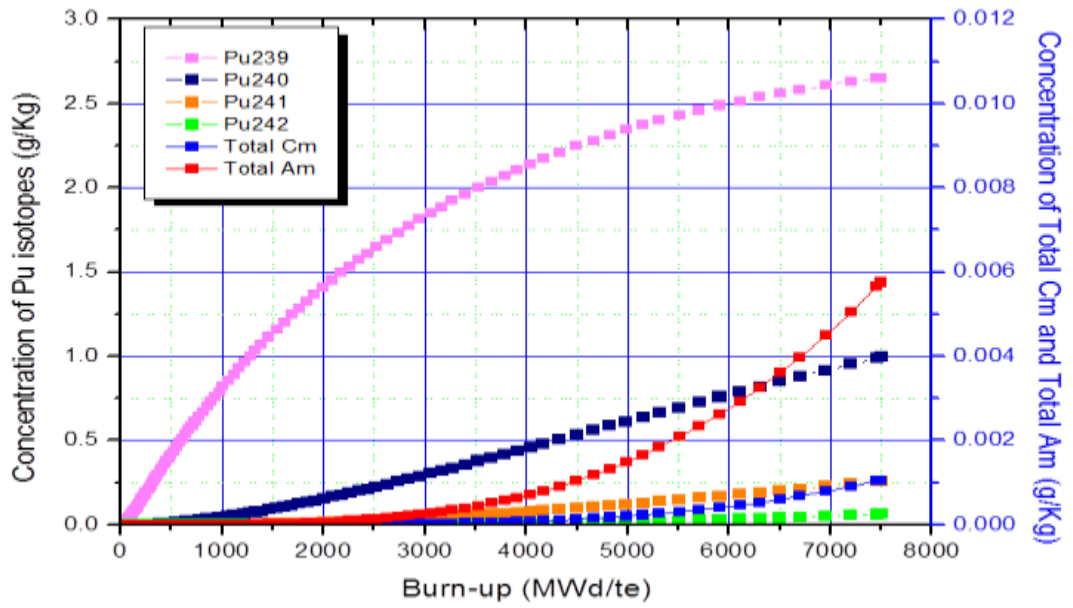
The actinides and fission products generated during irradiation and decay have been formulated. The simultaneous solutions were obtained for 112 actinides and 619 fission products using the newly developed IGDC code. As mentioned in Chapter -3, the spectrum average one-group section was generated for each of these using the PT-

HWR spectrum. The other inputs viz. decay constants, the energy liberated during the decay of isotopes, dose conversion factors, fission yield, and branching ratios have been mentioned in Chapter-1 and Annexure-4. The PT-HWR fuel has been simulated with variable time steps derived from the NDF (Numerical differentiation Formulae) formalism. The first level of analysis results is the number density of different fission products and actinides, the Bateman equations' solution. In the next level, these nuclide densities are then converted into the concentration of different isotopes with respect to the base fuel's heavy metal content [70]. Variation of important radio-nuclides for PT-HWR fuel, as calculated by IGDC, is shown in Figure 5.2 to 5.9. These sets of results are presented for the irradiation inside the PT-HWR core during the residence time of the fuel.



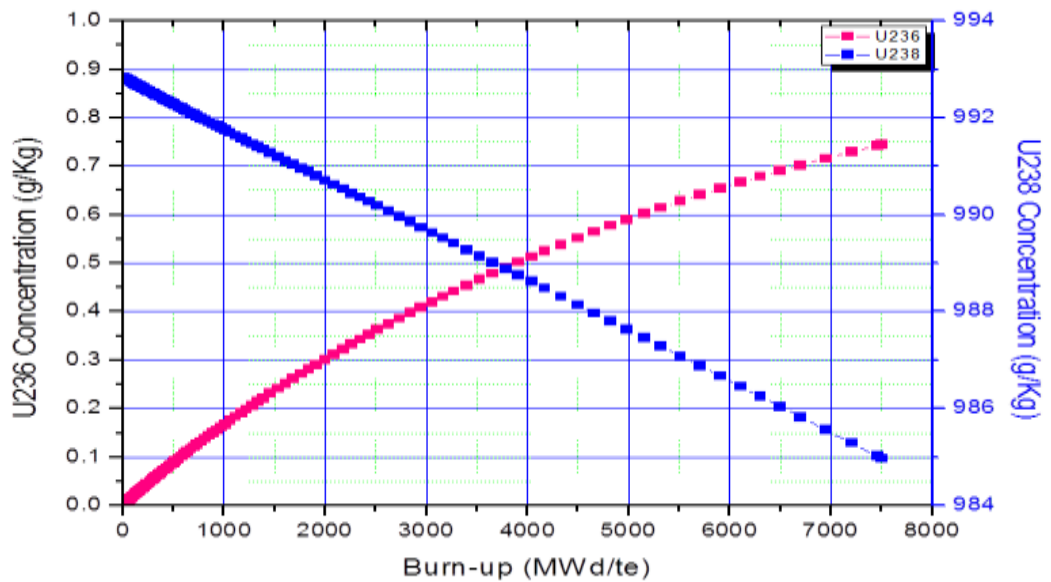
N.B.: Initial Heavy mass of the fuel bundle is approximately 13.4 kg.

Figure 5.2: Variation of uranium and plutonium isotopes with burn-up



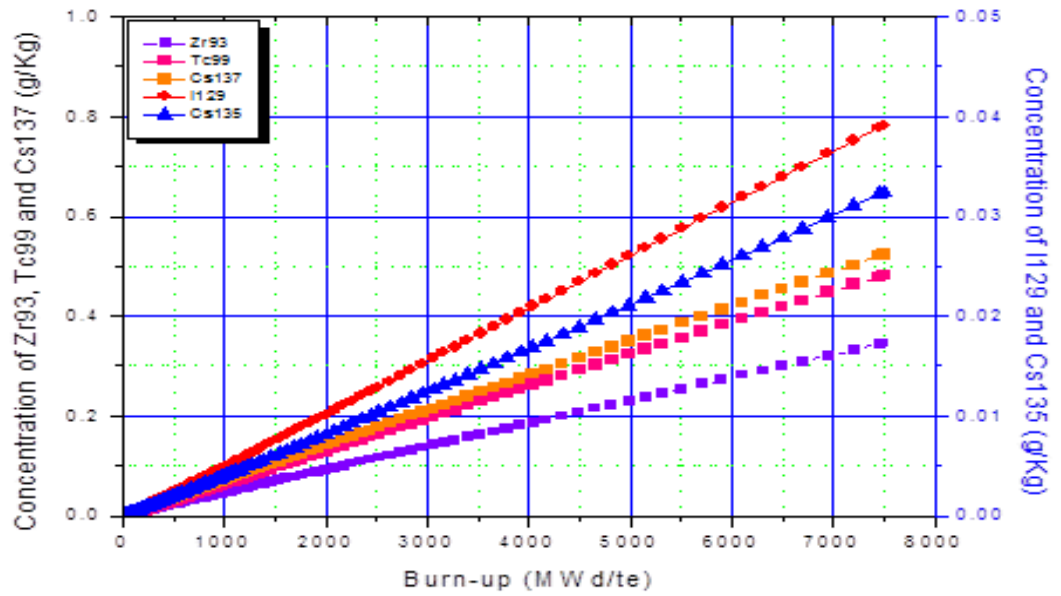
N.B.: Initial Heavy mass of the fuel bundle is approximately 13.4 kg.

Figure 5.3: Variation of plutonium, americium & curium with burn-up



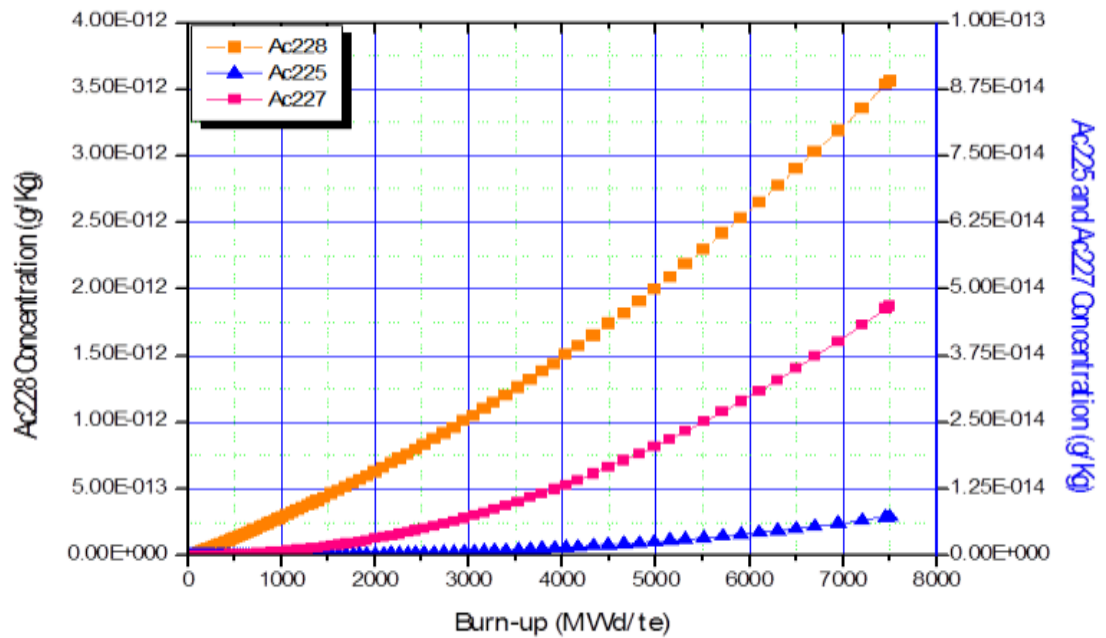
N.B.: Initial Heavy mass of the fuel bundle is approximately 13.4 kg.

Figure 5.4: Variation of U^{236} and U^{238} concentration with burn-up



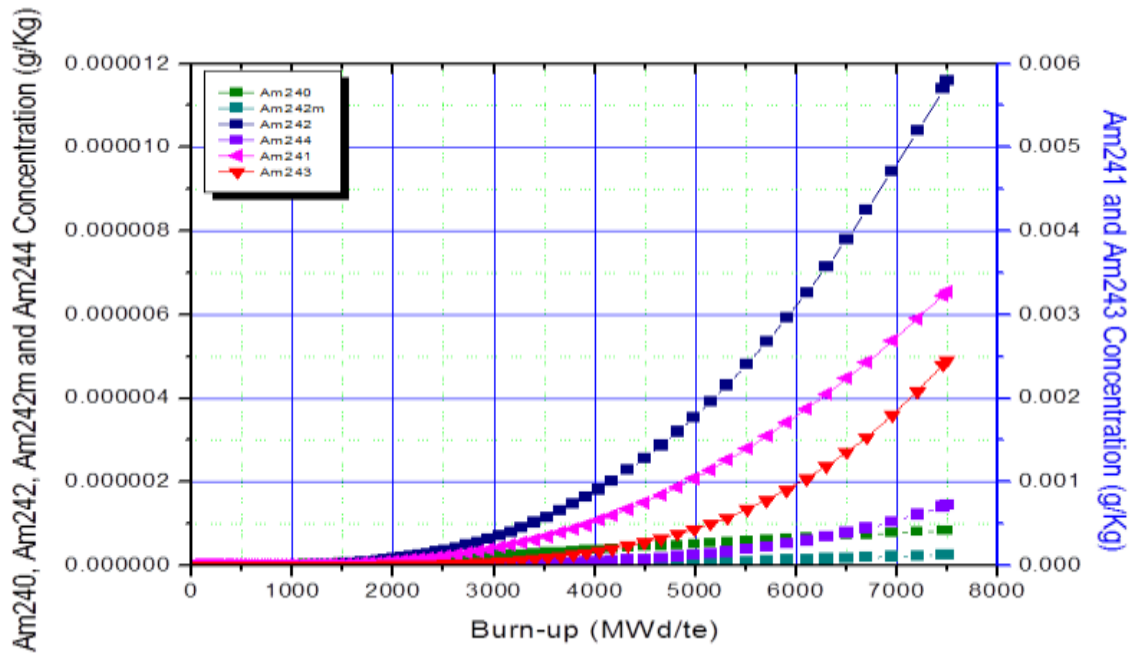
N.B.: Initial Heavy mass of the fuel bundle is approximately 13.4 kg.

Figure 5.5: Variation of non-saturating fission products with burn-up



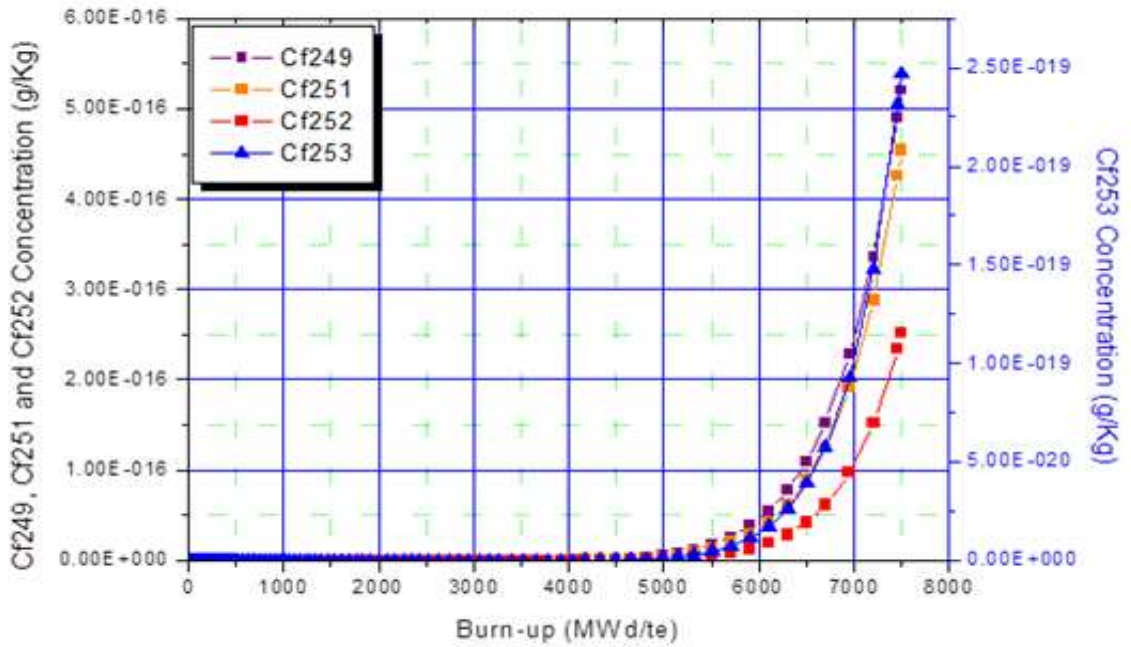
N.B.: Initial Heavy mass of the fuel bundle is approximately 13.4 kg.

Figure 5.6: Generation of actinium isotopes with burn-up



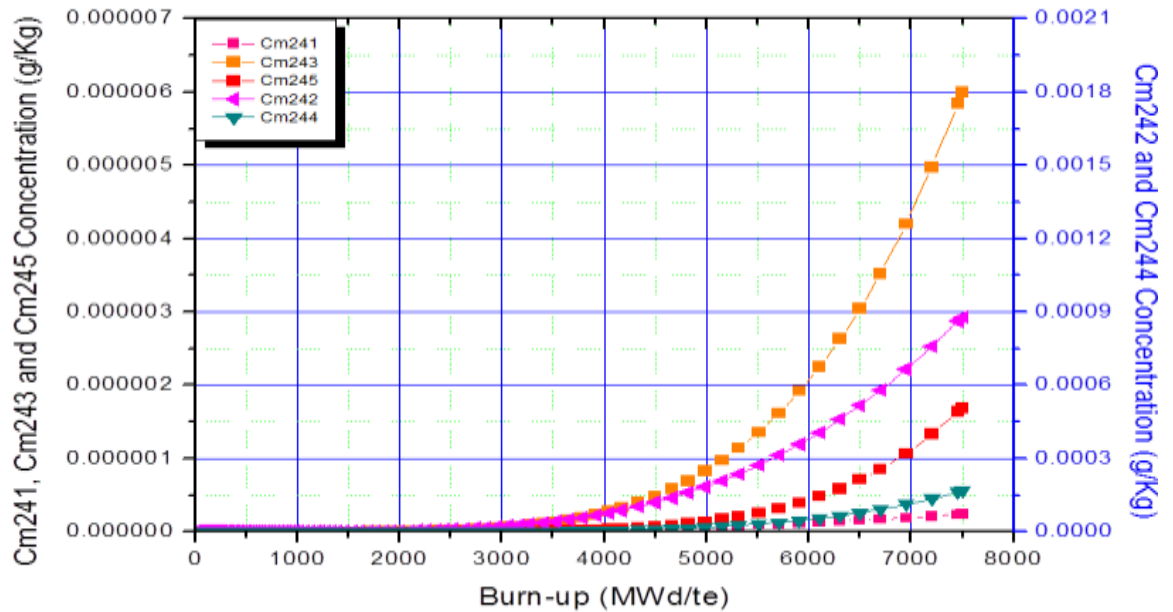
N.B.: Initial Heavy mass of the fuel bundle is approximately 13.4 kg.

Figure 5.7: Generation of americium isotopes with burn-up



N.B.: Initial Heavy mass of the fuel bundle is approximately 13.4 kg.

Figure 5.8: Generation of californium isotopes with burn-up



N.B.: Initial Heavy mass of the fuel bundle is approximately 13.4 kg.

Figure 5.9: Generation of curium isotopes with burn-up

5.3 NON-LINEAR COUPLING OF NEUTRON FLUX

The use of the K-S family of NDFs in the fuel cycle analysis code IGDC is new and has not been done before. K-S family of NDFs used in IGDC can handle the non-linear set of first-order differential equations. Therefore explicit flux variation can be coupled with Bateman equations, and hence neutron flux need not be treated as constant for the time step of integration as in the other codes. The variation of U^{235} concentration with and without the nonlinear coupling of neutron flux is shown in Figure 5.10, which shows a change in the concentration from 2.0565 to 1.9819 g/kg at 8000 MWd/te burn-up for natural uranium fuel, if nonlinear coupling of neutron flux is taken into account. The comparison of isotopic concentration at different burn-ups with nonlinear coupling

(which is used in IGDC) and without nonlinear coupling (which is generally used in matrix exponential methods such as ORIGEN2) of neutron flux is given in Table 5.8.

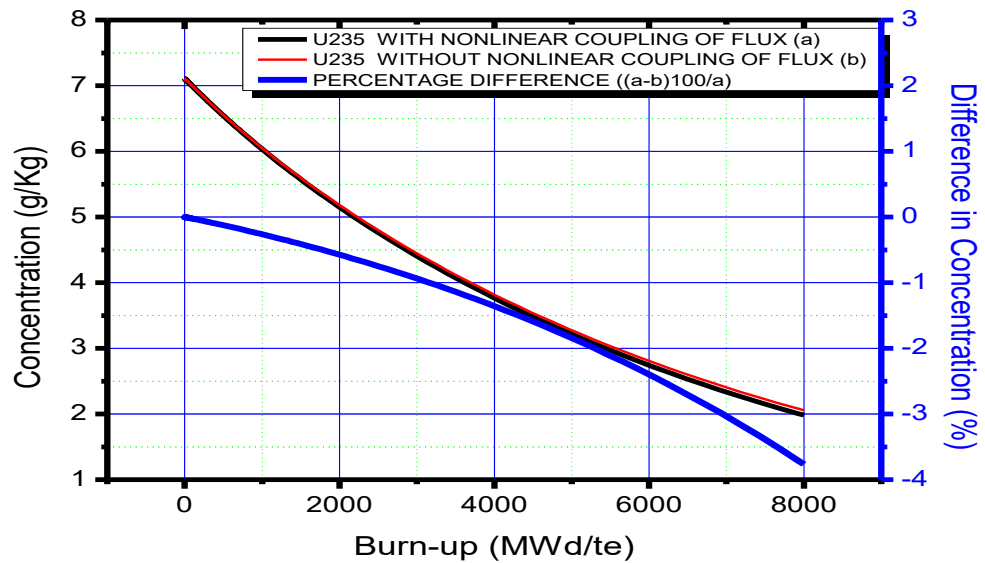


Figure 5.10: ²³⁵U Concentration with/without nonlinear coupling of neutron flux

Table 5.8: Comparison of concentration of U²³⁵ and Pu²³⁹

Burn-up (MWd/t)	U ²³⁵ Concentration with the nonlinear coupling of neutron flux (g/kg) (a)	U ²³⁵ Concentration without nonlinear coupling of neutron flux (g/kg) Col (b)	<u>Difference</u> ((a-b)/100/a) (%)	Pu ²³⁹ Concentration with nonlinear coupling of neutron flux (g/kg) c	Pu ²³⁹ Concentration without nonlinear coupling of neutron flux (g/kg) d	<u>Difference</u> ((c-d)/100/c) (%)
0	7.11	7.11	0.00	0	0	0.00
1000	6.0682	6.0822	-0.23	0.784	0.7843	-0.04
2000	5.1587	5.1843	-0.50	1.4035	1.4042	-0.05
3000	4.4506	4.4848	-0.77	1.8059	1.8067	-0.04
4000	3.832	3.8732	-1.08	2.1015	2.1024	-0.04
5000	3.237	3.2846	-1.47	2.3379	2.3388	-0.04
6000	2.7971	2.8489	-1.85	2.4832	2.484	-0.03
7000	2.3653	2.4209	-2.35	2.602	2.6028	-0.03
8000	1.9819	2.0565	-3.76	2.6883	2.6857	0.10

5.4 RADIO-ACTIVITY AND RADIO-TOXICITIES

After estimating the concentration of the radionuclide during irradiation, it is also essential to evaluate the activity in the fuel. A radioisotope decays in a number of ways, e.g., it can decay via β^- , β^+ , α , isomeric transition, or spontaneous fission. Therefore, the activity of the sample will depend upon their respective decay constants and branching ratios. The activity of a particular isotope is estimated as:

$$A_i = \sum_k (BR)_k N_i \lambda_{ik} \quad (5.1)$$

Where,

A_i is the specific activity of i^{th} isotope at time t ;

N_i is the number density of the i^{th} isotope at time t

λ_{ik} is the decay constant of the i^{th} isotope via k mode and

$(BR)_k$ is the branching ratio of k mode.

The spent fuel radioactivity is a crucial safety aspect for the reactor operation and the back end of the fuel cycle, namely reprocessing and safe disposal. The spent fuel activity in Ci/te has been estimated over millions of years. It is worth mentioning that the NDF is an efficient mathematical tool that allows solving several nuclides with varying half-lives and several branching in a single simulation.

The results have also been grouped as actinides and fission products separately to understand their behavior. The variation of activity of fission products and actinides after fuel discharge at 7500 MWd/te as calculated by IGDC is shown in Figure 5.11, which indicates that approximately 99% of the total initial activity of the discharge fuel will be reduced in about 30 years. The natural radioactivity from un-irradiated uranium is also presented in this graph. A critical comparison of the specific activity of spent

fuel and natural uranium can also be observed in this figure, which shows that about 99.99% of the fission product activity of PT-HWR spent fuel reduces in 1000 years and lies in the range of activity of the natural uranium. However, it can also be seen that fission product activity in spent fuel reduces to below the activity of natural uranium in 10^6 years.

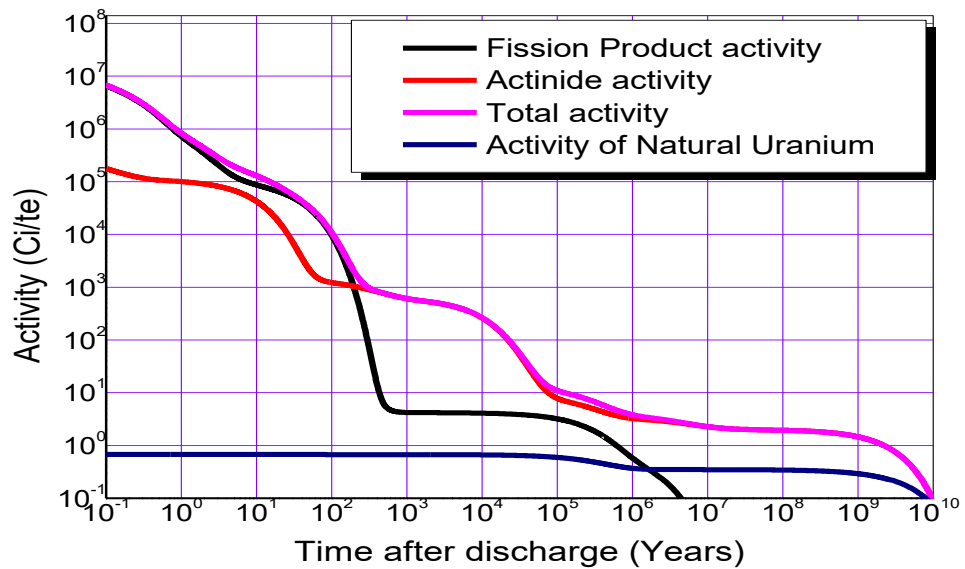


Figure 5.11: Variation of activity in PT-HWR fuel (Long Time Scale - LTS)

The above figure shows that fission product activity remains constant from 700 to 10^5 years. This phenomenon is mainly because the activity of most of the fission products decays down during the period of 700 years, but the fission product Tc^{99} , which have a fairly long half of about 211100 years, i.e., about 0.21 MY and therefore its activity (about 3.2 Ci/te) decays very slowly.

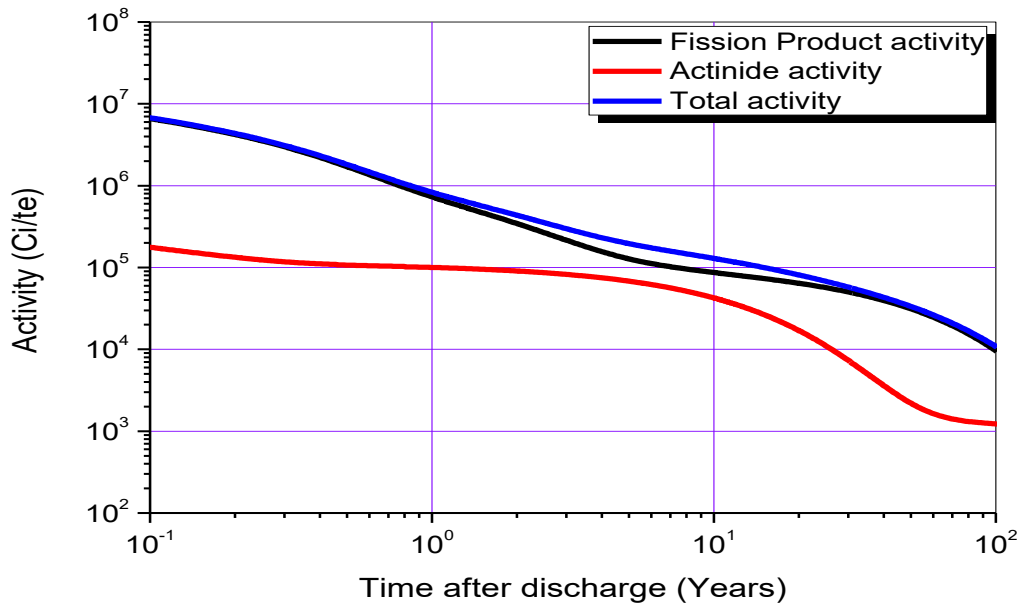


Figure 5.12: Variation of activity in PT-HWR fuel (Short Time Scale - STS)

From a closed cycle point of view and reprocessing angle, the activities due to actinides and fission products are given over the period of 0-100 years in Figure 5.12; the maximum contributors from FPs are Sr^{90} , Y^{90} , Cs^{137} and $\text{Ba}^{137\text{m}}$. Estimating radioactivity for discharge burn-up of 7500 MWd/te at various time intervals after shut down was calculated using "IGDC" and compared with the estimations by other codes. The comparison of specific activity is given in Table 5.9. The aim here is to benchmark the time evolution of the actinides and fission products using the novel method of solution developed in IGDC.

Table 5.9: Comparison of specific activity in the discharged fuel of PT-HWR

Time after shut down (Sec)	Time after shut down (Years)	Specific Activity (Curie/tonne)	Specific Activity (Curie/tonne)	Specific Activity (Curie/tonne)	<u>Percentage difference in Specific Activity (%)</u>	<u>Percentage difference in Specific Activity (%)</u>
		a	b	c	((a-c)100/a)	((b-c)100/b)
		ARGENTINA Ref: [57]	PAKISTAN Ref: [57]	IGDC (Present Study)		
0.00E+00	0.00E+00	1.50E+08	1.51E+08	1.25E+08	16.7	17.2
5.00E+00	1.59E-07	1.39E+08	1.39E+08	1.15E+08	17.3	17.3
1.00E+01	3.17E-07	1.34E+08	1.34E+08	1.10E+08	17.9	17.9
1.00E+02	3.17E-06	1.08E+08	1.09E+08	9.33E+07	13.6	14.4
1.00E+03	3.17E-05	7.43E+07	7.54E+07	7.24E+07	2.6	4.0
1.00E+04	3.17E-04	4.75E+07	4.85E+07	4.78E+07	-0.6	1.4
1.00E+05	3.17E-03	2.86E+07	2.84E+07	3.23E+07	-12.9	-13.7
1.00E+06	3.17E-02	1.38E+07	1.37E+07	1.20E+07	13.0	12.4
1.00E+07	3.17E-01	3.48E+06	3.49E+06	2.96E+06	14.9	15.2
1.00E+08	3.17E+00	2.38E+05	2.47E+05	2.85E+05	-19.7	-15.4

In this benchmark, Argentina and Pakistan used the computer code ORIGEN, which uses a matrix exponential method for solving Bateman equations, whereas IGDC uses the Klopfenstein-Shampine family of NDFs. This may be the reason for the reasonably matching values of Argentina & Pakistan and minor differences in the estimation of radioactivity by IGDC. At small times after shutdown IGDC is overpredicting w.r.t to ORIGEN whereas at larger times after shutdown IGDC seems to underpredict, the deviations are within the acceptable limits for such long duration fuel cycle analysis.

Another critical parameter from radiological protection point of view is the radiotoxicity. Specific radiotoxicity of a particular isotope is estimated as:

$$R_i(t) = A_i(t) \times (DCF)_i \quad (5.2)$$

Where $R_i(t)$ is the specific radiotoxicity of the i^{th} isotope and $(DCF)_i$ is the dose conversion factor (Sv/BQ) of the i^{th} isotope.

Dose conversion factors (DCFs) are extracted from International Commission on Radiological Protection (ICRP) publication-119 [17]. Ingestion and inhalation radio-toxicities are given in Table 5.10 and are shown in Figure 5.13 and Figure 5.14, respectively.

Table 5.10: Radio-toxicity in the discharged fuel in PT-HWR

Time after discharge (Days)	Ingestion radio-toxicity by an infant (Sv/tonne)	Ingestion radio-toxicity by an adult (Sv/tonne)	Ingestion radio-toxicity by a 15-year-old person (Sv/tonne)	Ingestion radio-toxicity by a 10-year-old person (Sv/tonne)	Inhalation radio-toxicity of 1 AMAD particle (Sv/tonne)	Inhalation radio-toxicity of 5 AMAD particle (Sv/tonne)
0.00E+00	3.06E+10	3.02E+09	4.24E+09	6.67E+09	5.00E+09	4.41E+09
1.00E+02	2.71E+09	2.51E+08	3.51E+08	4.92E+08	2.52E+09	1.72E+09
2.00E+02	1.66E+09	1.60E+08	2.34E+08	3.00E+08	2.05E+09	1.38E+09
3.00E+02	1.23E+09	1.24E+08	1.88E+08	2.24E+08	1.80E+09	1.20E+09
4.00E+02	1.01E+09	1.05E+08	1.64E+08	1.86E+08	1.64E+09	1.09E+09
5.00E+02	8.65E+08	9.27E+07	1.49E+08	1.61E+08	1.54E+09	1.02E+09
1.00E+03	5.38E+08	6.40E+07	1.12E+08	1.05E+08	1.31E+09	8.69E+08
2.00E+03	3.95E+08	4.88E+07	9.19E+07	7.75E+07	1.24E+09	8.26E+08
3.00E+03	3.63E+08	4.40E+07	8.40E+07	6.99E+07	1.23E+09	8.26E+08
4.00E+03	3.45E+08	4.09E+07	7.83E+07	6.50E+07	1.23E+09	8.27E+08
5.00E+03	3.29E+08	3.84E+07	7.34E+07	6.09E+07	1.23E+09	8.26E+08
6.00E+03	3.15E+08	3.62E+07	6.89E+07	5.72E+07	1.22E+09	8.24E+08
7.00E+03	3.02E+08	3.42E+07	6.48E+07	5.39E+07	1.22E+09	8.20E+08
8.00E+03	2.90E+08	3.24E+07	6.10E+07	5.08E+07	1.21E+09	8.16E+08
9.00E+03	2.79E+08	3.07E+07	5.75E+07	4.79E+07	1.20E+09	8.10E+08
1.00E+04	2.68E+08	2.91E+07	5.42E+07	4.52E+07	1.19E+09	8.04E+08
1.00E+05	8.81E+07	5.14E+06	5.07E+06	5.62E+06	7.32E+08	4.88E+08
1.00E+06	4.94E+07	2.94E+06	2.83E+06	3.18E+06	3.64E+08	2.37E+08
1.00E+07	8.51E+06	4.83E+05	4.90E+05	5.52E+05	6.05E+07	3.98E+07
1.00E+08	5.51E+05	2.21E+04	3.99E+04	4.05E+04	2.89E+06	2.11E+06
1.00E+09	1.58E+05	7.97E+03	1.81E+04	1.48E+04	8.27E+05	6.05E+05

N. B.: AMAD (Activity Median Aerodynamic Diameter): Inhalation is a route for internal exposure to radioactive aerosols. Aerosol's size distribution, and in particular its activity median aerodynamic diameter (AMAD) is essential for determining the fractional deposition of inhaled particles in the respiratory tract and the resulting doses. 1/5AMAD refers to the 1/5 μm diameter size of the aerosol particle

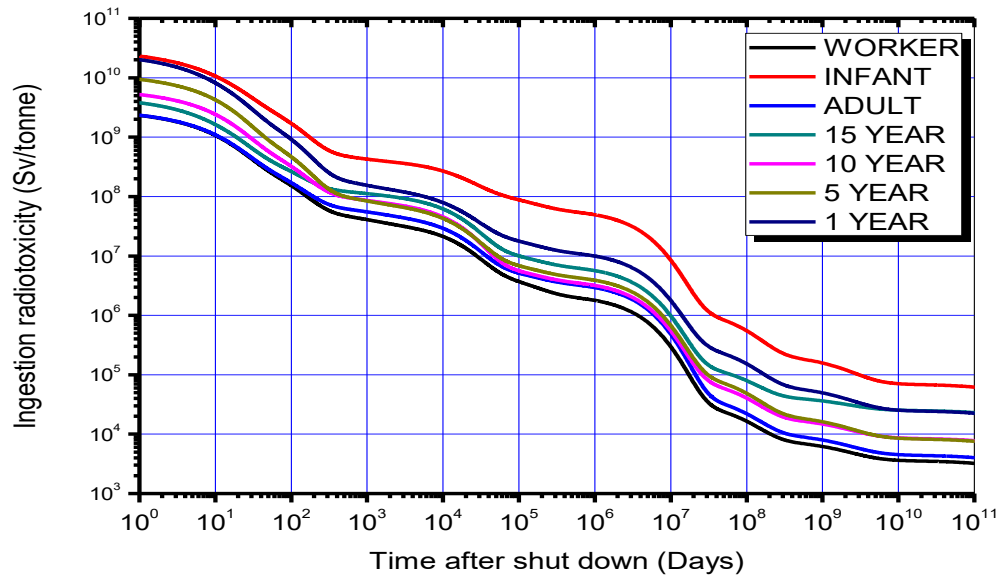


Figure 5.13: Radio-toxicity due to ingestion by different recipients

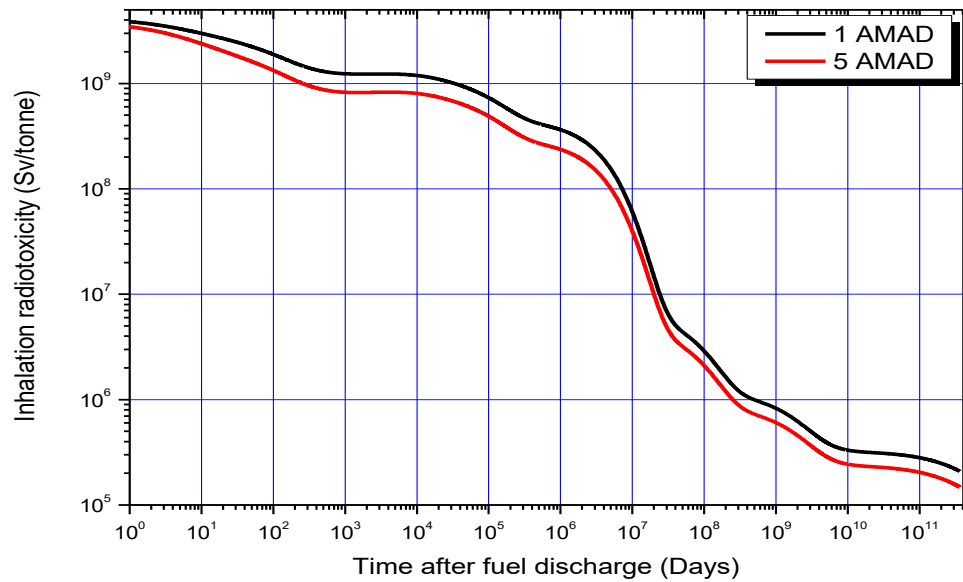


Figure 5.14: Inhalation radio-toxicity of different size particles

Figure 5.13 also shows a transition in the trend for a 15-year-old child after about 1000 days of fuel discharge, i.e., its radiotoxicity is higher than that of the 10-year-old child. This is mainly because the dose conversion factor of ^{226}Ra and ^{228}Ra is higher for a 15-year-old child than a five or 10-year-old child and an adult worker. Figure 5.13 shows that for the same quantity of material ingestion, radio-toxicity for an infant is more than that for an adult. Figure 5.14 shows that smaller diameter particles' inhalation radio-toxicity is more toxic than that of the higher diameter particle.

5.5 DECAY HEAT ANALYSIS

During the irradiation period, a number of fission products and actinides are generated and depleted in the nuclear fuel; these radioisotopes continue to produce heat via decay even after reactor shutdown or after the discharge of the fuel, and this residual heat is called thermal or total decay heat and gamma decay heat is the heat produced due to gamma decay only. Decay heat is defined as:

$$\text{Decay heat } D_i = \sum_k (BR)_k N_i \lambda_{ik} E_{ik} \quad (5.3)$$

Where $D_i(t)$ is the decay heat of the i^{th} isotope at time t ; N_i is the number density of the i^{th} isotope at time t , λ_{ik} is the decay constant of the i^{th} isotope via k mode; $(BR)_k$ is the branching ratio of k mode, E_{ik} is the energy liberated for the decay of i^{th} nuclei via k^{th} decay mode.

To estimate the decay heat as a function of time in the spent fuel of PT-HWR discharged at 7500 MWd/te, simulations were done in two steps with computer code IGDC. In the first step, the in-core irradiation of the 19 element PHWR fuel was simulated with IGDC up to 7500 MWd/te burn-up with the initial values of radio-isotopic

concentrations same as those of natural uranium. Initial average neutron flux for natural uranium fuelled 220 MWe class of PT-HWR using equation (1.3) was estimated to be 2.03×10^{14} n/cm²/s.

In the next step, the analysis of the discharged fuel was done. Simulations were done with IGDC with the initial values of radio-isotopic concentrations the same as those of accumulated values of radio-isotopes at 7500 MWd/Te burn-up obtained in the first step. The initial value of neutron flux in this step was assumed to be zero (as this simulation is for spent fuel i.e., discharged from the core).

Concentrations of different radio-isotopes as a function of time obtained in this step were utilized to estimate the total and gamma decay heat using equation (5-3). In the estimation of decay heat, decay data were utilized from ENSDF files, and energy liberated via different decay modes from various isotopes are extracted from the “JENDL FP Decay Data File 2011 and Fission Yields Data File 2011”. Decay factor and decay heat are shown in Figure 5.15 and Figure 5.16, respectively. Figure 5.15 shows the variation of fractional power after discharge, whereas Figure 5.16 shows the variation of specific heat content in the spent fuel after discharge. Gamma and thermal decay heat calculated by the computer code IGDC were compared with the results presented in IAEA TECDOC-887 using other codes are given in Table 5.11 and Table 5.12.

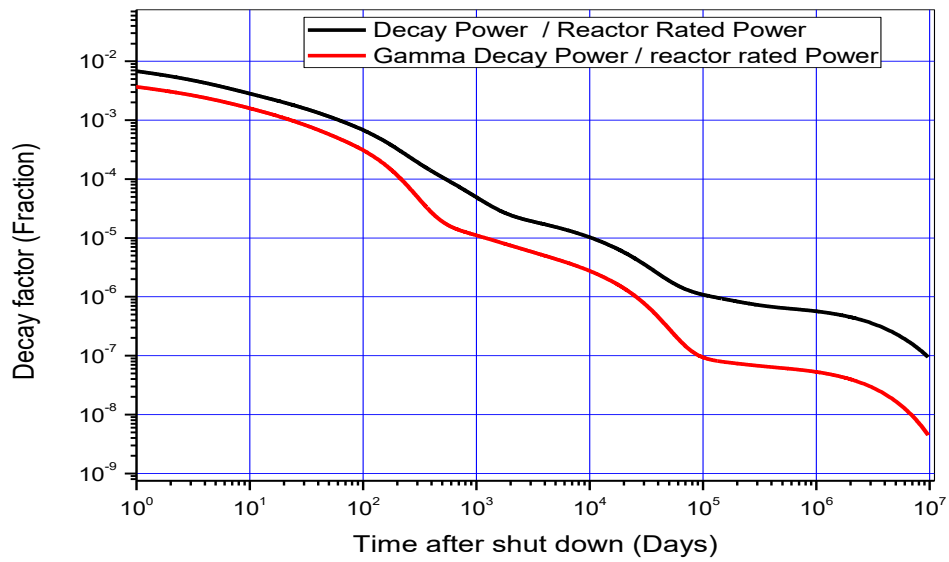


Figure 5.15: Variation of total decay factor and gamma decay factor

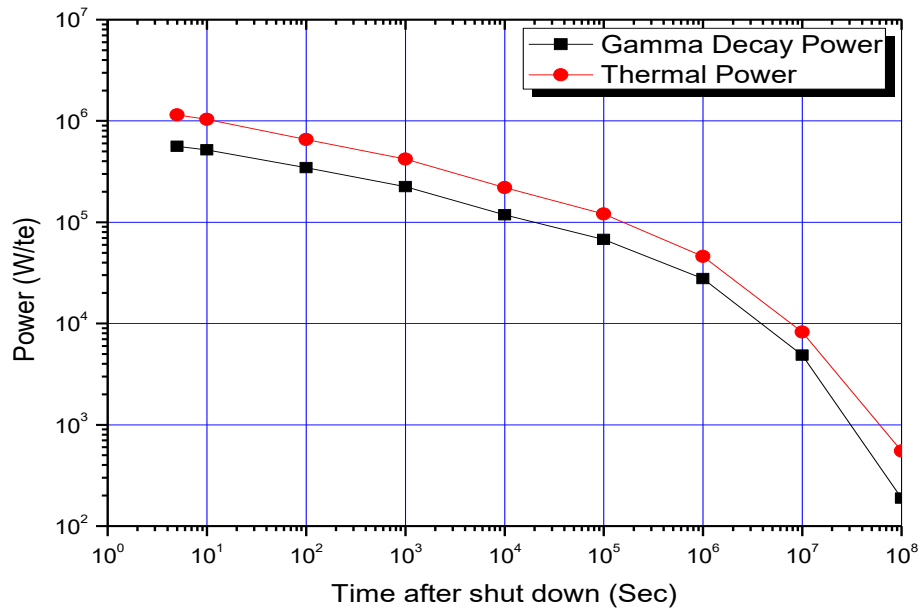


Figure 5.16: Variation of thermal and gamma decay power after shut down

Table 5.11: Gamma decay power after shut down at 7500 MWd/t in PT-HWR

Time after shut down (Sec)	Time after shut down (Days)	Gamma decay power (Watt/tonne)	Gamma decay power (Watt/tonne)	Gamma decay power (Watt/tonne)	Percentage difference in Gamma decay power (%)	Percentage difference in Gamma decay power (%)
		ARGENTINA Ref: 57] a	PAKISTAN Ref: 57] b	IGDC [Present study] c	((a-c)100/a)	((b-c)100/b)
0.00E+00	0.00E+00	5.93E+05	5.95E+05	6.14E+05	-3.54	-3.19
5.00E+00	5.79E-05	5.76E+05	5.77E+05	5.29E+05	8.16	8.32
1.00E+01	1.16E-04	5.65E+05	5.66E+05	4.90E+05	13.27	13.43
1.00E+02	1.16E-03	4.89E+05	4.88E+05	3.48E+05	28.83	28.69
1.00E+03	1.16E-02	3.25E+05	3.23E+05	2.26E+05	30.46	30.03
1.00E+04	1.16E-01	1.54E+05	1.53E+05	1.20E+05	22.08	21.57
1.00E+05	1.16E+00	8.02E+04	7.84E+04	6.87E+04	14.34	12.37
1.00E+06	1.16E+01	3.51E+04	3.42E+04	2.86E+04	18.52	16.37
1.00E+07	1.16E+02	6.60E+03	6.36E+03	5.07E+03	23.18	20.28
1.00E+08	1.16E+03	2.45E+02	1.70E+02	1.97E+02	19.59	-15.88

Table 5.12: Thermal decay power after shut down at 7500 MWd/t in PT-HWR

Time after shut down (Sec)	Time after shut down (Days)	Thermal decay power (Watt/tonne)	Thermal decay power (Watt/tonne)	Thermal decay power (Watt/tonne)	Percentage difference in Thermal decay power (%)	Percentage difference in thermal decay power (%)
		ARGENTINA Ref: [18] a	PAKISTAN Ref: [18] b	IGDC [Present study] c	((a-c)100/a)	((b-c)100/b)
0.00E+00	0.00E+00	1.68E+06	1.69E+06	1.25E+06	25.60	26.04
5.00E+00	5.79E-05	1.49E+06	1.49E+06	1.06E+06	28.86	28.86
1.00E+01	1.16E-04	1.40E+06	1.40E+06	9.65E+05	31.07	31.07
1.00E+02	1.16E-03	1.06E+06	1.06E+06	6.67E+05	37.08	37.08
1.00E+03	1.16E-02	6.08E+05	6.10E+05	4.30E+05	29.28	29.51
1.00E+04	1.16E-01	2.82E+05	2.83E+05	2.28E+05	19.15	19.43
1.00E+05	1.16E+00	1.40E+05	1.37E+05	1.27E+05	9.29	7.30
1.00E+06	1.16E+01	6.26E+04	6.16E+04	5.14E+04	17.89	16.56
1.00E+07	1.16E+02	1.44E+04	1.42E+04	1.17E+04	18.75	17.61
1.00E+08	1.16E+03	9.16E+02	8.46E+02	8.18E+02	10.70	3.31

The difference between the estimations of decay heat through IGDC and other codes may be due to the difference in the method of computations. However, decay heat

estimations by IGDC are also experimentally validated and will be discussed in the validation section.

5.5.1 DECAY HEAT FACTOR FOR ACTINIDES & FISSION PRODUCTS

Decay heat fraction is the ratio of heat produced at any instant to the initial heat produced at the time of discharge of the fuel and is therefore a dimensionless quantity. Fission product and actinide decay heat fractions for the discharged fuel from PT-HWR type of reactors of burn-up steps of 1000, 4000, 7500, 10000, 12500, 15000 & 20000 MWd/te and cooling time up to 30 years were estimated using the computer code IGDC and are given in Tables 5.13 and 5.14.

Table 5.13: Decay heat fraction at cooling period = 0 Years

Burn-Up (MWd/te)	Decay heat fraction (Cooling Time = 0 Years)		
	Actinides	Fission products	Total
1000	4.224E-03	5.909E-02	6.331E-02
4000	4.137E-03	6.003E-02	6.417E-02
7500	4.327E-03	6.033E-02	6.466E-02
10000	4.468E-03	6.045E-02	6.492E-02
12500	4.584E-03	6.056E-02	6.514E-02
15000	4.676E-03	6.065E-02	6.532E-02
20000	4.806E-03	6.079E-02	6.560E-02

Table 5.14: Variation of decay heat fraction at cooling period = 30 Years

Burn-Up (MWd/te)	Decay heat fraction (Cooling Time = 30 Years)		
	Actinides	Fission products	Total
1000	1.66E-08	1.46E-11	1.66E-08
4000	4.47E-08	5.75E-11	4.47E-08
7500	6.37E-08	1.06E-10	6.38E-08
10000	7.21E-08	1.40E-10	7.22E-08
12500	7.76E-08	1.73E-10	7.78E-08
15000	8.29E-08	2.06E-10	8.31E-08
20000	8.89E-08	2.68E-10	8.92E-08

Variation of decay heat due to fission products and actinides and given in Table 5.15.

Table 5.15: Variation of actinide and fission product decay heat with a time

Time after discharge (years)	Actinides (Watt/te)	Fission Products (Watt/te)	Total Decay Heat (Watt/te)	Actinides (%)	Fission Products (%)
0.00E+00	8.38E+04	1.17E+06	1.25E+06	7	93
1.00E+00	9.07E+01	2.75E+03	2.84E+03	3	97
1.00E+01	4.71E+01	2.44E+02	2.91E+02	16	84
1.00E+02	2.67E+01	2.82E+01	5.49E+01	49	51
1.00E+03	1.34E+01	2.73E-03	1.34E+01	100	0
1.00E+04	6.16E+00	2.20E-03	6.16E+00	100	0

Figure 5.17 shows that initially, the decay heat contribution is mainly due to the fission products, whereas as time passes, actinide contribution to the decay heat increases. It is also seen that after 100 years, the decay heat contribution from actinides and fission products are almost equal. This discrimination of the decay heat from actinides and fission products as a function of time is essential in the facilities where partitioning of actinides and fission products is being carried out to minimize radioactive waste [71].

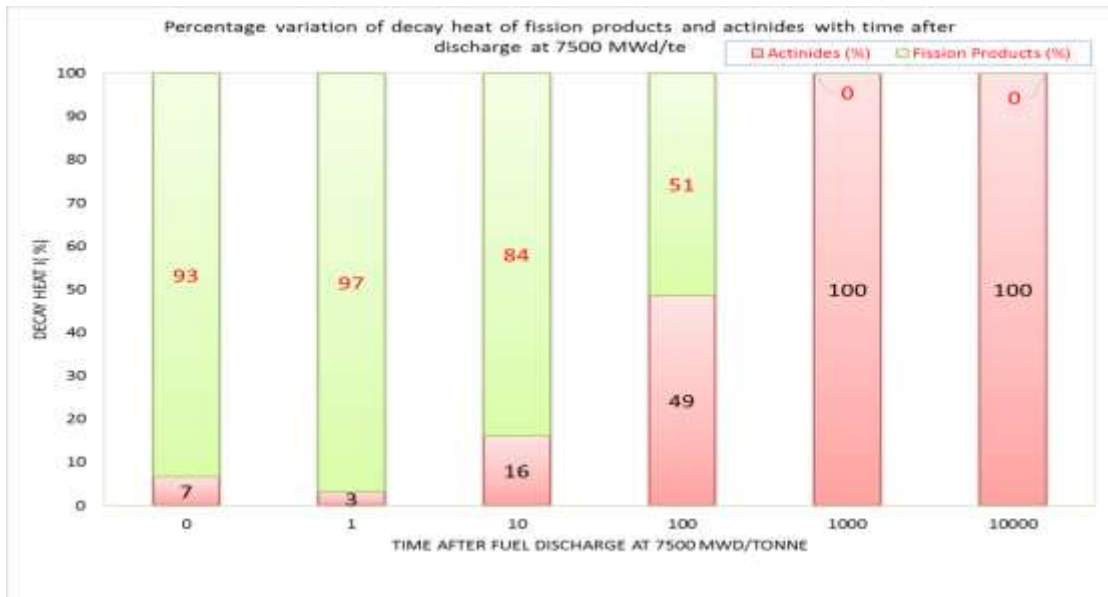


Figure 5.17: Decay heat (W/te) contribution of fission products and actinides

5.5.2 DECAY FACTOR FOR ALPHA, BETA, AND GAMMA EMITTERS

Break-up of the decay heat with respect to the heating due to alpha, beta, and gamma radiations is also a specific requirement for handling spent fuel. The contribution of alpha, beta, and gamma radiations in the decay heat is also significant with respect to the reprocessing of spent fuel. The decay heat fraction for an alpha, beta, and gamma radiations for the discharged fuel from PT-HWRs of burn-up steps of 1000, 4000, 7500, 10000, 12500, 15000 and 20000 MWd/te and cooling time up to about 30 years is evaluated. A comparison of decay fraction due to alpha, beta, and gamma radiations are given in Table 5.16 and 5.17 for the cooling period 0 and 30 years, respectively.

Table 5.16: Variation of decay heat fraction at cooling period = 0 Years

Burn-Up (MWd/te)	Decay heat fraction (Cooling Time = 0 Years)			
	Alpha emitter	Beta emitter	Gamma emitter	Total
1000	0.000E+00	3.221E-02	3.110E-02	6.331E-02
4000	1.033E-06	3.260E-02	3.156E-02	6.417E-02
7500	6.197E-06	3.292E-02	3.172E-02	6.466E-02
10000	1.653E-05	3.311E-02	3.180E-02	6.492E-02
12500	3.099E-05	3.325E-02	3.186E-02	6.514E-02
15000	4.855E-05	3.337E-02	3.191E-02	6.532E-02
20000	8.728E-05	3.352E-02	3.199E-02	6.560E-02

Table 5.17: Variation of decay heat fraction at cooling period = 30 Years

Burn-Up (MWd/te)	Decay heat fraction (Cooling Time = 30 Years)			
	Alpha emitter	Beta emitter	Gamma emitter	Total
1000	1.613E-08	1.642E-10	2.756E-10	1.657E-08
4000	4.313E-08	2.818E-10	1.323E-09	4.473E-08
7500	6.057E-08	4.269E-10	2.772E-09	6.377E-08
10000	6.807E-08	5.185E-10	3.594E-09	7.219E-08
12500	7.300E-08	5.971E-10	4.164E-09	7.776E-08
15000	7.776E-08	6.740E-10	4.640E-09	8.307E-08
20000	8.332E-08	8.028E-10	5.029E-09	8.915E-08

Table 5.16 and Table 5.17 describes a significant result of the transition of decay heat production initially by beta & gamma emitters to the alpha emitters afterward. This is because fission products are generally beta and gamma emitters in contrast to the alpha emitters actinides (half-life higher than the fission products). The contribution of different actinides in spent fuel after discharge is given in Table 5.18 below.

Table 5.18: Decay heat contribution of different actinides after discharge

Element	Time after discharge at 7500 MWd/te (in Years)					
	0	1.00E+00	1.00E+01	1.00E+02	1.00E+03	1.00E+04
	Decay Heat (Watt/te)					
U	4.25E+04	4.70E+01	1.97E+01	2.19E-02	2.08E-02	2.21E-02
Np	4.12E+04	2.46E-03	3.86E-03	4.92E-03	4.97E-03	4.31E-03
Cm	1.09E+02	2.39E+01	7.77E-01	6.61E-01	3.83E-02	4.72E-06
Pu	4.20E+01	1.66E+01	1.57E+01	1.30E+01	1.14E+01	5.60E+00
Am	2.50E+01	3.21E+00	1.09E+01	1.30E+01	1.97E+00	5.24E-01
Pa	5.51E-03	5.49E-03	5.61E-03	5.70E-03	5.72E-03	5.73E-03
Th	1.91E-04	1.55E-04	1.34E-04	1.42E-04	4.02E-04	2.70E-03
Ra	1.18E-04	3.25E-05	9.43E-06	8.10E-06	2.78E-05	5.84E-04
Ac	5.71E-05	1.05E-09	1.52E-08	4.00E-06	2.26E-04	2.16E-03
Bk	5.99E-10	2.83E-13	1.54E-22	0	0	0
Cf	1.57E-11	1.30E-11	4.27E-12	4.15E-13	2.45E-14	1.64E-17
Es	1.01E-13	2.06E-23	0	0	0	0
Total (actinides)	8.39E+04	9.07E+01	4.71E+01	2.67E+01	1.34E+01	6.16E+00

The table shows that the initial contribution in decay heat is through uranium. This initial contribution of uranium in decay heat is mainly from two of its isotopes viz. ^{239}U ($t_{1/2}\sim 23$ minutes) and ^{237}U ($t_{1/2}=6.75$ days). However, as time progresses, the contribution of plutonium dominates mainly due to ^{243}Pu ($t_{1/2}=4.956$ hours), ^{240}Pu ($t_{1/2}=6564$ years), ^{239}Pu ($t_{1/2}=2.411\text{e}4$ years), and ^{238}Pu ($t_{1/2}=87.7$ years). However, due to the short half-life of ^{243}Pu , its decay heat contribution dies down soon, and other plutonium isotopes (^{240}Pu , ^{239}Pu , and ^{238}Pu) continues to contribute to decay heat. Table 5.19 provides the contribution of different actinide isotopes in decay heat.

Table 5.19: Isotopic contribution to decay heat from individual actinides

Nuclide	Half-life	Time after discharge at 7500 MWd/te (in Years)					
	Sec	0.00E+00	1.00E+00	1.00E+01	1.00E+02	1.00E+03	1.00E+04
		Decay Heat (Watt/te)					
²³⁹ U	1.38E+03	4.22E+04	0.00E+00	0.00E+00	0.00E+00	0.00E+00	0.00E+00
²³⁷ U	5.83E+05	2.91E+02	4.70E+01	1.97E+01	3.47E-03	2.63E-07	1.30E-07
²⁴² Cm	1.41E+07	1.09E+02	2.34E+01	1.12E-04	2.45E-05	4.94E-11	0.00E+00
²⁴⁰ Pu	2.07E+11	7.08E+00	7.07E+00	7.07E+00	7.00E+00	6.37E+00	2.56E+00
²³⁹ Pu	7.61E+11	5.13E+00	5.26E+00	5.26E+00	5.23E+00	4.97E+00	3.03E+00
²³⁸ Pu	2.77E+09	3.42E+00	3.44E+00	2.99E+00	7.31E-01	5.76E-07	0.00E+00
²⁴¹ Am	1.37E+10	3.80E-01	1.76E+00	9.48E+00	1.15E+01	6.68E-01	1.17E-06
²⁴⁰ Am	1.83E+05	1.37E+00	1.43E+00	1.43E+00	1.42E+00	1.29E+00	5.18E-01
²⁴¹ Pu	4.51E+08	8.61E-01	7.81E-01	3.27E-01	5.77E-05	4.38E-09	2.17E-09
²⁴⁴ Cm	5.71E+08	4.88E-01	4.56E-01	2.30E-01	2.51E-04	5.01E-31	0.00E+00
²⁴¹ Cm	2.83E+06	1.51E-02	9.58E-02	5.41E-01	6.61E-01	3.83E-02	6.70E-08

The contribution of different fission products in spent fuel after discharge is given in Table 5.20 below.

Table 5.20: Decay heat of fission products after discharge (in Watt/te)

Element	Time after discharge at 7500 MWd/te (in Years)			
	0	1.00E+00	1.00E+01	1.00E+02
Rb	1.23E+05	1.25E-06	3.24E-09	3.24E-09
Y	1.00E+05	2.50E+02	1.09E+02	1.28E+01
La	9.65E+04	6.00E-05	2.76E-13	2.76E-13
Cs	9.36E+04	1.43E+02	2.86E+01	2.95E+00
I	9.09E+04	1.78E-06	1.78E-06	1.78E-06
Sr	8.83E+04	4.72E+01	2.28E+01	2.67E+00
Nb	7.78E+04	1.95E+02	2.00E-05	5.44E-05
Kr	6.32E+04	2.95E+00	1.65E+00	5.30E-03
Ba	5.79E+04	9.42E+01	7.66E+01	9.82E+00
Xe	5.43E+04	2.59E-08	0	0
Te	5.31E+04	9.86E-01	1.89E-02	3.57E-12
Zr	5.10E+04	9.55E+01	3.89E-05	3.89E-05

Element	Time after discharge at 7500 MWd/te (in Years)			
	0	1.00E+00	1.00E+01	1.00E+02
Br	3.69E+04	0	0	0
Sb	3.65E+04	2.85E+00	2.99E-01	4.03E-04
Tc	2.95E+04	1.74E-03	1.74E-03	1.74E-03
Mo	2.82E+04	5.79E-33	0	0
Pr	2.66E+04	1.57E+03	5.43E-01	0
Ce	2.09E+04	1.41E+02	4.84E-02	0
Se	1.23E+04	1.13E-07	1.13E-07	1.13E-07
Sn	8.60E+03	8.91E-02	2.06E-03	5.23E-04
As	3.92E+03	7.09E-18	7.09E-18	7.09E-18
Ru	3.28E+03	3.86E+00	2.38E-03	0
Nd	2.97E+03	8.22E-08	3.93E-12	3.93E-12
Pm	2.55E+03	1.87E+01	1.75E+00	1.05E-10
Rh	2.30E+03	1.73E+02	3.84E-01	1.96E-15
Ge	1.61E+03	0	0	0
In	5.35E+02	2.81E-16	2.81E-16	2.81E-16
Ag	2.97E+02	4.65E-05	5.22E-09	0
Ga	2.80E+02	0	0	0
Eu	2.65E+02	3.81E+00	1.81E+00	1.34E-03
Sm	2.23E+02	5.38E-03	5.01E-03	2.50E-03
Cd	1.66E+02	3.29E-03	8.41E-05	1.05E-06
Pd	8.73E+01	1.58E-07	1.58E-07	1.58E-07
Zn	3.63E+01	0	0	0
Cu	1.04E+00	0	0	0
Ga	5.64E-01	8.72E-03	6.87E-07	1.73E-12
Tb	1.45E-01	2.39E-03	5.44E-17	0
Ni	2.29E-02	0	0	0
Dy	3.62E-03	0	0	0
Ho	6.07E-04	1.02E-10	1.02E-10	9.67E-11
Total FPs	1.17E+06	2.74E+03	2.44E+02	2.83E+01

The table shows that the initial contribution to decay heat is through Rubidium (Rb). However, as time progresses, the contribution of yttrium (Y) dominates. Table 5.21 provides the contribution of different fission product isotopes in decay heat.

Table 5.21: FP isotopes contributing to the decay heat over time

Nuclide	Half-life	Time after discharge at 7500 MWd/te (in Years)			
	Sec	0.00E+00	1.00E+00	1.00E+01	1.00E+02
		Decay Heat (Watt/te)			
¹⁴⁴ Pr	1.04E+03	3.89E+03	1.57E+03	5.42E-01	0.00E+00
⁹⁵ Nb	3.02E+06	4.58E+03	1.95E+02	7.86E-14	0.00E+00
¹⁰⁶ Rh	3.01E+01	6.45E+02	1.73E+02	3.84E-01	0.00E+00
¹⁴⁴ Ce	2.46E+07	3.41E+02	1.40E+02	4.84E-02	0.00E+00
⁹⁰ Y	2.30E+05	1.37E+02	1.35E+02	1.09E+02	1.28E+01
¹³⁴ Cs	6.52E+07	1.60E+02	1.14E+02	5.63E+00	5.81E-13
⁹⁵ Zr	5.53E+06	4.95E+03	9.55E+01	3.77E-14	0.00E+00
^{137m} Ba	1.53E+02	9.65E+01	9.42E+01	7.66E+01	9.82E+00
⁹¹ Y	5.06E+06	6.41E+03	8.57E+01	1.19E-15	0.00E+00
^{89m} Y	1.57E+01	4.35E+03	2.93E+01	8.98E-19	0.00E+00
⁹⁰ Sr	9.09E+08	2.90E+01	2.84E+01	2.28E+01	2.67E+00
¹³⁷ Cs	9.49E+08	2.90E+01	2.83E+01	2.30E+01	2.95E+00
⁸⁹ Sr	4.37E+06	2.80E+03	1.88E+01	5.78E-19	0.00E+00
¹⁴⁷ Pm	8.28E+07	2.30E+01	1.87E+01	1.75E+00	1.05E-10
¹⁵⁴ Eu	2.71E+08	3.92E+00	3.61E+00	1.75E+00	1.33E-03
⁸⁵ Kr	3.39E+08	3.14E+00	2.95E+00	1.65E+00	5.30E-03
¹²⁵ Sb	8.71E+07	3.59E+00	2.85E+00	2.99E-01	5.65E-11
¹⁰³ Ru	3.39E+06	1.75E+03	2.79E+00	2.24E-25	0.00E+00
¹⁰⁶ Ru	3.21E+07	2.12E+00	1.07E+00	2.38E-03	0.00E+00
^{144m} Pr	4.32E+02	2.57E+00	1.06E+00	3.64E-04	0.00E+00
¹⁴¹ Ce	2.81E+06	1.47E+03	6.18E-01	0.00E+00	0.00E+00
¹²⁷ Te	3.37E+04	3.45E+01	5.60E-01	5.01E-10	0.00E+00
^{127m} Te	9.42E+06	2.11E+00	2.16E-01	1.94E-10	0.00E+00
¹⁵⁵ Eu	1.50E+08	2.28E-01	1.97E-01	5.32E-02	1.21E-07
^{103m} Rh	3.37E+03	1.13E+02	1.80E-01	1.45E-26	0.00E+00
^{125m} Te	4.96E+06	1.72E-01	1.79E-01	1.89E-02	3.57E-12
^{95m} Nb	3.12E+05	8.37E+00	1.66E-01	6.56E-17	0.00E+00

Table 5.21 and Figures 5.18 shows that initially, Praseodymium-144 (^{144}Pr), Niobium-95 (^{95}Nb), Zirconium (^{95}Zr), Yttrium-89m,91 (^{91}Y and $^{89\text{m}}\text{Y}$), and Strontium-89 (^{89}Sr) contribution in decay heat is higher. From this analysis it is seen that, as time progresses, the contribution from Yttrium-90 (^{90}Y) Strontium-90 (^{90}Sr), Cesium-137 (^{137}Cs) and Barium-137m ($^{137\text{m}}\text{Ba}$) dominates. Figure 5.19 show that most of the isotopes' decay heat reduces with time, whereas decay heat due to ^{241}Am increases initially to about 35 years and decreases afterward. This is due to the decay of ^{241}Pu ($t_{1/2} \sim 1.4$ years) into comparatively higher half-life isotope ^{241}Am ($t_{1/2} \sim 432$ years). It is also observed that decay heat due to ^{238}Pu ($t_{1/2} \sim 8.83$ years), ^{242}Cm ($t_{1/2} \sim 0.045$ years), and ^{244}Cm ($t_{1/2} \sim 1.82$ years) reduces very fast due to their short half-lives (0.045 & 1.82 years respectively) on the other hand due to longer half-life of ^{239}Pu ($t_{1/2} \sim 2400$ years) and ^{240}Pu ($t_{1/2} \sim 659$ years) their decay heat remains about constant.

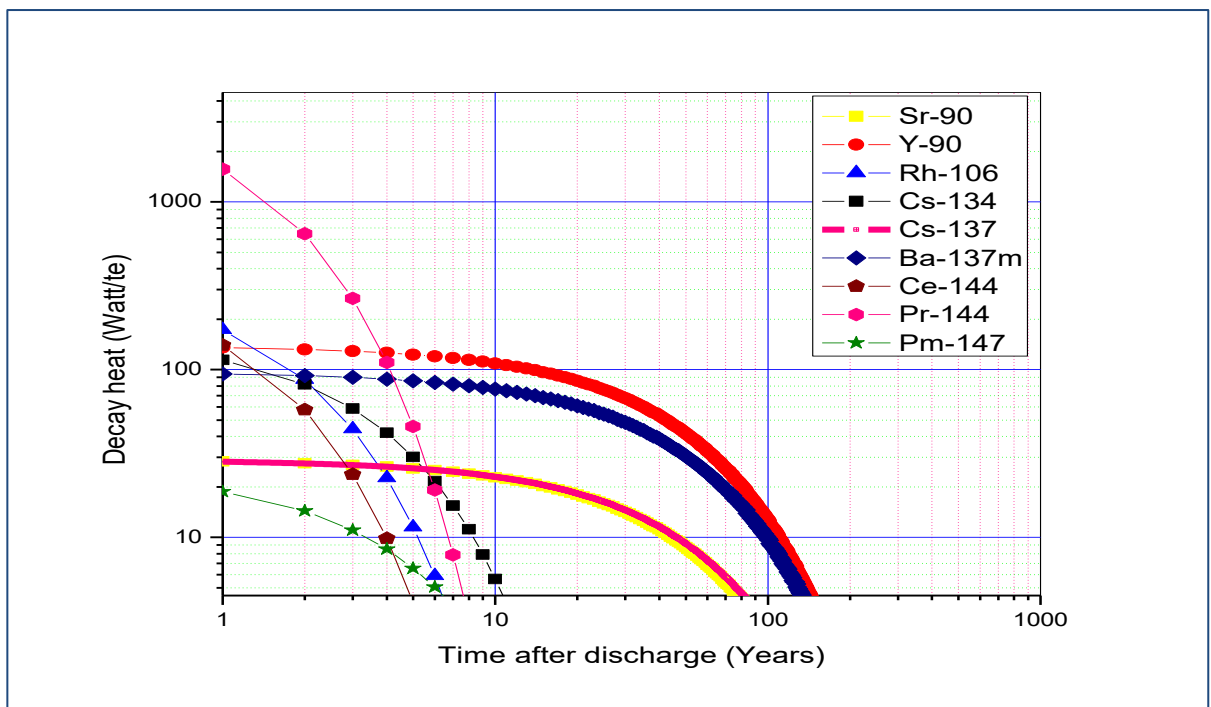


Figure 5.18: Variation of decay heat of essential fission products

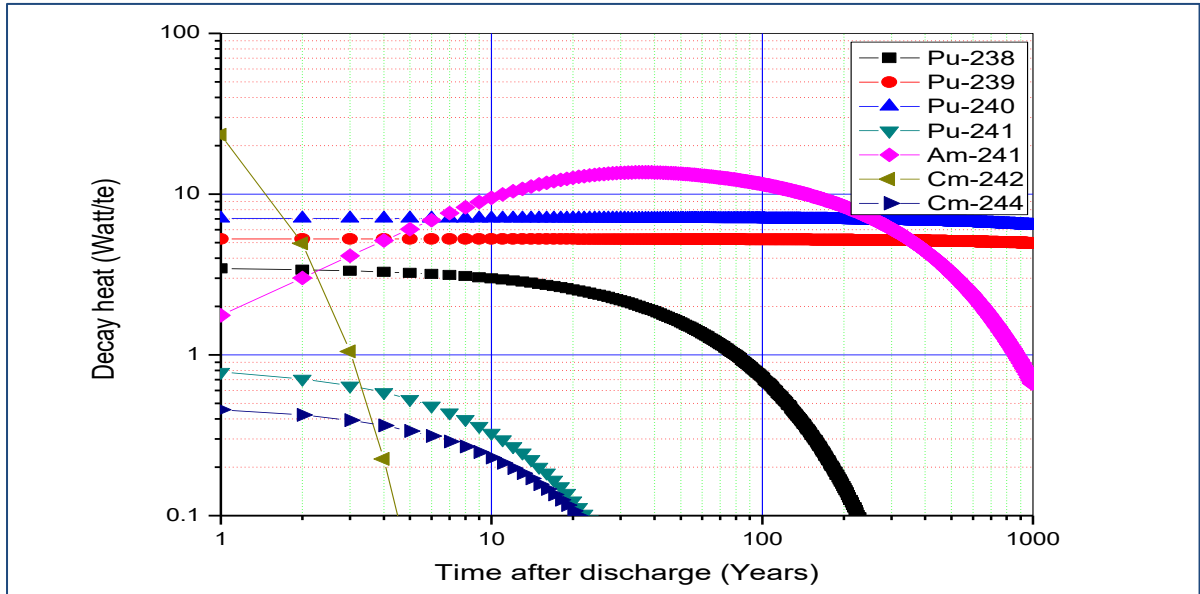


Figure 5.19: Variation of decay heat of important actinides

5.6 NEUTRON ABSORPTION

In a PT-HWR, various fission products are generated with irradiation. These fission products have different absorption characteristics and hence affect the core reactivity in a different manner.

To estimate the core reactivity accurately, identification of absorption characteristics of all the fission products is necessary. The effect of reactivity on several nuclides for MSR has been reported. The research stresses that the determination of reactivity impact of different fission products is crucial in salt cleanup systems of MSRs (Molten Salt Reactors) [72]. Therefore the estimation of reactivity equivalence of different fission products is extremely important.

In this research work, the effective worth of each neutron absorbing poison is estimated. In thermal reactors, Xe-135 is the poison with the maximum reactivity worth by virtue

of its high capture cross-section for thermal neutrons. The neutron poisoning in thermal reactors w.r.t to Xe-135 can be an essential factor for continuous operation.

5.6.1 POISONING FACTOR OF DIFFERENT FISSION PRODUCTS

Neutron poisoning of Xe-135 was discovered by John Archibald Wheeler in 1944 at Hanford B-Reactor while investigating reactor power run down after start-up by carefully analyzing the list of fission products of uranium fission [73]. It is also known that there are other isotopes also possible for poisoning in a reactor. To estimate the reactivity of the core, fission products other than Xe-135 having absorption characteristics should be accounted for explicitly. From a detailed simulation in IGDC, the most reactive fission products have been determined, and subsequently, their poisoning effect is also estimated.

The poisoning factor due to essential fission products at 4000 MWd/te and 7500 MWd/te burn-up is estimated and is summarized in Table 5.22.

Table 5.22: Poisoning factor and the nature of essential Fission Products

Fission Product	Poisoning factor at 4000 MWd/te (mK)	Poisoning factor at 7500 MWd/te (mK)	Nature	Fission Product	Poisoning factor at 4000 MWd/te (mK)	Poisoning factor at 7500 MWd/te (mK)	Nature
Xe135 *	29.59	28.48	S	Cd113	0.44	0.43	S
Sm149	6.26	6.12	S	Eu154	0.44	1.23	N
Nd143	5.55	9.64	N	Xe133	0.36	0.36	S
Xe135m	4.28	4.28	S	Ru101	0.32	0.59	N
Rh105	4.03	4	S	Nd147	0.3	0.3	S
Sm151	4.01	4.42	N	La139	0.27	0.5	N
Rh103	3.33	6.66	N	I129	0.26	0.49	N
Xe131	2.63	4.76	N	Pr141	0.24	0.51	N
Te127m	2.57	3.25	N	Ce141	0.21	0.21	S
Pm147	2.04	3.32	N	Pd108	0.2	0.36	N

Fission Product	Poisoning factor at 4000 MWd/te (mK)	Poisoning factor at 7500 MWd/te (mK)	Nature	Fission Product	Poisoning factor at 4000 MWd/te (mK)	Poisoning factor at 7500 MWd/te (mK)	Nature
Sm152	1.8	3.15	N	Pr143	0.2	0.2	S
Cs133	1.56	2.91	N	Mo95	0.19	0.53	N
Eu155	1.22	1.94	N	Pm149	0.17	0.18	S
Tc99	1.14	2.12	N	Pd107	0.13	0.23	N
Nd145	0.95	1.73	N	Pm148	0.13	0.22	N
Eu153	0.79	1.71	N	Cs134	0.1	0.31	N
Ag109	0.75	1.32	N	I127	0.06	0.12	N
Sm150	0.65	1.18	N	In115	0.06	0.11	N
Pd105	0.49	0.9	N	Sb125	0.06	0.1	N
Gd157	0.47	0.48	S	Sm147	0.05	0.17	N

Note: S denotes Saturated Fission Product, and N denotes Non-Saturated Fission Products

* Equilibrium load of Xe-135 in a PHWR is about 28 mk, which is achieved in about 50 hrs of reactor operation, but as burn-up increases due to the build-up of plutonium, equilibrium Xe-135 increases. Furthermore, it decreases due to an increase in the poison factor of non-saturating fission products.

5.5.2 RELATIVE ABSORPTION OF NEUTRON

In this research work, an exhaustive analysis of the relative absorption characteristics of fission products produced in the nuclear reactor is carried out. The **Relative importance factor of fission product w.r.t. Xe-135 (RELIFIX)** is also defined and estimated, which helps in understanding the level of impact of a particular fission product on core parameters with respect to Xenon-135. Relative absorption data may be utilized to estimate a specific fission product's contribution to core excess reactivity. Since the Xenon poison in a reactor is dependent on the power level, a direct correlation of excess reactivity due to all neutron poisons w.r.t Xe¹³⁵ is found to be useful

information. Xe^{135} is established to have the highest relative absorption and impact on the reactivity of the Pressure Tube type Heavy Water Reactor (PT-HWR).

Therefore, to understand the importance of fission products other than Xe^{135} on core reactivity, the term “**Relative importance factor of fission product w.r.t. Xe^{135} (RELIFIX)**” is defined as:

$$(RELIFIX)_i = \frac{\text{Relative absorption of } i\text{th fission product}}{\text{Relative absorption of } Xe - 135} \quad (5.4)$$

RELIFIX parameters of different fission products are given in Table 5.23. In this analysis, a fission product is said to be saturating or non-saturating based on the turning tangent method, i.e., the nature of the relative absorption slope. This table shows that next to Xe^{135} , fission product Nd^{143} is having the highest importance factor and is a non-saturating fission product. This table also indicates that commonly considered fission product poisons Xe^{135} , Sm^{149} , and Rh^{105} are not the only saturating fission products, but there are other saturating fission products even though with low RELIFIX parameter.

Table 5.23: RELIFIX parameters of essential fission products

Fission Product	RELIFIX at 4000 MWd/te	RELIFIX at 7500 MWd/te	Fission Product	RELIFIX at 4000 MWd/te	RELIFIX at 7500 MWd/te
Xe135	1.00E+00	1.00E+00	Gd157	1.57E-02	1.68E-02
Sm149	2.12E-01	2.15E-01	Eu154	1.48E-02	4.31E-02
Nd143	1.88E-01	3.38E-01	Cd113	1.48E-02	1.50E-02
Xe135m	1.45E-01	1.50E-01	Xe133	1.21E-02	1.26E-02
Rh105	1.36E-01	1.40E-01	Ru101	1.07E-02	2.07E-02
Sm151	1.36E-01	1.55E-01	Nd147	1.03E-02	1.07E-02
Rh103	1.12E-01	2.34E-01	La139	9.10E-03	1.76E-02
Xe131	8.88E-02	1.67E-01	I129	8.79E-03	1.72E-02
Te127m	8.70E-02	1.14E-01	Pr141	8.15E-03	1.78E-02

Fission Product	RELIFIX at 4000 MWd/te	RELIFIX at 7500 MWd/te	Fission Product	RELIFIX at 4000 MWd/te	RELIFIX at 7500 MWd/te
Pm147	6.88E-02	1.16E-01	Ce141	7.10E-03	7.47E-03
Sm152	6.07E-02	1.10E-01	Pr143	6.89E-03	7.16E-03
Cs133	5.28E-02	1.02E-01	Pd108	6.61E-03	1.28E-02
Eu155	4.14E-02	6.80E-02	Mo95	6.26E-03	1.88E-02
Tc99	3.87E-02	7.44E-02	Pm149	5.80E-03	6.14E-03
Nd145	3.20E-02	6.06E-02	Pm148	4.29E-03	7.69E-03
Eu153	2.67E-02	5.99E-02	Pd107	4.26E-03	8.24E-03
Ag109	2.52E-02	4.63E-02	I131	3.26E-03	3.38E-03
Sm150	2.19E-02	4.15E-02	Cs134	3.22E-03	1.09E-02
Pd105	1.64E-02	3.17E-02	Zr95	2.60E-03	2.97E-03

5.7 SUMMARY

In this research, the nuclear fuel cycle analysis code is developed. It is utilized to estimate piled up isotopic inventory, decay heat, activity, radio-toxicity, and poisoning factors of different fission products for fuel irradiated in PT-HWR.

The benchmarking for actinides and fission product inventory has shown that IGDC can predict within 10-15%. The powerful NDF method used to solve the nuclide densities in IGDC renders it a valuable tool for detailed fuel cycle analysis. From this analysis, it is concluded that for the same quantity of material ingestion, radio-toxicity for an infant is more than that of an adult. The inhalation radio-toxicity of smaller diameter particles is more toxic than the higher diameter particle.

Estimation of decay heat is an important safety aspect of the nuclear reactor. The results of the research work contain a vast amount of information not only on the variation of total decay heat but also on the isotopic contribution of the decay heat as a function of time. This information may be utilized for designing the shutdown cooling equipment

for the transport of spent fuel, reprocessing, partitioning of fission products, and the importance of nuclear fission produced isotopes in Radio Thermo-Generators (RTGs) [74]. IGDC has been developed, taking into account these multidimensional requirements of precise estimation of decay heat.

Experimental verification of the decay heat was carried out with the measured decay heat of Douglas Point Reactor. The difference between measured and estimated (through IGDC) total decay heat $\leq \pm 15.0\%$ compared to the measurement and irradiation history uncertainty of $\pm 7.0\%$. The unaccounted difference may be attributed to the different factors viz. exact weight of uranium in the fuel assembly, uncertainties in the cross-sections fission yield data, decay data, and the number of isotopes considered for analysis.

1. The versatility of the code IGDC and its application for use in the back-end analysis of spent fuel for PT-HWR is established with this validation. Two modes of benchmarking were taken up. The isotopic concentrations were compared through inter-code comparison and with published experimental results. The decay heat simulations were benchmarked with the experiments in Ontario Hydro. The significant observations for PT-HWR fuel cycle analysis are:

- Initially, after the discharge of the fuel from the reactor, the decay heat factor for actinides is smaller as compared to the fission products, which is mainly because actinide inventory is less as compared to fission products inventory in the spent fuel and their decay constants are lower than fission products.

- However, the decay factor of actinides dominates over fission products afterward, which is mainly because most of the fission products have half-lives smaller as compared to that of the actinides.
- 2. Similarly, the initial decay heat factor for alpha emitters is smaller than the beta and gamma emitters. However, the trend reverses afterward, and the decay factor of alpha emitters dominates over that of beta and gamma emitters. This trend reversal is mainly because most actinides are alpha emitter and fission products are beta and gamma emitters.
- 3. Isotopic decay heat analysis shows that reactor-produced isotopes ^{90}Sr and ^{137}Cs may be good candidates for RTGs because of their relatively long half-life and decay heat content.

The versatility of the code IGDC and its application for use in the back-end analysis of spent fuel for PT-HWR is established with this validation.

Present work is only an initiation towards the comprehensive fuel cycle analysis. An extensive work should be done in this area to maintain this code for catering the future requirements. The next chapter is devoted to summarizing the overall research work and discussing only some of the future work, which can be done to maintain the code's versatility.

6.0 SUMMARY OF THE RESEARCH WORK DONE

In this research work on nuclear fuel cycle analysis, modeling of fission generated radio-nuclides and actinides generated through neutron activation or radio-active decay of other radionuclides was carried out. This model and nuclear data libraries developed in chapter-3 were utilized for developing an indigenous nuclear fuel burn-up code **Isotopic Generation and Depletion Code: IGDC**. The use of efficient and new numerical techniques is the major novelty of this research. The significant outcome of the study is to have an own tool developed for the Indian community to reduce the dependence on foreign codes and resolve accessibility problems.

6.1 NUMERICAL METHOD OF IGDC

This code is developed using the Klopfenstein-Shampine family of NDF, an algorithm mainly meant for a stiff set of linear or nonlinear ODEs. It is well suited for the nuclear fuel cycle analysis, in which burn-up differential equations of various isotopes are coupled and highly stiff in nature. It is worth mentioning that this scheme is independent of the decay half-lives of the individual isotopes and hence a powerful method to obtain a solution of all isotopes simultaneously.

6.2 BENCHMARKING OF IGDC

Computational performance of a computer code depends upon several factors like time of execution, CPU memory used during execution, language used in the code, hardware architecture, and accuracy of the computation. Currently, the program is run on 64-bit computer architecture, and the code is developed in MATLAB-14. Among all the factors of the computational performance, the accuracy of the code is of prime importance. For this, the results of essential isotopes are compared with the experimental data for activities and concentrations.

The second comparison is carried out for clearance potential indexes, which shows that this index for the computer code IGDC and ORIGEN-ARP for different isotopes are of the same order.

Theoretical benchmarking of the code is carried out with the results available from different codes. The estimation of the concentration of ^{235}U and ^{239}Pu at 4000 MWd/te and 8000 MWd/te burn-up by the code “IGDC” is comparable with those estimated by other codes.

6.3 DECAY HEAT ANALYSIS WITH IGDC

The decay heat analysis provides inputs to several safety evaluations, such as designing the shutdown cooling, handling of spent fuel, transportation of irradiated fuel. An estimate of decay heat from each isotope is crucial for fuel performance and irradiation behavior studies. For reprocessing and effective isotope separation for various applications too, decay heat forms a core parameter. Another aspect of the fuel cycle is the partitioning of fission products and the importance of nuclear fission produced

isotopes in RTGs. Therefore, there is a multidimensional requirement of precise estimation of decay heat. It has been established that IGDC can estimate the decay heat and the nuclide inventories within calculation uncertainties.

6.4 ANALYSIS FOR NEUTRON ABSORBING ISOTOPES

Core reactivity depends on the balance between different production and loss mechanisms. During reactor operation, depending on the burn-up, several nuclides are present, and they contribute to this reactivity in different ways. Also, the concentration of fission products and actinides change with irradiation in a nuclear reactor. The IGDC code that has been developed can simulate different nuclides simultaneously and study the relative behavior of the various isotopes present at any instant. It is well known that neutron poisoning in thermal reactors is due to Xe^{135} . A new approach has been used to estimate the reactivity effect of every isotope in relation to absorption in Xe^{135} . We define a parameter RELIFIX, *Relative importance factor of fission product w.r.t. Xe^{135} (RELIFIX)*, which is the ratio of absorption of any fission product to that in Xe^{135} . Relative absorption data may be utilized further to estimate a particular fission product's contribution to core excess reactivity.

6.5 IMPORTANT CONCLUSIONS OF ANALYSIS USING IGDC

In this research work, the developed computer code IGDC is used for nuclear fuel cycle analysis of PT-HWR. The critical conclusion reported in this research include:

- Burn-up equations model, which was used to be solved mainly using the matrix exponential method, can also be solved numerically using Gears BDF / Klopfenstein – Shampine family of NDFs on the MATLAB platform.
- The indigenous code analysis confirms that the activities due to fission products in the discharged fuel of 220 MWe PT-HWR reduce by approximately 99% in about 30 years, and activities due to actinides, especially Pu, reduces to 96 % during this period.
- The activity from all fission products in the spent fuel from PT-HWR remains higher than the activity of uranium metal (or ore) for about 10^5 years. This is mainly due to the long term fission product ^{99}Tc , even though the contribution due to ^{99}Tc is negligible compared to the total activity.
- Initially, the decay heat contribution is mainly due to the fission products, whereas as time passes, actinide contribution to the decay heat increases. It is also seen that after 100 years, the decay heat contribution from actinides and fission products are almost equal. This discrimination of the decay heat from actinides and fission products as a function of time is essential in the facilities where partitioning of actinides and fission products is being carried out to minimize radioactive waste.
- The difference between measured and estimated (through IGDC) total decay heat $\leq \pm 15.0$ % compared to the measurement and irradiation history uncertainty of ± 7.0 %. As already explained, the unaccounted difference may be attributed to the different factors viz. exact weight of uranium in the fuel

assembly, uncertainties in the cross-sections fission yield data, decay data, and the number of isotopes considered for analysis.

- Initially, after the discharge of the fuel from the reactor, the decay heat factor for actinides is smaller than the fission products, which is mainly because actinide inventory is less compared to fission products inventory in the spent fuel. However, the decay factor of actinides dominates over fission products afterward, which is mainly because most of the fission products have half-lives smaller as compared to that of the actinides.
- Similarly, initially decay heat factor for alpha emitters is smaller as compared to the beta and gamma emitters. However, the trend reverses afterward, and the decay factor of alpha emitters dominates over that of beta and gamma emitters. This is mainly because most actinides are alpha emitter, and fission products are beta and gamma emitters.
- Isotopic decay heat analysis shows that reactor-produced isotopes ^{90}Sr and ^{137}Cs may be the right candidate for RTGs because of their relatively long half-life and decay heat content.
- As for neutron absorption by generated fission products is concerned, exhaustive analysis for about 620 isotopes was carried out. It was found that about 40 fission products have higher relative neutron absorption characteristics. These includes Xenon-135, Samarium-149, Rhodium-103, Promethium-147, Cesium-133, Samarium-151, Technetium-99, Samarium-152, Samarium-150, Rhodium-105, Europium-153, Europium-155,

Molibdenum-95, Neodymium-143 and Neodymium-145, etc. These isotopes should be accounted for an accurate estimation of core parameters.

- The new term “RELative Importance factor of Fission product w.r.t. Xe-135 (RELIFIX)” defined in this research work helps to understand the level of impact of a particular fission product on core reactivity.

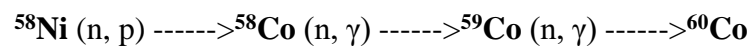
6.6 FUTURE WORK WITH IGDC

Various aspects of the nuclear fuel cycle like radioactivity, radio-toxicity, decay heat, relative absorption, etc. are covered in the present form of the developed code IGDC for PT-HWR. However, it is understood that the nuclear fuel cycle analysis is an extremely complicated subject. It is not possible to comprehend all the aspects of a different type of reactor that can be covered within one research work. Therefore, future work will be focused on the following elements:

1. Understanding the difference in measured and estimated decay heat and minimizing them.
2. Validate the code against the experimental data available for PWR / BWR fuel assemblies.
3. Validate the decay heat contribution of different isotopes with the available post-irradiation examination results for various reactor types.
4. A thorough analysis of the reactor produced materials that can be used for RTGs.
5. The burn-up code IGDC is developed using a new method based on Klopfenstein-Shampine Numerical Differentiation Formula (NDF), therefore

benchmarking the results of this code with other burn-up codes viz. DRAGON or SERPENT will be very useful and will be the subject of future development.

6. This code assumes a spatially homogenized model for the burn-up calculations using spectrum averaged one group cross-sections. Therefore, for the more realistic estimates, an independent transport solver may be coupled with the developed IGDC code in the future.
7. The calculations will also be checked for high burn-up fuels viz. slightly enriched uranium (SEU), ^{239}Pu mixed with ^{232}Th , and other likely combinations in the future.
8. Since the contribution of activation products is very small for PT-HWR, activation products are not considered for the present nuclear fuel cycle study. However, for other reactors, activation products contribute significantly and must be accounted. For example, this source is the more significant following shutdown of a fast reactor, with the formation of ^{22}Na and ^{24}Na by activation of the sodium coolant, and ^{58}Co and ^{60}Co from the activation of the nickel content of the steel structures in the reactor core:



Up to ~ 10% of the decay heat at five years cooling time arises primarily from ^{60}Co [6]. Therefore, the inclusion of activation products in IGDC will be taken up for future development.

9. The effect of burn-up dependent cross-sections on the isotopic analysis during in-core irradiation will be studied.

10. Future work will also be focused on understanding the significant discrepancies and exploring the data and decay chains to minimize them. A detailed comparison of IGDC results with experimental data will also be made in the future. Comparing long-term variation of specific activities of the spent fuel discharged at different burn-ups in natural and enriched fuel, component-wise contribution in decay heat and relative neutron absorption of different isotopes is the subject of future development.
11. An exhaustive study on all the radioisotope's clearance potential level may be carried out to understand the impact of spent fuel on the environment.
12. The choice of the group structure can have a significant impact on the fuel cycle analysis work. A future investigation on the effect of group structure on the code results may also be carried out in the future.

The versatility of the code IGDC and its application for use in the in-situ and back-end analysis of spent fuel for PT-HWR is established with the theoretical and experimental validation carried out in this research work. This research work is an entirely indigenous effort and had been benchmarked with computer codes and experimental data available, which are usually used for this purpose. The future work mentioned here may not be the imminent concluding work but may show a pathway from where analysis may be initiated in the future.

Present research work is disseminated in all the preceding six chapters. However, it is necessary to provide supplementary information to the main thesis. This additional information is provided in four annexures.

The decay chain of fission products

Fission products in nuclear fission are the isotopes of different elements that remain after fragmentation of a large nucleus when it undergoes nuclear fission. Typically, a large nucleus like that of uranium or plutonium fissions by splitting into two smaller nuclei, few neutrons, the release of energy (kinetic energy of the nuclei), and gamma rays. Fission product yields have been measured for major (e.g., U^{233} , U^{235} , Pu^{239}) and minor actinides (e.g., U^{238} , Np^{237}) using neutron sources (accelerators, etc.). Measurements have been done at thermal neutron energy and higher energies. Models have been used to extrapolate and interpolate to unknown isotopes and neutron energies. Based on these experimental and model results, the fission yields in the libraries and fission product decay chains have been created.

Fission products formed in nuclear fission are highly ionized and unstable. These fission products undergo a series of radioactive decay viz. β^- decay, β^+ decay, isomeric transition, and $\beta^- n$ decay until stabilized. The series of decay chains of fission products along with their branching ratios are shown below [6]:

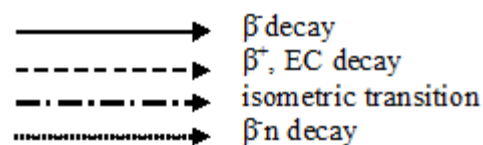
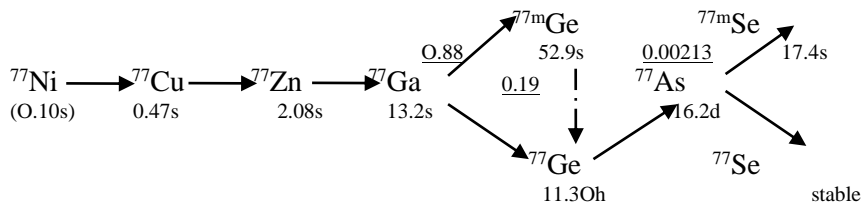
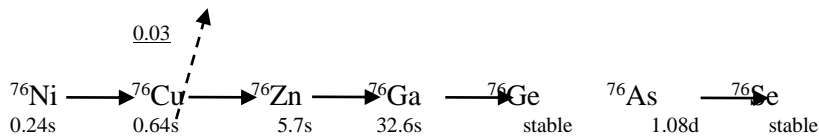
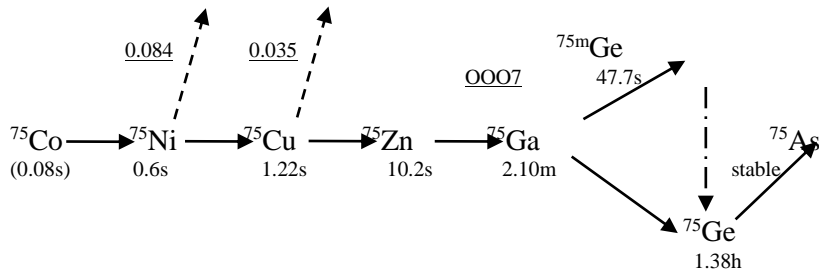
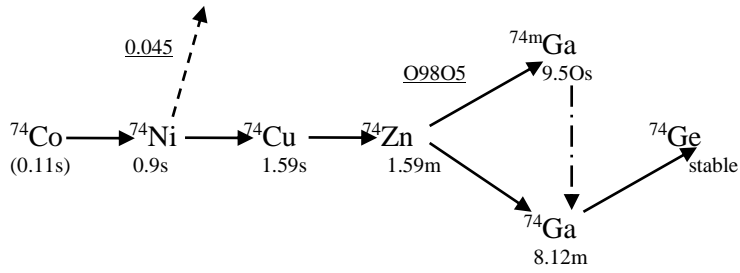
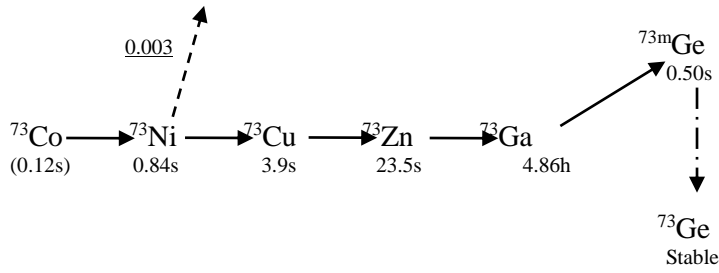
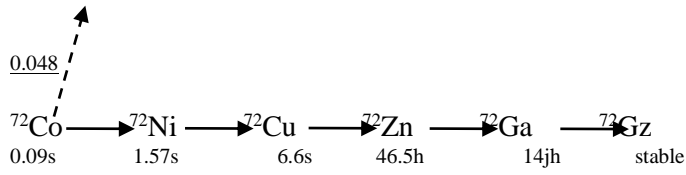
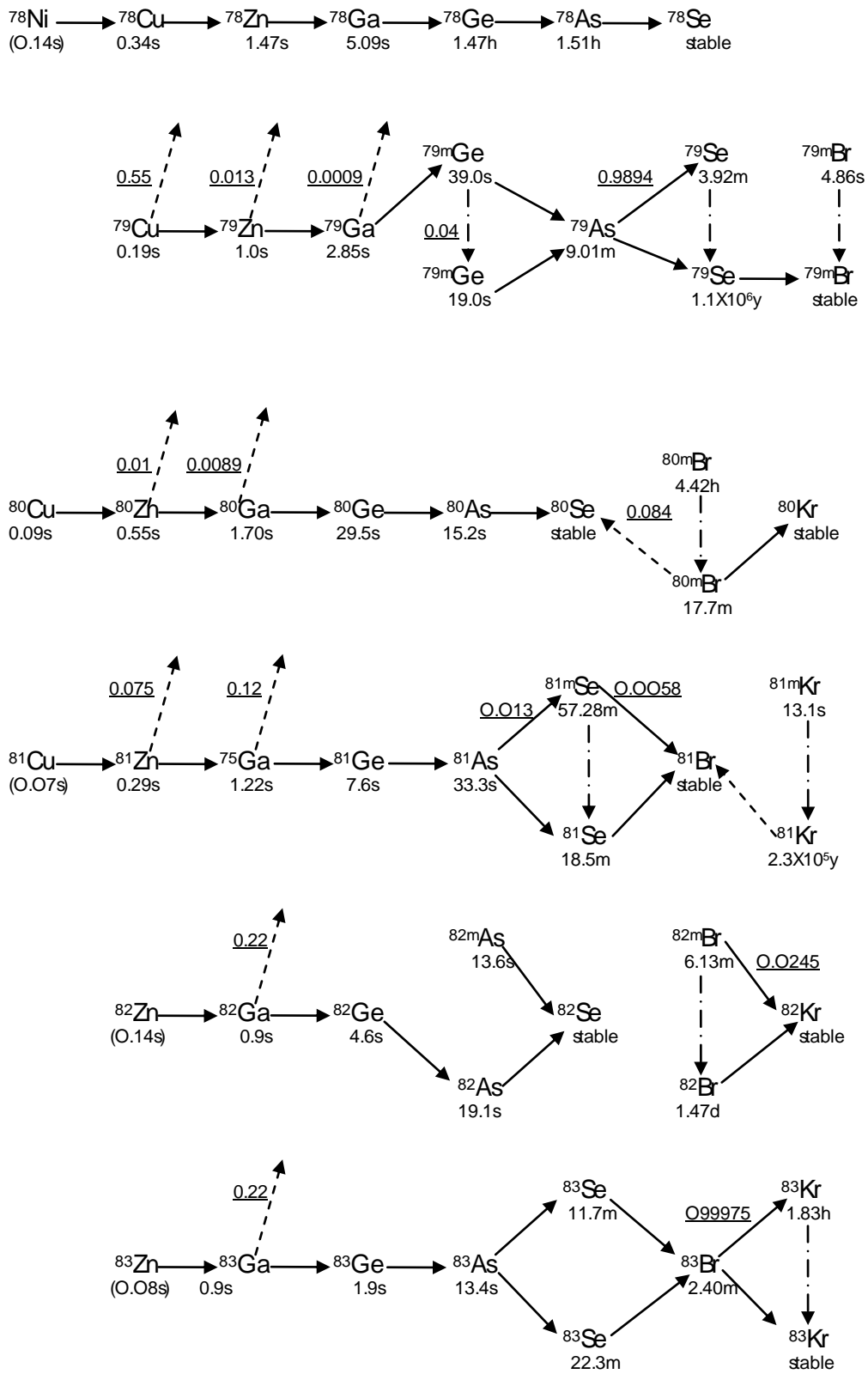
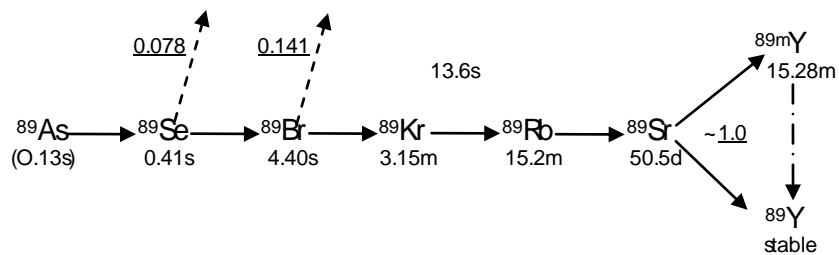
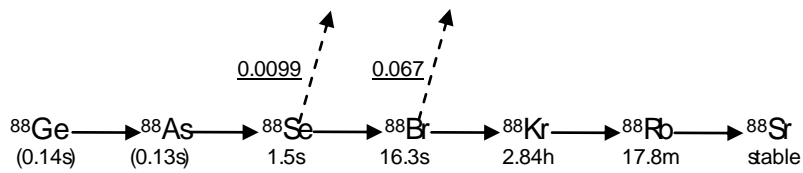
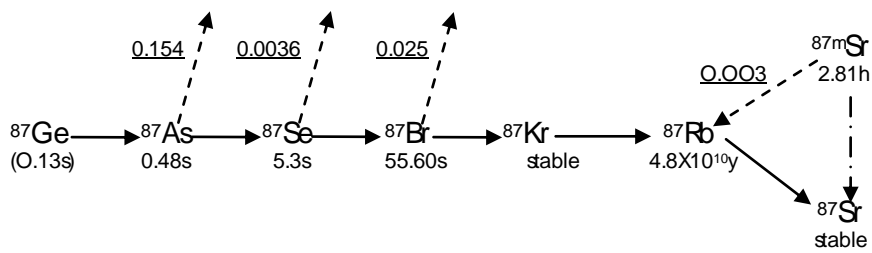
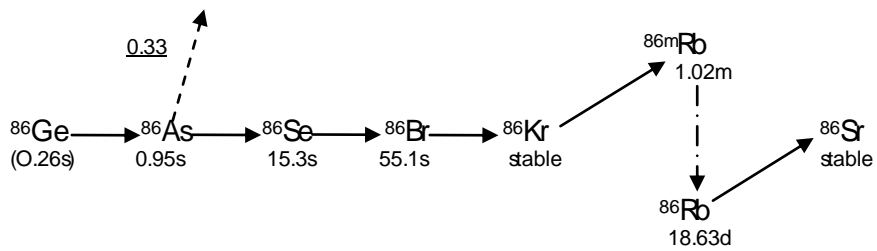
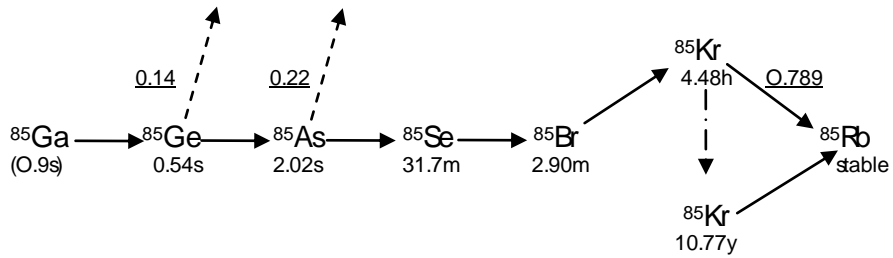
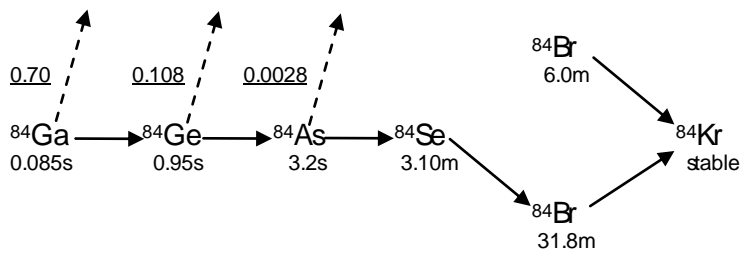


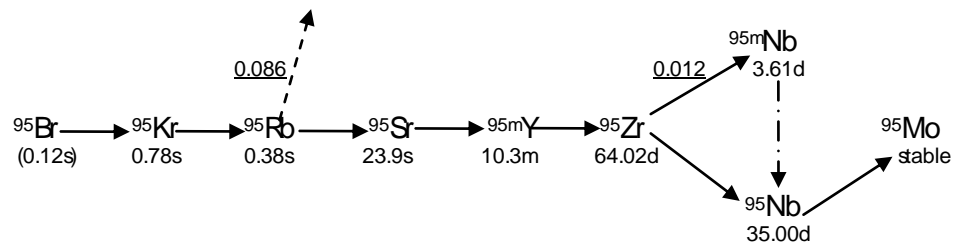
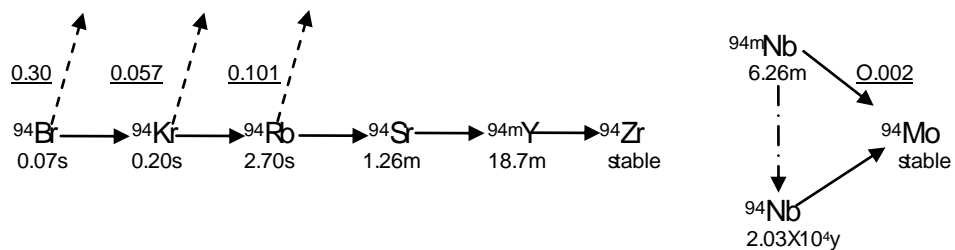
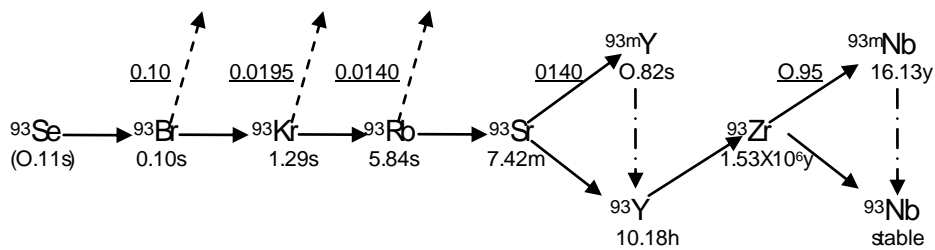
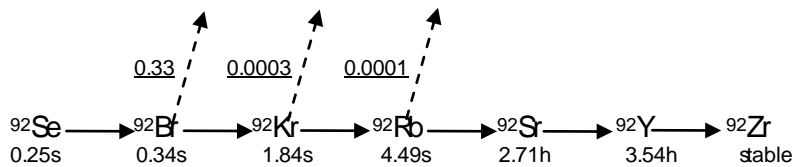
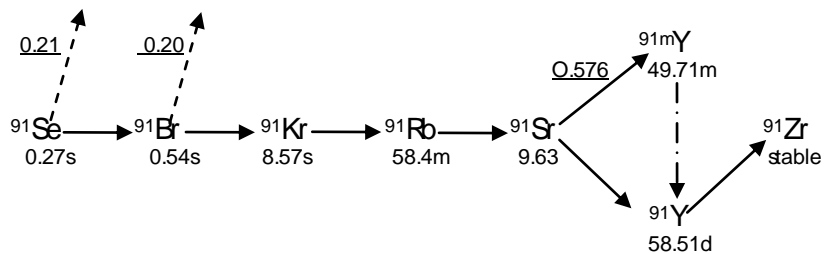
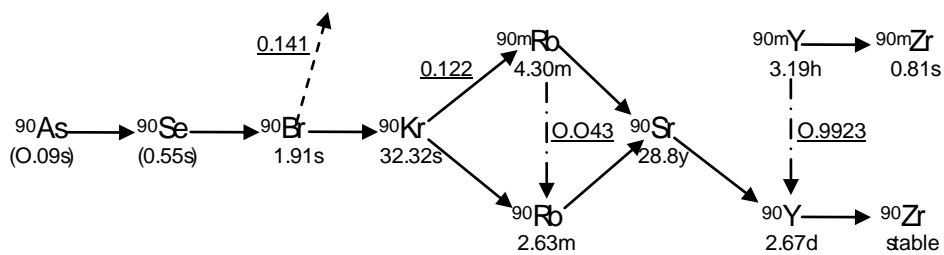
Figure A1. 1: Radioactive decay chains of fission products

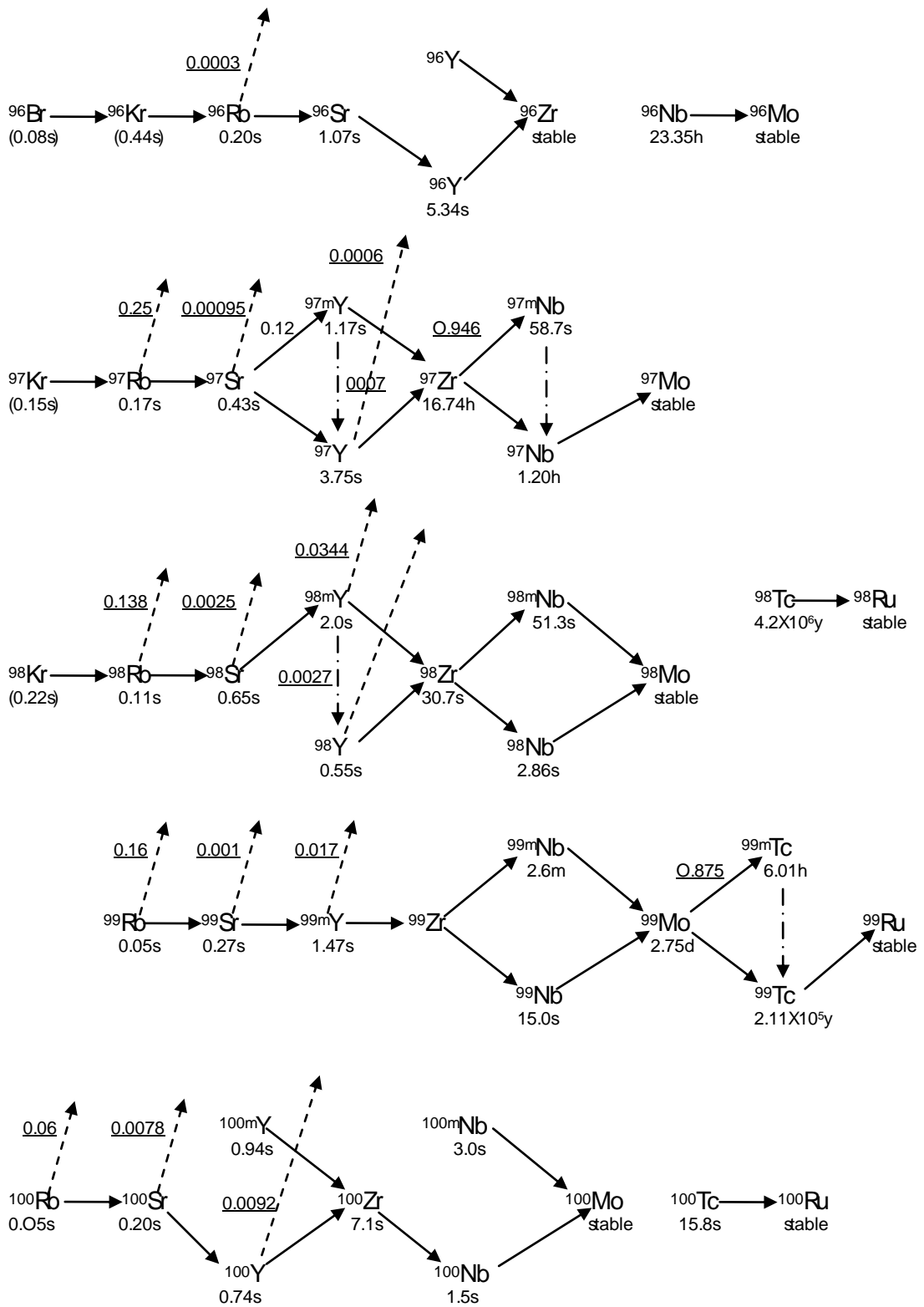
Note: Different radioactive decays are symbolized by different arrows in all the decay chains, as shown in Figure A1.1.

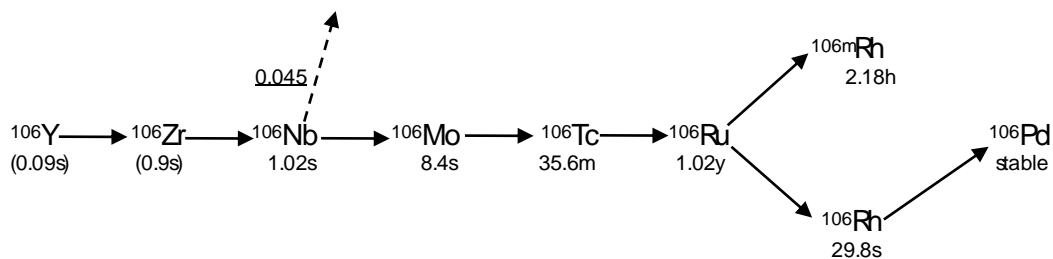
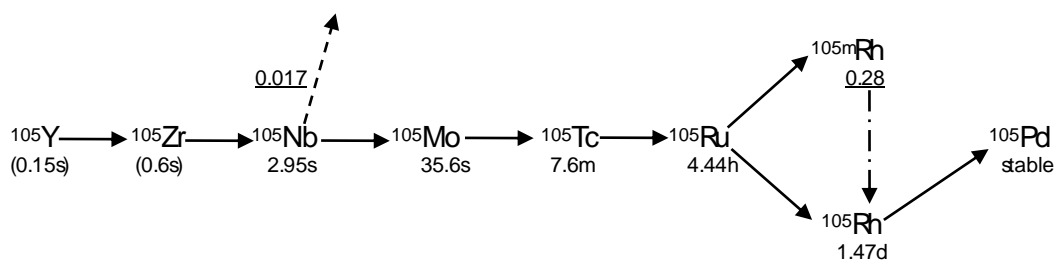
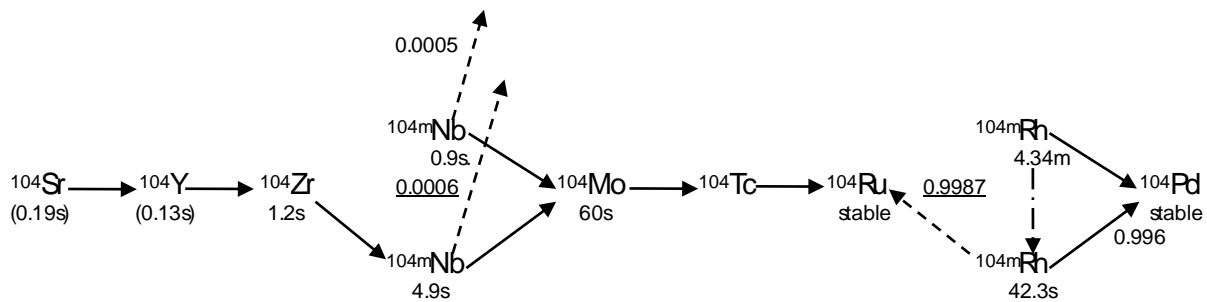
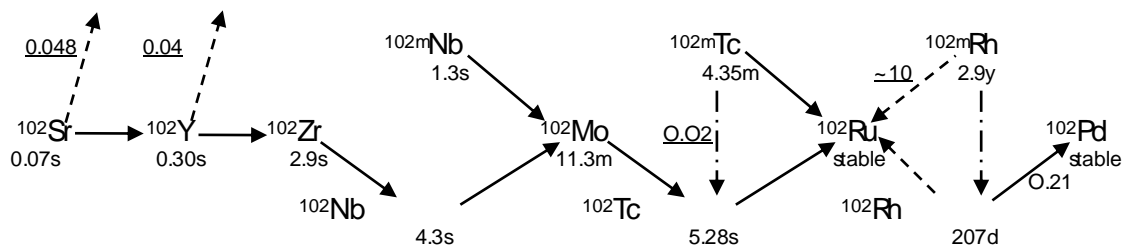
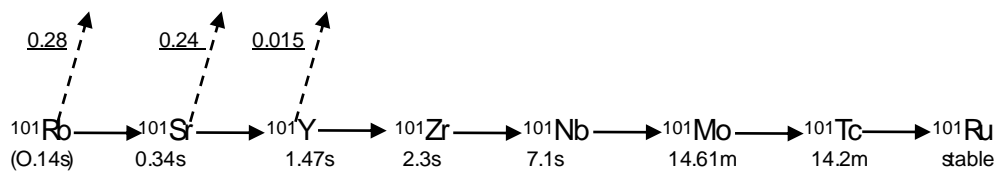


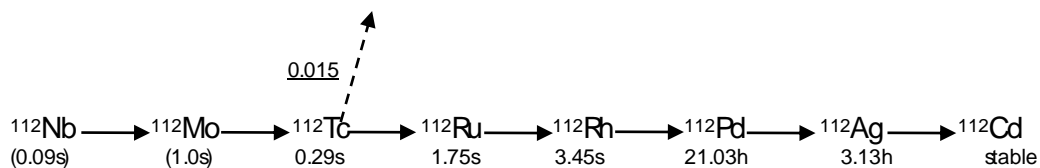
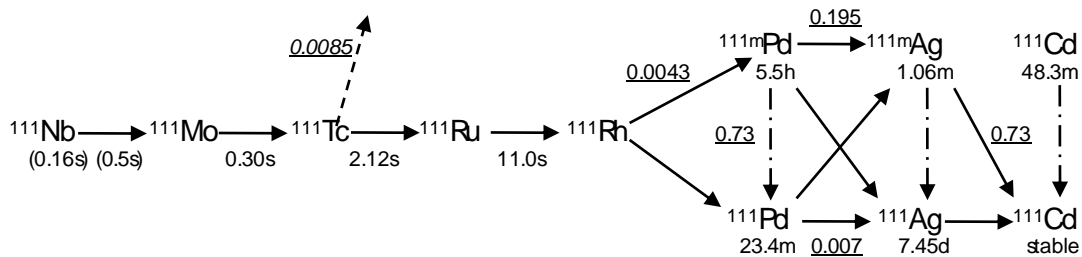
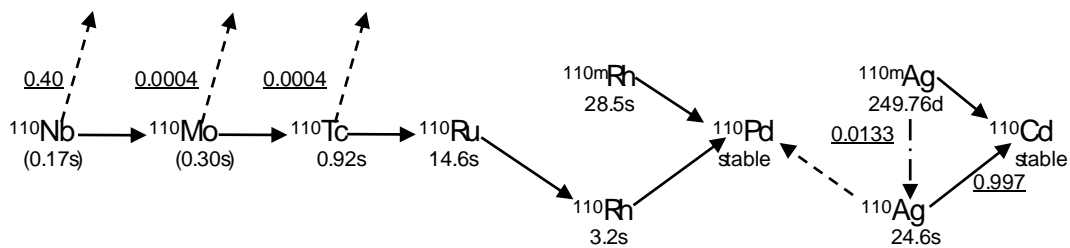
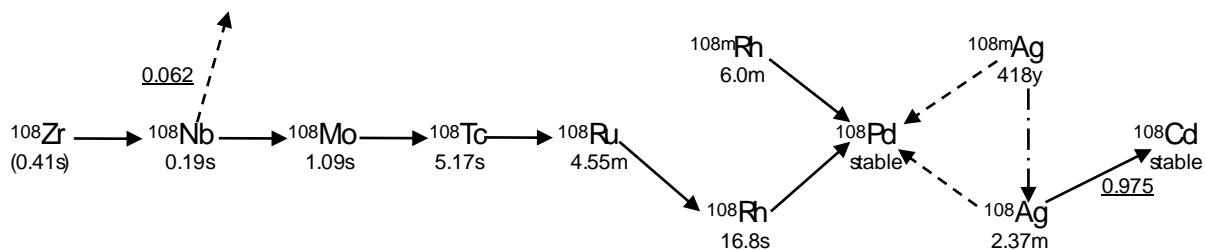
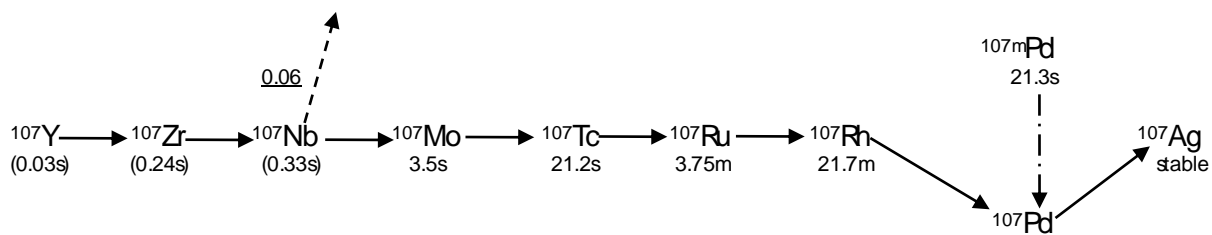


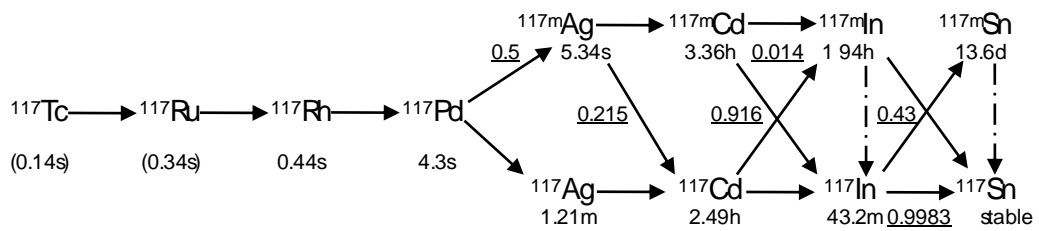
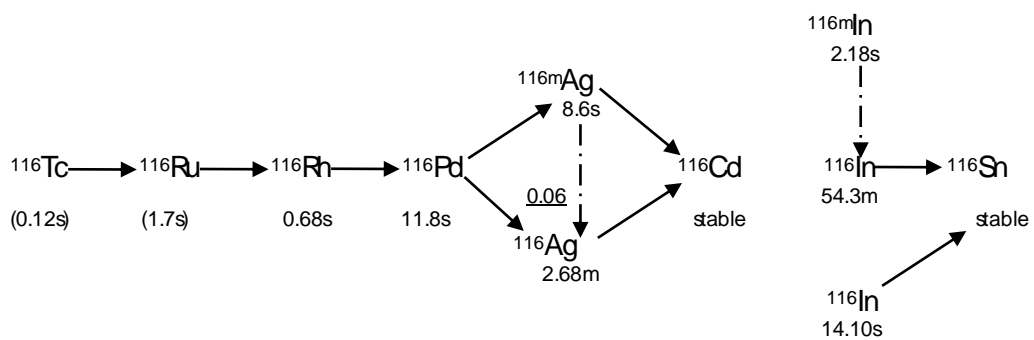
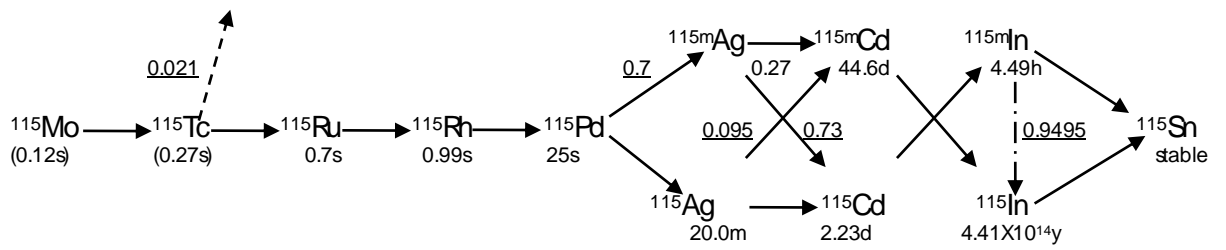
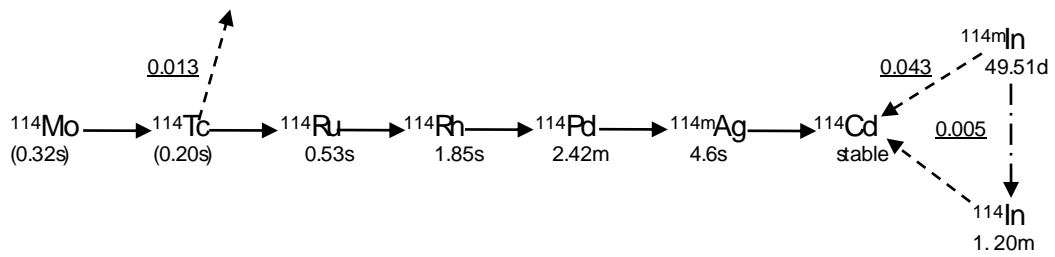
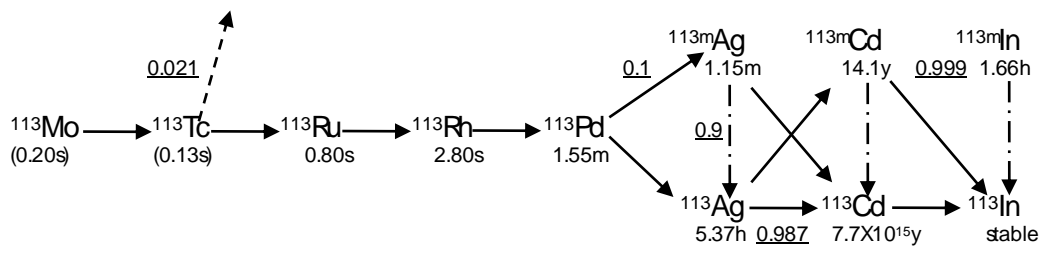


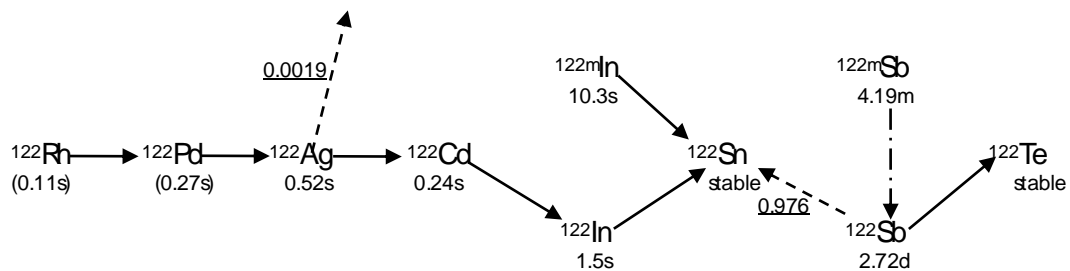
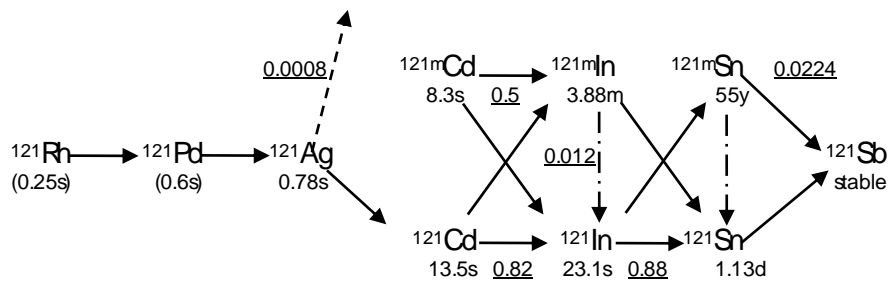
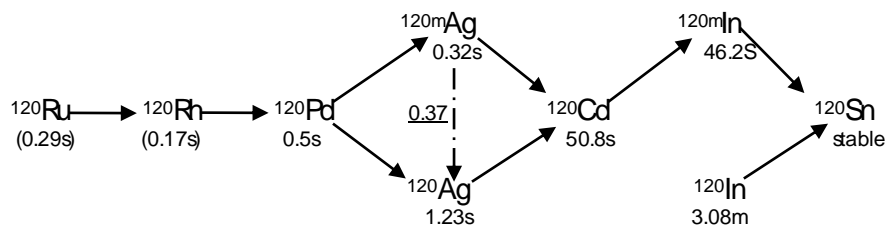
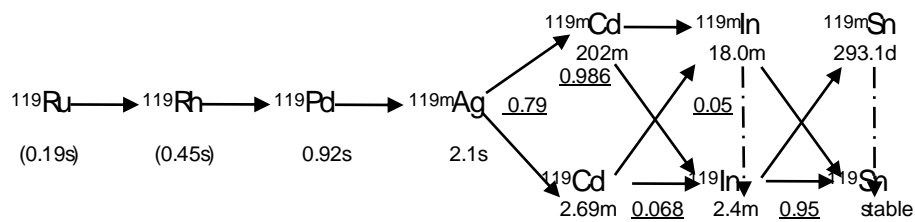
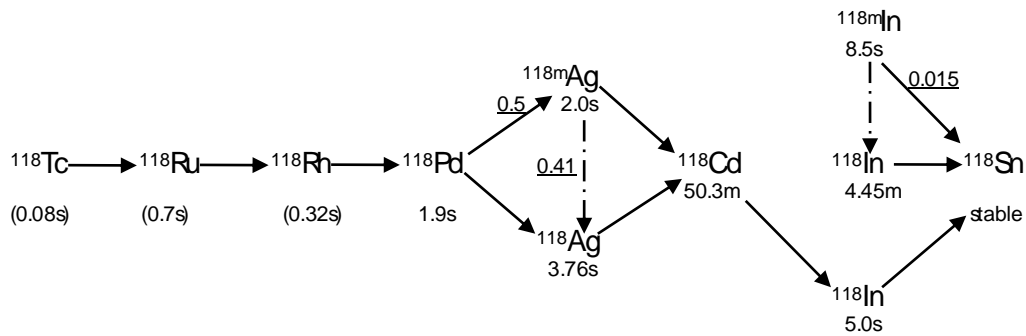


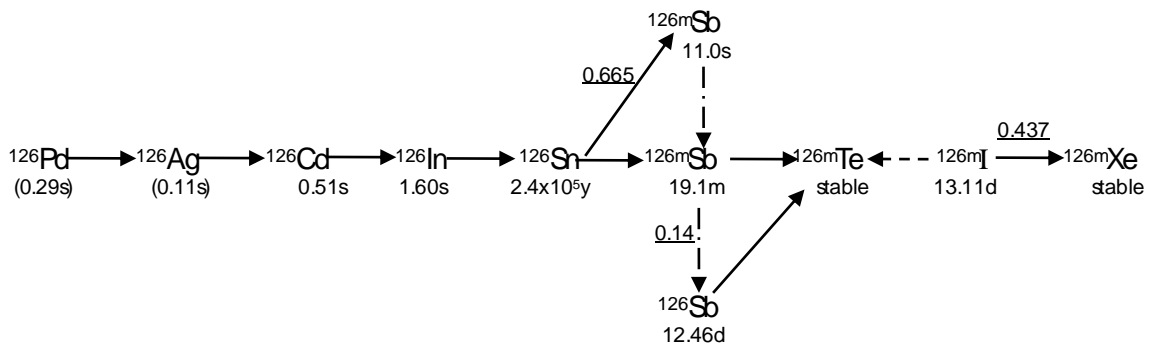
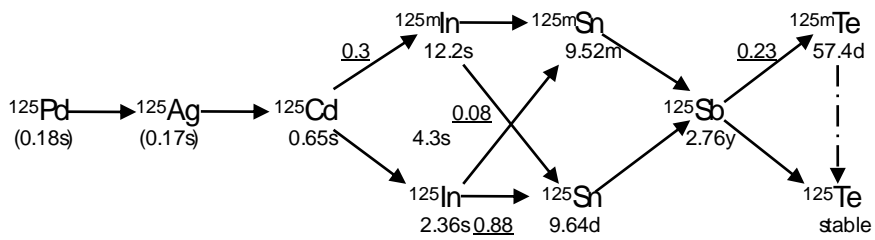
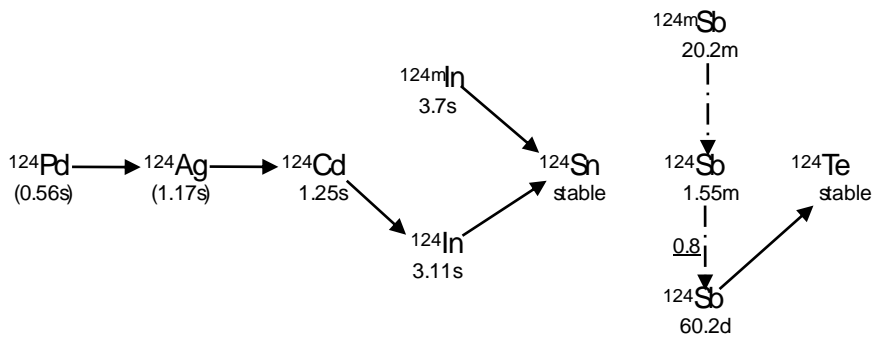
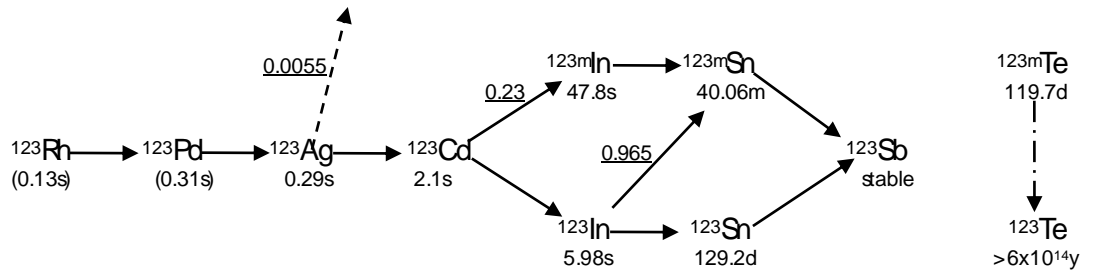


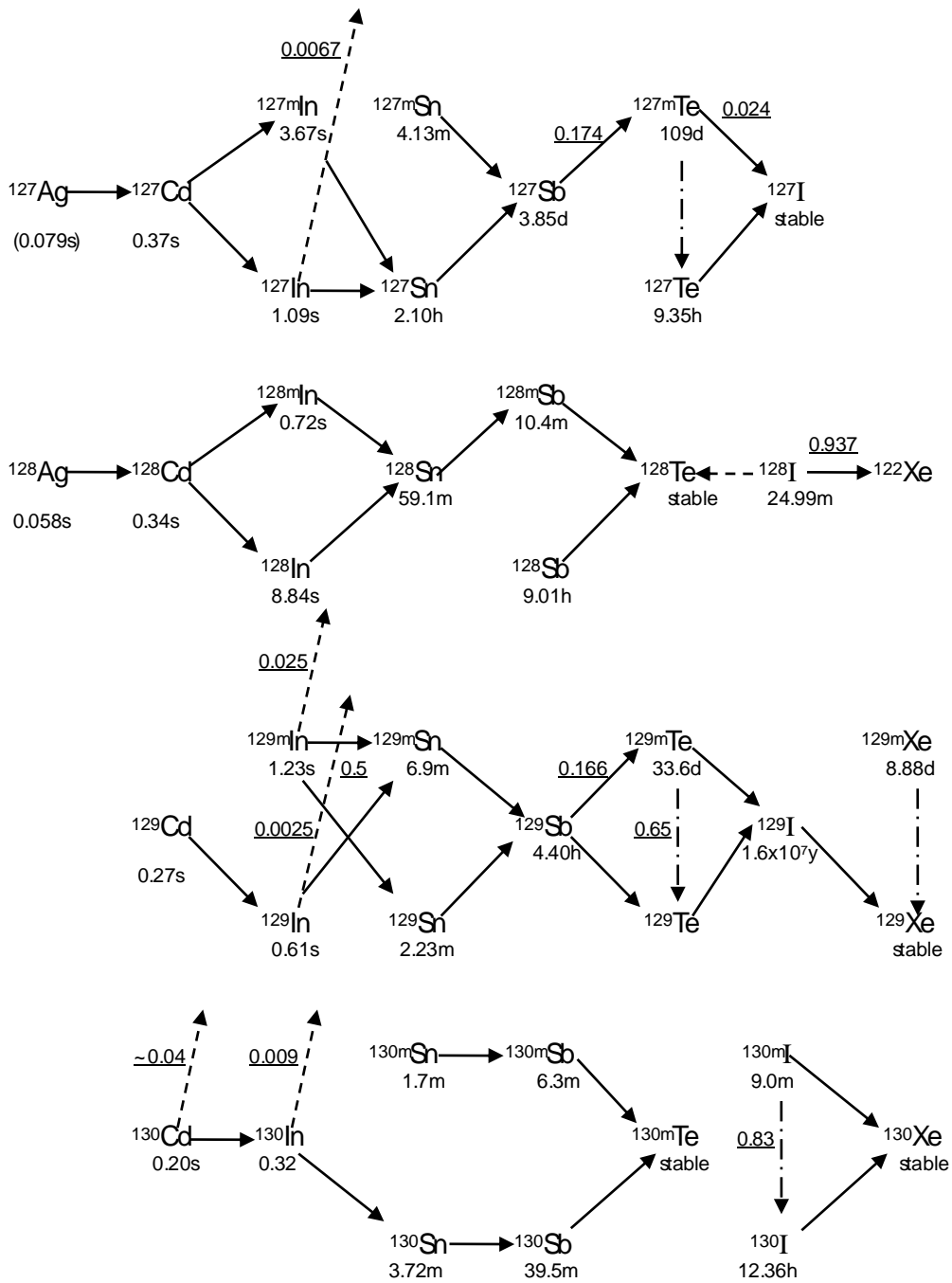


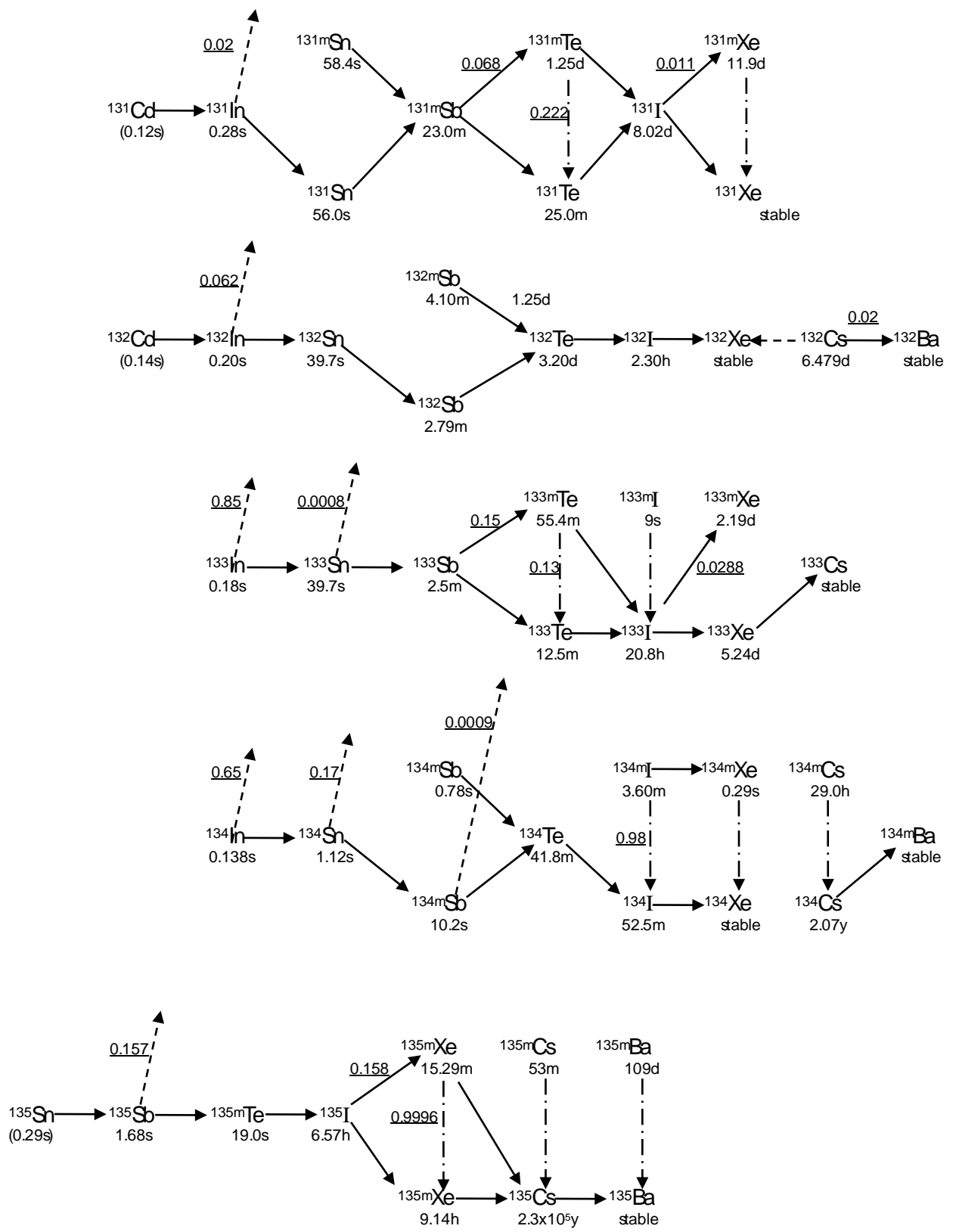


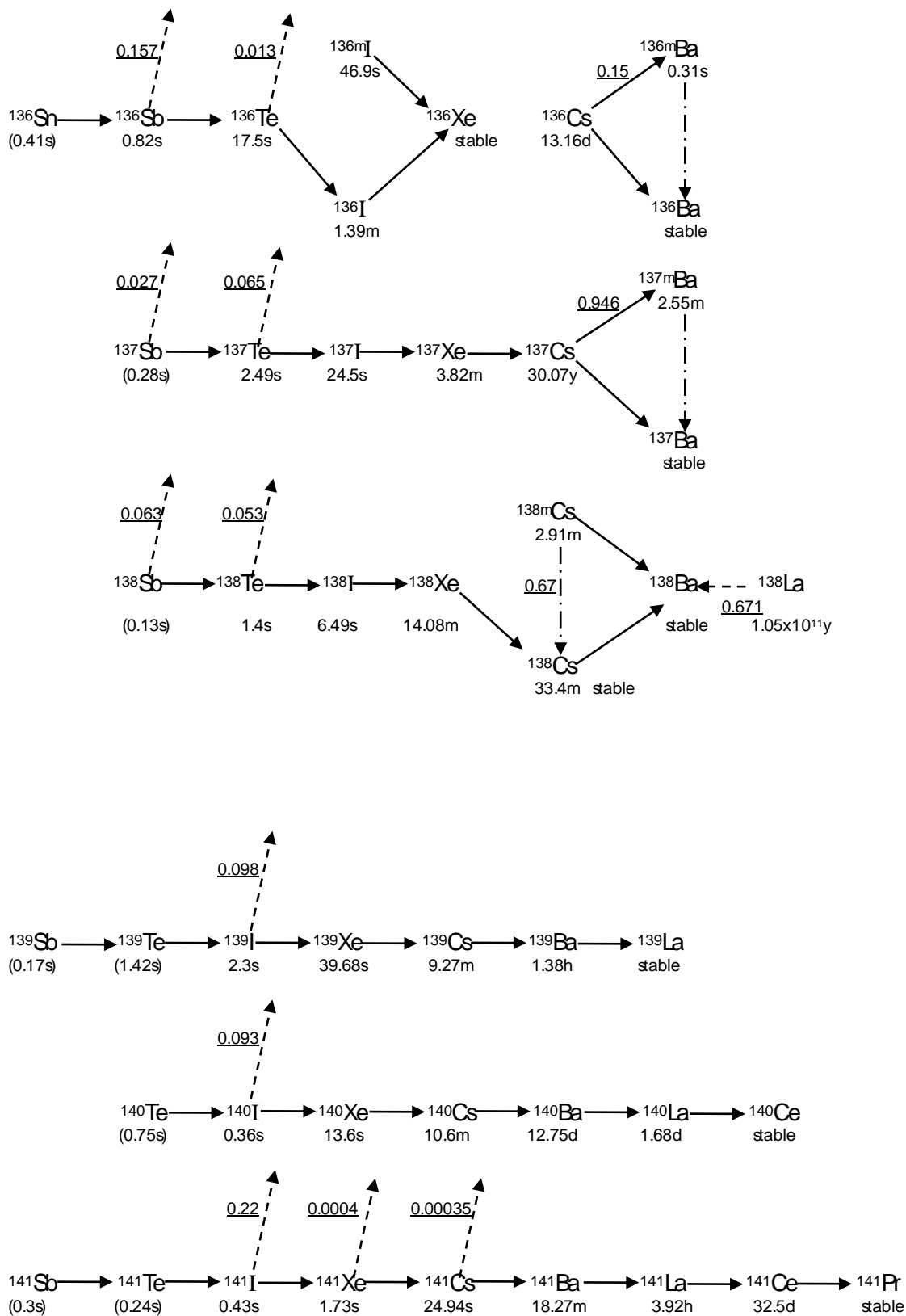


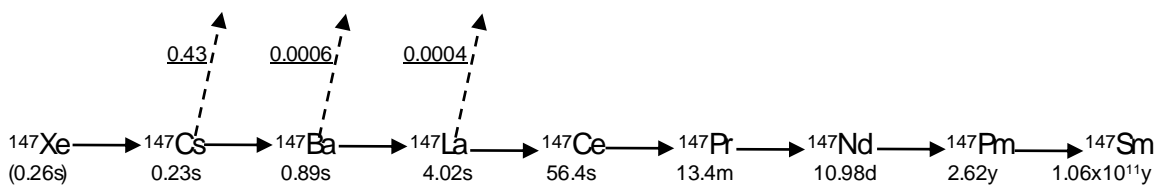
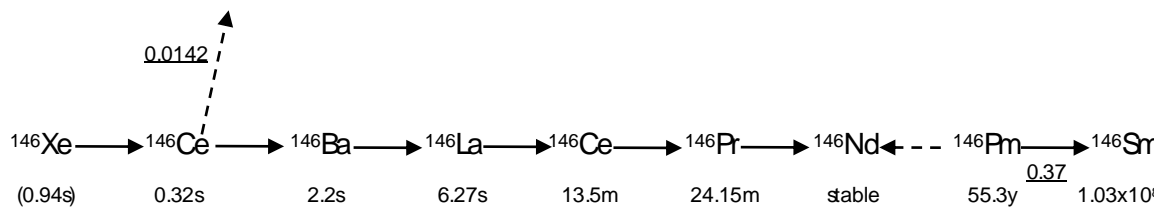
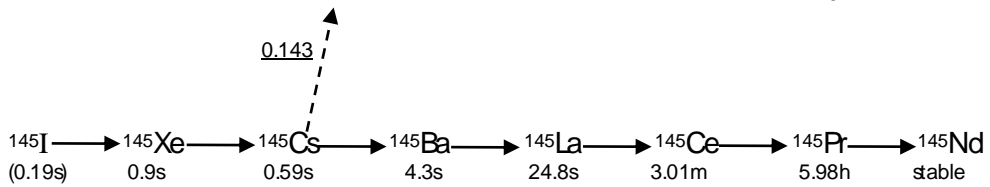
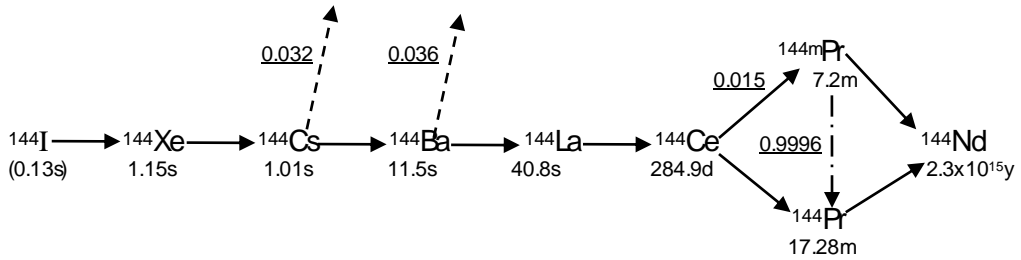
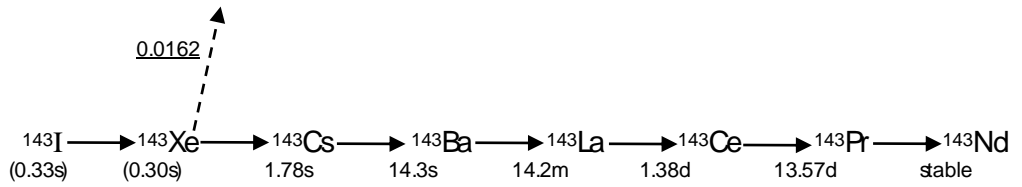
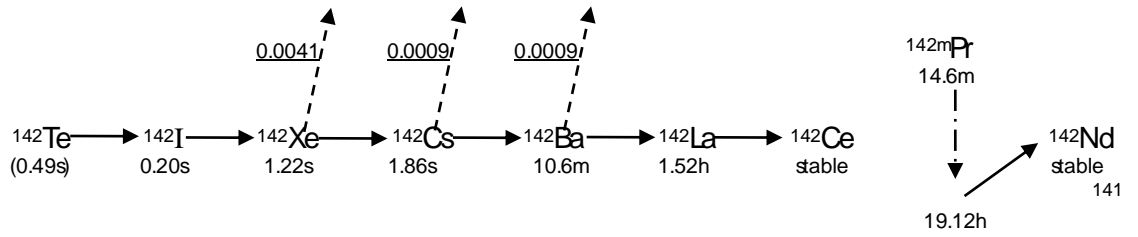


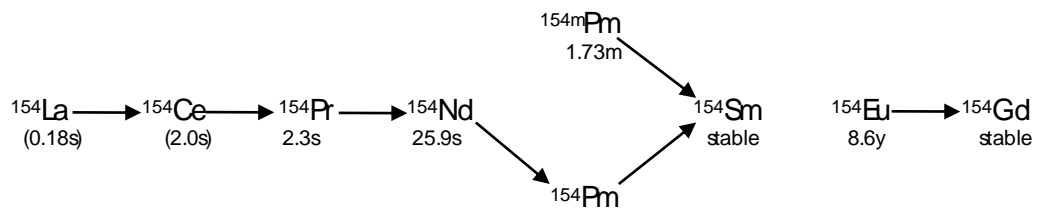
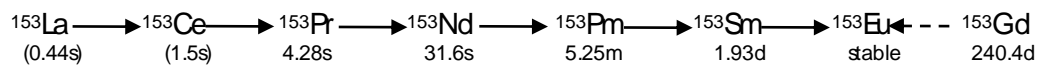
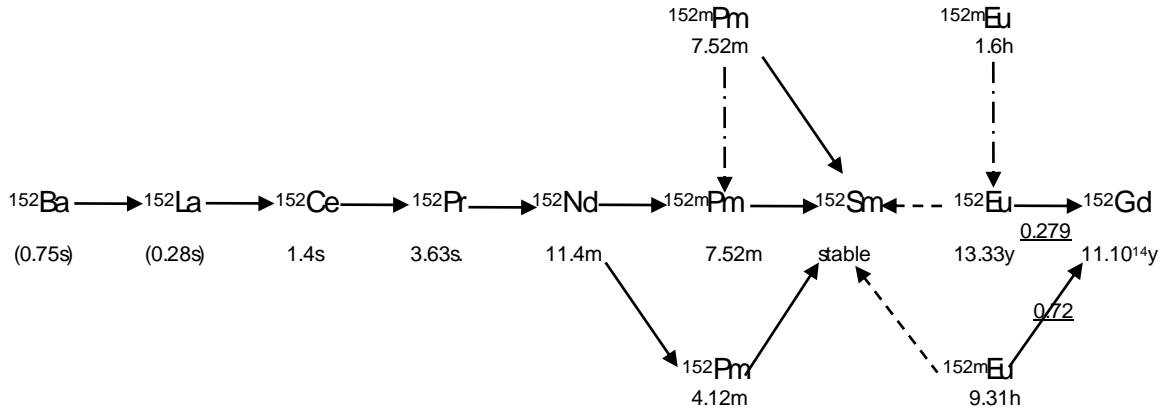
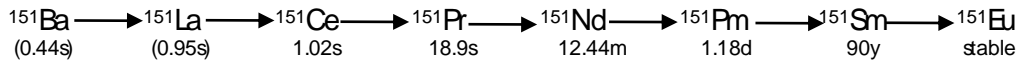
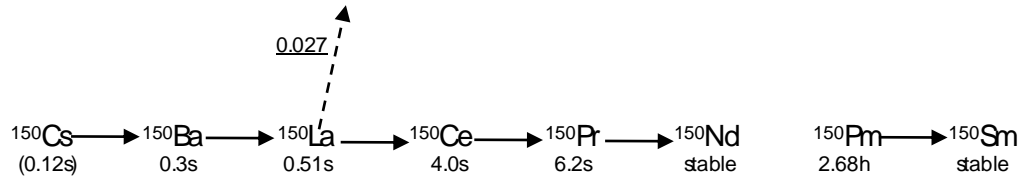
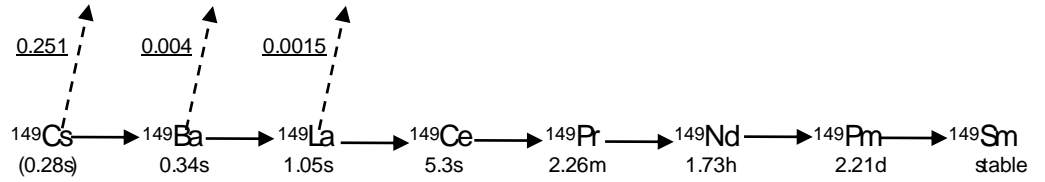
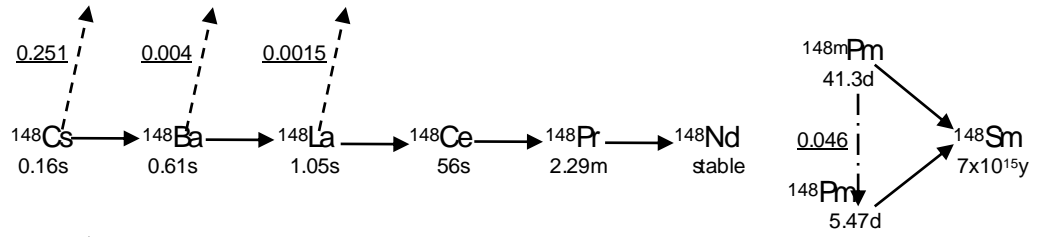


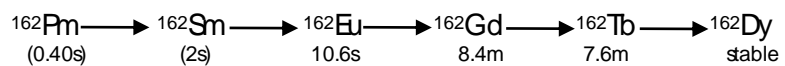
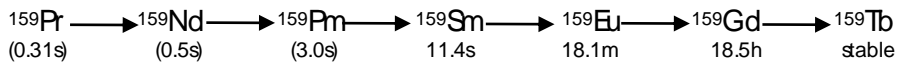
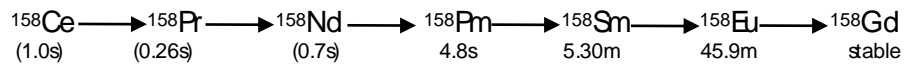
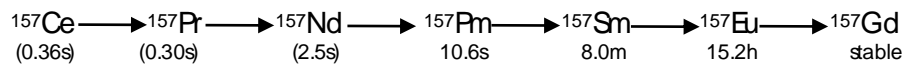
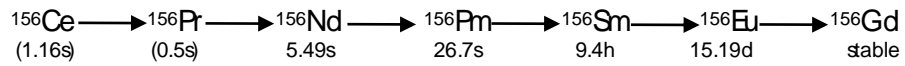


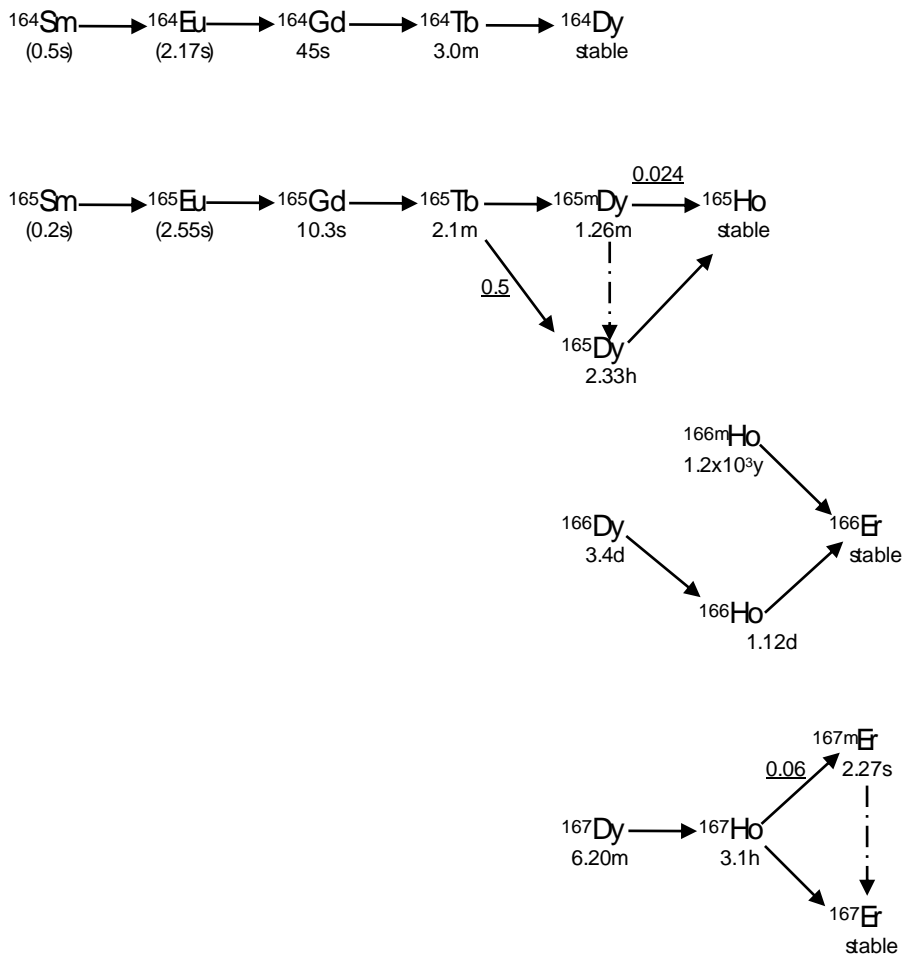












All the fission product chains have been explicitly modeled in IGDC. Nuclear fission typically breaks a heavy nucleus into two fission fragments (say ^{140}Xe -140 and ^{96}Sr are two of the nuclides that fission produces). Initially, the fission fragments are highly excited and get rid of excitation energy by emitting neutrons and gamma rays. Most fission neutrons are emitted almost immediately ($\sim 10^{-17}$ s) after the fission occurs; these are known as prompt fission neutrons, while the gamma rays are known as prompt

gammas. Following de-excitation, a nucleus formed by fission does not have sufficient excitation energy to throw off any more neutrons.

Name “**Fission products**” applies to all decay chain members, including the original fission fragments. The term “**Fragment**” describes the initial flying pieces that de-excite before they come to rest as fission products. The majority of fission products have half-lives that range from fractions of a second to about 30 years [75]. In 1 ton of CANDU spent fuel, about 12 kilograms is the fission products [76]. Fission products and their decay chains are given in this annexure are utilized for the modeling of the generation and decay of radioisotopes in a nuclear reactor. Fission products are highly charged and unstable and hence emits energy via different decay modes until it reaches a stable nucleus. This decay of fission products forms a chain called decay chain, which terminates on a stable nucleus, as shown in this annexure.

Generation and depletion of actinides

Besides the fission products, other elements are known as **actinides**, which are also found in the core of nuclear reactors; these are heavy nuclei and contribute to the fuel's radioactivity. Actinides are produced by neutron capture and also by radioactive decays of the parent nuclides. These 'transuranic' nuclei, heavier than uranium, are produced by neutron captures, which do not lead to nuclear fission. Their name comes from the element actinium ($Z=89$), a heavy metal that precedes uranium in Mendeleev's periodic table [76].

Long-lived actinides (e.g., Neptunium Np, americium Am, curium Cm) produced inside the nuclear reactor forms the long-lived radioactive waste and is associated with its radiotoxicity. The actinides formed by the capture of neutrons undergo a series of radioactive decay and form other actinides in the nuclear reactor. The decay chains of all the actinides followed in the IGDC code are presented here. The series of generation and decay chains of actinides along with their branching ratios are also shown below [6]:

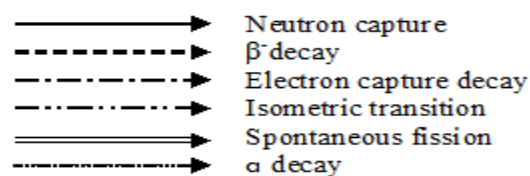
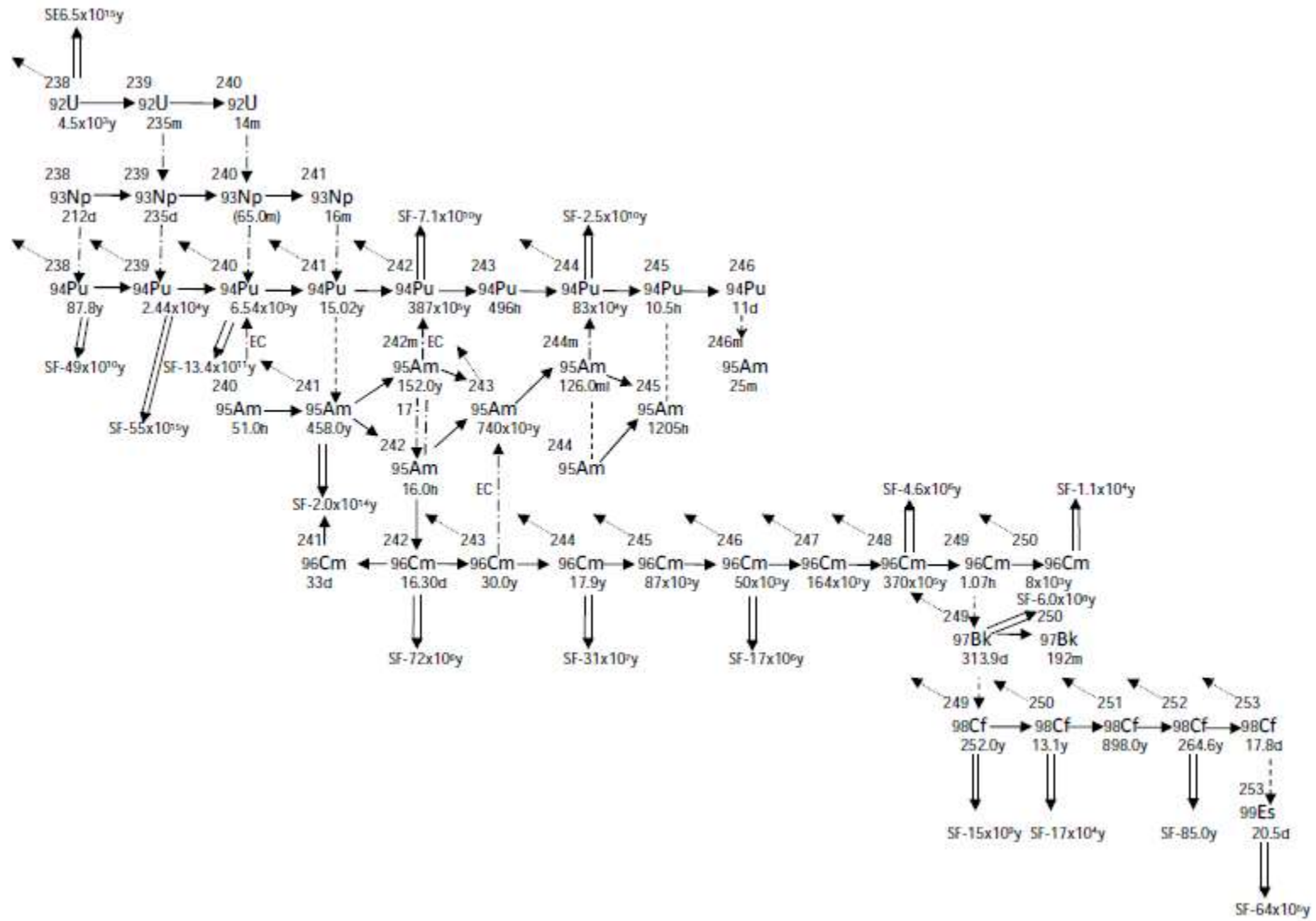
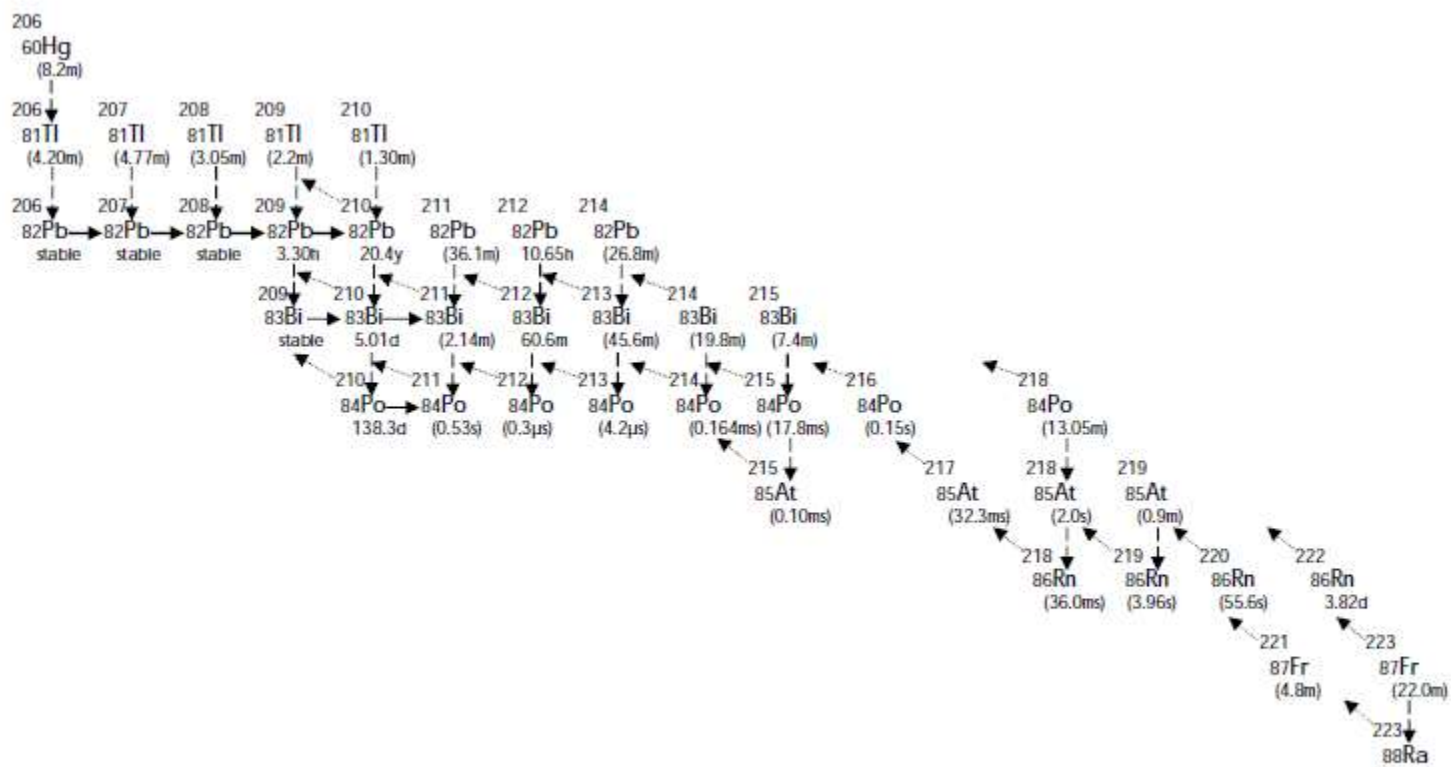


Figure A2. 1: Radioactive decay chains of actinides

Note: Different radioactive decays are symbolized by different arrows in all the decay chains, as shown in Figure A2.1.





It may be noted that actinide decay times cover a large range. Also, the actinide chain is exhaustive, and data also may not exist for certain isotopes. In 1 ton of CANDU spent fuel, about 6 kilograms of actinides are formed [76]. The composition of these actinides can be estimated by solving the burn-up equations of actinides. These equations can be developed using the generation and decay chains provided in this annexure.

Numerical Methods for ODEs

A3-1. Introduction

The equations in which the unknown function appears as derivative or the differential are called differential equations. Differential equations arise whenever some continuously varying quantities (modeled by functions viz. concentration of different isotopes changes always in a nuclear reactor fuel under irradiation) and their rates of change in space or time (expressed as derivatives) is known or assumed or postulated **[Error! Reference source not found.]**. These differential equations are found in many branches of science, e.g., such as Bateman or burn-up equations and Inhour equations in Reactor Physics. This makes the role of differential equations prominent in science and technology.

The rate of change of a radioactive substance is proportional to its concentration. This rate is called the radioactive decay rate. If $N(t)$ represents the concentration of the substance at any time t , the radioactive decay rate $\frac{dN}{dt}$ is proportional to $N(t)$. Then the rate of decomposition is modeled by

$$\frac{dN}{dt} = -KN, N(0) = N_0 \quad (1)$$

Where Minus sign indicates that the concentration of the substance is decreasing, and K is the constant of proportionality.

A physical situation concerned with the rate of change of one quantity with respect to another gives rise to a differential equation. Consider the first-order ordinary differential equation [78]

$$\frac{dy}{dx} = f(x, y), y(x_0) = y_0 \quad (2)$$

Many analytical techniques exist for solving such equations, but these methods can be applied to solve only a selected class of differential equations. However, a majority of differential equations appearing in physical problems cannot be solved analytically. Thus it becomes essential to discuss their solution by numerical methods. In numerical methods, one should not hope for finding a relation between variables; instead, one finds the numerical values of the dependent variable for certain values of the independent variable. It must be noted that even the differential equations which are solvable by analytical methods can be solved numerically as well. Therefore, the equations that are tough enough to be solved through analytical methods may be solved using numerical methods. Problems in which all the conditions are specified at the initial point only are called **initial-value problems**. For example, the problem is given by Eq. (1), and (2) are the initial value problem. To obtain a unique solution of n^{th} order ordinary differential equation, it is necessary to specify n values of the dependent variable and its derivative at specific independent variable values.

A3-2. Methods of solution of initial value problem

Generally, there are two ways to solve the initial value problem-

- Analytical Method
- Numerical Method

A3-2.1. Analytical method

The separation of variables is a technique commonly used to solve ordinary differential equations. If $\phi(x)$ is a solution, so is $c\phi(x)$, where c is an arbitrary (non-zero) constant, then it is considered as a linear differential equation and is called homogeneous. In this case, we use a homogeneous method. The integrating factor is commonly used to solve the ordinary differential equation but is also used within multivariable calculus when multiplying through by an integrating factor allows an inexact differential to be made into an exact differential. Not all first-order equations can be rearranged in this way, so this technique is not always appropriate.

Further, it is impossible to perform the integration even if the variables are separable [79]. It is also to be noted that these differential equations can be nonlinear and stiff also. In these cases, the above methods are very time taking and may not the solution too. Therefore, we need appropriate numerical methods to provide a quick and correct solution with a specified minimum error.

A3-2.2. Numerical method

Numerical methods [**Error! Reference source not found.**] for ordinary differential equations are used to find numerical approximations to the Initial Value Problem solution. Their use is also known as "numerical integration", although this term is sometimes taken to mean integrals' computation. *Solving the differential equation numerically is converting differential equations into an algebraic equation and solving it, and the solution method is called an integrator.* The numerical solutions are obtained step-by-step through a series of equal/unequal intervals of the independent variable. As

soon as the solution y has been obtained at $x = x_i$, the next step consists of evaluating y_{i+1} at $x = x_{i+1}$. The methods that require only the numerical value y_i to compute the next value y_{i+1} for solving Eqn. (2) given above are termed as single-step methods. The methods that require more than one previous value for the estimation of y_{i+1} are multistep methods.

A3-2.2.1. Single-step methods

Single-step methods require only one previous value for estimating the next value of the unknown variable. Here some essential single-step methods are described in the following sub-sections:

A3-2.2.1.1. Picard's method

Picard, a distinguished Professor of Mathematics at the University of Paris, France, was famous for his research on the Theory of Functions. The numerical method due to Picard is of considerable theoretical value. Practically, it is unsatisfactory because of the difficulties which arise in performing the necessary integrations. It is an iterative method and each step gives a better approximation of the required solution than the preceding one.

$$y_n = y_0 + \int_{x_0}^x f(x, y_{n-1}) dx \quad (3)$$

A3-2.2.1.2. Euler's method

The initial value problem is given as:

$$\frac{dy(x)}{dx} = f(x, y), \quad y(x_0) = y_0 \quad (4)$$

Estimating solutions at different base points $y(x_0 + h)$, $y(x_0 + 2h)$, $y(x_0 + 3h)$, can be obtained through Taylor series expansion (Here 'h' is the time step). A truncated Taylor series expansion is given as:

$$\begin{aligned}
 y(x_0 + h) &\approx \sum_{k=0}^n \frac{h^k}{k!} \left(\frac{d^k y}{dx^k} \Big|_{x=x_0, y=y_0} \right) \\
 &\approx y(x_0) + h \frac{dy}{dx} \Big|_{x=x_0, y=y_0} + \frac{h^2}{2!} \frac{d^2 y}{dx^2} \Big|_{x=x_0, y=y_0} + \dots + \frac{h^n}{n!} \frac{d^n y}{dx^n} \Big|_{x=x_0, y=y_0}
 \end{aligned} \tag{5}$$

The first-order Taylor series method is known as the Euler Method. Only the constant term and linear term are used in the Euler method. The error due to the use of the truncated Taylor series is of order $O(h^2)$.

$$y(x_0 + h) = y(x_0) + h \frac{dy}{dx} \Big|_{x=x_0, y=y_0} + O(h^2)$$

Notation:

$$x_n = x_0 + nh, \quad y_n = y(x_n),$$

$$\frac{dy}{dx} \Big|_{x=x_i, y=y_i} = f(x_i, y_i)$$

Euler Method

$$y_{i+1} = y_i + h f(x_i, y_i) \tag{6}$$

Euler's method is the simplest one-step method and has a limited application because of its low accuracy. This method yields a solution of an ordinary differential equation in the form of a set of tabulated values.

$$y_{n+1} = y_n + hf(x_n, y_n) \tag{7}$$

Formula (7) is called Euler's forward Formula. In this method, equation (6) is an explicit equation and is used for non-stiff problems. Backward Euler method is used

for stiff first-order ordinary differential equations as it is A-stable i.e. stability independent of time step “h” and is given by

$$y_{n+1} = y_n + hf(x_{n+1}, y_{n+1}) \quad (8)$$

A3-2.2.1.3. Modified Euler’s method

The modified Euler’s method gives a more significant improvement in accuracy over the original Euler’s method. This is also called the trapezoidal method. In each integration step, the average value of the beginning and end of the interval is considered.

$$y_{n+1} = y_n + \frac{h}{2} [f(x_n, y_n) + f(x_{n+1}, y_{n+1})] \quad (9)$$

A3-2.2.1.4. RungeKutta second order method

More efficient methods of accuracy were developed by two German Mathematicians, Carl Runge (1856-1927) and Wilhelm Kutta (1867-1944). These methods are well-known as Runge-Kutta methods. Their orders distinguish them in the sense that they agree with Taylor’s series solution up to h^r where r is the order of the method [81]. As in Taylor’s method, these methods do not demand prior computation of higher $y(x)$ derivatives. In place of these derivatives, extra values of the given function $f(x, y)$ are used.

$$k1 = hf(x_n, y_n) \quad (10)$$

$$k2 = hf(x_{n+h}, y_{n+k1}) \quad (11)$$

$$y_{n+1} = y_n + \frac{1}{2}(k1 + k2) \quad (12)$$

A3-2.2.1.5. RungeKutta fourth-order method

The fourth-order Runge-Kutta method is used widely for finding the numerical solutions of linear or non-linear ordinary differential equations. Runge-Kutta methods

are referred to as single-step methods. The major disadvantage of Runge-Kutta methods is that they use many more evaluations of the derivative $f(x, y)$ to obtain the same accuracy compared with multi-step methods. A class of techniques known as Runge-Kutta methods combines the advantage of high order accuracy with the property of being one step.

$$k_1 = hf(x_n, y_n) \quad (13)$$

$$k_2 = hf(x_{n+h/2}, y_{n+k_1/2}) \quad (14)$$

$$k_3 = hf(x_{n+h/2}, y_{n+k_2/2}) \quad (15)$$

$$k_4 = hf(x_{n+h}, y_{n+k_3}) \quad (16)$$

$$y_{n+1} = y_n + \frac{1}{6}(k_1 + 2k_2 + 2k_3 + k_4) \quad (17)$$

A3-2.2.1.6. Numerical Solution of stiff differential equations

Stiff differential equations have both slow and fast varying components. In this situation, if the time step of integration is very small, the computation time will be considerable. On the other hand, if the time step of integration is chosen to be very large, fast varying components will be lost.

In this condition, an implicit method algorithm viz. Backward Euler Method can be applied. Stiffness is usually associated with differential equations viz. system of first-order coupled differential equations. However, some characteristics of a particular numerical method applied to a stiff system can be studied when the method is applied to a single equation [82].

Example-1: Solve the following problem from $t = 0$ to $t = 10$,

$$\frac{dy_1}{dt} = -y_1, y_1(0) = 1.5 \quad (18)$$

Solution: The analytical solution for this equation is $y_1 = 1.5e^{-t} = 1.5e^{-10}$.

If we want to solve the following equation numerically, the stable step size with Euler's method is limited by $|1+h\lambda|\leq 1$ (Stability condition), where h is the time step size (Δt) and λ is -1.

i.e. for stability, $|1-\Delta t| \leq 1$, i.e. $\Delta t \leq 2$, therefore at least $\frac{10}{2} = 5$ -time steps are necessary to integrate to $t = 10$.

Example-2: Solve the following problem from $t = 0$ to $t = 10$,

$$\frac{dy_2}{dt} = -1000y_2, y_2(0) = 0.5 \quad (19)$$

Solution: The analytical solution for this equation is $y_2 = 0.5e^{-1000t}$.

For this system, the largest step size we can use is $1000\Delta t \leq 2$ or $\Delta t \leq 0.002$. If we want to integrate to $t = 10$, we would need $\frac{10}{0.002} = 5000$ integration steps.

Note: The stiff problem arises when the solution contains both terms $1.5e^{-t}$ and $0.5e^{-1000t}$. In this case to integrate upto $t = 10$ so that the term $1.5e^{-t}$ can become sufficiently small and we will need 5,000 integration steps to satisfy the stability requirement. Consider the following linear system of differential equations:

$$\frac{dy_1}{dt} = -500.5 y_1 + 499.5 y_2 \quad ; y_1(0) = 2 \quad (20)$$

$$\frac{dy_2}{dt} = 499.5 y_1 - 500.5 y_2 \quad ; y_2(0) = 1 \quad (21)$$

The system can be written in matrix form as

$$\frac{dy}{dt} = Ay \quad (22)$$

Where,

$$\mathbf{y} = \begin{bmatrix} y_1 \\ y_2 \end{bmatrix} \text{ and } \mathbf{A} = \begin{bmatrix} -500.5 & 499.5 \\ 499.5 & -500.5 \end{bmatrix} \quad (23)$$

Substitute a solution of the form $\mathbf{y} = \mathbf{k}e^{\lambda t}$ into equation (22) we obtain

$$\lambda \mathbf{k}e^{\lambda t} - \mathbf{A}\mathbf{k}e^{\lambda t} = 0 \quad (24)$$

or

$$(\lambda \mathbf{I} - \mathbf{A})\mathbf{k} = 0 \quad (25)$$

The homogeneous equation (19) will have nontrivial solutions when

$$|(\lambda \mathbf{I} - \mathbf{A})| = 0 \quad (26)$$

$$\begin{vmatrix} \lambda + 500.5 & -499.5 \\ -499.5 & \lambda + 500.5 \end{vmatrix} = 0 \quad (27)$$

On solving, $\lambda_1 = -1$ and $\lambda_2 = -1000$

λ_1 and λ_2 are the eigenvalues of \mathbf{A} . The constant vector \mathbf{k} can now be evaluated

For $\lambda_1 = -1$

$$\begin{vmatrix} 499.5 & -499.5 \\ -499.5 & 499.5 \end{vmatrix} \begin{bmatrix} k_1 \\ k_2 \end{bmatrix} = 0 \Rightarrow \mathbf{k}_1 = C_1 \begin{bmatrix} 1 \\ 1 \end{bmatrix}$$

For $\lambda_2 = -1000$

$$\begin{vmatrix} -499.5 & -499.5 \\ -499.5 & -499.5 \end{vmatrix} \begin{bmatrix} k_1 \\ k_2 \end{bmatrix} = 0 \Rightarrow \mathbf{k}_2 = C_2 \begin{bmatrix} 1 \\ -1 \end{bmatrix}$$

The solution is then written as

$$\mathbf{y} = \mathbf{k}_1 e^{\lambda_1 t} + \mathbf{k}_2 e^{\lambda_2 t} = C_1 \begin{bmatrix} 1 \\ 1 \end{bmatrix} e^{-t} + C_2 \begin{bmatrix} 1 \\ -1 \end{bmatrix} e^{-1000t}$$

The constant C_1 and C_2 can be determined from the initial conditions

$$y_1(0) = 2 = C_1 + C_2$$

$$y_2(0) = 1 = C_1 - C_2$$

Solving the above two linear equations we obtain $C_1 = 1.5$ and $C_2 = 0.5$.

When we solve this system of equations numerically, we must integrate to $t = 10$ to see the full evolution of y_1 and y_2 . However, the largest step size is limited by

$$|\lambda_{\max}|\Delta t \leq 2 \Rightarrow \Delta t \leq \frac{2}{1000} = 0.002$$

The above condition requires 5,000 iteration steps. Therefore, the largest step size is governed by the largest eigenvalue, and the smallest eigenvalue usually controls the final time. The stiffness ratio SR of a system of differential equations is defined as

$$SR = \frac{\max |\operatorname{Re} \lambda_i|}{\min |\operatorname{Re} \lambda_i|} \quad (28)$$

A system is stiff if its SR is about 10^3 or higher. When the SR approaches 10^6 the system is very stiff. The stiffness can also be defined for a system of nonlinear equations

$$\frac{dy_i}{dt} = f(t, y_1, \dots, y_n) \quad ; \quad i = 1, 2, \dots, n \quad (29)$$

The equations can be linearized about the solution at a given time t_m

$$\frac{dy_i}{dt} = f(\mathbf{y}(t)) + \sum_{j=1}^n \frac{\partial y_i}{\partial y_j} (y_j - y_j(t)) \quad (30)$$

The eigenvalues of the Jacobian matrix \mathbf{A} are then calculated where $A_{ij} = \frac{\partial f_i}{\partial y_j}$. The

stiffness is then applied to that particular time t_m . The problem created by stiff differential equations can be alleviated by step size control using an adjustable step size to maintain a certain error tolerance. The step size can be adjusted using the empirical method, local truncation error, or integration method with a built-in error estimate.

A3-2.2.2. Baily's criteria for step size

One empirical technique for step size control is Bailey's criterion for a system of equations as follows:

$$\frac{dy_i}{dt} = f(t, y_1, \dots, y_n) \quad ; \quad i = 1, 2, \dots, n \quad (31)$$

Consider y_{i+1} at time step $t + \Delta t$ and $y_i^{(0)}$ at time step t . Compute $\Delta y_i = |y_{i+1} - y_i^{(0)}|$ for $i = 1, 2, \dots, n$. If all $\Delta y_i / y_i < 0.01$, double the step size. If any $\Delta y_i / y_i > 0.01$, half the step size. Otherwise keep the same step size. The step size can be checked by this criterion every 5-10 time steps.

Another simple procedure for controlling the step size is to do the calculations at each interval twice: Once with the full step size, and then repeat the calculations over the same interval with step size half that of the first one. This calculation will produce an estimated error that can be used to check the step size. For example, if the truncation error E is second-order $O(h^2)$, it can be written as $E = C h^2$. The constant C can be estimated as follow:

With full step size h

$$y_1 = y(0)(exact) + Ch^2 \quad (32)$$

With half the step size

$$y_2 = y(0)(exact) + C\left(\frac{h}{2}\right)^2 \quad (33)$$

The error can then be estimated

$$y_1 - y_2 = Ch^2 - C\left(\frac{h}{2}\right)^2 \text{ i.e. } E = \frac{3}{4}Ch^2 = \frac{4}{3}(y_1 - y_2) \quad (34)$$

With this information, h can be reduced if E is less than some error tolerance. Some integration methods have an estimate of the local error, for example, the Runge - Kutta method with the following formula:

$$y_{n+1} = y_n + \frac{1}{6}(k_1 + 4k_4 + k_5), \quad E \approx \frac{1}{30}(2k_1 - 9k_3 + 8k_4 - k_5) \quad (35)$$

Where,

$$\begin{aligned}
k_1 &= hf(x_n, y_n) \\
k_2 &= hf(x_n + \frac{1}{3}h, y_n + \frac{1}{3}k_1) \\
k_3 &= hf(x_n + \frac{1}{3}h, y_n + \frac{1}{6}k_1 + \frac{1}{6}k_2) \\
k_4 &= hf(x_n + \frac{1}{2}h, y_n + \frac{3}{8}k_3) \\
k_5 &= hf(x_n + \frac{1}{2}h, y_n + \frac{1}{2}k_1 - \frac{3}{2}k_3 + 2k_4)
\end{aligned}$$

A3-2.2.3. Multi-step methods

In single-step methods like Euler and Runge-Kutta methods, the estimates of y_{i+1} depend only on y_i and x_i . In the two-step method, estimates of y_{i+1} depend on y_i, y_{i-1}, x_i , and x_{i-1} . In a three-step method, estimates of y_{i+1} depend on $y_i, y_{i-1}, y_{i-2}, x_i, x_{i-1}$, and x_{i-2} . As the number of steps is increasing the accuracy of the method increases. Adam-Moulton method, Gears Backward Differentiation Formulae, and Shampine Numerical Differentiation Formulae methods are multi-step methods.

A3-2.2.4. Numerical solution with Multi-step methods[83]

In higher-order multi-step methods, the general-purpose method of resolution for the equation

$$\frac{dy}{dt} = f(y, t), y(t_0) = x_0$$

is given by:

$$y_{n+1} = \sum_{i=0}^p a_i y_{n-i} + h \sum_{i=-1}^p b_i f(y_{n-i}, t_{n-i}) \quad (36)$$

With $b_{-1} = 0$, the method is explicit and not suitable for obtaining the correct and stable solution. When $b_{-1} \neq 0$, the method is implicit and suitable for solving stiff problems.

For differential equation systems describing the burn-up equations, the eigenvalues strongly vary. This kind of differential equation system is called stiff.

For a polynomial of order k , the number of required coefficients is.

$$2p + 3 \geq k + 1 \quad (37)$$

These co-efficient should satisfy $x^{n+1} = x(t^{n+1})$. The following equation system can achieve this:

$$\sum_{i=0}^p a_i = 1 \ \& \ \sum_{i=1}^p (-i)^j a_i + j \sum_{i=-1}^p (-i)^{j-1} b_i = 1 \ \text{for } j = 1, 2, 3, \dots, k \quad (38)$$

The different linear multistep integration methods constructed by the equation system (38) vary in the equality condition corresponding with (37) and the choice of coefficients, which are set to zero.

A3-2.2.5. Gears BDF method[83]

The Gear formulae (also called BDF - Backward Differentiation Formulae) have great importance within the multi-step integration methods used in solving stiff ODEs. The conditions:

$$p = k - 1 \ \text{and} \ b_0 = b_1 = \dots = b_{k-1} = 0 \quad (39)$$

is set to satisfy the equation system (38). The equation system of the BDF coefficients of order 4 is as follows:

$$\begin{bmatrix} 0 & 1 & 1 & 1 & 1 \\ 1 & 0 & -1 & -2 & -3 \\ 2 & 0 & 1 & 4 & 9 \\ 3 & 0 & -1 & -8 & -27 \\ 4 & 0 & 1 & 16 & 81 \end{bmatrix} \cdot \begin{bmatrix} b_{-1} \\ a_0 \\ a_1 \\ a_2 \\ a_3 \end{bmatrix} = \begin{bmatrix} 1 \\ 1 \\ 1 \\ 1 \\ 1 \end{bmatrix} \quad (40)$$

Order $k=1$ yields the implicit Euler method. The example given in the equation system (40) results in the following integration formula.

$$\begin{aligned} y_{n+1} &= a_0 y_n + a_1 y_{n-1} + a_2 y_{n-2} + a_3 y_{n-3} + h b_{-1} f(y_{n+1}, t_{n+1}) \\ &= \frac{48}{25} y_n - \frac{36}{25} y_{n-1} + \frac{16}{25} y_{n-2} - \frac{3}{25} y_{n-3} + h \frac{12}{25} f(y_{n+1}, t_{n+1}) \end{aligned} \quad (41)$$

There is no more stable second-order integration method than the Gear's method of second order. Only implicit Gear methods with order $k \leq 6$ are zero stable. Backward differentiation formulae (BDF) for the order $k = 1, 2, 3, 4, 5$ and 6 are as follows:

$k=1,$

$$y_{n+1} = y_n + h f_{n+1} \quad (42)$$

$k=2,$

$$y_{n+1} = \left(\frac{4}{3}\right) y_n - \left(\frac{1}{3}\right) y_{n-1} + \left(\frac{2}{3}\right) h f_{n+1} \quad (43)$$

$k=3,$

$$y_{n+1} = \left(\frac{18}{11}\right) y_n - \left(\frac{9}{11}\right) y_{n-1} + \left(\frac{2}{11}\right) y_{n-2} + \left(\frac{6}{11}\right) h f_{n+1} \quad (44)$$

$k=4,$

$$y_{n+1} = \left(\frac{48}{25}\right) y_n - \left(\frac{36}{25}\right) y_{n-1} + \left(\frac{16}{25}\right) y_{n-2} - \left(\frac{3}{25}\right) y_{n-3} + \left(\frac{12}{25}\right) h f_{n+1} \quad (45)$$

$k=5,$

$$\begin{aligned} y_{n+1} &= \left(\frac{300}{137}\right) y_n - \left(\frac{300}{137}\right) y_{n-1} + \left(\frac{200}{137}\right) y_{n-2} - \left(\frac{75}{137}\right) y_{n-3} + \left(\frac{12}{137}\right) y_{n-4} \\ &\quad + \left(\frac{60}{137}\right) h f_{n+1} \end{aligned} \quad (46)$$

BDFs provides the possibility to use high-order formulae in highly stable schemes, but their most significant drawback is the higher-order formula's poor stability properties. Several efforts to derive methods with better accuracy and stability properties than those in BDFs have been made.

One of the modifications made to the BDFs in this line is the NDFs (Numerical Differentiation Formulae) done by Klopfenstein and Shampine. It is a computationally cheap modification that consists of anticipating a difference of the order (n+1) term multiplied by a constant $k\gamma_k$ in the BDF formulae of order k. This term is equivalent to the error in the (k)th term occurring in the BDFs and thus reduces the error constant of BDF and owing to which larger time step can be taken with the same accuracy as of BDFs and not much less stable. Then the k-step NDF of order k is

$$\sum_{m=1}^k \frac{1}{m} \nabla^m y_{n+1} = hf_{n+1} + k\gamma_k (y_{n+1} - y_{n+1}^{[0]}) \quad (47)$$

Where “k” is a scalar parameter and $\gamma_k = \sum_{j=1}^k \frac{1}{j}$

Klopfenstein found numerically the value of “k” that maximizes the angle of A-stability. The addition of this new term has this advantage of giving rise to the same accuracy and higher stability for stiff ODEs than BDFs but with a bigger time step. This method is well applied for the solution of Bateman equations.

A3-2.2.6. Adams-Bashford Method[83]

The Adams-Bashford algorithm is an explicit multi-step integration method whence

$$p = k - 1 \quad \text{and} \quad a_1 = a_2 = \dots = a_{k-1} = 0 \quad \text{and} \quad b_{-1} = 0 \quad (48)$$

is set to satisfy the equation system (38). The equation system of the Adams-Bashford coefficients of order 4 is as follows.

$$\begin{bmatrix} 1 & 0 & 0 & 0 & 0 \\ 0 & 1 & 1 & 1 & 1 \\ 0 & 0 & -2 & -4 & -6 \\ 0 & 0 & 3 & 12 & 27 \\ 0 & 0 & -4 & -32 & -108 \end{bmatrix} \cdot \begin{bmatrix} a_0 \\ b_0 \\ b_1 \\ b_2 \\ b_3 \end{bmatrix} = \begin{bmatrix} 1 \\ 1 \\ 1 \\ 1 \\ 1 \end{bmatrix} \quad (49)$$

This equation system results in the following integration formula.

$$\begin{aligned} y_{n+1} &= a_0 y_n + h b_0 f(y_n, t_n) + h b_1 f(y_{n-1}, t_{n-1}) + h b_2 f(y_{n-2}, t_{n-2}) \\ &\quad + h b_3 f(y_{n-3}, t_{n-3}) \\ &= y_n + h \frac{55}{24} f(y_n, t_n) - h \frac{59}{24} f(y_{n-1}, t_{n-1}) + h \frac{37}{24} f(y_{n-2}, t_{n-2}) - \\ &\quad h \frac{9}{24} f(y_{n-3}, t_{n-3}) \end{aligned} \quad (50)$$

The Adams-Bashford formula of order 1 yields the (explicit) forward Euler integration method.

A3-2.2.7. Adams-Moulton Method[83]

The Adams-Moulton algorithm is an implicit multi-step integration method whence

$$p = k - 2 \quad \text{and} \quad a_1 = a_2 = \dots = a_{k-2} = 0 \quad (51)$$

is set to satisfy the equation system (38). The equation system of the Adams-Moulton coefficients of order 4 is as follows.

$$\begin{bmatrix} 1 & 0 & 0 & 0 & 0 \\ 0 & 1 & 1 & 1 & 1 \\ 0 & 2 & 0 & -2 & -4 \\ 0 & 3 & 0 & 3 & 12 \\ 0 & 4 & 0 & -4 & -32 \end{bmatrix} \cdot \begin{bmatrix} a_0 \\ b_{-1} \\ b_0 \\ b_1 \\ b_2 \end{bmatrix} = \begin{bmatrix} 1 \\ 1 \\ 1 \\ 1 \\ 1 \end{bmatrix} \quad (52)$$

This equation system results in the following integration formula.

$$\begin{aligned}
y_{n+1} &= a_0 y_n + h b_{-1} f(y_{n+1}, t_{n+1}) + h b_0 f(y_n, t_n) + h b_1 f(y_{n-1}, t_{n-1}) \\
&\quad + h b_2 f(y_{n-2}, t_{n-2}) \\
&= y_n + h \frac{9}{24} f(y_{n+1}, t_{n+1}) + h \frac{19}{24} f(y_n, t_n) - h \frac{5}{24} f(y_{n-1}, t_{n-1}) + \\
&\quad h \frac{1}{24} f(y_{n-2}, t_{n-2}) \tag{53}
\end{aligned}$$

The Adams-Moulton formula of order one yields the (implicit) backward Euler integration method, and the formula of order two yields the trapezoidal rule.

A3-2.2.8. Predictor-corrector methods[83]

Various integration methods have been discussed so far. The elementary and linear multistep methods (to get more accurate methods) always assumed $\mathbf{a-1}=-\mathbf{1}$ in its general form. Explicit methods were encountered by $\mathbf{b-1=0}$ and implicit methods by $\mathbf{b-1}\neq\mathbf{0}$. Explicit methods have been shown to have a limited area of stability and implicit methods to have a larger range of stability. With increasing order \mathbf{k} , the linear multistep methods interval of absolute stability (intersection of the area of absolute stability in the complex plane with the real axis) decreases except for the implicit Gear formulae.

For these reasons, implicit methods can be used to obtain solutions of ordinary differential equation systems describing so-called stiff problems. Now considering, e.g., the implicit Adams-Moulton formulae of order 3:

$$y_{n+1} = y_n + h \frac{5}{12} f(y_{n+1}, t_{n+1}) + h \frac{8}{12} f(y_n, t_n) - h \frac{1}{24} f(y_{n-1}, t_{n-1}) \tag{54}$$

Clarifies that \mathbf{f}^{n+1} is necessary to calculate y_{n+1} . Every implicit integration method has this particular property. The above equation can be solved using iteration. This iteration is said to be convergent if the integration method is consistent and zero-stable. A linear multistep method that is at least first-order is called a consistent method. Zero-stability and consistency are necessary for convergence. The iteration introduces a second index \mathbf{m} .

$$y_{n+1}^{m+1} = y_n + h \frac{5}{12} f^m(y_{n+1}, t_{n+1}) + h \frac{8}{12} f(y_n, t_n) - h \frac{1}{24} f(y_{n-1}, t_{n-1}) \quad (55)$$

This iteration will converge for an arbitrary initial guess y_{n+1}^0 only limited by the step size \mathbf{h} . In practice, successive iterations are processed unless

$$|y_{n+1}^{m+1} - y_{n+1}^m| < \varepsilon_{abs} + \varepsilon_{rel} \cdot |y_{n+1}^m| \quad (56)$$

The disadvantage of this method is that the number of iterations until it converges, is unknown. Alternatively, it is possible to use a fixed number of correction steps. A cheap way of providing an excellent initial guess y_{n+1}^0 is using an explicit integration method, e.g., the Adams-Bashford formula of order 3.

$$y_{n+1}^0 = y_n + h \frac{23}{12} f(y_n, t_n) - h \frac{16}{12} f(y_{n-1}, t_{n-1}) + h \frac{5}{12} f(y_{n-2}, t_{n-2}) \quad (57)$$

Equation (57) requires no iteration process and can be used to obtain the initial guess. The combination of evaluating a single explicit integration method (the predictor step) to provide an excellent initial guess for the successive evaluation of an implicit method (the corrector step) using iteration is called the predictor-corrector method. The

motivation using an implicit integration method is its fitness for solving stiff problems. The explicit method (though possibly unstable) is used to provide an excellent initial guess for the corrector steps.

A3-2.2.9. Adaptive step-size control[83]

For all numerical integration methods used for the burn-up analysis of nuclear reactors, the choice of a proper step-size is essential. If the step-size is too large, the results become inaccurate or even completely wrong when the region of absolute stability is left. And if the step-size is too small, the calculation requires more time than necessary without raising the accuracy. Usually, a chosen initial step-size cannot be used overall the requested time of calculation because short-lived isotopes will die out within a short duration of time, and then for long-lived isotopes, one must change the time step from small to large. The technique of changing the time step is described in this section. A step-size \mathbf{h} is chosen such that

$$\varepsilon_{LTE} < \varepsilon_{abs} + \varepsilon_{rel} \cdot |y_{n+1}^m| \quad (58)$$

Consider the following step error ratio

$$q = \frac{\varepsilon_{LTE}}{\varepsilon_{LTE} < \varepsilon_{abs} + \varepsilon_{rel} \cdot |y_{n+1}^m|} \quad (59)$$

The algorithm for step-size control is as follows:

The initial step size \mathbf{h} is chosen sufficiently small. After each integration step, every step-error ratio gets computed, and the largest value of q (say \mathbf{q}_{max}) is then checked.

If $q_{\max} \neq 1$, then a reduction of the current step-size is necessary. As new step-size, the following expression is used

$$h^{n+1} = \left(\frac{\varepsilon}{q_{\max}} \right)^{\frac{1}{k+1}} \cdot h^n \quad (60)$$

Where “ k ” is the order of the corrector-predictor method.

A3-2.2.10. Some basic concepts

This section shall define some concepts involved in the ordinary differential equations and their numerical solutions [84].

A3-2.2.10.1. Differential equation

An equation involving one or more unknown function (dependent variables) and its derivatives with respect to one or more known functions (independent variables) is called a **differential equation**.

For example,

1. $x \frac{dy}{dx} = 2y$ and
2. $x \frac{\partial z}{\partial x} + y \frac{\partial z}{\partial y} - z = 0$ are differential equations.

Differential equations of the form-1, involving derivatives w.r.t. a single independent variable are called **ordinary differential equations** (ODEs) whereas, those involving derivatives w.r.t. two or more independent variables are **partial differential equations** (PDEs). Differential equations of the form-2 is an example of PDE.

A3-2.2.10.2. Order and degree of Differential equation

The **order** of a differential equation is the order of the highest order derivative appearing in the equation. The **degree** is the highest exponent of the highest order derivative after the equation has been rationalized, i.e., after it has been expressed in the form free from radicals and any fractional power of the derivatives or negative power. For example, equation

$$\left(\frac{d^3y}{dx^3}\right)^2 + 2\frac{d^2y}{dx^2} - \frac{dy}{dx} + x^2\left(\frac{dy}{dx}\right)^3 = 0 \text{ is of } \mathbf{third} \text{ order and } \mathbf{second} \text{ degree and equation}$$

$y = x \frac{dy}{dx} + \frac{a}{dy/dx}$ is of the **first-order** and **second** degree as it can be written in the form

$$y \frac{dy}{dx} = x \left(\frac{dy}{dx}\right)^2 + a$$

A3-2.2.10.3. Linear and non-linear Differential equation

When the dependent variable and its derivatives occur in the first degree only and not as higher powers or products, the equation is **linear**; otherwise, it is **nonlinear**. For example, the equation $\frac{d^2y}{dx^2} + y = x^2$ is a linear ODE, whereas $(x+y)^2 \frac{dy}{dx} = 1$ is a nonlinear

ODE. Similarly, $\frac{\partial^2 z}{\partial x^2} + \frac{\partial^2 z}{\partial y^2} - \left(\frac{\partial^2 z}{\partial x \partial y}\right)^2 = 0$, it is a nonlinear partial differential equation (PDE).

A3-2.2.10.4. Initial and boundary value problem

The **general solution** of an n^{th} order ODE contains n arbitrary constants. To determine these arbitrary constants, we require n conditions. Suppose all these conditions are given at one point. In that case, these conditions are known as **initial conditions**, and the differential equation, together with the initial conditions, is called an **initial value problem** (IVP). The n^{th} -order IVP, along with associated initial conditions, can be written as:

$$y^n(t) = f(t, y, y', y'', \dots, y^{(n-1)}) \quad (61)$$

$$y^{(p)}(t_0) = y_0^{(p)}, p = 0, 1, 2, \dots, n - 1. \quad (62)$$

We are required to find the solution $y(t)$ for $t > t_0$. If the n conditions are prescribed at more than one point, then these conditions are known as **boundary conditions**. These conditions are usually defined at two points, say t_0 and t_a , and we are required to find the solution $y(t)$ between $t_0 < t < t_a$. The differential equation, together with the boundary conditions, is then known as a **boundary value problem** (BVP).

A3-2.2.10.5. Existence and uniqueness of the solution

It is known that the n^{th} order IVP (38) is equivalent to solving the following system of n first-order equations: Hence, it is sufficient to study numerical methods for the solution of the first order IVP.

$$y' = f(t, y), y(t_0) = y_0 \quad (63)$$

Before attempting to obtain numerical solutions to the equation (63), we must ensure that the problem has a unique solution. The following theorem provides the existence and uniqueness of the solution to IVP (63).

Theorem 1: If $f(t, y)$ satisfies the conditions

- i) $f(t, y)$ is a real function
- ii) $f(t, y)$ is bounded and continuous for $t \in [t_0, b]$ and $y \in] - \infty, \infty [$
- iii) there exists a constant L such that for any $t \in [t_0, b]$ and for any two numbers y_1 and y_2

$$|f(t, y_1) - f(t, y_2)| \leq L |y_1 - y_2|$$

then for any y_0 , the IVP (63) has a unique solution. This condition is called the **Lipchitz condition**, and L is called the **Lipchitz constant**.

We assume the existence and uniqueness of the solution and that $f(t, y)$ has continuous partial derivatives w.r.t. t and y of an as high order as we desire.

A3-2.2.10.6. Solving differential equation numerically

Let us assume that $[t_0, b]$ be an interval over which the IVP solution (63) is required. If we subdivide the interval $[t_0, b]$ into n subintervals using a step size $h = \left[\frac{t_n - t_0}{n} \right]$, where $t_n = b$, we obtain the **mesh points** or **grid points** $t_0, t_1, t_2, \dots, t_n$. We can then write $t_k = t_0 + kh$, $k = 0, 1, \dots, n$. A numerical method for the IVP solution (63) will produce approximate values y_k at the grid points t_k in a step-by-step manner, i.e., values of y_1, y_2, \dots , etc. in unit order.

A3-2.2.10.7. Error in numerical solution and concept of order

Remember that the approximate values y_k may contain truncation and round-off errors. We shall now discuss the construction of numerical methods and related basic concepts with reference to a simple ODE.

$$\frac{dy}{dt} = \lambda y, t \in [a, b], \quad y(t_0) = y_0, \quad (64)$$

Where λ is a constant.

Let the domain $[a, b]$ be subdivided into N intervals and let the grid points be defined by,

$$t_j = t_0 + jh, j = 0, 1, \dots, N$$

Where, $t_0 = a$ and $t_N = t_0 + Nh = b$.

Separating the variables and integrating, we find that the exact solution of Eqn. (64) is

$$y(t) = y(t_0) e^{\lambda(t-t_0)}. \quad (65)$$

In order to obtain a relation between the solutions at two successive points, $t = t_n$ and t_{n+1} in Eqn. (65), we use,

$$y(t_n) = y(t_0) e^{\lambda(t_n - t_0)} \text{ and } y(t_{n+1}) = y(t_0) e^{\lambda(t_{n+1} - t_0)}, \text{ Dividing we get}$$

$$\frac{y(t_{n+1})}{y(t_n)} = \frac{e^{\lambda t_{n+1}}}{e^{\lambda t_n}} = e^{\lambda(t_{n+1} - t_n)} \quad (66)$$

Hence we have,

$$y(t_{n+1}) = e^{\lambda h} y(t_n), n = 0, 1, \dots, N-1. \quad (67)$$

Eqn. (66) gives the required relation between $y(t_n)$ and $y(t_{n+1})$. Setting $n = 0, 1, 2, \dots, N-1$, successively, we can find $y(t_1), y(t_2), \dots, y(t_N)$ from the given value $y(t_0)$. An approximate method or a numerical method can be obtained by approximating $e^{\lambda h}$ in Eqn. (67). For example, we may use the following polynomial approximations,

$$e^{\lambda h} = 1 + \lambda h + O(|\lambda h|^2) \quad (68)$$

$$e^{\lambda h} = 1 + \lambda h + \frac{\lambda^2 h^2}{2} + O(|\lambda h|^3) \quad (69)$$

$$e^{\lambda h} = 1 + \lambda h + \frac{\lambda^2 h^2}{2} + \frac{\lambda^3 h^3}{6} + O(|\lambda h|^4) \quad (70)$$

.....

Let us retain $(p + 1)$ terms in the expansion of $e^{\lambda h}$ and denote the approximation to $e^{\lambda h}$ by $E(\lambda h)$. The numerical method for obtaining the approximate values y_n of the exact solution $y(t_n)$ can then be written as

$$y_{n+1} = E(\lambda h) y_n, \quad n = 0, 1, \dots, N-1 \quad (71)$$

The truncation error (T.E.) of the method is defined by

$TE = y(t_{n+1}) - y_{n+1}$. Since $(p + 1)$ terms are retained in the expansion of $e^{\lambda h}$, we have

$$\begin{aligned} TE &= \left(1 + \lambda h + \dots + \frac{(\lambda h)^p}{p!} + \frac{(\lambda h)^{p+1}}{(p+1)!} e^{\theta \lambda h} \right) - \left(1 + \lambda h + \dots + \frac{(\lambda h)^p}{p!} \right) \\ &= \frac{(\lambda h)^{p+1}}{(p+1)!} e^{\theta \lambda h}, \quad 0 < \theta < 1 \end{aligned}$$

The TE is of order $p+1$, and the numerical method is called of order p . The order of an integration method equals the power of the step size up to which the Taylor series's approximate solution is considered.

A3-2.2.10.8. Concept of stability

The concept of stability is essential in a numerical method. We say that a numerical method is **stable** if the error at any stage, i.e., $y_n - y(t_n) = \epsilon_n$ remains bounded as $n \rightarrow \infty$.

Let us examine the stability of the numerical method (71). Putting $y_{n+1} = y(t_{n+1}) + \epsilon_{n+1}$ and $y_n = y(t_n) + \epsilon_n$ in Eqn. (71), we get

$$y(t_{n+1}) + \varepsilon_{n+1} = E(\lambda h) [y(t_n) + \varepsilon_n] \text{ or } \varepsilon_{n+1} = E(\lambda h) [y(t_n) + \varepsilon_n] - y(t_{n+1})$$

Which on using eqn. (67) becomes $\varepsilon_{n+1} = E(\lambda h) [y(t_n) + \varepsilon_n] - e^{\lambda h} y(t_n)$

$$\varepsilon_{n+1} = [E(\lambda h) - e^{\lambda h}] y(t_n) + E(\lambda h) \varepsilon_n \quad (72)$$

We **note** from Eqn. (72) that the error at t_{n+1} consists of two parts. The first part $E(\lambda h) - e^{\lambda h}$ is the **local truncation error (LTE)** and can be made as small as we like by suitably determining $E(\lambda h)$. The second part $E(\lambda h) \varepsilon_n$ is the **propagation error** from the previous step t_n to t_{n+1} and will not grow if $|E(\lambda h)| < 1$. If $|E(\lambda h)| < 1$, then as $n \rightarrow \infty$ the propagation error tends to zero and the method is said to be absolutely stable. Further, a numerical method is said to be **relatively stable** if $|E(\lambda h)| \leq e^{\lambda h}$, $\lambda > 0$. The polynomial approximations (68), (69), and (70) always give relatively stable methods. Let us now find when the methods $y_{n+1} = E(\lambda h) y_n$ are absolutely stable where $E(\lambda h)$ is given by (68) (69) or (70). These methods are given by

First order: $y_{n+1} = (1 + \lambda h) y_n$

Second order: $y_{n+1} = \left(1 + \lambda h + \frac{\lambda^2 h^2}{2}\right) y_n$ and

Third order: $y_{n+1} = \left(1 + \lambda h + \frac{\lambda^2 h^2}{2} + \frac{\lambda^3 h^3}{6}\right) y_n$

Let us examine the conditions for absolute stability in various methods:

First order: $|1 + \lambda h| \leq 1$ or $-1 \leq 1 + \lambda h \leq 1$ or $-2 \leq \lambda h \leq 0$

Second order: $\left|1 + \lambda h + \frac{\lambda^2 h^2}{2}\right| \leq 1$ or $-1 \leq 1 + \lambda h + \frac{\lambda^2 h^2}{2} \leq 1$

The right inequality gives $\lambda h \left(1 + \frac{\lambda h}{2}\right) \leq 0$ i.e., $\lambda h \leq 0$ and $1 + \frac{\lambda h}{2} \geq 0$.

The second condition gives $-2 \leq \lambda h$. Hence the right inequality gives $-2 \leq \lambda h \leq 0$.

The left inequality gives $2 + \lambda h + \frac{\lambda^2 h^2}{2} \geq 0$.

For $-2 \leq \lambda h \leq 0$, this equation is always satisfied. Hence the stability condition is $-2 \leq \lambda h \leq 0$.

Third-order: $\left| 1 + \lambda h + \frac{\lambda^2 h^2}{2} + \frac{\lambda^3 h^3}{6} \right| \leq 1$ Using the right and left inequalities, we get $-2.5 \leq \lambda h \leq 0$. These intervals for λh are known as **stability intervals**.

A3-3. Summary

Different numerical methods for handling the stiff and non-stiff system of coupled linear and nonlinear ordinary differential equations are described in this annexure. One-step and linear multistep methods (LMM) are also described to handle the stiff system of equations viz. set of coupled isotopic generation and depletions equations. For highly stiff differential equations, the Gears BDF method or Shampine NDF formulae can be used. These methods can be easily applied to the system of equations using MATLAB.

Nuclear data for fuel cycle analysis

A4-1. INTRODUCTION

A vast amount of nuclear data are available and distributed through various agencies viz—National Nuclear Data Centre of Brookhaven National Laboratory's (BNL).

Burn-up code IGDC developed in this research work also requires nuclear data viz. decay data, fission yield data, branching ratios, dose conversion factors, and energy released during radio-isotope decay, etc. The extraction of these data from the available resources is described in this annexure.

A4-2. BROOKHAVEN NATIONAL LABORATORY'S (BNL)

The National Nuclear Data Centre (NNDC) of Brookhaven National Laboratory's (BNL) collects, evaluates, and disseminates nuclear physics data for basic nuclear research and applied nuclear technologies. The data center contains experimental information on nuclear structure and nuclear reactions, evaluates them employing nuclear physics theory and expertise in evaluating experimental techniques to provide recommended results, maintains nuclear databases, and uses modern information technology to disseminate the results. There are two other major data banks operated by international organizations, one in Paris and another in Vienna [85]. Various information available on these data centers is shown in Figure A4.1.

Main	Structure & Decay	Reactions	Bibliography	Networks & Links	Publications	Meetings
AMDC Atomic Mass Data Center, Q-value Calculator	Atlas of Neutron Resonances Parameters & thermal values	CapGam Thermal Neutron Capture γ -rays	Chart of Nuclides Basic properties of atomic nuclei			
Covariances of Neutron Reactions	CSEWG Cross Section Evaluation Working Group	CSISRS alias EXFOR Nuclear reaction experimental data	ENDF Evaluated Nuclear (reaction) Data File, Sigma			
ENSDF Evaluated Nuclear Structure Data File	IRDF IRDFF International Reactor Dosimetry and Fusion File	MIRD Medical Internal Radiation Dose				
NMMSS & DoE NMIRDC Safeguards & inventory decay data standards	NSR Nuclear Science References	Nuclear Data Sheets Nuclear structure & decay data journal, Special Issues on reaction data	Nuclear Wallet Cards Ground & isomeric states properties, Homeland Security version			
NucRates MACS & Astro-physical reaction rates	NuDat Nuclear structure & decay Data	USNDP U.S. Nuclear Data Program	USNDP/CSEWG GForge Collaboration Server			
XUNDL Experimental Un-evaluated Nuclear Data List						

Figure A4. 1: National Nuclear Data Centre of BNL

NNDC website can be accessed through www.nndc.bnl.gov.

A4-3. DECAY-DATA LIBRARY

Decay data are extracted from **nudat** (NUDAT), and **nuclear wallet cards** linked to the National Nuclear Data Centre of Brookhaven National Laboratory's (BNL) and converted to the decay constants for using them burn-up code IGDC. We have extracted data for about 800 radionuclides of interest. Decay constants of important radionuclides are summarized in Table A4.1.

Table A4. 1: Decay data of radio-isotopes for PT-HWR

Isotope	Effective Decay Constant (Sec-1)										
Ni72	4.42E-01	As82	3.63E-02	Y92	5.44E-05	Mo103	1.03E-02	Cd111m	2.38E-04	Cs138	3.46E-04
Cu72	1.05E-01	Se82	2.67E-28	Kr93	5.39E-01	Tc103	1.28E-02	Ru112	3.96E-01	In121m	2.98E-03
Zn72	4.14E-06	Br82m	1.88E-03	Rb93	1.19E-01	Ru103	2.04E-07	Pd112	9.16E-06	In121	3.00E-02
Ga72	1.37E-05	Br82	5.46E-06	Sr93	1.56E-03	Rh103m	2.06E-04	Ag112	6.15E-05	Sn121	7.12E-06
Cu73	1.65E-01	Ge83	3.75E-01	Y93	1.89E-05	Pd103	4.72E-07	Rh113	2.48E-01	Sn121m	5.01E-10
Zn73	2.95E-02	As83	5.17E-02	Zr93	1.44E-14	Nb104	1.44E-01	Pd113	7.45E-03	Cd122	1.32E-01
Ga73	3.96E-05	Se83	5.18E-04	Nb93m	1.36E-09	Mo104	1.16E-02	Ag113m	1.01E-02	Sb122	2.95E-06
Cu74	4.25E-01	Se83m	9.89E-03	Rb94	2.57E-01	Tc104	6.31E-04	Ag113	3.59E-05	Sb122m	1.31E+03
Zn74	7.25E-03	Kr83m	1.05E-04	Sr94	9.21E-03	Rh104	1.64E-02	Cd113m	1.56E-09	In122m	6.73E-02
Ga74m	7.30E-02	As84	1.54E-01	Y94	6.18E-04	Rh104m	2.67E-03	Cd113	2.73E-24	In123	1.12E-01
Ga74	1.42E-03	Se84	3.54E-03	Nb94m	1.84E-03	Nb105	2.35E-01	In113m	1.16E-04	Sn123	6.21E-08
Cu75	5.66E-01	Br84	3.64E-04	Nb94	1.08E-12	Mo105	1.95E-02	Pd114	4.78E-03	In123m	1.46E-02
Zn75	6.80E-02	Br84m	1.93E-03	Sr95	2.90E-02	Tc105	1.52E-03	Ag114	1.51E-01	Sn123m	2.88E-04
Ga75	5.50E-03	As85	3.42E-01	Y95	1.12E-03	Ru105	4.34E-05	In114m	1.62E-07	Cd124	5.55E-01
Ge75	1.40E-04	Se85	2.19E-02	Zr95	1.25E-07	Rh105	5.45E-06	In114	9.64E-03	Pm149	3.63E-06
Ge75m	1.45E-02	Br85	3.98E-03	Nb95	2.29E-07	Rh105m	1.73E-02	Pd115	2.77E-02	Sn126	9.50E-14
Zn76	1.22E-01	Kr85m	4.30E-05	Nb95m	2.22E-06	Nb106	7.45E-01	Ag115	5.78E-04	Sb126m	6.03E-04
Ga76	2.13E-02	Kr85	2.04E-09	Sr96	6.48E-01	Mo106	7.94E-02	Ag115m	3.85E-02	I126	6.21E-07
As76	7.34E-06	Se86	4.53E-02	Y96m	7.22E-02	Ru106	2.16E-08	Cd115	3.60E-06	In127m	1.89E-01
Zn77	3.33E-01	Br86	1.26E-02	Y96	1.30E-01	Rh106	2.30E-02	Cd115m	1.80E-07	Sn127	9.17E-05
Ga77	5.25E-02	Rb86m	1.14E-02	Zr96	1.10E-27	Mo107	1.98E-01	In115m	4.29E-05	Sn127m	2.80E-03
Ge77	1.70E-05	Rb86	4.30E-07	Nb96	8.25E-06	Tc107	3.27E-02	In115	4.99E-23	Sb127	2.08E-06
Ge77m	1.31E-02	Se87	1.31E-01	Y97	1.85E-01	Ru107	3.08E-03	Pd116	5.87E-02	Te127m	7.36E-08
As77	4.96E-06	Br87	1.25E-02	Zr97	1.15E-05	Rh107	5.32E-04	Ag116	3.01E-03	Te127	2.06E-05
Se77m	3.99E-02	Kr87	1.51E-04	Nb97m	1.18E-02	Pd107	3.38E-15	Ag116m	3.47E-02	Sn128	1.96E-04
Zn78	4.72E-01	Rb87	4.56E-19	Y98m	3.47E-01	Pd107m	3.25E-02	Cd116	6.67E-28	Sb128m	1.11E-03
Ga78	1.36E-01	Sr87m	6.84E-05	Zr98	2.26E-02	Mo108	6.36E-01	In116m	2.13E-04	Sb128	2.14E-05
Ge78	1.31E-04	Se88	4.53E-01	Nb98	2.42E-01	Tc108	1.34E-01	In116	4.92E-02	Sn129	5.18E-03
As78	1.27E-04	Br88	4.26E-02	Nb98m	2.25E-04	Ru108	2.54E-03	Ag117	9.52E-03	Eu163	6.44E-02
Ga79	2.43E-01	Kr88	6.78E-05	Tc98	5.21E-15	Rh108	4.13E-02	Cd117	7.74E-05	Pb212	1.81E-05
Ge79m	1.78E-02	Rb88	6.50E-04	Y99	4.69E-01	Ag108m	5.02E-11	Cd117m	5.73E-05	Pb214	4.31E-04
Ge79	3.65E-02	Br89	1.58E-01	Zr99	3.30E-01	Ag108	4.85E-03	In117m	9.94E-05	Bi209	1.16E-27
As79	1.28E-03	Kr89	3.67E-03	Nb99m	4.44E-03	Tc109	8.06E-01	In117	2.67E-04	Bi210	1.60E-06
Se79m	2.95E-03	Rb89	7.63E-04	Mo99	2.92E-06	Ru109	2.01E-02	Sn117m	5.90E-07	Bi211	5.40E-03
Se79	5.83E-14	Sr89	1.59E-07	Tc99m	3.20E-05	Rh109	8.67E-03	Pd118	3.65E-01	Bi212	1.91E-04

Isotope	Effective Decay Constant (Sec-1)										
Br79m	1.43E-01	Y89m	4.43E-02	Tc99	1.04E-13	Pd109	1.41E-05	Ag118	1.84E-01	Bi213	2.53E-04
Ga80	4.08E-01	Br90	3.61E-01	Zr100	9.76E-02	Pd109m	2.46E-03	Cd118	2.30E-04	Bi214	5.81E-04
Ge80	2.35E-02	Kr90	2.14E-02	Nb100	4.62E-01	Ag109m	1.75E-02	In118m	2.60E-03	Bi215	1.50E-03
As80	4.56E-02	Rb90m	2.69E-03	Nb100m	2.32E-01	Cd109	1.74E-08	In118	1.39E-01	Fr221	2.36E-03
Br80	6.53E-04	Rb90	4.39E-03	Mo100	3.01E-27	Ru110	5.98E-02	Cd119m	5.25E-03	Fr223	5.25E-04
Br80m	4.36E-05	Sr90	7.63E-10	Tc100	4.48E-02	Rh110	2.43E-02	Cd119	4.29E-03	Po210	5.80E-08
Ga81	5.70E-01	Y90m	6.04E-05	Zr101	3.01E-01	Rh110m	2.17E-01	In119m	6.42E-04	Rn221	4.50E-04
Ge81	9.12E-02	Y90	3.01E-06	Mo101	7.91E-04	Ag110	2.82E-02	In119	4.81E-03	Cm241	2.45E-07
As81	2.08E-02	Kr91	8.09E-02	Tc101	8.14E-04	Ag110m	3.21E-08	Sn119m	2.74E-08	Sb124	1.33E-07
Se81	6.26E-04	Rb91	1.19E-02	Zr102	2.39E-01	Ru111	3.27E-01	Ag120	5.64E-01	In124m	1.87E-01
Se81m	2.02E-04	Sr91	2.00E-05	Nb102	1.61E-01	Rh111	6.30E-02	Cd120	1.36E-02	In125	2.94E-01
Kr81	9.63E-14	Y91	1.37E-07	Nb102m	5.33E-01	Pd111m	3.50E-05	In120m	1.50E-02	In125m	5.68E-02
Kr81m	5.29E-02	Y91m	2.32E-04	Mo102	1.02E-03	Pd111	4.94E-04	In120	2.25E-01	Sb125	7.96E-09
Ge82	1.52E-01	Kr92	3.77E-01	Rh102m	5.87E-09	Ag111	1.08E-06	Cd121	5.13E-02	Sn125m	1.21E-03
As82m	5.10E-02	Sr92	7.10E-05	Rh102	3.87E-08	Ag111m	1.07E-02	Cd121m	8.35E-02	Sn125	8.32E-07
Sn130m	6.80E-03	Cs138m	3.97E-03	Nd150	2.42E-27	Gd163	1.02E-02	Cm242	4.92E-08	Te125m	1.40E-07
I130m	1.31E-03	La138	2.15E-19	Pm150	7.18E-05	Tb163	5.92E-04	Cm243	7.55E-10	Sb126	6.50E-07
I130	1.56E-05	I139	3.04E-01	Ce151	3.94E-01	Gd164	1.54E-02	Cm244	1.21E-09	In124	2.22E-01
Sn131	1.24E-02	Cs139	1.25E-03	Pr151	3.67E-02	Tb164	3.85E-03	Cm245	2.59E-12	Te123	2.39E-25
Sb131	5.02E-04	Ba139	1.39E-04	Nd151	9.29E-04	Eu165	2.51E-01	Cm246	4.62E-12	Te123m	6.73E-08
Te131m	5.79E-06	Cs140	1.09E-02	Pm151	6.78E-06	Tb165	5.46E-03	Cm247	1.41E-15	Po218	3.73E-03
I131	1.00E-06	Ba140	6.29E-07	Sm151	2.48E-10	Dy165m	9.19E-03	Cm248	6.31E-14	Pb211	3.20E-04
Xe131m	6.76E-07	La140	4.78E-06	Eu151	1.29E-26	Dy165	8.25E-05	Cm249	1.80E-04	Sb129	4.38E-05
Sb132	4.14E-03	Xe141	4.01E-01	Pr152	1.91E-01	Dy166	2.36E-06	Cm250	2.65E-12	Te129	1.66E-04
Sb132m	2.82E-03	Cs141	2.79E-02	Nd152	1.01E-03	Ho166	7.18E-06	Bk249	2.51E-08	Te129m	2.39E-07
Te132	2.50E-06	Ba141	6.32E-04	Pm152	2.81E-03	Ho166m	1.82E-11	Bk250	5.99E-05	I129	1.40E-15
I132	8.39E-05	La141	4.91E-05	Pm152m	1.54E-03	Dy167	1.86E-03	Es253	3.92E-07	Xe129m	9.04E-07
Cs132	1.24E-06	Ce141	2.47E-07	Eu152	1.62E-09	Ho167	6.19E-05	Cf249	6.26E-11	Sn130	3.11E-03
Sn133	4.78E-01	Xe142	5.68E-01	Gd152	2.04E-22	Er167m	3.06E-01	Cf250	1.68E-09	Sb130	2.92E-04
Sb133	4.62E-03	Cs142	4.12E-01	Eu152m	2.07E-05	Y97m	5.92E-01	Cf251	2.45E-11	Te130	2.78E-29
Te133m	2.09E-04	Ba142	1.09E-03	Pr153	1.62E-01	U232	3.19E-10	Cf252	8.30E-09	Sb130m	1.83E-03
Te133	9.24E-04	Ce142	4.39E-25	Pm153	2.20E-03	U233	1.38E-13	Cf253	4.50E-07	Sn129m	1.67E-03
I133	9.26E-06	Pr142	1.01E-05	Gd153	3.34E-08	U234	8.95E-14	Ac225	8.02E-07	Te128	2.85E-33
I133m	7.70E-02	Pr142m	7.88E-04	Nd154	2.68E-02	U235	3.12E-17	Ac226	6.56E-06	I128	4.62E-04
Xe133	1.53E-06	Cs143	3.87E-01	Pm154	4.31E-03	U236	9.38E-16	Ac227	1.01E-09	Rn219	1.75E-01
Xe133m	3.66E-06	Ba143	4.78E-02	Pm154m	6.67E-03	U237	1.19E-06	Ac228	3.13E-05	Ba137m	4.53E-03
Sn134	6.60E-01	Ce143	5.83E-06	Eu154	2.55E-09	U238	4.92E-18	Hg206	1.39E-03	Te138	4.95E-01
Sb134m	6.88E-02	Pr143	5.91E-07	Pr155	2.68E-01	U239	4.93E-04	Tl206	2.75E-03	I138	1.11E-01

Isotope	Effective Decay Constant (Sec-1)										
Te134	2.76E-04	Ba144	6.03E-02	Nd155	7.79E-02	U240	1.36E-05	Tl207	2.42E-03	Xe138	8.20E-04
I134	2.20E-04	La144	1.70E-02	Pm155	1.67E-02	Pu236	7.69E-09	Tl208	3.78E-03	Sm148	3.15E-24
I134m	3.28E-03	Ce144	2.82E-08	Eu155	4.62E-09	Pu237	1.78E-07	Tl210	8.89E-03	Pm148m	1.94E-07
Xe134	3.79E-31	Pr144	6.68E-04	Nd156	1.26E-01	Pu238	2.50E-10	Th226	3.78E-04	Pr149	5.11E-03
Cs134m	6.61E-05	Pr144m	1.60E-03	Pm156	2.60E-02	Pu239	9.11E-13	Th227	4.29E-07	Nd149	1.11E-04
Cs134	1.06E-08	Nd144	9.63E-24	Sm156	2.05E-05	Pu240	3.35E-12	Th228	1.15E-08	Sm162	2.89E-01
Sb135	4.13E-01	La145	2.80E-02	Eu156	5.28E-07	Pu241	1.54E-09	Th229	2.99E-12	Eu162	6.54E-02
I135	2.93E-05	Ce145	3.84E-03	Nd157	1.28E-01	Pu242	5.88E-14	Th230	2.91E-13	Gd162	1.38E-03
Xe135	2.11E-05	Pr145	3.22E-05	Pm157	6.56E-02	Pu243	3.89E-05	Th231	7.55E-06	Sm163	2.29E-01
Xe135m	7.56E-04	Ba146	3.12E-01	Sm157	1.44E-03	Pu244	2.71E-16	Th232	1.56E-18	Np237	1.02E-14
Cs135	9.50E-15	Ce146	8.55E-04	Eu157	1.27E-05	Pu245	1.83E-05	Th234	3.33E-07	Np239	3.40E-06
Cs135m	2.18E-04	Pr146	4.78E-04	Sm158	2.18E-03	Pu246	7.40E-07	Th235	1.63E-03	Np240	1.87E-04
Ba135m	6.71E-06	Sm146	2.13E-16	Eu158	2.52E-04	Am240	3.79E-06	Ra223	7.02E-07	Np241	8.31E-04
Te136	3.93E-02	La147	1.73E-01	Sm159	6.10E-02	Am241	5.08E-11	Ra224	2.19E-06	Pa234	2.87E-05
I136	8.31E-03	Ce147	1.23E-02	Eu159	6.38E-04	Am242m	1.56E-10	Ra225	5.39E-07	Pa235	4.79E-04
Xe136	6.08E-29	Pr147	8.62E-04	Gd159	1.04E-05	Am242	1.20E-05	Ra226	1.37E-11	Pb209	5.92E-05
I136m	1.48E-02	Nd147	7.31E-07	Pm160	2.72E-01	Am243	2.98E-12	Ra227	2.74E-04	Pb210	9.89E-10
Cs136	6.10E-07	Pm147	8.37E-09	Eu160	1.82E-02	Am244m	4.44E-04	Ra228	3.82E-09	Cs137	7.30E-10
Te137	2.78E-01	Sm147	2.07E-19	Tb160	1.11E-07	Am244	1.90E-05	Pa231	6.70E-13	Pm148	1.49E-06
I137	2.83E-02	La148	5.50E-01	Eu161	2.67E-02	Am245	9.39E-05	Pa232	6.08E-06	Tb161	1.16E-06
Xe137	3.03E-03	Pr148	5.05E-03	Gd161	3.15E-03	Am246	2.10E-06	Pa233	2.97E-07	Np236	1.43E-13

A4-4. DATA LIBRARY FOR DOSE CONVERSION FACTORS

Inhalation and ingestion dose conversion factors are the factors that are used to convert the activity of inhalation or ingestion into their corresponding radiation dose. The unit of these conversion factors is Sievert per Becquerel. Inhalation dose factors depend upon the size and nature of the radio-isotope. In contrast, ingestion dose conversion factors depend upon the age of the recipient and the nature of the radio-isotopes. The data library of these conversion factors is generated using ICRP publication 118 [17] and is given in Table A4.2.

Table A4. 2: Dose conversion factors

Isotope	For inhalation		For ingestion						
	1 AMAD particle	5 AMAD particle	Worker	Infant	1-year-old Public	5-year-old Public	10-year-old Public	15-year-old Public	Adult Public
	Dose Conversion factor (Sv/Bq)								
Rh103m	1.89E-12	2.03E-12	3.80E-12	4.70E-11	2.70E-11	1.30E-11	7.40E-12	4.80E-12	3.80E-12
Y91m	1.05E-11	1.45E-11	1.10E-11	9.20E-11	6.00E-11	3.30E-11	2.10E-11	1.40E-11	1.10E-11
Pr142m	6.90E-12	9.15E-12	1.70E-11	2.00E-10	1.20E-10	6.20E-11	3.70E-11	2.10E-11	1.70E-11
Tc101	1.09E-11	1.80E-11	1.90E-11	2.40E-10	1.30E-10	6.10E-11	3.50E-11	2.40E-11	1.90E-11
Cs135m	1.30E-11	2.40E-11	1.90E-11	1.30E-10	8.60E-11	4.90E-11	3.20E-11	2.30E-11	1.90E-11
Cs134m	1.50E-11	2.60E-11	2.00E-11	2.10E-10	1.20E-10	5.90E-11	3.50E-11	2.50E-11	2.00E-11
Tc99m	1.55E-11	2.45E-11	2.20E-11	2.00E-10	1.30E-10	7.20E-11	4.30E-11	2.80E-11	2.20E-11
Rh107	1.45E-11	2.37E-11	2.40E-11	2.90E-10	1.60E-10	7.90E-11	4.50E-11	3.10E-11	2.40E-11
Se81	1.18E-11	1.90E-11	2.70E-11	3.40E-10	1.90E-10	9.00E-11	5.10E-11	3.40E-11	2.70E-11
U239	1.93E-11	2.87E-11	2.75E-11	3.40E-10	1.90E-10	9.30E-11	5.40E-11	3.50E-11	2.70E-11
In113m	1.50E-11	2.55E-11	2.80E-11	3.00E-10	1.80E-10	9.30E-11	6.20E-11	3.60E-11	2.80E-11
Sm155	1.70E-11	2.80E-11	2.90E-11	3.60E-10	2.00E-10	9.70E-11	5.50E-11	3.70E-11	2.90E-11
Am244m	7.90E-11	6.20E-11	2.90E-11	3.70E-10	2.00E-10	9.60E-11	5.50E-11	3.70E-11	2.90E-11
Nd151	1.75E-11	2.85E-11	3.00E-11	3.40E-10	2.00E-10	9.70E-11	5.70E-11	3.80E-11	3.00E-11
Br80	8.15E-12	1.40E-11	3.10E-11	3.90E-10	2.10E-10	1.00E-10	5.80E-11	3.90E-11	3.10E-11
In117	2.30E-11	3.80E-11	3.10E-11	3.30E-10	1.90E-10	9.70E-11	5.80E-11	3.90E-11	3.10E-11
Cm249	3.20E-11	5.10E-11	3.10E-11	3.90E-10	2.20E-10	1.10E-10	6.10E-11	4.00E-11	3.10E-11
Sr87m	1.70E-11	2.85E-11	3.15E-11	2.40E-10	1.70E-10	9.00E-11	5.60E-11	3.60E-11	3.00E-11
Sb128m	1.30E-11	2.25E-11	3.30E-11	3.70E-10	2.10E-10	1.00E-10	6.00E-11	4.10E-11	3.30E-11
Pr147	1.85E-11	2.95E-11	3.30E-11	3.90E-10	2.20E-10	1.10E-10	6.10E-11	4.20E-11	3.30E-11
Am246m	2.30E-11	3.80E-11	3.40E-11	3.90E-10	2.20E-10	1.10E-10	6.40E-11	4.40E-11	3.40E-11
Am246	2.30E-11	3.80E-11	3.40E-11	3.90E-10	2.20E-10	1.10E-10	6.40E-11	4.40E-11	3.40E-11
Ba142	1.60E-11	2.70E-11	3.50E-11	3.60E-10	2.20E-10	1.10E-10	6.60E-11	4.30E-11	3.50E-11
Sb126m	1.65E-11	2.80E-11	3.60E-11	3.90E-10	2.20E-10	1.10E-10	6.60E-11	4.50E-11	3.60E-11
Pd107	2.19E-10	1.25E-10	3.70E-11	4.40E-08	2.80E-10	1.40E-10	8.10E-11	4.60E-11	3.70E-11
Sn123m	2.10E-11	3.40E-11	3.80E-11	4.70E-10	2.60E-10	1.30E-10	7.30E-11	4.90E-11	3.80E-11
Mo101	2.10E-11	3.60E-11	4.20E-11	4.80E-10	2.70E-10	1.30E-10	7.60E-11	5.20E-11	4.10E-11
Ge75	2.65E-11	4.05E-11	4.60E-11	5.50E-10	3.10E-10	1.50E-10	8.70E-11	5.90E-11	4.60E-11
Y95	1.65E-11	2.55E-11	4.60E-11	5.70E-10	3.10E-10	1.50E-10	8.70E-11	5.90E-11	4.60E-11
I128	1.40E-11	2.20E-11	4.60E-11	5.70E-10	3.30E-10	1.60E-10	8.90E-11	6.00E-11	4.60E-11
Rb89	1.40E-11	2.50E-11	4.70E-11	5.40E-10	3.00E-10	1.50E-10	8.60E-11	5.90E-11	4.70E-11
In119m	1.45E-11	2.35E-11	4.70E-11	5.90E-10	3.20E-10	1.60E-10	8.80E-11	6.00E-11	4.70E-11
Se83	2.60E-11	4.35E-11	4.90E-11	4.60E-10	2.90E-10	1.50E-10	8.70E-11	5.90E-11	4.70E-11
Pr144	1.85E-11	2.95E-11	5.00E-11	6.40E-10	3.50E-10	1.70E-10	9.50E-11	6.50E-11	5.00E-11
Se81m	3.20E-11	4.90E-11	5.60E-11	6.00E-10	3.70E-10	1.80E-10	1.10E-10	6.70E-11	5.30E-11
La143	1.70E-11	2.65E-11	5.60E-11	6.90E-10	3.90E-10	1.90E-10	1.10E-10	7.10E-11	5.60E-11
Pb209	1.80E-11	3.20E-11	5.70E-11	5.70E-10	3.80E-10	1.90E-10	1.10E-10	6.60E-11	5.70E-11
Ag115	2.47E-11	3.77E-11	6.00E-11	7.20E-10	4.10E-10	2.00E-10	1.20E-10	7.70E-11	6.00E-11
Am245	5.30E-11	7.60E-11	6.20E-11	6.80E-10	4.50E-10	2.20E-10	1.30E-10	7.90E-11	6.20E-11

Isotope	For inhalation		For ingestion						
	1 AMAD particle	5 AMAD particle	Worker	Infant	1-year-old Public	5-year-old Public	10-year-old Public	15-year-old Public	Adult Public
	Dose Conversion factor (Sv/Bq)								
Te129	2.75E-11	4.30E-11	6.30E-11	7.50E-10	4.40E-10	2.10E-10	1.20E-10	8.00E-11	6.30E-11
In116m	3.90E-11	6.75E-11	6.40E-11	5.80E-10	3.60E-10	1.90E-10	1.20E-10	8.00E-11	6.40E-11
Ba141	2.20E-11	3.50E-11	7.00E-11	7.60E-10	4.70E-10	2.30E-10	1.30E-10	8.60E-11	7.00E-11
Te133	2.35E-11	4.10E-11	7.20E-11	8.40E-10	6.30E-10	3.30E-10	1.60E-10	1.10E-10	7.20E-11
Y94	2.85E-11	4.50E-11	8.10E-11	9.90E-10	5.50E-10	2.70E-10	1.50E-10	1.00E-10	8.10E-11
Tc104	2.70E-11	4.35E-11	8.10E-11	1.00E-09	5.30E-10	2.60E-10	1.50E-10	1.00E-10	8.00E-11
Np240	8.70E-11	1.30E-10	8.20E-11	8.70E-10	5.20E-10	2.60E-10	1.60E-10	1.00E-10	8.20E-11
Ho167	7.10E-11	1.00E-10	8.30E-11	8.80E-10	5.50E-10	2.80E-10	1.70E-10	1.00E-10	8.30E-11
Ra227	2.80E-10	2.10E-10	8.40E-11	1.10E-09	4.30E-10	2.50E-10	1.70E-10	1.30E-10	8.10E-11
Pu243	8.35E-11	1.10E-10	8.50E-11	1.00E-09	6.20E-10	3.10E-10	1.80E-10	1.10E-10	8.50E-11
In115m	4.25E-11	6.60E-11	8.60E-11	9.60E-10	6.00E-10	3.00E-10	1.80E-10	1.10E-10	8.60E-11
Te131	3.05E-11	5.35E-11	8.70E-11	9.00E-10	6.60E-10	3.50E-10	1.90E-10	1.20E-10	8.70E-11
Br84	3.10E-11	5.10E-11	8.80E-11	1.00E-09	5.80E-10	2.80E-10	1.60E-10	1.10E-10	8.80E-11
Rb88	1.70E-11	2.80E-11	9.00E-11	1.10E-09	6.20E-10	3.00E-10	1.70E-10	1.20E-10	9.00E-11
Sb130	4.45E-11	7.70E-11	9.10E-11	9.10E-10	5.40E-10	2.80E-10	1.70E-10	1.20E-10	9.10E-11
Cs138	2.60E-11	4.60E-11	9.20E-11	1.10E-09	5.90E-10	2.90E-10	1.70E-10	1.20E-10	9.20E-11
Eu158	4.80E-11	7.50E-11	9.40E-11	1.10E-09	6.20E-10	3.10E-10	1.80E-10	1.20E-10	9.40E-11
Sm151	3.70E-09	2.60E-09	9.80E-11	1.50E-09	6.40E-10	3.30E-10	2.00E-10	1.20E-10	9.80E-11
Sb131	4.45E-11	7.10E-11	1.00E-10	1.10E-09	7.30E-10	3.90E-10	2.10E-10	1.40E-10	1.00E-10
Pu237	3.45E-10	2.95E-10	1.00E-10	1.10E-09	6.90E-10	3.60E-10	2.20E-10	1.30E-10	1.00E-10
Br80m	5.55E-11	7.90E-11	1.10E-10	1.40E-09	8.00E-10	3.90E-10	2.30E-10	1.40E-10	1.10E-10
Nb98m	6.00E-11	9.75E-11	1.10E-10	1.20E-09	7.10E-10	3.60E-10	2.20E-10	1.40E-10	1.10E-10
Te134	6.05E-11	9.65E-11	1.10E-10	1.10E-09	7.50E-10	3.90E-10	2.20E-10	1.40E-10	1.10E-10
I134	4.80E-11	7.90E-11	1.10E-10	1.10E-09	7.50E-10	3.90E-10	2.10E-10	1.40E-10	1.10E-10
Dy165	6.10E-11	8.70E-11	1.10E-10	1.30E-09	7.90E-10	3.90E-10	2.30E-10	1.40E-10	1.10E-10
Bi214	1.06E-08	1.65E-08	1.10E-10	1.40E-09	7.40E-10	3.60E-10	2.10E-10	1.40E-10	1.10E-10
Ge78	7.25E-11	1.11E-10	1.20E-10	1.20E-09	7.00E-10	3.60E-10	2.20E-10	1.50E-10	1.20E-10
Nb93m	1.03E-09	5.75E-10	1.20E-10	1.50E-09	9.10E-10	4.60E-10	2.70E-10	1.50E-10	1.20E-10
In117m	5.20E-11	8.25E-11	1.20E-10	1.40E-09	8.60E-10	4.30E-10	2.50E-10	1.60E-10	1.20E-10
Ba139	3.50E-11	5.50E-11	1.20E-10	1.40E-09	8.40E-10	4.10E-10	2.40E-10	1.50E-10	1.20E-10
Nd149	8.75E-11	1.25E-10	1.20E-10	1.40E-09	8.70E-10	4.30E-10	2.60E-10	1.60E-10	1.20E-10
Bk250	9.60E-10	7.10E-10	1.40E-10	1.50E-09	8.50E-10	4.40E-10	2.70E-10	1.70E-10	1.40E-10
Pb214	2.90E-09	4.80E-09	1.40E-10	2.70E-09	1.00E-09	5.20E-10	3.10E-10	2.00E-10	1.40E-10
Sn128	7.50E-11	1.23E-10	1.50E-10	1.60E-09	9.70E-10	4.90E-10	3.00E-10	1.90E-10	1.50E-10
Y90m	9.80E-11	1.30E-10	1.70E-10	1.80E-09	1.20E-09	6.10E-10	3.70E-10	2.20E-10	1.70E-10
Te127	8.10E-11	1.26E-10	1.70E-10	1.50E-09	1.20E-09	6.20E-10	3.60E-10	2.10E-10	1.70E-10
La142	7.45E-11	1.25E-10	1.80E-10	1.90E-09	1.10E-09	5.80E-10	3.50E-10	2.30E-10	1.80E-10
Pb211	3.90E-09	5.60E-09	1.80E-10	3.10E-09	1.40E-09	7.10E-10	4.10E-10	2.70E-10	1.80E-10
Pd103	2.80E-10	2.37E-10	1.90E-10	2.20E-09	1.40E-09	7.20E-10	4.30E-10	2.40E-10	1.90E-10
Sn127	9.95E-11	1.60E-10	2.00E-10	2.00E-09	1.30E-09	6.60E-10	4.00E-10	2.50E-10	2.00E-10

Isotope	For inhalation		For ingestion						
	1 AMAD particle	5 AMAD particle	Worker	Infant	1-year-old Public	5-year-old Public	10-year-old Public	15-year-old Public	Adult Public
	Dose Conversion factor (Sv/Bq)								
Bi213	2.00E-08	2.95E-08	2.00E-10	2.50E-09	1.40E-09	6.70E-10	3.90E-10	2.50E-10	2.00E-10
As78	9.20E-11	1.40E-10	2.10E-10	2.00E-09	1.40E-09	7.00E-10	4.10E-10	2.70E-10	2.10E-10
Sn121	1.42E-10	1.90E-10	2.30E-10	2.60E-09	1.70E-09	8.40E-10	5.00E-10	2.80E-10	2.30E-10
Sm156	2.10E-10	2.80E-10	2.50E-10	2.80E-09	1.80E-09	9.00E-10	5.40E-10	3.10E-10	2.50E-10
Ga73	1.04E-10	1.50E-10	2.60E-10	3.00E-09	1.90E-09	9.30E-10	5.50E-10	3.30E-10	2.60E-10
Ru105	1.40E-10	2.07E-10	2.60E-10	2.70E-09	1.80E-09	9.10E-10	5.50E-10	3.30E-10	2.60E-10
Pm147	4.65E-09	3.35E-09	2.60E-10	3.60E-09	1.90E-09	9.60E-10	5.70E-10	3.20E-10	2.60E-10
Pm150	1.35E-10	2.05E-10	2.60E-10	2.80E-09	1.70E-09	8.70E-10	5.20E-10	3.20E-10	2.60E-10
Bi212	1.97E-08	2.70E-08	2.60E-10	3.20E-09	1.80E-09	8.70E-10	5.00E-10	3.30E-10	2.60E-10
Gd153	2.00E-09	1.95E-09	2.70E-10	2.90E-09	1.80E-09	9.40E-10	5.80E-10	3.40E-10	2.70E-10
Zr93	1.26E-08	1.24E-08	2.80E-10	1.20E-09	7.60E-10	5.10E-10	5.80E-10	8.60E-10	1.10E-09
Cd117	1.34E-10	2.07E-10	2.80E-10	2.90E-09	1.90E-09	9.50E-10	5.70E-10	3.50E-10	2.80E-10
Cd117m	1.70E-10	2.73E-10	2.80E-10	2.60E-09	1.70E-09	9.00E-10	5.60E-10	3.50E-10	2.80E-10
Te133m	1.02E-10	1.55E-10	2.80E-10	3.10E-09	2.40E-09	1.30E-09	6.30E-10	4.10E-10	2.80E-10
I132	9.60E-11	2.00E-10	2.90E-10	3.00E-09	2.40E-09	1.30E-09	6.20E-10	4.10E-10	2.90E-10
Am242	1.60E-08	1.20E-08	3.00E-10	5.00E-09	2.20E-09	1.10E-09	6.40E-10	3.70E-10	3.00E-10
Eu155	6.50E-09	4.70E-09	3.20E-10	4.30E-09	2.20E-09	1.10E-09	6.80E-10	4.00E-10	3.20E-10
Ge77	2.55E-10	3.50E-10	3.30E-10	3.00E-09	1.80E-09	9.90E-10	6.20E-10	4.10E-10	3.30E-10
Sn119m	1.15E-09	9.30E-10	3.40E-10	4.10E-09	2.50E-09	1.30E-09	7.50E-10	4.30E-10	3.40E-10
Th226	5.70E-08	7.60E-08	3.55E-10	4.40E-09	2.40E-09	1.20E-09	6.70E-10	4.50E-10	3.50E-10
La141	1.09E-10	1.65E-10	3.60E-10	4.30E-09	2.60E-09	1.30E-09	7.60E-10	4.50E-10	3.60E-10
Rh105	2.46E-10	3.33E-10	3.70E-10	4.00E-09	2.70E-09	1.30E-09	8.00E-10	4.60E-10	3.70E-10
Sn121m	2.50E-09	2.14E-09	3.80E-10	4.60E-09	2.70E-09	1.40E-09	8.20E-10	4.70E-10	3.80E-10
Pr145	1.65E-10	2.55E-10	3.90E-10	4.70E-09	2.90E-09	1.40E-09	8.50E-10	4.90E-10	3.90E-10
As77	3.80E-10	4.20E-10	4.00E-10	2.70E-09	2.90E-09	1.50E-09	8.70E-10	5.00E-10	4.00E-10
Sb129	1.75E-10	2.75E-10	4.20E-10	4.30E-09	2.80E-09	1.50E-09	8.80E-10	5.30E-10	4.20E-10
Ag112	1.44E-10	2.17E-10	4.30E-10	4.90E-09	3.00E-09	1.50E-09	8.90E-10	5.40E-10	4.30E-10
Ac228	1.83E-08	1.77E-08	4.30E-10	7.40E-09	2.80E-09	1.40E-09	8.70E-10	5.30E-10	4.30E-10
Ba135m	1.50E-10	2.30E-10	4.50E-10	3.30E-09	2.90E-09	1.50E-09	8.50E-10	4.70E-10	4.30E-10
Sr92	1.70E-10	2.60E-10	4.60E-10	3.40E-09	2.70E-09	1.40E-09	8.20E-10	4.80E-10	4.30E-10
Am244	1.90E-09	1.50E-09	4.60E-10	4.90E-09	3.10E-09	1.60E-09	9.60E-10	5.80E-10	4.60E-10
Y92	1.95E-10	2.75E-10	4.90E-10	5.90E-09	3.60E-09	1.80E-09	1.00E-09	6.20E-10	4.90E-10
Gd159	1.90E-10	2.85E-10	4.90E-10	5.70E-09	3.60E-09	1.80E-09	1.10E-09	6.20E-10	4.90E-10
Cs132	2.40E-10	3.80E-10	5.00E-10	2.70E-09	1.80E-09	1.10E-09	7.70E-10	5.70E-10	5.00E-10
Eu152m	2.20E-10	3.20E-10	5.00E-10	5.70E-09	3.60E-09	1.80E-09	1.10E-09	6.20E-10	5.00E-10
Pa234	3.90E-10	5.65E-10	5.10E-10	5.00E-09	3.20E-09	1.70E-09	1.00E-09	6.40E-10	5.10E-10
Br82	5.05E-10	7.60E-10	5.40E-10	3.70E-09	2.60E-09	1.50E-09	9.50E-10	6.40E-10	5.40E-10
Pd109	2.73E-10	3.93E-10	5.50E-10	6.30E-09	4.10E-09	2.00E-09	1.20E-09	6.80E-10	5.50E-10
Nb95m	8.05E-10	8.10E-10	5.60E-10	6.40E-09	4.10E-09	2.10E-09	1.20E-09	7.10E-10	5.60E-10
Nb95	1.50E-09	1.30E-09	5.80E-10	4.60E-09	3.20E-09	1.80E-09	1.10E-09	7.40E-10	5.80E-10

Isotope	For inhalation		For ingestion						
	1 AMAD particle	5 AMAD particle	Worker	Infant	1-year-old Public	5-year-old Public	10-year-old Public	15-year-old Public	Adult Public
	Dose Conversion factor (Sv/Bq)								
Am240	4.40E-10	5.90E-10	5.80E-10	4.70E-09	3.30E-09	1.80E-09	1.20E-09	7.30E-10	5.80E-10
Eu157	3.20E-10	4.40E-10	6.00E-10	6.70E-09	4.30E-09	2.20E-09	1.30E-09	7.50E-10	6.00E-10
Sr91	2.90E-10	4.30E-10	7.05E-10	5.20E-09	4.00E-09	2.10E-09	1.20E-09	7.40E-10	6.50E-10
Sn117m	1.30E-09	1.30E-09	7.10E-10	7.70E-09	5.00E-09	2.50E-09	1.50E-09	8.80E-10	7.10E-10
Ce141	3.35E-09	2.90E-09	7.10E-10	8.10E-09	5.10E-09	2.60E-09	1.50E-09	8.80E-10	7.10E-10
Fr222	1.40E-08	2.10E-08	7.10E-10	6.20E-09	3.90E-09	2.00E-09	1.30E-09	8.50E-10	7.20E-10
Tb161	1.20E-09	1.20E-09	7.20E-10	8.30E-09	5.30E-09	2.70E-09	1.60E-09	9.00E-10	7.20E-10
Pu245	4.65E-10	6.30E-10	7.20E-10	8.00E-09	5.10E-09	2.60E-09	1.50E-09	8.90E-10	7.20E-10
Pa232	6.35E-09	4.40E-09	7.20E-10	7.20E-09	4.30E-09	2.30E-09	1.40E-09	8.90E-10	7.20E-10
Ru103	1.86E-09	1.59E-09	7.30E-10	7.10E-09	4.60E-09	2.40E-09	1.50E-09	9.20E-10	7.30E-10
Pm151	4.35E-10	6.25E-10	7.30E-10	8.00E-09	5.10E-09	2.60E-09	1.60E-09	9.10E-10	7.30E-10
Sm153	6.10E-10	6.80E-10	7.40E-10	8.40E-09	5.40E-09	2.70E-09	1.60E-09	9.20E-10	7.40E-10
Sb128	3.35E-10	5.65E-10	7.60E-10	6.30E-09	4.50E-09	2.40E-09	1.50E-09	9.50E-10	7.60E-10
U237	1.20E-09	1.18E-09	7.65E-10	8.30E-09	5.40E-09	2.80E-09	1.60E-09	9.50E-10	7.60E-10
Tc99	2.10E-09	1.80E-09	7.80E-10	1.00E-08	4.80E-09	2.30E-09	1.30E-09	8.20E-10	6.40E-10
Np239	9.00E-10	1.10E-09	8.00E-10	8.90E-09	5.70E-09	2.90E-09	1.70E-09	1.00E-09	8.00E-10
Te125m	1.91E-09	1.79E-09	8.70E-10	1.30E-08	6.30E-09	3.30E-09	1.90E-09	1.10E-09	8.70E-10
Pa233	3.40E-09	3.00E-09	8.70E-10	9.70E-09	6.20E-09	3.20E-09	1.90E-09	1.10E-09	8.70E-10
Zr95	4.17E-09	3.60E-09	8.80E-10	8.50E-09	5.60E-09	3.00E-09	1.90E-09	1.20E-09	9.50E-10
Np238	2.00E-09	1.70E-09	9.10E-10	9.50E-09	6.20E-09	3.20E-09	1.90E-09	1.10E-09	9.10E-10
Cm241	3.40E-08	2.60E-08	9.10E-10	1.10E-08	5.70E-09	3.00E-09	1.90E-09	1.10E-09	9.10E-10
I135	3.30E-10	4.60E-10	9.30E-10	1.00E-08	8.90E-09	4.70E-09	2.20E-09	1.40E-09	9.30E-10
Mo99	6.00E-10	7.30E-10	9.70E-10	5.50E-09	3.50E-09	1.80E-09	1.10E-09	7.60E-10	6.00E-10
Bk249	1.50E-07	1.00E-07	9.70E-10	2.20E-08	2.90E-09	1.90E-09	1.40E-09	1.10E-09	9.70E-10
Pm149	6.90E-10	7.90E-10	9.90E-10	1.20E-08	7.40E-09	3.70E-09	2.20E-09	1.20E-09	9.90E-10
Ga72	4.30E-10	7.00E-10	1.10E-09	1.00E-08	6.80E-09	3.60E-09	2.20E-09	1.40E-09	1.10E-09
Nb96	6.65E-10	9.85E-10	1.10E-09	9.20E-09	6.30E-09	3.40E-09	2.20E-09	1.40E-09	1.10E-09
Sb125	2.95E-09	2.50E-09	1.10E-09	1.10E-08	6.10E-09	3.40E-09	2.10E-09	1.40E-09	1.10E-09
La138	1.06E-07	1.11E-07	1.10E-09	1.30E-08	4.60E-09	2.70E-09	1.90E-09	1.30E-09	1.10E-09
Ce143	7.75E-10	9.75E-10	1.10E-09	1.20E-08	8.00E-09	4.10E-09	2.40E-09	1.40E-09	1.10E-09
Nd147	2.15E-09	2.00E-09	1.10E-09	1.20E-08	7.80E-09	3.90E-09	2.30E-09	1.30E-09	1.10E-09
U240	4.37E-10	6.67E-10	1.10E-09	1.30E-08	8.10E-09	4.10E-09	2.40E-09	1.40E-09	1.10E-09
Y93	4.20E-10	5.85E-10	1.20E-09	1.40E-08	8.50E-09	4.30E-09	2.50E-09	1.40E-09	1.20E-09
Rh102	4.00E-09	2.93E-09	1.20E-09	1.20E-08	7.40E-09	3.90E-09	2.40E-09	1.40E-09	1.20E-09
Pr143	2.20E-09	2.05E-09	1.20E-09	1.40E-08	8.70E-09	4.30E-09	2.60E-09	1.50E-09	1.20E-09
Ag111	1.20E-09	1.22E-09	1.30E-09	1.40E-08	9.30E-09	4.60E-09	2.70E-09	1.60E-09	1.30E-09
Pr142	5.45E-10	7.20E-10	1.30E-09	1.50E-08	9.80E-09	4.90E-09	2.90E-09	1.60E-09	1.30E-09
Bi210	4.26E-08	3.07E-08	1.30E-09	1.50E-08	9.70E-09	4.80E-09	2.90E-09	1.60E-09	1.30E-09
Zn72	1.20E-09	1.50E-09	1.40E-09	8.70E-09	8.60E-09	4.50E-09	2.80E-09	1.70E-09	1.40E-09
Cd115	8.13E-10	1.01E-09	1.40E-09	1.40E-08	9.70E-09	4.90E-09	2.90E-09	1.70E-09	1.40E-09

Isotope	For inhalation		For ingestion						
	1 AMAD particle	5 AMAD particle	Worker	Infant	1-year-old Public	5-year-old Public	10-year-old Public	15-year-old Public	Adult Public
	Dose Conversion factor (Sv/Bq)								
Te123m	2.44E-09	2.30E-09	1.40E-09	1.90E-08	8.80E-09	4.90E-09	2.80E-09	1.70E-09	1.40E-09
Eu152	3.90E-08	2.70E-08	1.40E-09	1.60E-08	7.40E-09	4.10E-09	2.60E-09	1.70E-09	1.40E-09
Ho166	6.60E-10	8.30E-10	1.40E-09	1.60E-08	1.00E-08	5.20E-09	3.10E-09	1.70E-09	1.40E-09
Cf253	1.20E-06	1.00E-06	1.40E-09	1.00E-07	1.10E-08	6.00E-09	3.70E-09	1.80E-09	1.40E-09
Rb87	5.10E-10	7.60E-10	1.50E-09	1.50E-08	1.00E-08	5.20E-09	3.10E-09	1.80E-09	1.50E-09
As76	7.40E-10	9.20E-10	1.60E-09	1.00E-08	1.10E-08	5.80E-09	3.40E-09	2.00E-09	1.60E-09
Tb160	6.60E-09	5.40E-09	1.60E-09	1.60E-08	1.00E-08	5.40E-09	3.30E-09	2.00E-09	1.60E-09
Dy166	1.80E-09	1.80E-09	1.60E-09	1.90E-08	1.20E-08	6.00E-09	3.60E-09	2.00E-09	1.60E-09
Se79	2.05E-09	2.35E-09	1.65E-09	4.10E-08	2.80E-08	1.90E-08	1.40E-08	4.10E-09	2.90E-09
Nb94	2.75E-08	1.61E-08	1.70E-09	1.50E-08	9.70E-09	5.30E-09	3.40E-09	2.10E-09	1.70E-09
Sb122	6.95E-10	9.15E-10	1.70E-09	1.80E-08	1.20E-08	6.10E-09	3.70E-09	2.10E-09	1.70E-09
Sb127	1.03E-09	1.22E-09	1.70E-09	1.70E-08	1.20E-08	5.90E-09	3.60E-09	2.10E-09	1.70E-09
Pm148m	5.15E-09	4.20E-09	1.80E-09	1.50E-08	1.00E-08	5.50E-09	3.50E-09	2.20E-09	1.70E-09
Te131m	9.85E-10	1.40E-09	1.90E-09	2.00E-08	1.40E-08	7.80E-09	4.30E-09	2.70E-09	1.90E-09
Cd109	6.70E-09	6.37E-09	2.00E-09	2.10E-08	9.50E-09	5.50E-09	3.50E-09	2.40E-09	2.00E-09
I130	6.90E-10	9.60E-10	2.00E-09	2.10E-08	1.80E-08	9.80E-09	4.60E-09	3.00E-09	2.00E-09
Cs135	7.10E-10	9.90E-10	2.00E-09	4.10E-09	2.30E-09	1.70E-09	1.70E-09	2.00E-09	2.00E-09
La140	8.50E-10	1.25E-09	2.00E-09	2.00E-08	1.30E-08	6.80E-09	4.20E-09	2.50E-09	2.00E-09
Eu154	5.00E-08	3.50E-08	2.00E-09	2.50E-08	1.20E-08	6.50E-09	4.10E-09	2.50E-09	2.00E-09
Ho166m	1.10E-07	7.80E-08	2.00E-09	2.60E-08	9.30E-09	5.30E-09	3.50E-09	2.40E-09	2.00E-09
Zr97	7.87E-10	1.15E-09	2.10E-09	2.20E-08	1.40E-08	7.30E-09	4.40E-09	2.60E-09	2.10E-09
Sn123	4.45E-09	3.60E-09	2.10E-09	2.50E-08	1.60E-08	7.80E-09	4.60E-09	2.60E-09	2.10E-09
Eu156	3.30E-09	3.00E-09	2.20E-09	2.20E-08	1.50E-08	7.50E-09	4.60E-09	2.70E-09	2.20E-09
Tc98	4.55E-09	3.80E-09	2.30E-09	2.30E-08	1.20E-08	6.10E-09	3.70E-09	2.50E-09	2.00E-09
Ag108m	1.60E-08	1.05E-08	2.30E-09	2.10E-08	1.10E-08	6.50E-09	4.30E-09	2.80E-09	2.30E-09
Te127m	4.40E-09	4.10E-09	2.30E-09	4.10E-08	1.80E-08	9.50E-09	5.20E-09	3.00E-09	2.30E-09
Fr223	9.10E-10	1.30E-09	2.30E-09	2.60E-08	1.70E-08	8.30E-09	5.00E-09	2.90E-09	2.40E-09
Y91	7.55E-09	5.65E-09	2.40E-09	2.80E-08	1.80E-08	8.80E-09	5.20E-09	2.90E-09	2.40E-09
Sb126	1.90E-09	2.45E-09	2.40E-09	2.00E-08	1.40E-08	7.60E-09	4.90E-09	3.10E-09	2.40E-09
Sr89	4.25E-09	3.50E-09	2.45E-09	3.60E-08	1.80E-08	8.90E-09	5.80E-09	4.00E-09	2.60E-09
Sb124	3.70E-09	3.30E-09	2.50E-09	2.50E-08	1.60E-08	8.40E-09	5.20E-09	3.20E-09	2.50E-09
Ba140	1.00E-09	1.60E-09	2.50E-09	3.20E-08	1.80E-08	9.20E-09	5.80E-09	3.70E-09	2.60E-09
Rh102m	9.93E-09	7.63E-09	2.60E-09	1.90E-08	1.00E-08	6.40E-09	4.30E-09	3.00E-09	2.60E-09
Y90	1.45E-09	1.65E-09	2.70E-09	3.10E-08	2.00E-08	1.00E-08	5.90E-09	3.30E-09	2.70E-09
Pm148	2.05E-09	2.15E-09	2.70E-09	3.00E-08	1.90E-08	9.70E-09	5.80E-09	3.30E-09	2.70E-09
Rb86	9.60E-10	1.30E-09	2.80E-09	3.10E-08	2.00E-08	9.90E-09	5.90E-09	3.50E-09	2.80E-09
Ag110m	8.23E-09	6.63E-09	2.80E-09	2.40E-08	1.40E-08	7.80E-09	5.20E-09	3.40E-09	2.80E-09
Pu241	5.05E-07	3.32E-07	2.83E-09	5.60E-08	5.70E-09	5.50E-09	5.10E-09	4.80E-09	4.80E-09
Te129m	3.80E-09	3.60E-09	3.00E-09	4.40E-08	2.40E-08	1.20E-08	6.60E-09	3.90E-09	3.00E-09
Cs136	1.30E-09	1.90E-09	3.00E-09	1.50E-08	9.50E-09	6.10E-09	4.40E-09	3.40E-09	3.00E-09

Isotope	For inhalation		For ingestion						
	1 AMAD particle	5 AMAD particle	Worker	Infant	1-year-old Public	5-year-old Public	10-year-old Public	15-year-old Public	Adult Public
	Dose Conversion factor (Sv/Bq)								
Sn125	1.96E-09	2.05E-09	3.10E-09	3.50E-08	2.20E-08	1.10E-08	6.70E-09	3.80E-09	3.10E-09
Cd115m	6.17E-09	5.80E-09	3.30E-09	4.10E-08	1.90E-08	9.70E-09	6.90E-09	4.10E-09	3.30E-09
Pu246	7.30E-09	6.75E-09	3.30E-09	3.60E-08	2.30E-08	1.20E-08	7.10E-09	4.10E-09	3.30E-09
Th234	6.80E-09	5.55E-09	3.40E-09	4.00E-08	2.50E-08	1.30E-08	7.40E-09	4.20E-09	3.40E-09
Te132	2.00E-09	2.70E-09	3.70E-09	4.80E-08	3.00E-08	1.60E-08	8.30E-09	5.30E-09	3.80E-09
In114m	7.60E-09	8.45E-09	4.10E-09	5.60E-08	3.10E-08	1.50E-08	9.00E-09	5.20E-09	4.10E-09
I133	1.50E-09	2.10E-09	4.30E-09	4.90E-08	4.40E-08	2.30E-08	1.00E-08	6.80E-09	4.30E-09
Te123	3.30E-09	3.90E-09	4.40E-09	2.00E-08	9.30E-09	6.90E-09	5.40E-09	4.70E-09	4.40E-09
Sn126	1.90E-08	1.60E-08	4.70E-09	5.00E-08	3.00E-08	1.60E-08	9.80E-09	5.90E-09	4.70E-09
Ce144	4.15E-08	2.60E-08	5.20E-09	6.60E-08	3.90E-08	1.90E-08	1.10E-08	6.50E-09	5.20E-09
Pb212	1.90E-08	3.30E-08	5.90E-09	1.50E-07	6.30E-08	3.30E-08	2.00E-08	1.30E-08	6.00E-09
Es253	2.50E-06	2.10E-06	6.10E-09	1.70E-07	4.50E-08	2.30E-08	1.40E-08	7.60E-09	6.10E-09
Ru106	3.20E-08	2.06E-08	7.00E-09	8.40E-08	4.90E-08	2.50E-08	1.50E-08	8.60E-09	7.00E-09
Th227	8.70E-06	6.90E-06	8.65E-09	3.00E-07	7.00E-08	3.60E-08	2.30E-08	1.50E-08	8.80E-09
Ac226	7.98E-07	7.13E-07	1.00E-08	1.40E-07	7.60E-08	3.80E-08	2.30E-08	1.30E-08	1.00E-08
Cm242	4.80E-06	3.70E-06	1.20E-08	5.90E-07	7.60E-08	3.90E-08	2.40E-08	1.50E-08	1.20E-08
Cs137	4.80E-09	6.70E-09	1.30E-08	2.10E-08	1.20E-08	9.60E-09	1.00E-08	1.30E-08	1.30E-08
Sr90	8.70E-08	5.35E-08	1.54E-08	2.30E-07	7.30E-08	4.70E-08	6.00E-08	8.00E-08	2.80E-08
Np236	3.00E-06	2.00E-06	1.70E-08	1.90E-07	2.40E-08	1.80E-08	1.80E-08	1.80E-08	1.70E-08
Cs134	6.80E-09	9.60E-09	1.90E-08	2.60E-08	1.60E-08	1.30E-08	1.40E-08	1.90E-08	1.90E-08
I131	7.60E-09	1.10E-08	2.20E-08	1.80E-07	1.80E-07	1.00E-07	5.20E-08	3.40E-08	2.20E-08
Cd113m	6.33E-08	6.47E-08	2.30E-08	1.20E-07	5.60E-08	3.90E-08	2.90E-08	2.40E-08	2.30E-08
Ac225	5.22E-06	4.40E-06	2.40E-08	4.60E-07	1.80E-07	9.10E-08	5.40E-08	3.00E-08	2.40E-08
Cd113	6.60E-08	6.80E-08	2.50E-08	1.00E-07	4.80E-08	3.70E-08	3.00E-08	2.60E-08	2.50E-08
U238	3.46E-06	2.63E-06	2.58E-08	3.40E-07	1.20E-07	8.00E-08	6.80E-08	6.70E-08	4.50E-08
U236	3.77E-06	2.94E-06	2.70E-08	3.50E-07	1.30E-07	8.40E-08	7.00E-08	7.00E-08	4.70E-08
U235	3.67E-06	2.83E-06	2.72E-08	3.50E-07	1.30E-07	8.50E-08	7.10E-08	7.00E-08	4.70E-08
U234	4.05E-06	3.18E-06	2.87E-08	3.70E-07	1.30E-07	8.80E-08	7.40E-08	7.40E-08	4.90E-08
I126	1.00E-08	1.40E-08	2.90E-08	2.10E-07	2.10E-07	1.30E-07	6.80E-08	4.50E-08	2.90E-08
U233	4.16E-06	3.25E-06	2.93E-08	3.80E-07	1.40E-07	9.20E-08	7.80E-08	7.80E-08	5.10E-08
In115	2.70E-07	2.80E-07	3.20E-08	1.30E-07	6.40E-08	4.80E-08	4.30E-08	3.60E-08	3.20E-08
Gd152	1.32E-05	1.35E-05	4.10E-08	1.20E-06	1.20E-07	7.70E-08	5.30E-08	4.30E-08	4.10E-08
Sm147	8.90E-06	6.10E-06	4.90E-08	1.40E-06	1.40E-07	9.20E-08	6.40E-08	5.20E-08	4.90E-08
Pu236	1.38E-05	1.02E-05	5.35E-08	2.10E-06	2.20E-07	1.40E-07	1.00E-07	8.50E-08	8.70E-08
Th228	3.35E-05	2.35E-05	5.35E-08	3.70E-06	3.70E-07	2.20E-07	1.40E-07	9.40E-08	7.20E-08
Sm146	9.90E-06	6.70E-06	5.40E-08	1.50E-06	1.50E-07	1.00E-07	7.00E-08	5.80E-08	5.40E-08
Ra224	2.90E-06	2.40E-06	6.50E-08	2.70E-06	6.60E-07	3.50E-07	2.60E-07	2.00E-07	6.50E-08
Cf252	1.80E-05	1.30E-05	9.00E-08	5.00E-06	5.10E-07	3.20E-07	1.90E-07	1.00E-07	9.00E-08
Ra225	5.80E-06	4.80E-06	9.50E-08	7.10E-06	1.20E-06	6.10E-07	5.00E-07	4.40E-07	9.90E-08
Ra223	6.90E-06	5.70E-06	1.00E-07	5.30E-06	1.10E-06	5.70E-07	4.50E-07	3.70E-07	1.00E-07

Isotope	For inhalation		For ingestion						
	1 AMAD particle	5 AMAD particle	Worker	Infant	1-year-old Public	5-year-old Public	10-year-old Public	15-year-old Public	Adult Public
	Dose Conversion factor (Sv/Bq)								
I129	3.70E-08	5.10E-08	1.10E-07	1.80E-07	2.20E-07	1.70E-07	1.90E-07	1.40E-07	1.10E-07
Np237	2.10E-05	1.50E-05	1.10E-07	2.00E-06	2.10E-07	1.40E-07	1.10E-07	1.10E-07	1.10E-07
Cm244	2.50E-05	1.70E-05	1.20E-07	2.90E-06	2.90E-07	1.90E-07	1.40E-07	1.20E-07	1.20E-07
Pu238	2.90E-05	2.05E-05	1.40E-07	4.00E-06	4.00E-07	3.10E-07	2.40E-07	2.20E-07	2.30E-07
Pu242	2.90E-05	1.94E-05	1.45E-07	4.00E-06	4.00E-07	3.20E-07	2.60E-07	2.30E-07	2.40E-07
Pu244	2.85E-05	1.87E-05	1.46E-07	4.00E-06	4.10E-07	3.20E-07	2.60E-07	2.30E-07	2.40E-07
Th230	2.65E-05	1.76E-05	1.49E-07	4.10E-06	4.10E-07	3.10E-07	2.40E-07	2.20E-07	2.10E-07
Cm243	2.90E-05	2.00E-05	1.50E-07	3.20E-06	3.30E-07	2.20E-07	1.60E-07	1.40E-07	1.50E-07
Pu239	3.10E-05	2.02E-05	1.52E-07	4.20E-06	4.20E-07	3.30E-07	2.70E-07	2.40E-07	2.50E-07
Pu240	3.10E-05	2.02E-05	1.52E-07	4.20E-06	4.20E-07	3.30E-07	2.70E-07	2.40E-07	2.50E-07
Th232	3.25E-05	2.05E-05	1.56E-07	4.60E-06	4.50E-07	3.50E-07	2.90E-07	2.50E-07	2.30E-07
Cf250	3.20E-05	2.20E-05	1.60E-07	5.70E-06	5.50E-07	3.70E-07	2.30E-07	1.70E-07	1.60E-07
U232	1.54E-05	1.18E-05	1.84E-07	2.50E-06	8.20E-07	5.80E-07	5.70E-07	6.40E-07	3.30E-07
Am242m	3.50E-05	2.40E-05	1.90E-07	3.10E-06	3.00E-07	2.30E-07	2.00E-07	1.90E-07	1.90E-07
Cm247	3.60E-05	2.50E-05	1.90E-07	3.40E-06	3.50E-07	2.60E-07	2.10E-07	1.90E-07	1.90E-07
Am241	3.90E-05	2.70E-05	2.00E-07	3.70E-06	3.70E-07	2.70E-07	2.20E-07	2.00E-07	2.00E-07
Am243	3.90E-05	2.70E-05	2.00E-07	3.60E-06	3.70E-07	2.70E-07	2.20E-07	2.00E-07	2.00E-07
Cm245	4.00E-05	2.70E-05	2.10E-07	3.70E-06	3.70E-07	2.80E-07	2.30E-07	2.10E-07	2.10E-07
Cm246	4.00E-05	2.70E-05	2.10E-07	3.70E-06	3.70E-07	2.80E-07	2.20E-07	2.10E-07	2.10E-07
Po210	1.80E-06	1.46E-06	2.40E-07	2.60E-05	8.80E-06	4.40E-06	2.60E-06	1.60E-06	1.20E-06
Ra226	3.20E-06	2.20E-06	2.80E-07	4.70E-06	9.60E-07	6.20E-07	8.00E-07	1.50E-06	2.80E-07
Th229	8.20E-05	5.85E-05	3.40E-07	1.10E-05	1.00E-06	7.80E-07	6.20E-07	5.30E-07	4.90E-07
Cf249	6.60E-05	4.50E-05	3.50E-07	9.00E-06	8.70E-07	6.40E-07	4.70E-07	3.80E-07	3.50E-07
Cf251	6.70E-05	4.60E-05	3.60E-07	9.10E-06	8.80E-07	6.50E-07	4.70E-07	3.90E-07	3.60E-07
Ra228	2.60E-06	1.70E-06	6.70E-07	3.00E-05	5.70E-06	3.40E-06	3.90E-06	5.30E-06	6.90E-07
Pb210	8.90E-07	1.10E-06	6.80E-07	8.40E-06	3.60E-06	2.20E-06	1.90E-06	1.90E-06	6.90E-07
Pa231	8.10E-05	5.30E-05	7.10E-07	1.30E-05	1.30E-06	1.10E-06	9.20E-07	8.00E-07	7.10E-07
Cm248	1.40E-04	9.50E-05	7.70E-07	1.40E-05	1.40E-06	1.00E-06	8.40E-07	7.70E-07	7.70E-07
Ac227	2.72E-04	2.76E-04	1.10E-06	3.30E-05	3.10E-06	2.20E-06	1.50E-06	1.20E-06	1.10E-06
Cm250	7.90E-04	5.40E-04	4.40E-06	7.80E-05	8.20E-06	6.00E-06	4.90E-06	4.40E-06	4.40E-06

A4-5. DECAY ENERGY DATA LIBRARY

The energy liberated during radioactive decay of an isotope is an essential factor for estimating decay heat. “JENDL FP Decay Data File 2011 and Fission Yields Data File 2011” is a source of data for the energy of isotopic decay. These data were extracted for about 800 nuclei of interest and are annexed in Table A4.3.

Table A4. 3: Energy released in radio-isotopic decay

Isotope	Energy Released in Decay (eV)			Isotope	Energy Released in Decay (eV)			Isotope	Energy Released in Decay (eV)		
	Alpha	Beta	Gamma		Alpha	Beta	Gamma		Alpha	Beta	Gamma
Ni72	0.00E+00	2.10E+06	8.40E+05	Ag110	0.00E+00	1.18E+06	3.07E+04	Pr145	0.00E+00	6.75E+05	1.86E+04
Cu72	0.00E+00	2.49E+06	2.82E+06	Ag110m	0.00E+00	6.80E+04	2.76E+06	Nd145	0.00E+00	0.00E+00	0.00E+00
Zn72	0.00E+00	9.59E+04	1.50E+05	Cd110	0.00E+00	0.00E+00	0.00E+00	Ba146	0.00E+00	1.18E+06	8.33E+05
Ga72	0.00E+00	4.76E+05	2.77E+06	Ru111	0.00E+00	1.87E+06	9.62E+05	La146	0.00E+00	2.35E+06	1.49E+06
Ge72	0.00E+00	0.00E+00	0.00E+00	Rh111	0.00E+00	1.08E+06	8.98E+05	Ce146	0.00E+00	1.95E+05	3.16E+05
Cu73	0.00E+00	1.99E+06	7.72E+05	Pd111m	0.00E+00	1.90E+05	1.50E+05	Pr146	0.00E+00	1.32E+06	1.01E+06
Zn73	0.00E+00	1.54E+06	1.17E+06	Pd111	0.00E+00	8.32E+05	4.68E+04	Nd146	0.00E+00	0.00E+00	0.00E+00
Ga73	0.00E+00	4.47E+05	3.41E+05	Ag111	0.00E+00	3.51E+05	2.65E+04	Sm146	2.53E+06	0.00E+00	0.00E+00
Ge73	0.00E+00	0.00E+00	0.00E+00	Ag111m	0.00E+00	5.51E+04	4.78E+03	La147	0.00E+00	1.63E+06	9.36E+05
Cu74	0.00E+00	2.51E+06	3.21E+06	Cd111	0.00E+00	0.00E+00	0.00E+00	Ce147	0.00E+00	8.59E+05	1.08E+06
Zn74	0.00E+00	5.78E+05	8.60E+05	Cd111m	0.00E+00	1.05E+05	2.84E+05	Pr147	0.00E+00	7.50E+05	8.14E+05
Ga74m	0.00E+00	0.00E+00	3.60E+04	Ru112	0.00E+00	1.11E+06	7.25E+05	Nd147	0.00E+00	2.67E+05	1.44E+05
Ga74	0.00E+00	9.90E+05	3.03E+06	Rh112	0.00E+00	2.48E+06	1.16E+06	Pm147	0.00E+00	6.19E+04	4.36E+00
Ge74	0.00E+00	0.00E+00	0.00E+00	Pd112	0.00E+00	8.90E+04	5.13E+03	Sm147	2.31E+06	0.00E+00	0.00E+00
Cu75	0.00E+00	2.69E+06	1.09E+06	Ag112	0.00E+00	1.42E+06	6.90E+05	La148	0.00E+00	2.67E+06	1.26E+06
Zn75	0.00E+00	1.94E+06	1.82E+06	Cd112	0.00E+00	0.00E+00	0.00E+00	Ce148	0.00E+00	6.01E+05	3.26E+05
Ga75	0.00E+00	1.25E+06	3.78E+05	Rh113	0.00E+00	1.62E+06	2.95E+05	Pr148	0.00E+00	1.69E+06	1.24E+06
Ge75	0.00E+00	4.20E+05	3.50E+04	Pd113	0.00E+00	1.37E+06	1.21E+05	Nd148	0.00E+00	0.00E+00	0.00E+00
Ge75m	0.00E+00	7.80E+04	5.78E+04	Ag113m	0.00E+00	1.97E+05	2.12E+05	Pm148	0.00E+00	7.29E+05	5.74E+05
As75	0.00E+00	0.00E+00	0.00E+00	Ag113	0.00E+00	7.64E+05	7.19E+04	Sm148	1.99E+06	0.00E+00	0.00E+00
Zn76	0.00E+00	1.59E+06	5.23E+05	Cd113m	0.00E+00	1.85E+05	8.22E+01	Pm148m	0.00E+00	1.68E+05	1.99E+06
Ga76	0.00E+00	1.80E+06	2.80E+06	Cd113	0.00E+00	9.26E+04	0.00E+00	La149	0.00E+00	1.78E+06	1.09E+06
Ge76	0.00E+00	0.00E+00	0.00E+00	In113m	0.00E+00	1.34E+05	2.61E+05	Ce149	0.00E+00	1.18E+06	1.05E+06
As76	0.00E+00	1.06E+06	4.17E+05	In113	0.00E+00	0.00E+00	0.00E+00	Pr149	0.00E+00	9.53E+05	6.16E+05
Se76	0.00E+00	0.00E+00	0.00E+00	Rh114	0.00E+00	2.74E+06	1.75E+06	Nd149	0.00E+00	5.30E+05	3.84E+05
Zn77	0.00E+00	2.54E+06	1.94E+06	Pd114	0.00E+00	5.33E+05	2.59E+04	Pm149	0.00E+00	3.66E+05	1.19E+04
Ga77	0.00E+00	2.04E+06	7.89E+05	Ag114	0.00E+00	2.15E+06	2.59E+05	Sm149	0.00E+00	0.00E+00	0.00E+00
Ge77	0.00E+00	6.42E+05	1.08E+06	Cd114	0.00E+00	0.00E+00	0.00E+00	Ce150	0.00E+00	6.89E+05	4.40E+05
Ge77m	0.00E+00	9.70E+05	7.40E+04	In114m	0.00E+00	1.43E+05	8.00E+04	Pr150	0.00E+00	1.90E+06	5.60E+05
As77	0.00E+00	2.26E+05	8.10E+03	In114	0.00E+00	7.74E+05	2.14E+03	Nd150	0.00E+00	0.00E+00	0.00E+00
Se77	0.00E+00	0.00E+00	0.00E+00	Pd115	0.00E+00	1.35E+06	1.25E+06	Pm150	0.00E+00	7.30E+05	1.47E+06
Se77m	0.00E+00	7.17E+04	8.89E+04	Ag115	0.00E+00	1.08E+06	4.80E+05	Sm150	0.00E+00	0.00E+00	0.00E+00
Zn78	0.00E+00	2.25E+06	1.53E+06	Ag115m	0.00E+00	1.00E+06	4.98E+05	Ce151	0.00E+00	1.44E+06	8.77E+05
Ga78	0.00E+00	2.58E+06	2.54E+06	Cd115	0.00E+00	3.19E+05	1.93E+05	Pr151	0.00E+00	1.23E+06	7.01E+05
Ge78	0.00E+00	2.27E+05	2.78E+05	Cd115m	0.00E+00	6.04E+05	3.30E+04	Nd151	0.00E+00	6.09E+05	8.51E+05

Isotope	Energy Released in Decay (eV)			Isotope	Energy Released in Decay (eV)			Isotope	Energy Released in Decay (eV)		
	Alpha	Beta	Gamma		Alpha	Beta	Gamma		Alpha	Beta	Gamma
As78	0.00E+00	1.26E+06	1.31E+06	In115m	0.00E+00	1.73E+05	1.63E+05	Pm151	0.00E+00	3.00E+05	3.28E+05
Se78	0.00E+00	0.00E+00	0.00E+00	In115	0.00E+00	1.52E+05	0.00E+00	Sm151	0.00E+00	1.98E+04	1.36E+01
Ga79	3.13E+04	2.45E+06	2.08E+06	Sn115	0.00E+00	0.00E+00	0.00E+00	Eu151	0.00E+00	0.00E+00	0.00E+00
Ge79m	0.00E+00	1.29E+06	1.78E+06	Pd116	0.00E+00	6.62E+05	6.04E+05	Ce152	0.00E+00	1.17E+06	7.78E+05
Ge79	0.00E+00	1.71E+06	3.09E+05	Ag116	0.00E+00	1.95E+06	1.75E+06	Pr152	0.00E+00	2.12E+06	1.68E+06
As79	0.00E+00	8.39E+05	3.38E+04	Ag116m	0.00E+00	1.39E+06	3.07E+06	Nd152	0.00E+00	3.30E+05	1.64E+05
Se79m	0.00E+00	8.30E+04	1.41E+04	Cd116	0.00E+00	0.00E+00	0.00E+00	Pm152	0.00E+00	1.33E+06	2.86E+05
Se79	0.00E+00	5.58E+04	0.00E+00	In116m	0.00E+00	3.14E+05	2.49E+06	Sm152	0.00E+00	0.00E+00	0.00E+00
Br79	0.00E+00	0.00E+00	0.00E+00	In116	0.00E+00	1.36E+06	1.96E+04	Pm152m	0.00E+00	9.20E+05	1.50E+06
Br79m	0.00E+00	4.70E+04	1.60E+05	Sn116	0.00E+00	0.00E+00	0.00E+00	Eu152	0.00E+00	1.24E+05	1.17E+06
Ga80	0.00E+00	3.12E+06	3.55E+06	Pd117	0.00E+00	1.92E+06	1.09E+06	Gd152	2.20E+06	0.00E+00	0.00E+00
Ge80	0.00E+00	8.15E+05	6.20E+05	Ag117m	0.00E+00	1.32E+06	8.32E+05	Eu152m	0.00E+00	5.12E+05	2.94E+05
As80	0.00E+00	2.15E+06	5.80E+05	Ag117	0.00E+00	1.10E+06	1.30E+06	Pr153	0.00E+00	1.70E+06	1.03E+06
Se80	0.00E+00	0.00E+00	0.00E+00	Cd117	0.00E+00	4.30E+05	1.08E+06	Nd153	0.00E+00	1.18E+06	2.80E+05
Br80	0.00E+00	7.26E+05	7.60E+04	Cd117m	0.00E+00	2.07E+05	2.04E+06	Pm153	0.00E+00	6.90E+05	7.63E+04
Br80m	0.00E+00	5.95E+04	2.42E+04	In117m	0.00E+00	4.31E+05	9.10E+04	Sm153	0.00E+00	2.67E+05	6.18E+04
Kr80	0.00E+00	0.00E+00	0.00E+00	In117	0.00E+00	2.64E+05	6.90E+05	Eu153	0.00E+00	0.00E+00	0.00E+00
Ga81	0.00E+00	2.36E+06	2.26E+06	Sn117m	0.00E+00	1.56E+05	1.58E+05	Gd153	0.00E+00	4.00E+04	1.05E+05
Ge81	0.00E+00	1.68E+06	2.96E+06	Sn117	0.00E+00	0.00E+00	0.00E+00	Pr154	0.00E+00	1.87E+06	2.41E+06
As81	0.00E+00	1.58E+06	2.32E+05	Pd118	0.00E+00	1.56E+06	4.14E+05	Nd154	0.00E+00	8.70E+05	4.65E+05
Se81	0.00E+00	6.11E+05	8.10E+03	Ag118m	0.00E+00	1.13E+06	1.85E+06	Pm154	0.00E+00	8.39E+05	1.78E+06
Se81m	0.00E+00	8.50E+04	1.81E+04	Ag118	0.00E+00	2.58E+06	1.57E+06	Sm154	0.00E+00	0.00E+00	0.00E+00
Br81	0.00E+00	0.00E+00	0.00E+00	Cd118	0.00E+00	1.61E+05	0.00E+00	Pm154m	0.00E+00	8.80E+05	1.78E+06
Kr81	0.00E+00	4.76E+03	7.28E+03	In118m	0.00E+00	6.10E+05	2.78E+06	Eu154	0.00E+00	2.72E+05	1.24E+06
Kr81m	0.00E+00	5.91E+04	1.31E+05	In118	0.00E+00	1.88E+06	7.80E+04	Gd154	0.00E+00	0.00E+00	0.00E+00
Ge82	0.00E+00	1.45E+06	7.65E+05	Sn118	0.00E+00	0.00E+00	0.00E+00	Pr155	0.00E+00	2.07E+06	1.48E+06
As82m	0.00E+00	1.82E+06	2.79E+06	Ag119	0.00E+00	1.84E+06	1.63E+06	Nd155	0.00E+00	1.37E+06	8.34E+05
As82	0.00E+00	2.92E+06	1.08E+06	Cd119m	0.00E+00	9.00E+05	1.95E+06	Pm155	0.00E+00	1.02E+06	6.33E+05
Se82	0.00E+00	0.00E+00	0.00E+00	Cd119	0.00E+00	8.20E+05	1.64E+06	Sm155	0.00E+00	5.68E+05	1.03E+05
Br82m	0.00E+00	5.20E+04	1.13E+04	In119m	0.00E+00	1.04E+06	1.28E+04	Eu155	0.00E+00	6.34E+04	6.13E+04
Br82	0.00E+00	1.46E+05	2.66E+06	In119	0.00E+00	6.30E+05	7.10E+05	Gd155	0.00E+00	0.00E+00	0.00E+00
Kr82	0.00E+00	0.00E+00	0.00E+00	Sn119	0.00E+00	0.00E+00	0.00E+00	Nd156	0.00E+00	1.12E+06	7.66E+05
Ge83	0.00E+00	2.69E+06	2.44E+06	Sn119m	0.00E+00	7.55E+04	1.15E+04	Pm156	0.00E+00	1.39E+06	1.73E+06
As83	0.00E+00	1.26E+06	2.75E+06	Ag120	0.00E+00	2.29E+06	2.88E+06	Sm156	0.00E+00	2.00E+05	1.14E+05
Se83	0.00E+00	5.00E+05	2.61E+06	Cd120	0.00E+00	6.77E+05	0.00E+00	Eu156	0.00E+00	4.50E+05	1.23E+06
Se83m	0.00E+00	1.27E+06	9.82E+05	In120m	0.00E+00	1.00E+06	3.00E+06	Gd156	0.00E+00	0.00E+00	0.00E+00

Isotope	Energy Released in Decay (eV)			Isotope	Energy Released in Decay (eV)			Isotope	Energy Released in Decay (eV)		
	Alpha	Beta	Gamma		Alpha	Beta	Gamma		Alpha	Beta	Gamma
Kr83m	0.00E+00	3.91E+04	2.77E+03	In120	0.00E+00	2.24E+06	3.31E+05	Nd157	0.00E+00	1.67E+06	1.14E+06
Kr83	0.00E+00	0.00E+00	0.00E+00	Sn120	0.00E+00	0.00E+00	0.00E+00	Pm157	0.00E+00	1.45E+06	8.41E+05
As84	0.00E+00	3.20E+06	3.15E+06	Cd121	0.00E+00	1.21E+06	1.66E+06	Sm157	0.00E+00	8.90E+05	4.09E+05
Se84	0.00E+00	5.40E+05	4.20E+05	Cd121m	0.00E+00	1.19E+06	2.13E+06	Eu157	0.00E+00	3.90E+05	2.91E+05
Br84	0.00E+00	1.23E+06	1.76E+06	In121m	0.00E+00	1.50E+06	6.40E+04	Gd157	0.00E+00	0.00E+00	0.00E+00
Kr84	0.00E+00	0.00E+00	0.00E+00	In121	0.00E+00	9.90E+05	9.30E+05	Pm158	0.00E+00	1.57E+06	2.16E+06
Br84m	0.00E+00	8.90E+05	2.77E+06	Sn121	0.00E+00	1.16E+05	0.00E+00	Sm158	0.00E+00	4.08E+05	5.55E+05
As85	0.00E+00	2.84E+06	3.01E+06	Sn121m	0.00E+00	3.40E+04	5.00E+03	Eu158	0.00E+00	8.90E+05	1.30E+06
Se85	0.00E+00	1.90E+06	2.08E+06	Sb121	0.00E+00	0.00E+00	0.00E+00	Gd158	0.00E+00	0.00E+00	0.00E+00
Br85	0.00E+00	1.04E+06	6.60E+04	Cd122	0.00E+00	7.97E+05	4.56E+05	Pm159	0.00E+00	1.78E+06	1.16E+06
Kr85m	0.00E+00	2.55E+05	1.57E+05	In122	0.00E+00	2.53E+06	6.40E+05	Sm159	0.00E+00	1.00E+06	9.65E+05
Kr85	0.00E+00	2.51E+05	2.23E+03	Sn122	0.00E+00	0.00E+00	0.00E+00	Eu159	0.00E+00	9.00E+05	3.07E+05
Rb85	0.00E+00	0.00E+00	0.00E+00	Sb122	0.00E+00	5.62E+05	4.45E+05	Gd159	0.00E+00	3.09E+05	5.67E+04
Se86	0.00E+00	1.44E+06	2.27E+06	Sb122m	0.00E+00	6.13E+04	7.22E+04	Tb159	0.00E+00	0.00E+00	0.00E+00
Br86	0.00E+00	1.90E+06	3.30E+06	In122m	0.00E+00	1.34E+06	3.06E+06	Pm160	0.00E+00	1.97E+06	2.50E+06
Kr86	0.00E+00	0.00E+00	0.00E+00	Cd123	0.00E+00	1.78E+06	2.02E+06	Sm160	0.00E+00	8.47E+05	6.90E+05
Rb86m	0.00E+00	9.70E+03	5.46E+05	In123	0.00E+00	1.36E+06	1.06E+06	Eu160	0.00E+00	1.17E+06	2.54E+06
Rb86	0.00E+00	6.68E+05	9.30E+04	Sn123	0.00E+00	5.23E+05	6.90E+03	Gd160	0.00E+00	0.00E+00	0.00E+00
Sr86	0.00E+00	0.00E+00	0.00E+00	Sb123	0.00E+00	0.00E+00	0.00E+00	Tb160	0.00E+00	2.58E+05	1.13E+06
Se87	0.00E+00	2.08E+06	2.64E+06	In123m	0.00E+00	2.03E+06	6.60E+04	Dy160	0.00E+00	0.00E+00	0.00E+00
Br87	0.00E+00	1.61E+06	3.34E+06	Sn123m	0.00E+00	4.79E+05	1.41E+05	Sm161	0.00E+00	1.51E+06	1.14E+06
Kr87	0.00E+00	1.33E+06	7.92E+05	Te123	0.00E+00	2.01E+03	2.46E+02	Eu161	0.00E+00	1.01E+06	1.01E+06
Rb87	0.00E+00	8.17E+04	0.00E+00	Te123m	0.00E+00	1.01E+05	1.48E+05	Gd161	0.00E+00	5.86E+05	3.93E+05
Sr87m	0.00E+00	6.50E+04	3.22E+05	Cd124	0.00E+00	1.14E+06	5.68E+05	Tb161	0.00E+00	1.96E+05	3.55E+04
Sr87	0.00E+00	0.00E+00	0.00E+00	In124	0.00E+00	2.05E+06	2.70E+06	Dy161	0.00E+00	0.00E+00	0.00E+00
Se88	0.00E+00	2.22E+06	2.03E+06	Sn124	0.00E+00	0.00E+00	0.00E+00	Sm162	0.00E+00	1.38E+06	8.78E+05
Br88	0.00E+00	2.30E+06	2.89E+06	Sb124	0.00E+00	3.90E+05	1.85E+06	Eu162	0.00E+00	1.40E+06	2.02E+06
Kr88	0.00E+00	3.70E+05	1.95E+06	In124m	0.00E+00	1.62E+06	3.80E+06	Gd162	0.00E+00	2.86E+05	5.37E+05
Rb88	0.00E+00	2.05E+06	6.77E+05	Sb124m	0.00E+00	1.14E+05	4.40E+05	Tb162	0.00E+00	5.31E+05	1.11E+06
Sr88	0.00E+00	0.00E+00	0.00E+00	Te124	0.00E+00	0.00E+00	0.00E+00	Dy162	0.00E+00	0.00E+00	0.00E+00
Br89	0.00E+00	2.37E+06	2.77E+06	In125	0.00E+00	1.81E+06	1.20E+06	Sm163	0.00E+00	1.67E+06	1.33E+06
Kr89	0.00E+00	1.38E+06	1.92E+06	In125m	0.00E+00	2.10E+06	6.72E+05	Eu163	0.00E+00	1.54E+06	1.07E+06
Rb89	0.00E+00	9.70E+05	2.24E+06	Sb125	0.00E+00	1.00E+05	4.37E+05	Gd163	0.00E+00	8.59E+05	9.61E+05
Sr89	0.00E+00	5.85E+05	0.00E+00	Sn125m	0.00E+00	8.06E+05	3.46E+05	Tb163	0.00E+00	3.62E+05	7.89E+05
Y89m	0.00E+00	7.25E+03	9.01E+05	Sn125	0.00E+00	8.00E+05	3.30E+05	Dy163	0.00E+00	0.00E+00	0.00E+00
Y89	0.00E+00	0.00E+00	0.00E+00	Te125	0.00E+00	0.00E+00	0.00E+00	Eu164	0.00E+00	1.56E+06	2.15E+06

Isotope	Energy Released in Decay (eV)			Isotope	Energy Released in Decay (eV)			Isotope	Energy Released in Decay (eV)		
	Alpha	Beta	Gamma		Alpha	Beta	Gamma		Alpha	Beta	Gamma
Br90	0.00E+00	2.90E+06	2.90E+06	Te125m	0.00E+00	1.04E+05	3.52E+04	Gd164	0.00E+00	7.18E+05	6.47E+05
Kr90	0.00E+00	1.36E+06	1.33E+06	In126	0.00E+00	2.40E+06	2.81E+06	Tb164	0.00E+00	7.50E+05	2.36E+06
Rb90m	0.00E+00	1.40E+06	3.24E+06	Sb126	0.00E+00	3.70E+05	2.76E+06	Dy164	0.00E+00	0.00E+00	0.00E+00
Rb90	0.00E+00	1.99E+06	2.16E+06	Sn126	0.00E+00	1.06E+05	5.60E+04	Eu165	0.00E+00	1.83E+06	1.41E+06
Sr90	0.00E+00	1.96E+05	0.00E+00	Sb126m	0.00E+00	6.50E+05	1.55E+06	Gd165	0.00E+00	1.23E+06	8.81E+05
Y90m	0.00E+00	4.53E+04	6.35E+05	Te126	0.00E+00	0.00E+00	0.00E+00	Tb165	0.00E+00	8.88E+05	8.49E+05
Y90	0.00E+00	9.34E+05	1.25E+00	I126	0.00E+00	1.60E+05	4.35E+05	Dy165m	0.00E+00	1.02E+05	1.90E+04
Zr90	0.00E+00	0.00E+00	0.00E+00	Xe126	0.00E+00	0.00E+00	0.00E+00	Dy165	0.00E+00	4.48E+05	2.30E+04
Kr91	0.00E+00	2.10E+06	1.75E+06	In127	1.75E+04	2.20E+06	1.60E+06	Ho165	0.00E+00	0.00E+00	0.00E+00
Rb91	0.00E+00	1.61E+06	2.34E+06	In127m	2.30E+04	2.90E+06	4.70E+05	Dy166	0.00E+00	1.67E+05	4.21E+04
Sr91	0.00E+00	6.50E+05	7.07E+05	Sn127	0.00E+00	5.70E+05	1.91E+06	Ho166	0.00E+00	6.94E+05	2.96E+04
Y91	0.00E+00	6.03E+05	3.10E+03	Sn127m	0.00E+00	8.90E+05	8.86E+05	Er166	0.00E+00	0.00E+00	0.00E+00
Y91m	0.00E+00	2.63E+04	5.28E+05	Sb127	0.00E+00	3.13E+05	6.93E+05	Ho166m	0.00E+00	1.44E+05	1.59E+06
Zr91	0.00E+00	0.00E+00	0.00E+00	Te127m	0.00E+00	7.59E+04	1.09E+04	Dy167	0.00E+00	7.10E+05	5.33E+05
Kr92	0.00E+00	2.00E+06	1.40E+06	I127	0.00E+00	0.00E+00	0.00E+00	Ho167	0.00E+00	2.10E+05	3.50E+05
Rb92	0.00E+00	2.90E+06	2.15E+06	Te127	0.00E+00	2.25E+05	4.90E+03	Er167m	0.00E+00	1.08E+05	9.82E+04
Sr92	0.00E+00	2.00E+05	1.34E+06	Sn128	0.00E+00	2.51E+05	6.00E+05	Er167	0.00E+00	0.00E+00	0.00E+00
Y92	0.00E+00	1.45E+06	2.52E+05	Sb128m	0.00E+00	9.50E+05	1.91E+06	Y97m	0.00E+00	2.42E+06	2.15E+06
Zr92	0.00E+00	0.00E+00	0.00E+00	Sb128	0.00E+00	4.80E+05	3.09E+06	U232	5.39E+06	1.45E+04	1.66E+03
Kr93	0.00E+00	2.88E+06	2.26E+06	Te128	0.00E+00	0.00E+00	0.00E+00	U233	4.89E+06	3.90E+03	2.34E+02
Rb93	0.00E+00	2.20E+06	2.27E+06	I128	0.00E+00	7.45E+05	6.76E+04	U234	4.84E+06	1.19E+04	1.41E+03
Sr93	0.00E+00	7.70E+05	2.02E+06	Xe128	0.00E+00	0.00E+00	0.00E+00	U235	4.41E+06	3.87E+04	1.65E+05
Y93	0.00E+00	1.17E+06	9.60E+04	In129m	2.70E+04	3.50E+06	2.75E+05	U236	4.55E+06	8.80E+03	1.20E+03
Zr93	0.00E+00	1.92E+04	0.00E+00	Sn129	0.00E+00	1.29E+06	1.01E+06	U237	0.00E+00	1.82E+05	1.39E+05
Nb93m	0.00E+00	2.67E+04	1.97E+03	Sn129m	0.00E+00	8.70E+05	2.32E+06	U238	4.26E+06	7.10E+03	1.00E+03
Nb93	0.00E+00	0.00E+00	0.00E+00	Sb129	0.00E+00	3.96E+05	1.37E+06	U239	0.00E+00	4.08E+05	5.09E+04
Rb94	0.00E+00	2.72E+06	3.66E+06	Te129	0.00E+00	5.40E+05	6.20E+04	U240	0.00E+00	1.23E+05	1.59E+03
Sr94	0.00E+00	7.33E+05	1.57E+06	Te129m	0.00E+00	2.69E+05	3.74E+04	Pu236	5.86E+06	9.60E+03	1.58E+03
Y94	0.00E+00	1.81E+06	7.70E+05	I129	0.00E+00	5.40E+04	2.46E+04	Pu237	3.37E+02	9.10E+03	5.31E+04
Zr94	0.00E+00	0.00E+00	0.00E+00	Xe129	0.00E+00	0.00E+00	0.00E+00	Pu238	5.58E+06	8.47E+03	1.42E+03
Nb94m	0.00E+00	3.42E+04	1.17E+04	Xe129m	0.00E+00	1.82E+05	5.12E+04	Pu239	5.24E+06	4.00E+03	5.03E+02
Nb94	0.00E+00	1.48E+05	1.57E+06	Sn130	0.00E+00	4.52E+05	9.36E+05	Pu240	5.24E+06	8.43E+03	1.34E+03
Mo94	0.00E+00	0.00E+00	0.00E+00	Sb130	0.00E+00	6.90E+05	3.27E+06	Pu241	1.20E+02	5.23E+03	1.78E+00
Sr95	0.00E+00	2.21E+06	1.54E+06	Te130	0.00E+00	0.00E+00	0.00E+00	Pu242	4.97E+06	6.60E+03	1.17E+03
Y95	0.00E+00	1.44E+06	1.11E+06	Sb130m	0.00E+00	8.30E+05	2.71E+06	Pu243	0.00E+00	1.63E+05	2.70E+04
Zr95	0.00E+00	1.18E+05	7.32E+05	Sn130m	0.00E+00	9.00E+05	2.07E+06	Pu244	4.65E+06	3.70E+03	1.30E+01

Isotope	Energy Released in Decay (eV)			Isotope	Energy Released in Decay (eV)			Isotope	Energy Released in Decay (eV)		
	Alpha	Beta	Gamma		Alpha	Beta	Gamma		Alpha	Beta	Gamma
Nb95	0.00E+00	4.45E+04	7.64E+05	I130m	0.00E+00	1.50E+05	1.10E+05	Pu245	0.00E+00	3.40E+05	3.96E+05
Nb95m	0.00E+00	1.69E+05	7.08E+04	I130	0.00E+00	2.79E+05	2.14E+06	Pu246	0.00E+00	1.01E+05	1.41E+05
Mo95	0.00E+00	0.00E+00	0.00E+00	Xe130	0.00E+00	0.00E+00	0.00E+00	Am240	1.02E+01	5.01E+04	1.01E+06
Sr96	0.00E+00	1.97E+06	1.35E+06	Sn131	0.00E+00	1.46E+06	1.19E+06	Am241	5.58E+06	2.90E+04	2.72E+04
Y96m	0.00E+00	1.61E+06	4.31E+06	Sn131m	0.00E+00	1.25E+06	1.89E+06	Am242m	2.40E+04	3.69E+04	3.86E+03
Y96	0.00E+00	2.66E+06	1.21E+06	Sb131	0.00E+00	6.50E+05	2.03E+06	Am242	0.00E+00	1.74E+05	1.72E+04
Zr96	0.00E+00	0.00E+00	0.00E+00	Te131	0.00E+00	7.12E+05	4.20E+05	Am243	5.36E+06	1.87E+04	5.66E+04
Nb96	0.00E+00	2.53E+05	2.46E+06	Te131m	0.00E+00	1.55E+05	1.37E+06	Am244m	0.00E+00	5.20E+05	1.51E+04
Mo96	0.00E+00	0.00E+00	0.00E+00	I131	0.00E+00	1.92E+05	3.82E+05	Am244	0.00E+00	3.10E+05	8.00E+05
Y97	0.00E+00	2.20E+06	1.82E+06	Xe131m	0.00E+00	1.43E+05	2.03E+04	Am245	0.00E+00	2.84E+05	3.18E+04
Zr97	0.00E+00	7.05E+05	1.87E+05	Xe131	0.00E+00	0.00E+00	0.00E+00	Am246m	0.00E+00	4.95E+05	9.77E+05
Nb97m	0.00E+00	0.00E+00	7.28E+05	Sn132	0.00E+00	7.20E+05	1.28E+06	Am246	0.00E+00	7.30E+05	8.90E+05
Mo97	0.00E+00	0.00E+00	0.00E+00	Sb132	0.00E+00	1.25E+06	2.60E+06	Np236	0.00E+00	2.10E+05	1.53E+05
Y98m	0.00E+00	2.50E+06	2.74E+06	Sb132m	0.00E+00	1.28E+06	2.63E+06	Np237	4.87E+06	4.99E+04	2.87E+04
Zr98	0.00E+00	9.10E+05	0.00E+00	Te132	0.00E+00	1.01E+05	2.34E+05	Np238	0.00E+00	2.11E+05	5.81E+05
Nb98	0.00E+00	1.63E+06	8.56E+05	I132	0.00E+00	4.93E+05	2.26E+06	Np239	0.00E+00	2.70E+05	1.75E+05
Mo98	0.00E+00	0.00E+00	0.00E+00	Xe132	0.00E+00	0.00E+00	0.00E+00	Np240	0.00E+00	5.30E+05	1.12E+06
Nb98m	0.00E+00	7.70E+05	2.81E+06	Cs132	0.00E+00	1.28E+04	7.14E+05	Np241	0.00E+00	4.40E+05	3.55E+04
Tc98	0.00E+00	1.18E+05	1.41E+06	Ba132	0.00E+00	0.00E+00	0.00E+00	Cm241	5.93E+04	1.06E+05	4.80E+05
Ru98	0.00E+00	0.00E+00	0.00E+00	Sn133	0.00E+00	3.40E+06	2.73E+05	Cm242	6.21E+06	6.71E+03	2.14E+01
Y99	0.00E+00	2.38E+06	1.15E+06	Sb133	0.00E+00	6.60E+05	2.74E+06	Cm243	5.93E+06	1.20E+05	1.28E+05
Zr99	0.00E+00	1.71E+06	8.44E+05	Te133m	0.00E+00	3.72E+05	1.86E+06	Cm244	5.89E+06	5.90E+03	1.65E+01
Nb99m	0.00E+00	1.18E+06	1.72E+06	Te133	0.00E+00	7.06E+05	1.20E+06	Cm245	5.48E+06	7.12E+04	9.75E+04
Nb99	0.00E+00	1.27E+06	6.22E+05	I133	0.00E+00	4.09E+05	6.12E+05	Cm246	5.47E+06	0.00E+00	0.00E+00
Mo99	0.00E+00	3.94E+05	1.48E+05	I133m	0.00E+00	4.91E+04	1.58E+06	Cm247	5.03E+06	1.09E+04	3.14E+05
Tc99m	0.00E+00	1.51E+04	1.27E+05	Xe133	0.00E+00	1.36E+05	4.71E+04	Cm248	4.72E+06	0.00E+00	0.00E+00
Tc99	0.00E+00	8.46E+04	7.00E-01	Xe133m	0.00E+00	1.91E+05	4.08E+04	Cm249	0.00E+00	2.77E+05	1.91E+04
Ru99	0.00E+00	0.00E+00	0.00E+00	Cs133	0.00E+00	0.00E+00	0.00E+00	Cm250	5.17E+06	3.77E+04	1.91E+04
Zr100	0.00E+00	1.11E+06	6.98E+05	Sn134	0.00E+00	2.53E+06	1.25E+06	Bk249	7.78E+01	3.24E+04	8.30E-02
Nb100	0.00E+00	2.54E+06	7.10E+05	Sb134m	0.00E+00	2.86E+06	2.06E+06	Bk250	0.00E+00	2.88E+05	8.97E+05
Nb100m	0.00E+00	2.00E+06	2.21E+06	Te134	0.00E+00	2.24E+05	8.71E+05	Es253	6.74E+06	1.29E+03	3.54E+02
Mo100	0.00E+00	0.00E+00	0.00E+00	I134	0.00E+00	6.34E+05	2.60E+06	Cf249	5.91E+06	6.60E+04	3.30E+05
Tc100	0.00E+00	1.32E+06	7.61E+04	I134m	0.00E+00	8.80E+04	2.44E+05	Cf250	6.12E+06	3.68E+03	8.90E+02
Ru100	0.00E+00	0.00E+00	0.00E+00	Xe134	0.00E+00	0.00E+00	0.00E+00	Cf251	5.88E+06	1.71E+05	1.10E+05
Zr101	0.00E+00	2.20E+06	1.09E+06	Cs134m	0.00E+00	1.05E+05	2.68E+04	Cf252	6.02E+06	3.95E+03	9.20E+02
Nb101	0.00E+00	1.86E+06	4.50E+05	Cs134	0.00E+00	1.64E+05	1.55E+06	Cf253	2.00E+04	7.23E+04	0.00E+00

Isotope	Energy Released in Decay (eV)			Isotope	Energy Released in Decay (eV)			Isotope	Energy Released in Decay (eV)		
	Alpha	Beta	Gamma		Alpha	Beta	Gamma		Alpha	Beta	Gamma
Mo101	0.00E+00	5.48E+05	1.47E+06	Ba134	0.00E+00	0.00E+00	0.00E+00	Ac225	5.88E+06	1.36E+04	1.15E+04
Tc101	0.00E+00	4.79E+05	3.37E+05	Sb135	0.00E+00	2.75E+06	6.70E+05	Ac226	4.90E+03	2.90E+05	1.32E+05
Ru101	0.00E+00	0.00E+00	0.00E+00	Te135	0.00E+00	2.08E+06	1.48E+06	Ac227	7.17E+04	1.21E+04	5.43E+02
Zr102	0.00E+00	1.25E+06	7.37E+05	I135	0.00E+00	3.39E+05	1.58E+06	Ac228	0.00E+00	4.10E+05	8.53E+05
Nb102	0.00E+00	2.28E+06	2.09E+06	Xe135	0.00E+00	3.20E+05	2.48E+05	Hg206	0.00E+00	4.20E+05	1.02E+05
Nb102m	0.00E+00	2.83E+06	1.46E+06	Xe135m	0.00E+00	9.73E+04	4.28E+05	Tl206	0.00E+00	5.38E+05	4.10E+01
Mo102	0.00E+00	3.50E+05	1.85E+04	Cs135	0.00E+00	7.57E+04	0.00E+00	Tl207	0.00E+00	4.95E+05	2.35E+03
Tc102	0.00E+00	1.94E+06	1.10E+05	Cs135m	0.00E+00	3.54E+04	1.60E+06	Tl208	0.00E+00	5.96E+05	3.38E+06
Ru102	0.00E+00	0.00E+00	0.00E+00	Ba135	0.00E+00	0.00E+00	0.00E+00	Tl209	0.00E+00	6.82E+05	2.14E+06
Rh102m	0.00E+00	5.56E+03	2.16E+06	Ba135m	0.00E+00	2.06E+05	6.11E+04	Tl210	0.00E+00	1.30E+06	2.76E+06
Rh102	0.00E+00	1.66E+05	4.99E+05	Te136	0.00E+00	1.30E+06	2.04E+06	Th226	6.42E+06	1.99E+04	8.50E+03
Pd102	0.00E+00	0.00E+00	0.00E+00	I136	0.00E+00	1.99E+06	2.35E+06	Th227	6.01E+06	5.20E+04	1.63E+05
Zr103	0.00E+00	2.46E+06	1.47E+06	Xe136	0.00E+00	0.00E+00	0.00E+00	Th228	5.50E+06	1.95E+04	3.06E+03
Nb103	0.00E+00	2.11E+06	9.82E+05	I136m	0.00E+00	2.68E+06	2.13E+06	Th229	5.01E+06	1.00E+05	9.42E+04
Mo103	0.00E+00	1.12E+06	1.13E+06	Cs136	0.00E+00	1.32E+05	1.44E+06	Th230	4.75E+06	1.32E+04	1.34E+03
Tc103	0.00E+00	7.04E+05	5.53E+05	Ba136	0.00E+00	0.00E+00	0.00E+00	Th231	0.00E+00	1.46E+05	2.31E+04
Ru103	0.00E+00	6.65E+04	4.96E+05	Te137	0.00E+00	2.17E+06	1.61E+06	Th232	4.07E+06	1.13E+04	1.08E+03
Rh103m	0.00E+00	3.48E+04	1.68E+03	I137	0.00E+00	1.89E+06	1.13E+06	Th233	0.00E+00	4.11E+05	3.56E+04
Rh103	0.00E+00	0.00E+00	0.00E+00	Xe137	0.00E+00	1.70E+06	1.90E+05	Th234	0.00E+00	5.88E+04	7.00E+03
Pd103	0.00E+00	4.97E+03	1.46E+04	Cs137	0.00E+00	1.87E+05	0.00E+00	Th235	0.00E+00	6.70E+05	5.20E+04
Nb104	0.00E+00	2.51E+06	3.38E+06	Ba137	0.00E+00	0.00E+00	0.00E+00	Ra223	5.77E+06	6.80E+04	1.38E+05
Mo104	0.00E+00	6.23E+05	5.85E+05	Ba137m	0.00E+00	6.36E+04	5.95E+05	Ra224	5.77E+06	2.27E+03	1.04E+04
Tc104	0.00E+00	8.50E+05	3.23E+06	Te138	0.00E+00	1.95E+06	1.07E+06	Ra225	1.72E+03	1.07E+05	1.38E+04
Ru104	0.00E+00	0.00E+00	0.00E+00	I138	0.00E+00	2.90E+06	1.42E+06	Ra226	4.86E+06	3.80E+03	7.37E+03
Rh104	0.00E+00	9.85E+05	1.20E+04	Xe138	0.00E+00	6.40E+05	1.13E+06	Ra227	0.00E+00	4.22E+05	1.37E+05
Rh104m	0.00E+00	8.31E+04	4.54E+04	Cs138	0.00E+00	1.24E+06	2.36E+06	Ra228	0.00E+00	9.90E+03	9.85E+02
Pd104	0.00E+00	0.00E+00	0.00E+00	Cs138m	0.00E+00	3.30E+05	7.07E+05	Pa231	5.01E+06	3.21E+04	3.97E+04
Nb105	0.00E+00	2.50E+06	1.40E+06	Ba138	0.00E+00	0.00E+00	0.00E+00	Pa232	0.00E+00	1.61E+05	9.33E+05
Mo105	0.00E+00	1.03E+06	2.40E+06	La138	0.00E+00	3.74E+04	1.23E+06	Pa233	0.00E+00	2.01E+05	2.19E+05
Tc105	0.00E+00	7.17E+05	1.83E+06	I139	0.00E+00	2.50E+06	6.62E+05	Pa234m	0.00E+00	8.10E+05	1.62E+04
Ru105	0.00E+00	4.13E+05	7.38E+05	Xe139	0.00E+00	1.81E+06	1.02E+06	Pa234	0.00E+00	4.07E+05	1.52E+06
Rh105	0.00E+00	1.54E+05	7.73E+04	Cs139	0.00E+00	1.66E+06	3.03E+05	Pa235	0.00E+00	4.76E+05	0.00E+00
Rh105m	0.00E+00	9.40E+04	3.46E+04	Ba139	0.00E+00	9.01E+05	4.60E+04	Pb206	0.00E+00	0.00E+00	0.00E+00
Pd105	0.00E+00	0.00E+00	0.00E+00	La139	0.00E+00	0.00E+00	0.00E+00	Pb207	0.00E+00	0.00E+00	0.00E+00
Nb106	0.00E+00	3.31E+06	2.55E+06	Xe140	0.00E+00	1.04E+06	1.47E+06	Pb208	0.00E+00	0.00E+00	0.00E+00
Mo106	0.00E+00	1.23E+06	7.46E+05	Cs140	0.00E+00	1.75E+06	2.22E+06	Pb209	0.00E+00	1.98E+05	0.00E+00

Isotope	Energy Released in Decay (eV)			Isotope	Energy Released in Decay (eV)			Isotope	Energy Released in Decay (eV)		
	Alpha	Beta	Gamma		Alpha	Beta	Gamma		Alpha	Beta	Gamma
Tc106	0.00E+00	1.46E+06	3.13E+06	Ba140	0.00E+00	3.20E+05	1.82E+05	Pb210	7.07E-02	3.33E+04	4.53E+03
Ru106	0.00E+00	1.00E+04	0.00E+00	La140	0.00E+00	5.35E+05	2.31E+06	Pb211	0.00E+00	4.50E+05	6.44E+04
Rh106	0.00E+00	1.41E+06	2.06E+05	Ce140	0.00E+00	0.00E+00	0.00E+00	Pb212	0.00E+00	1.73E+05	1.45E+05
Pd106	0.00E+00	0.00E+00	0.00E+00	Xe141	0.00E+00	2.40E+06	1.01E+06	Pb214	0.00E+00	2.91E+05	2.40E+05
Mo107	0.00E+00	2.32E+06	1.39E+06	Cs141	0.00E+00	1.94E+06	9.97E+05	Bi209	3.14E+06	0.00E+00	0.00E+00
Tc107	0.00E+00	1.28E+06	1.82E+06	Ba141	0.00E+00	9.46E+05	9.25E+05	Bi210	7.43E+03	3.89E+05	0.00E+00
Ru107	0.00E+00	1.06E+06	3.45E+05	La141	0.00E+00	9.63E+05	2.68E+04	Bi211	6.67E+06	1.31E+04	4.73E+04
Rh107	0.00E+00	4.30E+05	3.13E+05	Ce141	0.00E+00	1.70E+05	7.67E+04	Bi212	2.23E+06	5.04E+05	1.04E+05
Pd107	0.00E+00	9.60E+03	0.00E+00	Pr141	0.00E+00	0.00E+00	0.00E+00	Bi213	1.32E+05	4.41E+05	1.27E+05
Pd107m	0.00E+00	6.27E+04	1.52E+05	Xe142	0.00E+00	1.40E+06	1.58E+06	Bi214	1.32E+04	6.54E+05	1.48E+06
Ag107	0.00E+00	0.00E+00	0.00E+00	Cs142	0.00E+00	2.90E+06	9.50E+05	Bi215	0.00E+00	3.00E+05	7.00E+05
Mo108	0.00E+00	1.59E+06	1.15E+06	Ba142	0.00E+00	3.83E+05	1.04E+06	Fr221	6.47E+06	8.43E+03	2.88E+04
Tc108	0.00E+00	2.26E+06	2.99E+06	La142	0.00E+00	8.68E+05	2.37E+06	Fr222	0.00E+00	7.20E+05	1.79E+05
Ru108	0.00E+00	3.70E+05	6.30E+04	Ce142	0.00E+00	0.00E+00	0.00E+00	Fr223	0.00E+00	3.70E+05	5.60E+04
Rh108	0.00E+00	1.90E+06	3.20E+05	Pr142	0.00E+00	8.09E+05	5.80E+04	Po210	5.41E+06	7.80E-02	8.30E+00
Rh108m	0.00E+00	6.30E+05	2.72E+06	Pr142m	0.00E+00	0.00E+00	3.15E-07	Po218	6.11E+06	0.00E+00	0.00E+00
Pd108	0.00E+00	0.00E+00	0.00E+00	Nd142	0.00E+00	0.00E+00	0.00E+00	At218	6.81E+06	0.00E+00	0.00E+00
Ag108m	0.00E+00	4.78E+03	1.62E+06	Cs143	0.00E+00	1.94E+06	1.22E+06	At219	6.00E+06	0.00E+00	0.00E+00
Ag108	0.00E+00	6.08E+05	1.85E+04	Ba143	0.00E+00	1.24E+06	1.14E+06	Rn219	6.88E+06	6.70E+03	5.85E+04
Cd108	0.00E+00	0.00E+00	0.00E+00	La143	0.00E+00	1.50E+06	2.63E+05	Rn220	6.40E+06	0.00E+00	6.30E+02
Tc109	0.00E+00	2.14E+06	1.10E+06	Ce143	0.00E+00	4.31E+05	2.79E+05	Rn221	1.35E+06	3.60E+05	1.18E+05
Ru109	0.00E+00	1.04E+06	1.66E+06	Pr143	0.00E+00	3.15E+05	9.00E-03	Rn222	5.59E+06	0.00E+00	3.88E+02
Rh109	0.00E+00	9.50E+05	2.99E+05	Nd143	0.00E+00	0.00E+00	0.00E+00	Rh110	0.00E+00	1.15E+06	2.38E+06
Pd109	0.00E+00	3.61E+05	6.45E+02	Ba144	0.00E+00	9.46E+05	7.05E+05	Pd110	0.00E+00	0.00E+00	0.00E+00
Pd109m	0.00E+00	7.70E+04	1.11E+05	La144	0.00E+00	1.36E+06	2.33E+06	Rh110m	0.00E+00	2.10E+06	3.30E+05
Ag109	0.00E+00	0.00E+00	0.00E+00	Ce144	0.00E+00	9.11E+04	1.93E+04	Ba145	0.00E+00	1.31E+06	2.05E+06
Ag109m	0.00E+00	7.43E+04	1.12E+04	Pr144	0.00E+00	1.21E+06	2.89E+04	La145	0.00E+00	9.98E+05	1.73E+06
Cd109	0.00E+00	7.91E+04	2.67E+04	Pr144m	0.00E+00	4.28E+04	1.27E+04	Ce145	0.00E+00	5.38E+05	1.04E+06
Ru110	0.00E+00	6.59E+05	5.97E+05	Nd144	1.90E+06	0.00E+00	0.00E+00	-	-	-	-

A4-6. BRANCHING RATIO

A radio-isotope may decay via more than one decay mode, and in these cases, it becomes necessary to properly account for the branching into these modes in the burn-up code. Consider the following decay chain of U^{235} , as shown in Figure A4.2.

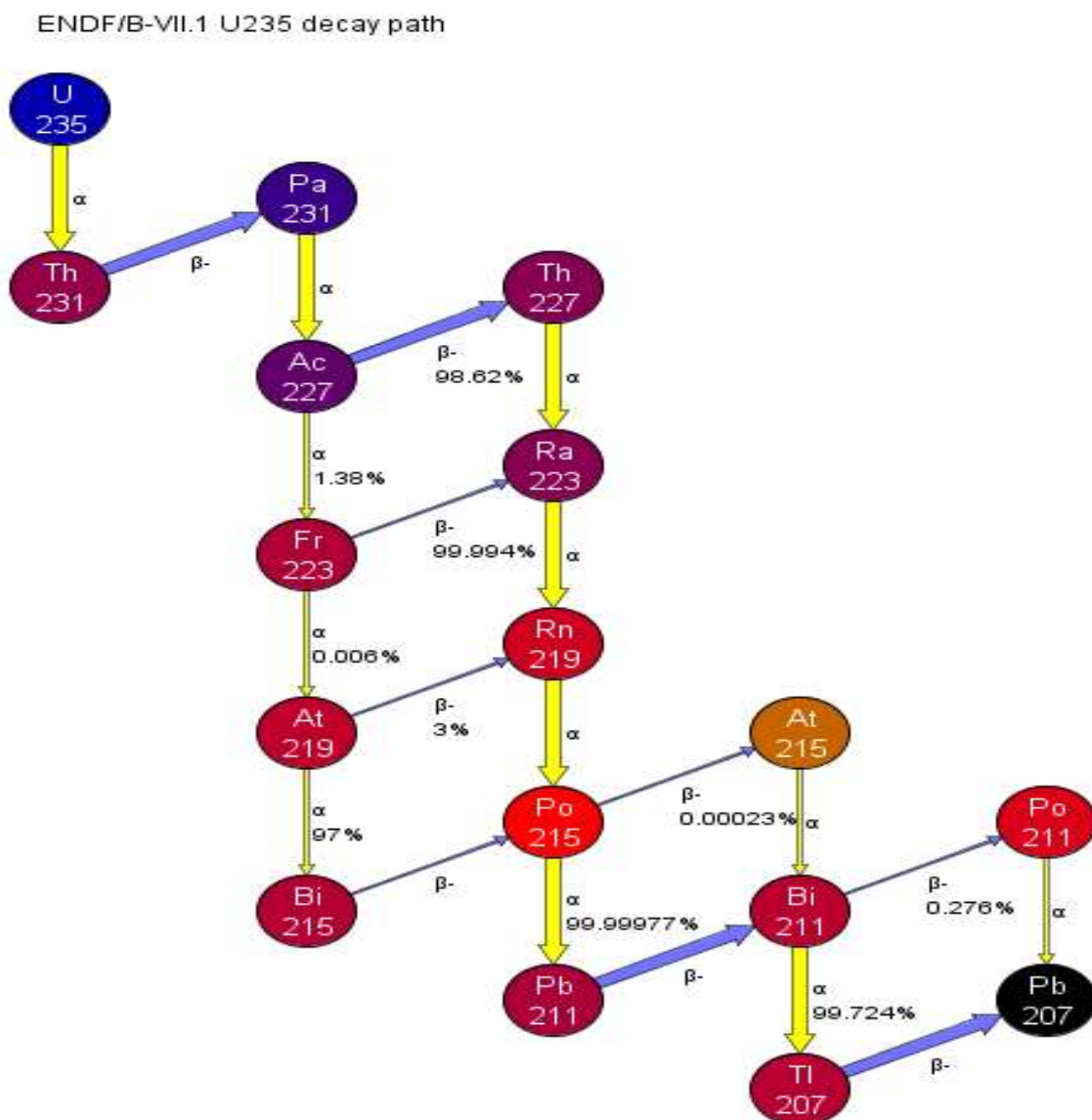


Figure A4. 2: Radioactive decay chain of U^{235}

As shown in Figure A4.2 of the U^{235} decay chain, Ac^{227} is converted to Th^{227} via 98.62% beta decay and Fr^{223} via 1.38% alpha decay. Hence branching ratio of Ac^{227} is 0.9862 for decay into Th^{227} and 0.0138 for decay into Fr^{223} . Decay chains of Am^{242} and Am^{242m} are shown in Figure A4.3 & Figure A4.4, respectively.

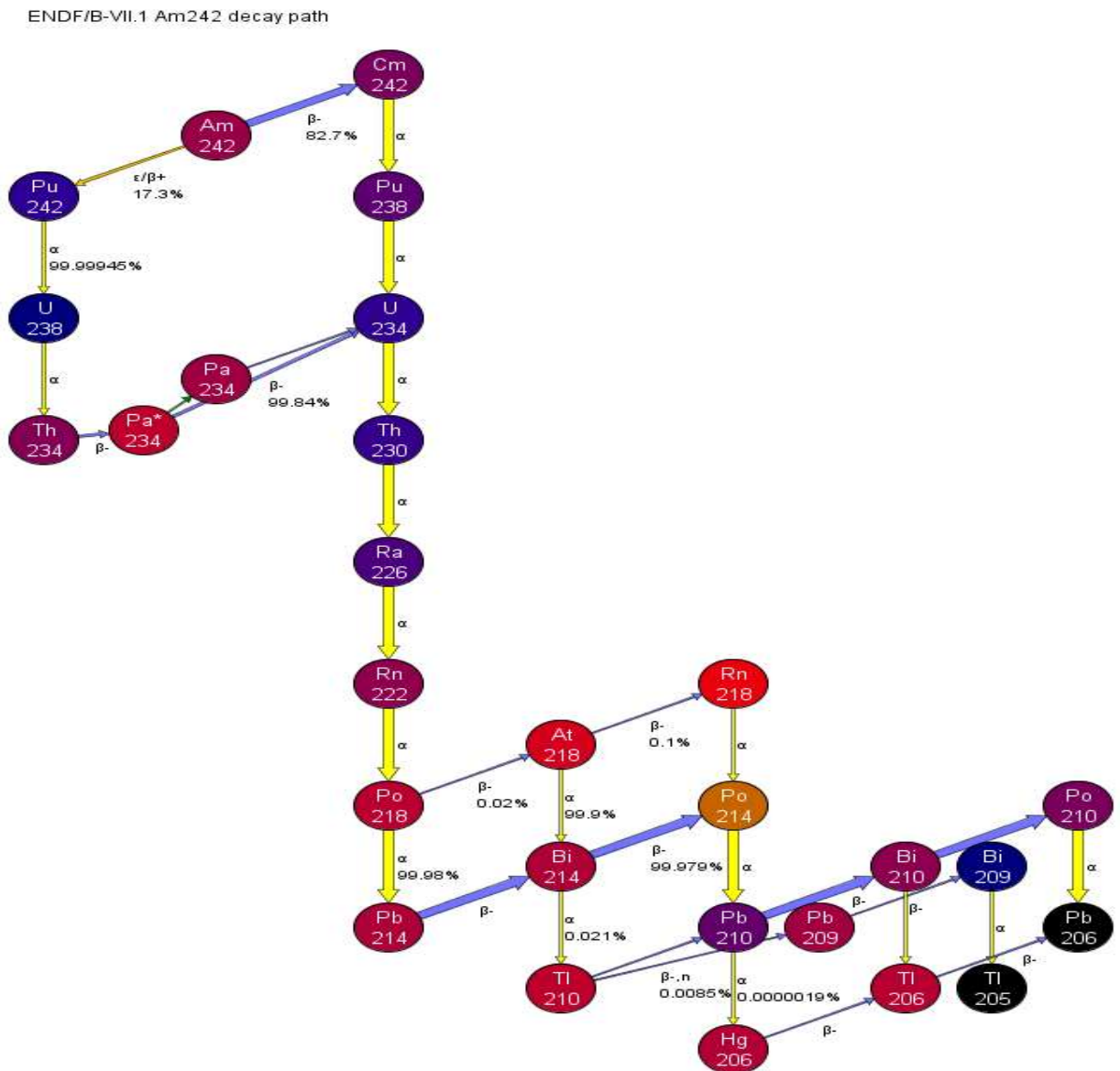


Figure A4. 3: Radioactive decay chain of Am^{242}

ENDF/B-VII.1 Am^{242m} decay path

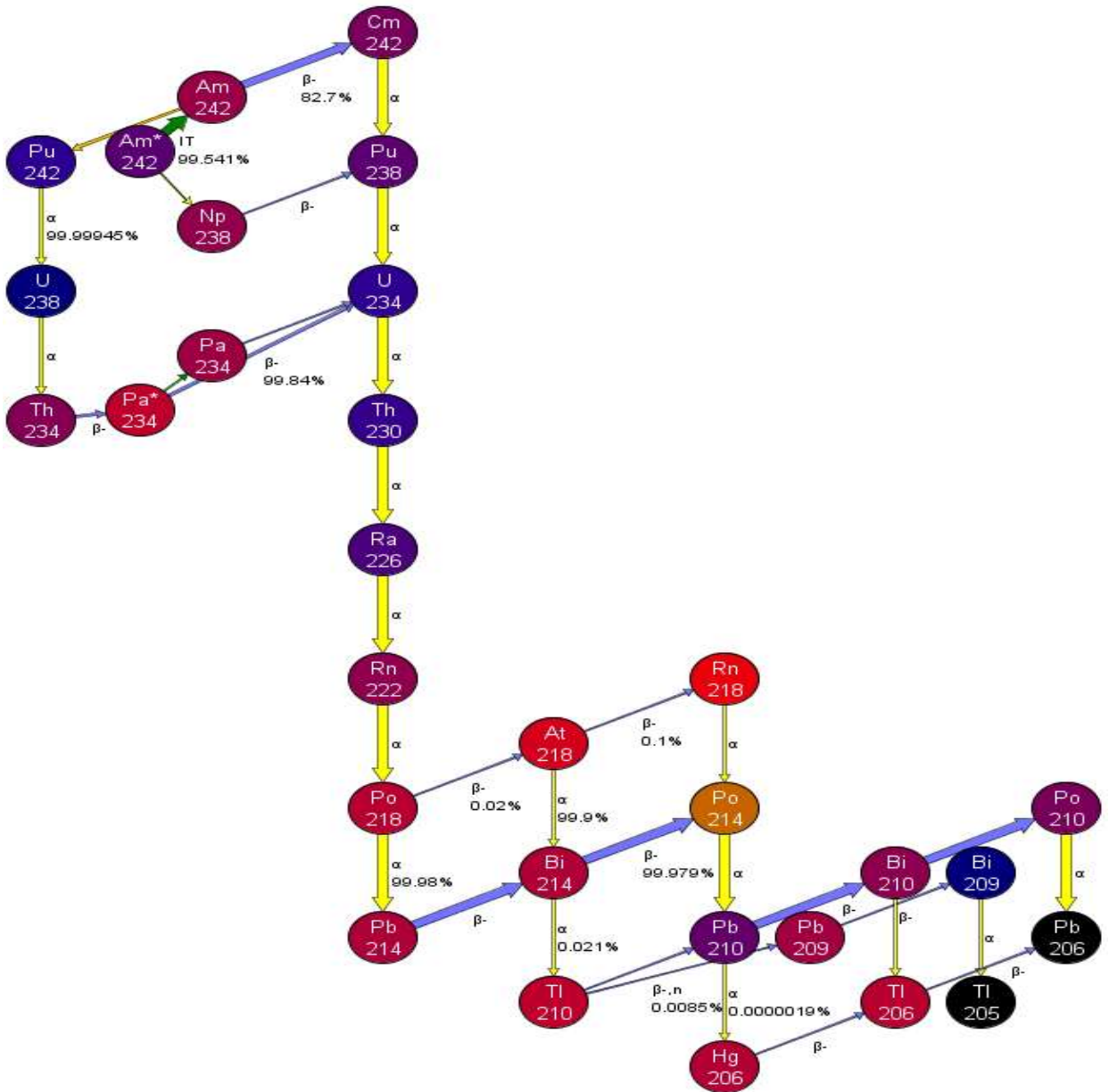


Figure A4. 4: Radioactive decay chain of Am^{242m}

A detailed description of decay chains with their branching ratios are given in annexure-1 & 2 and are properly accounted in the burn-up code IGDC.

A4-7. FISSION YIELD

Nuclear fission splits a heavy nucleus such as U^{235} or Pu^{239} into two lighter nuclei called fission products. **Fission yield** is the fraction of a fission product produced per fission. The parent independent yields mean expected numbers of each produced nuclide at the moment that fission occurs. The total expected number is two if fission is 2-body fission; however, the number is larger than two because actual fission yield data is included light nuclides produced by 3-body fission. The cumulative parent yields are the numbers, including the expected amount of products from parent nuclides by radioactive decay (basically β), and the total number is larger than 2. The Independent fission yield curve for 2-body fission plotted from data from JAEA nuclear data center and is shown in Figure-A4.5.

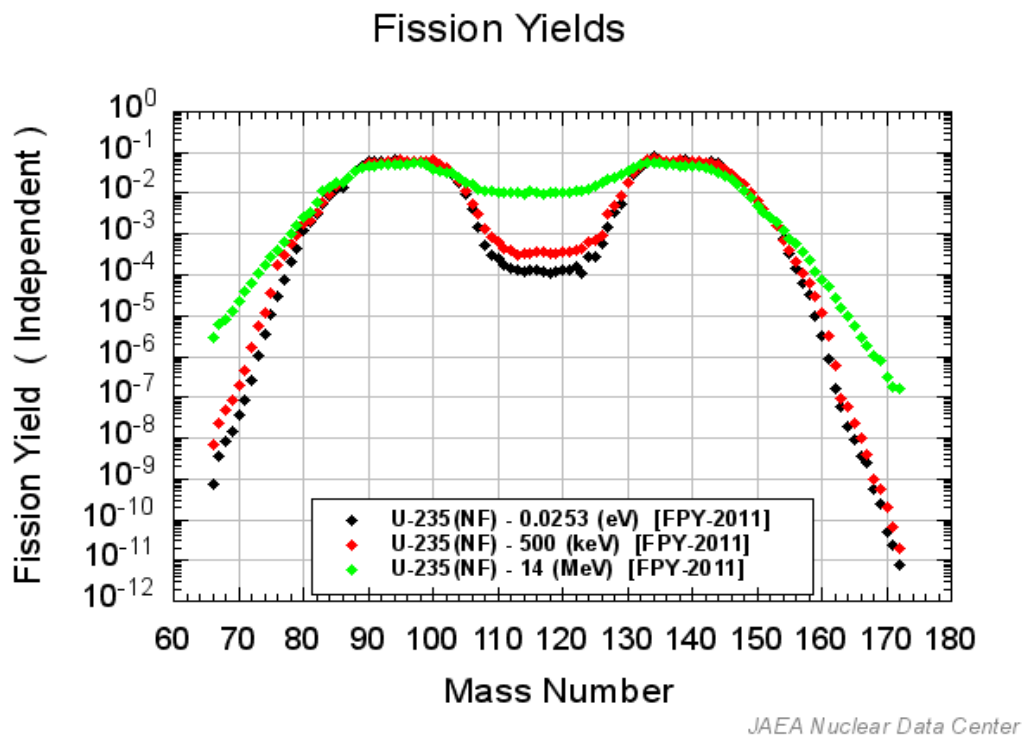


Figure A4. 5: Independent fission yield of U^{235}

As shown in Figure A4.5, nuclear fission is asymmetric for the low energy neutron and tends to be symmetric as the neutron energy increases. For burn-up codes, parent independent yields are used. Fission product yields are typically tabulated at discrete neutron energies such as thermal (0.0253 eV), fission (500 keV), and high energy (14 MeV). The yield for each fissionable nuclide is calculated by linearly interpolating the tabulated data at the computed spectrum averaged neutron energy (calculated from the fuel spectrum).

A4-8. SUMMARY

Methodologies for the generation of various nuclear data libraries to develop isotopic generation and depletion code of the current research viz. decay data library, fission yield library, the library for energy liberated during radioactive decay, dose conversion factor libraries, etc. are described in this annexure. The generated data libraries are used in the computer code IGDC.

References

1. H. Bateman, "The solution of a system of differential equations occurring in the theory of radioactive transformations," Proc. Cambridge Phil. Soc., 15, p. 423 (1910).
2. C. W. Gear, "Numerical initial value problems in ordinary differential equations, automatic computation", Prentice-Hall, Englewood Cliffs, NJ, 1971.
3. Lawrence F. Shampine and Mark W. Reichelt, "The MATLAB ODE suit", May 1997, SIAM Journal on Scientific Computing 18(1).
4. Allen G. Croff, "A User's Manual for the ORIGEN2 Computer Code," ORNL/TM-7175 (CCC-371), Oak Ridge National Laboratory, July 1980.
5. Technical Report Series No. 425, "Country Nuclear Fuel Cycle Profile", Second edition, IAEA, Vienna, 2005.
6. Nichols A. L., "Nuclear Data Requirements for Decay Heat Calculations", Lectures given at the workshop on nuclear reaction data and nuclear reactors: Physics, Design, and Safety, Trieste, 2002.
7. R. Crocker, "Fission product decay chains: Schematics with branching fractions, half-lives and literature references", US-NRDL, San Francisco, California, 94135.
8. M.B. Chadwick et al., "ENDF/B-VII.0: Next Generation Evaluated Nuclear Data Library for Nuclear Science and Technology" UCRL-JRNL-225066, 2006.
9. A.J. Koning and D. Rochman, "Modern Nuclear Data Evaluation with the TALYS Code System", Nuclear Data Sheets 113 (2012) 2841.

10. D.E.Cullen, "PREPRO2012: 2012 ENDF/B Pre-processing codes", IAEA-NDS-39, Rev. 15, October 2012, Nuclear Data Section, IAEA, Vienna.
11. Wikipedia contributors. (2020, August 31). Fission product yield. In *Wikipedia, The Free Encyclopedia*. Retrieved 13:43, December 9, 2020, from https://en.wikipedia.org/w/index.php?title=Fission_product_yield&oldid=975926511
12. Nicolas Soppera, Manuel Bossant, Oscar Cabellos, EmmericDupont, and Carlos J. D, JANIS: NEA JAVA-based Nuclear Data Information System, EPJ Web of Conferences 146, 07006 (2017).
13. The NUBASE evaluation of nuclear and decay properties - Audi, G. et al. Nucl. Phys. A729 (2003) 3-128. Dembia, CL, GD Recktenwald, MR Deinert (2013): Bondarenko method for obtaining group cross-sections in a multi-region collision probability model. Progress in Nuclear Energy, 67, 124-131.
14. J. K Tuli, Nuclear wallet cards for radioactive nuclides, (Seventh edition), April 2005, National nuclear data Centre, New York (www.nndc.bnl.gov).
15. J.K. Tuli, Evaluated nuclear structure data file: a manual for preparation of data sets, BNL-NCS-51655-01/02 Rev., Brookhaven National. Laboratory, (2001).
16. J KATAKURA, "JENDL FP Decay Data File 2011 and Fission Yields Data File 2011".
17. Eckerman K, Harrison J, Menzel HG, Clement CH., ICRP Publication 119: Compendium of dose coefficients based on ICRP Publication 60, Ann ICRP. 2012; 41 Suppl 1:1-130.

18. R.C. Bolles and N.E. Ballou, “Calculated activities and abundances of ^{235}U fission products”, U.S.N.R.D.L-456, 1959.
19. Andrej Trikov, “From basic nuclear data to applications”, “Jozef Stefan” Institute, Ljubljana, Slovenia, Lecture given at the “Workshop on Nuclear Data and Nuclear Reactors”, Physics, Design and Safety, Trieste 13 March-14 April 2000.
20. C. L. Dunford, “ENDF utility codes” Release 6.10 for ENDF-6 and ENDF-5, IAEA-NDS-29 Rev.7, Nov. 1995.
21. R. E. MacFarlane, A. C. Kahler, “Methods for Processing ENDF/B-VII with NJOY”, Nuclear Data Sheets, Volume 111, Issue 12, December 2010, Pages 2739-2890.
22. M. Gupta, M.A. Kellett, A.L. Nichols, O. Bersillon, “Decay Heat Calculations: Assessment of Fission Product Decay Data Requirements for Th/U Fuel”, IAEA Nuclear Data Section, Vienna International Centre, A-1400 Vienna, Austria, May.
23. Yuan, D., and Kernan, W., Explicit Solutions for Exit-only Radioactive Decay Chains, *J. of Applied Physics*, 101, 094907 (2007).
24. Pressyanov Dobromir S., Short Solution of the Radioactive Decay Chain Equations, *Am. J. Phys.* 70, 444–445 (2002).
25. Cetnar, J., Wallenius, J., Gudowski, W., “MCB: A continuous energy Monte-Carlo burn-up simulation code”, Proceedings of the Fifth International Information Exchange Meeting Mol, Belgium, November 25–27, AEN NEA OECD, pp. 523–527, (1998).

26. S.Nair, "RICE: A Reactor Inventory Code for calculating actinide and fission product arising's using a point source model, RD/B/N4138, IMAC/P(77)10, Central Electricity Generating Board", Berkeley Nuclear Laboratories (October 1977).
27. U. Fischer and H. W. Wiese, "Improved and Consistent Determination of the Nuclear Inventory of Spent PWR Fuel on the Basis of Cell-Burnup Methods Using KORIGEN," KFK-3014; ORNL-tr-5043 (January 1983).
28. K. Koyama, N. Yamano, S. Miyasaka, "A computer code for calculating radiation sources and analysing nuclide transmutations", JAERI-M 8229 (May 1979).
29. J. Sanz, O. Cabellos, and N. García-Herranz. "ACAB Inventory Code for Nuclear. Applications", User's Manual V.2008., 2008.
30. R. Srivenkatesan, "Literature Survey Report on Decay Heat Calculations: Nuclear Data, Methods, Codes and Validations", BRNS Project from MCNS, Manipal University, November 2014.
31. GokhanYesilyurt, Kevin T. Clarno, and Ian C. Gauld, "Modular ORIGEN-S for multi-physics code systems", Oak Ridge National Laboratory.
32. B. T. Rearden, M. A. Jessee, Editors, "SCALE code system", ORNL/TM-2005/39, Version 6.2.3, Oak Ridge National Laboratory.
33. Oak Ridge, TN 37831I. C. Gauld, D. L. Barnett, O. W. Hermann, S. M. Bowman, "OPUS/PlotOPUS: An ORIGEN-S Post-Processing Utility and Plotting Program for SCALE (NUREG/CR-6718)", Oak Ridge National Laboratory.

34. R. F. Burstall, "FISPIN A Computer Code for Nuclide Inventory Calculations," ND-R-328(R) (October 1979).
35. J Sidell (1976) "EXTRA: A Digital Computer Program for the Solution of Stiff Sets of Ordinary, Initial Value, First Order Differential Equations." AEEW-R799, UKAEA, Winfrith.
36. J.W. Eastwood and J.G. Morgan, "The FISPACT-II Detailed Design Document", Technical Report CEM/100421/SD/3 Issue 1, Culham Electromagnetics Ltd, November 2010.
37. R.A. Forrest, J. Kopecky, and J.-Ch. Sublet, "The European Activation File: EAF-2005", cross-section library, UKAEA FUS 515, EURATOM/UKAEA Fusion, January 2005.
38. J. Sanz, O. Cabellos and N. García-Herranz, "ACAB -2008: Activation Abacus Code V2008", NEA Data Bank NEA-1839, (2008).
39. Nair S. (1977) RICE—a reactor inventory code for calculating actinide and fission product arising using a point source model, CEGB Report RD/B/N4138.
40. Clarke, R.H. (1972) FISP, A Comprehensive Computer Program for Generating Fission Product Inventories, Health Physics, 23, 565-572;
41. Tobias, A. (1978) FISP5 – an extended and improved version of the fission product inventory code FISP, Central Electricity Generating Board Report RD/B/N4303.
42. A. Tobias, "Decay Heat", Progress in Nuclear Energy, Vol. 5, pp.1-93 (1979).

43. Kamatam Venkata Subbaiah, “ISOGEN: Interactive isotope generation and depletion code”, Manipal Centre for Natural Sciences, Radiation Protection and Environment- 2017, Manipal University, Manipal, Karnataka, India.
44. Jaakko Leppänen and Maria Pusa, “Burnup calculation capability in the psg2 / serpent Monte Carlo reactor physics code”, VTT Technical Research Centre of Finland, International Conference on Mathematics, Computational Methods & Reactor Physics (M&C 2009) Saratoga Springs, New York, May 3-7, 2009, on CD-ROM, American Nuclear Society, LaGrange Park, IL (2009).
45. Joel Rhodes, Kord Smith, and Deokjung Lee, “CASMO-5 Development and Applications”, StudsvikScandpower Inc., 504 Shoup Ave Suite #201, Idaho Falls, ID, 83402 USA.
46. Krishnani P. D., “CLUB—A multi-group Integral Transport theory code for analysis of cluster lattices”, *Ann. Nucl. Energy*, 9, 255 (1982).
47. Askew, J.R. Fayers, F.J., and Kemshell, P., 1966. A general description of the lattice code WIMS-D. *British nuclear energy society*, p. 564, Oct 1966.
48. Gregg, R. and C. Grove, “Analysis of the UK nuclear fission roadmap using the ORION fuel cycle modeling code,” *Proceedings of the IChemE Nuclear Fuel Cycle Conference*, Manchester, United Kingdom (2012).
49. Boucher, L., Grouiller, J.P., CEA Cadarache, DEN/CAD/SPRC (France) “COSI: a simulation software for a pool of reactors and fuel cycle plants”,
50. IAEA-TECDOC-1535, “Nuclear Fuel Cycle Simulation System (VISTA), February 2007.

51. A. Tsilanizara, C.M. Diop, B. Nimal, M. Detoc, Luneville, M. Chiron, T.D. Huynh, I. Bresard, M. Eid, J.C Klein, B. Roque, P. Marimbeau, C. Garzenne, J.M. Parize and C. Vergne, “DARWIN: An Evolution Code System for a Large Range of Applications”.
52. Alain Kavenoky and Richard Sanchez, “The APOLLO assembly spectrum code”, Département des Etudes Mécaniques et Thermiques, Centre d'Etudes Nucléaires de Saclay, 91191 Gif sur Yvette Cedex – France.
53. Axel Becker and Gerd Anton, “SNF: spent fuel analyses based on CASMO/SIMULATE in-core fuel management”, Studsvik Scandpower GmbH Norderstedt, Germany.
54. F. Michel-Sendis, “SFCOMPO-2.0: An OECD NEA database of spent nuclear fuel isotopic assays, reactor design specifications, and operating data”.
55. Alexandru Octavian Pavelescu, Dan Gabriel Gepraga, CANDU radiotoxicity inventories estimation – a calculated experiment cross-check for data verification and validation, Environmental Physics, October-2006.
56. I. C. Gauld, K. A. Litwin, “Verification and Validation of the ORIGEN-S code and Nuclear Data Libraries”, RC-1429, COG-I-95-150, Scientific Document Distribution Office (SDDO), AECL, Chalk River, Ontario, Canada K0J 1J0.
57. In-core fuel management benchmarks for PHWRs, IAEA TECDOC-887, 1996.
58. Bajaj, S.S., & Gore, A.R. (2006). The Indian PHWR. Nuclear Engineering and Design, 236(7-8), 701-722. doi:10.1016/j.nucengdes.2005.09.028.

59. R.E. Macfarlane, “An introduction to ENDF formats,” Lectures given at the workshop on nuclear data and nuclear reactors: Physics, Design, and Safety, Trieste, 2000.
60. M. Herman and A. Trkov, “ENDF-6 Formats Manual”, National Nuclear Data Center, Brookhaven National Laboratory, June-2009.
61. Tinus Keyser, “M.Eng (Nuclear) Minor Dissertation EEE5004Z Numerical simulation of nuclear reactor isotope depletion”, KYSTIN001, November 2017.
62. Basic Organization - T-2: LANL. <https://t2.lanl.gov/nis/endf/intro05.html>
63. Dembia, CL, GD Recktenwald, MR Deinert (2013): Bondarenko method for obtaining group cross-sections in a multi-region collision probability model. *Progress in Nuclear Energy*, 67, 124-131.
64. Dermott E. Cullen, “Groupie”, The nuclear data section, International Atomic Energy Agency, Vienna, Austria
65. J.L. Kloosterman, “Actinide data for transmutation studies”, ECN-I—94-056, February, 1995.
66. Edward Purba, “Compact numerical methods for stiff differential equations”, Sarjana S-1, Bandung Institute of Technology, Bandung, Indonesia, 1984.
67. P.P. Kruger, “Numerical methods to solve the fuel depletion equations for a nuclear reactor”, Dissertation submitted in partial fulfillment of the requirements for the degree Magister Scientiae in Physics at the Potchefstroomse Universiteit vir Christelike Hoer Onderwys.
68. Graham W. Griffith, “ Numerical analysis using R, Solutions to ODEs and PDFs”, Cambridge University Press”.

69. J.C. Tait, I.C. Gauld, and A.H. Kerr, “Validation Of The ORIGEN-S Code For Predicting Radionuclide Inventories In Used CANDU Fuel”, *Journal of Nuclear Materials* 223, 109–121 (1995).
70. Keith E. Holbert, “Nuclear Power Engineering”, EEE 460
71. “Actinide and Fission Product Partitioning and Transmutation”, Twelfth Information Exchange Meeting, Prague, Czech Republic, 24-27 September 2012, NEA/NSC/DOC (2013)3.
72. Merk B, Litskevich D, Gregg R, Mount AR. Demand driven salt clean-up in a molten salt fast reactor - Defining a priority list. *PLoS One*. 2018 Mar 1;13(3):e0192020. DOI: 10.1371/journal.pone.0192020. PMID: 29494604; PMCID: PMC5832222.
73. Paul L. Roggenkamp, “The Influence of Xenon-135 on Reactor Operation”, WSRC-MS-2000-00061.
74. Rod Adams, “RTG Heat Sources: Two Proven Materials” Archived 7 February 2012 at the Wayback Machine, 1 Sep 1996, and Retrieved 20 Jan 2012.
75. Conceptual Physics: Difference between Fission Fragments...
<http://www.conceptualphysicstoday.com/2015/02/difference-between-fission-fragments.html>
76. Youssef Mroueh, “The radioactive decays and heat emission of the CANDU reactor’s used fuel bundles”, Pickering-PN-CAC Meeting, October 19th, 2004.
77. Wikipedia contributors. (2014, May 11). Differential equation. In Wikipedia, The Free Encyclopedia. Retrieved 13:46, December 9, 2020, from

https://en.wikipedia.org/w/index.php?title=Differential_equation&oldid=608070296

78. M. Goyal, “Computer-Based Numerical & Statistical Techniques”, Jones & Bartlett Publishers, 2007.

79. Differential Equations - University of Manchester.

http://epsassets.manchester.ac.uk/medialand/maths/helm/19_2.pdf.

80. Wikipedia contributors. (2020, August 15). Numerical methods for ordinary differential equations. In Wikipedia, The Free Encyclopedia. Retrieved 13:57, December 9, 2020, from:

https://en.wikipedia.org/w/index.php?title=Numerical_methods_for_ordinary_differential_equations&oldid=973206689.

81. Ordinary Differential Equations 3-Numerical Analysis.

<https://www.docsity.com/en/ordinary-differential-equations-3-numerical-analysis-lecture-slides/168864>

82. Numerical Solution of Initial-Value Problems.

<https://www.cpp.edu/~tknguyen/egr511/Notes/Ch4-5.doc>.

83. Integration methods. <http://qucs.sourceforge.net/tech/node24.html>

84. Indira Gandhi National Open University.

<http://ignou.ac.in/userfiles/Unit-3-Block-3.doc>

85. National Nuclear Data Center | Global and Regional Solutions.

<https://www.bnl.gov/NST/NNDC.php>.